SKAと重力

– パルサーによる重力波直接観測と重力理論検証 –

井岡 邦仁 (KEK, 総研大)

KEK
HIGH ENERGY ACCELERATOR RESEARCH ORGANIZATION
The Graduate University for Advanced Studies
Sokendai

SKA2 Key Science Drivers

- ORIGINS
  - Neutral Hydrogen in the Universe from the Epoch of Re-ionisation to now
    - When did the first stars and galaxies form?
    - How did galaxies evolve?
    - Dark Energy, Dark Matter
  - Astro-biology
- FUNDAMENTAL FORCES
  - Pulsars, General Relativity and gravitational waves
  - Origin and evolution of cosmic magnetism
- TRANSIENTS (new phenomenon)

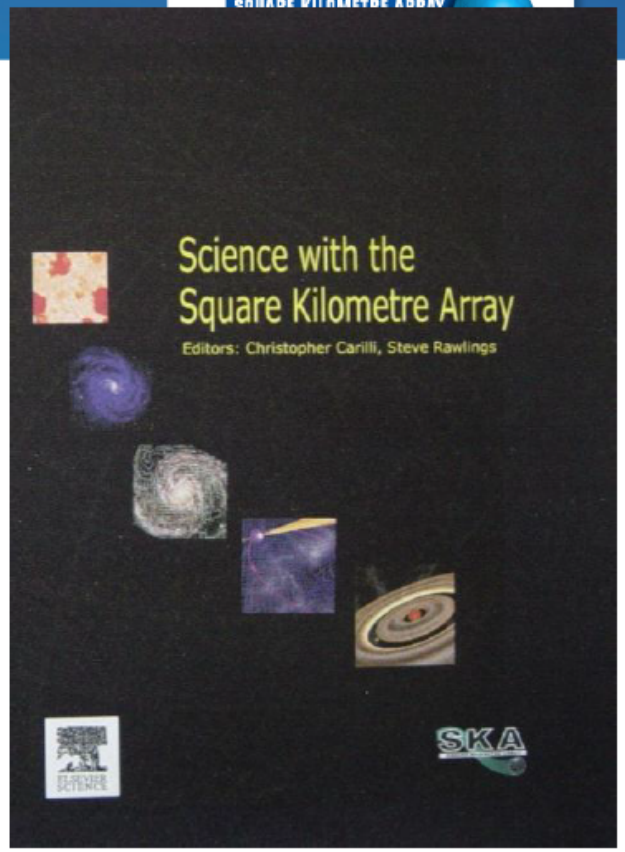

Science with the Square Kilometre Array
(2004, eds. C. Carilli & S. Rawlings, *New Astron. Rev.*, **48**)

SKA2 Key Science Drivers

- ORIGINS
  - Neutral Hydrogen in the Universe from the Epoch of Re-ionisation to now [SKA1]
    - When did the first stars and galaxies form?
    - How did galaxies evolve?
    - Dark Energy, Dark Matter
  - Astro-biology
- FUNDAMENTAL FORCES
  - Pulsars, General Relativity and gravitational waves [SKA1]
  - Origin and evolution of cosmic magnetism
- TRANSIENTS (new phenomenon)

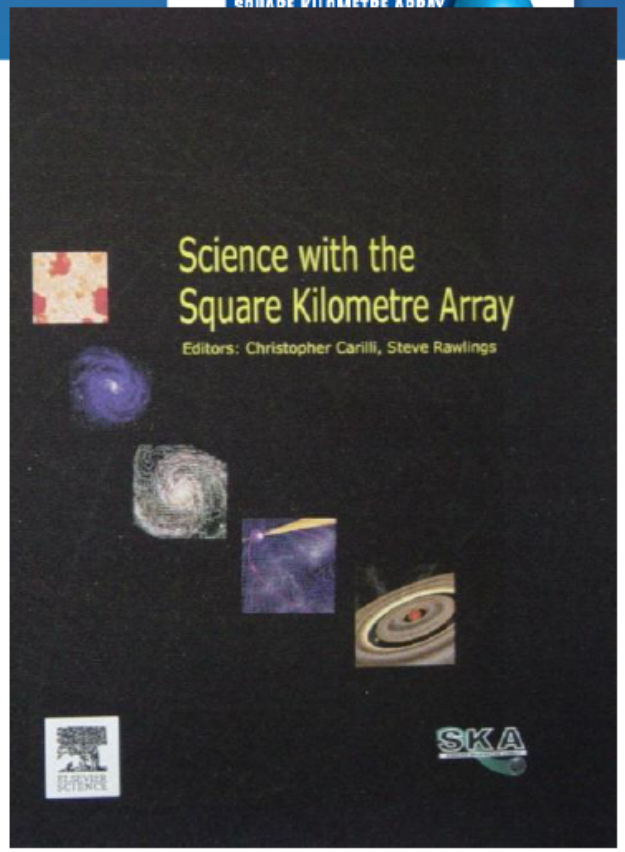

Science with the Square Kilometre Array
(2004, eds. C. Carilli & S. Rawlings, *New Astron. Rev.*, **48**)

SKA2 Key Science Drivers

- ORIGINS
  - Neutral Hydrogen in the Universe from the Epoch of Re-ionisation to now [SKA1]
    - When did the first stars and galaxies form?
    - How did galaxies evolve?
    - Dark Energy, Dark Matter
  - Astro-biology
- FUNDAMENTAL FORCES
  - Pulsars, General Relativity and gravitational waves [SKA1]
  - Origin and evolution of cosmic magnetism
- TRANSIENTS (new phenomenon)

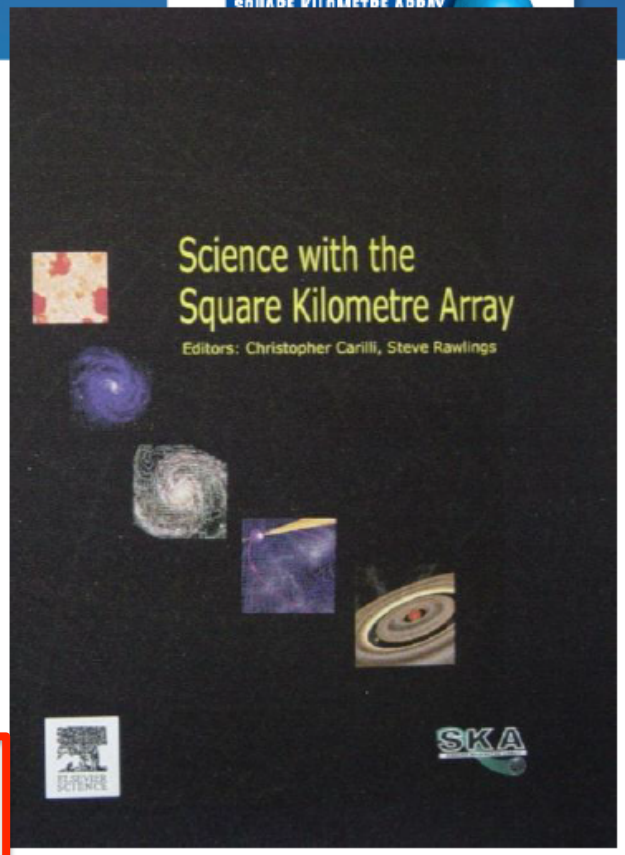

Science with the Square Kilometre Array
(2004, eds. C. Carilli & S. Rawlings, *New Astron. Rev.*, **48**)

Outline

- Pulsar
  - Finding all pulsars in the Milky Way
  - Super dense matter physics, etc.
- Strong-field tests of gravity
- Gravitational wave astronomy
  - Complementary to AdvLIGO, KAGRA, eLISA, DECIGO, CMB-pol, LiteBIRD

Pulsar

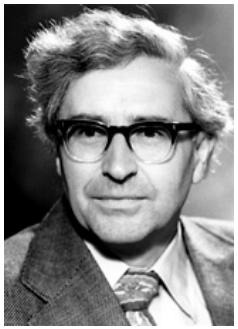

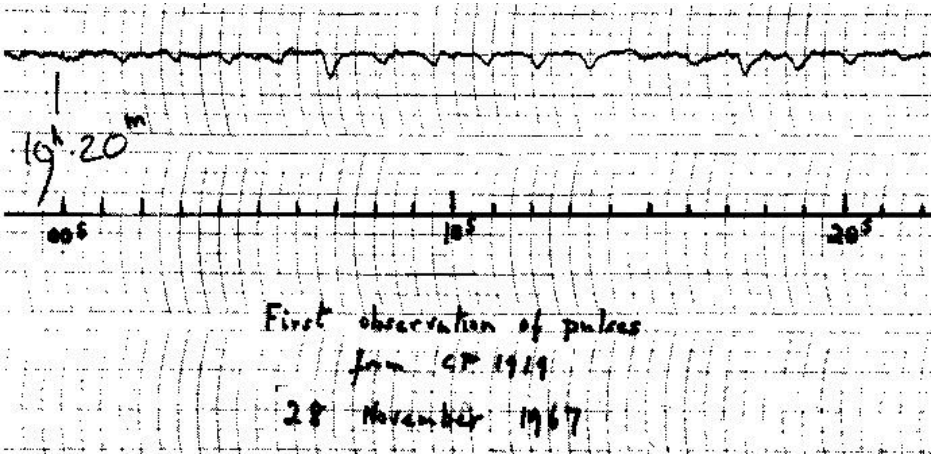

Bell (graduate), Hewish 1967
Discovered serendipitously
Nobel prize to Hewish 1974
(w/ Ryle; radio interferometer)

CP 1919 (PSR B1919+21) P=1.3373011 sec

$$\frac{GM}{R^2} > R\Omega^2$$ (Gravity>Centrifugal F)

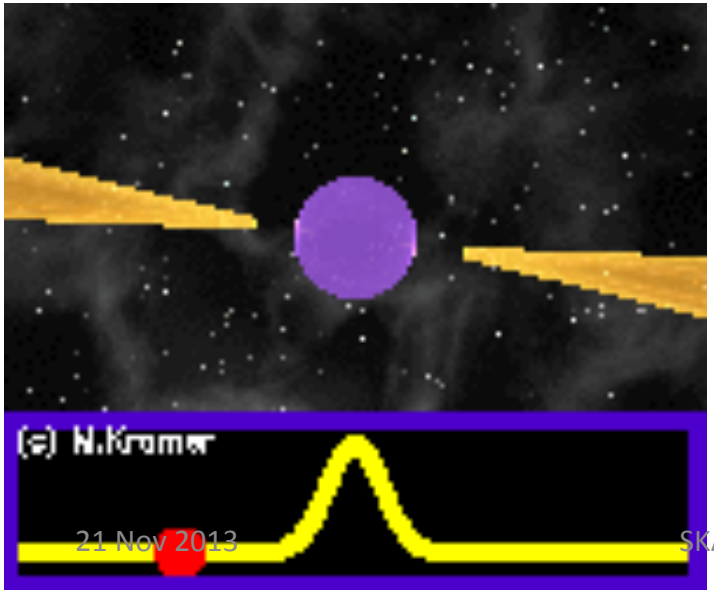

$$\bar{\rho} > \frac{3\Omega^2}{4\pi G} \sim 5\times10^{13}\,\mathrm{g\,cm^{-3}}$$

~ Nuclear density 3×10^{14} g/cm^3

⇒ ***Neutron star!***

Pulsars are Extreme

- ***Almost black holes (Strong gravity)***

$$\frac{E_{\text{gravity}}}{Mc^2} \approx 0.1\ (\text{NS}),\ 0.5\ (\text{BH}),\ 0.000001\ (\text{Sun})$$

- ***Super dense objects***
  - 10x nuclear density
  - B~$B_{QED} = m_e^2 c^3 / e\hbar = 4.4 \times 10^{13}\,\text{G}$
  - V>10^{12} Volt (>TeV accelerators)
  - Superfluid superconductor
- ***Super cosmic clocks***
  - e.g., PSR J0437-4715

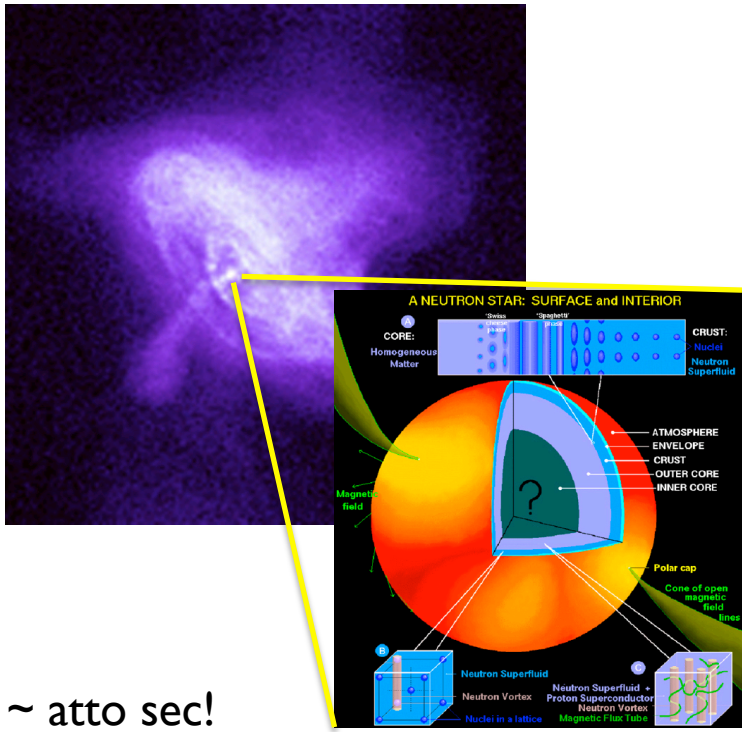

Δt ~ atto sec!

5.757451831072007 ± 0.000000000000008 ms

Pulsars to Probe Gravity

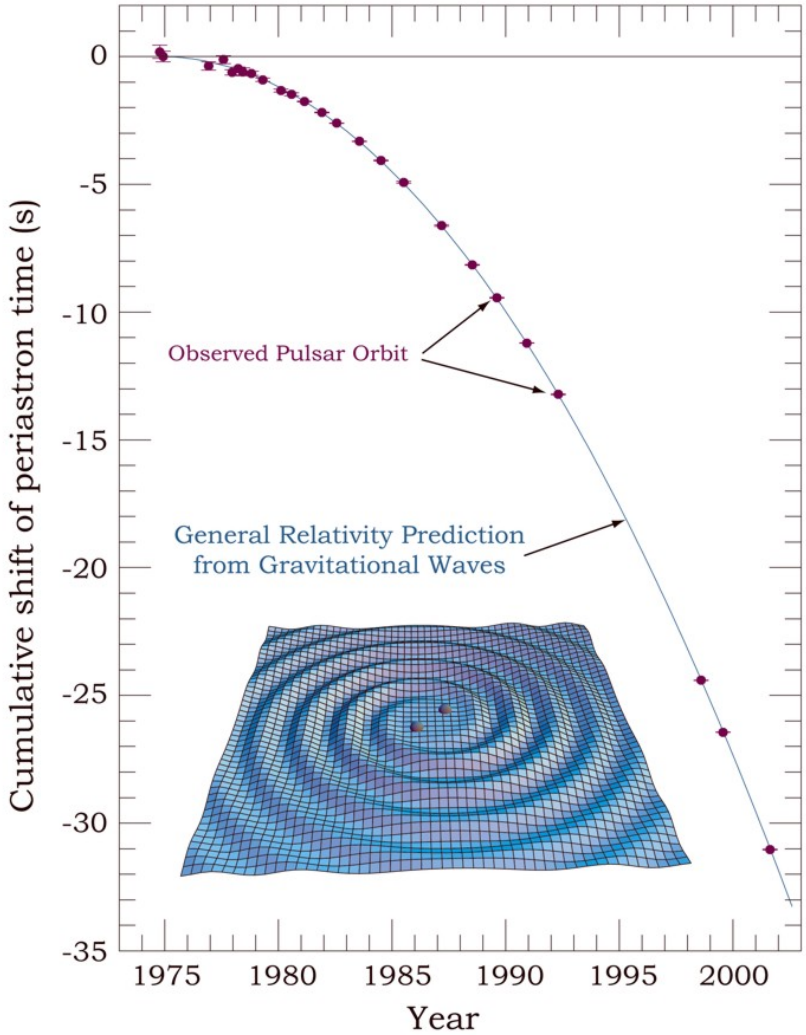

Binary PSR B1913+16

Orbit decay as predicted by General Relativity

First evidence of gravitational wave

Indirect detection

R. Hulse
J. Taylor
Arecibo in 74-75
Nobel prize1993

Pulsar Census

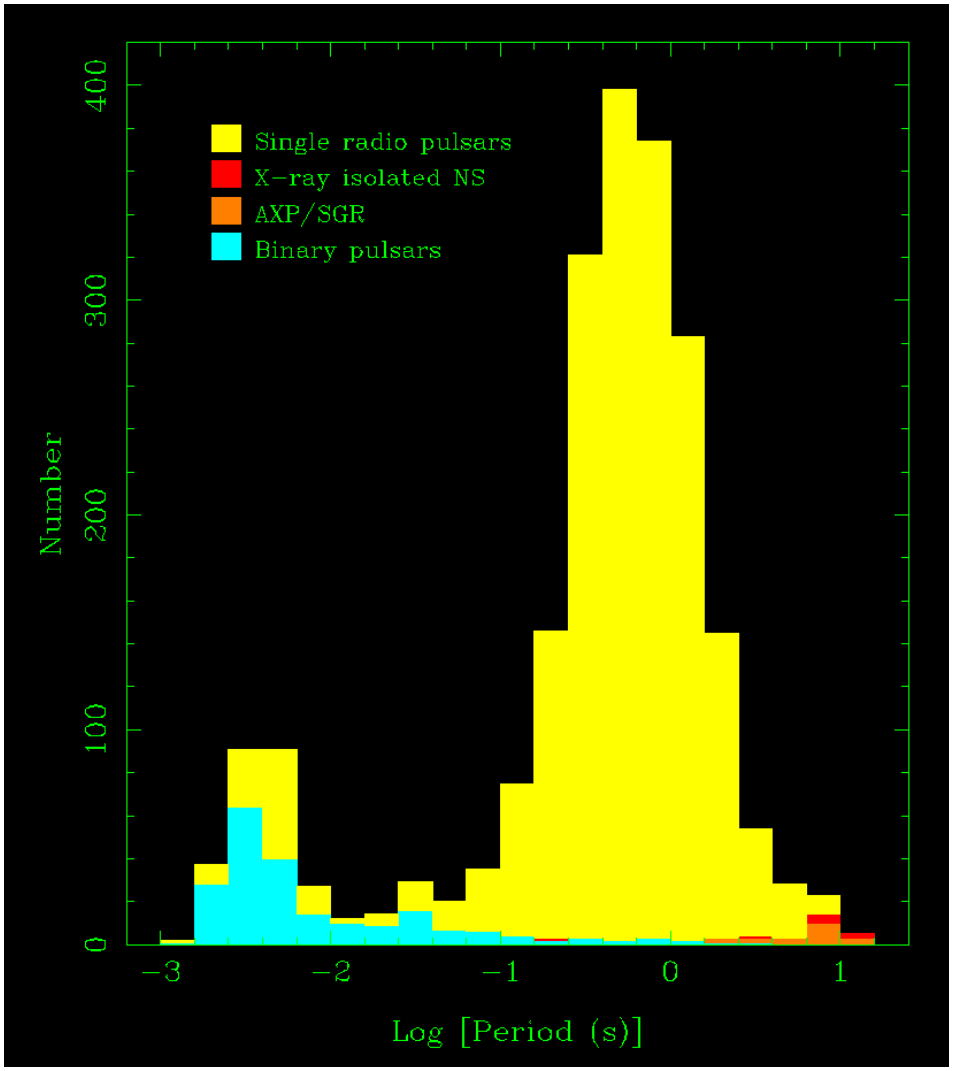

2213 known pulsars

2050 normal pulsars (via supernova)
302 msec pulsars (mostly binary; recycled)
213 in binary
142 in globular cluster
8 X-ray isolated NS
20 AXP/SGR
21 extragalactic

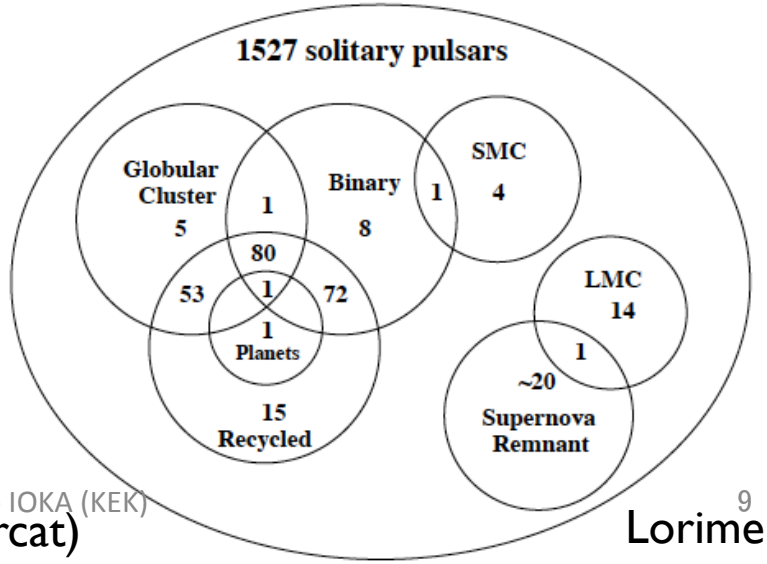

Manchester 13 (www.atnf.csiro.au/research/pulsar/psrcat)

Lorimer 08

$P\dot{P}$ Diagram

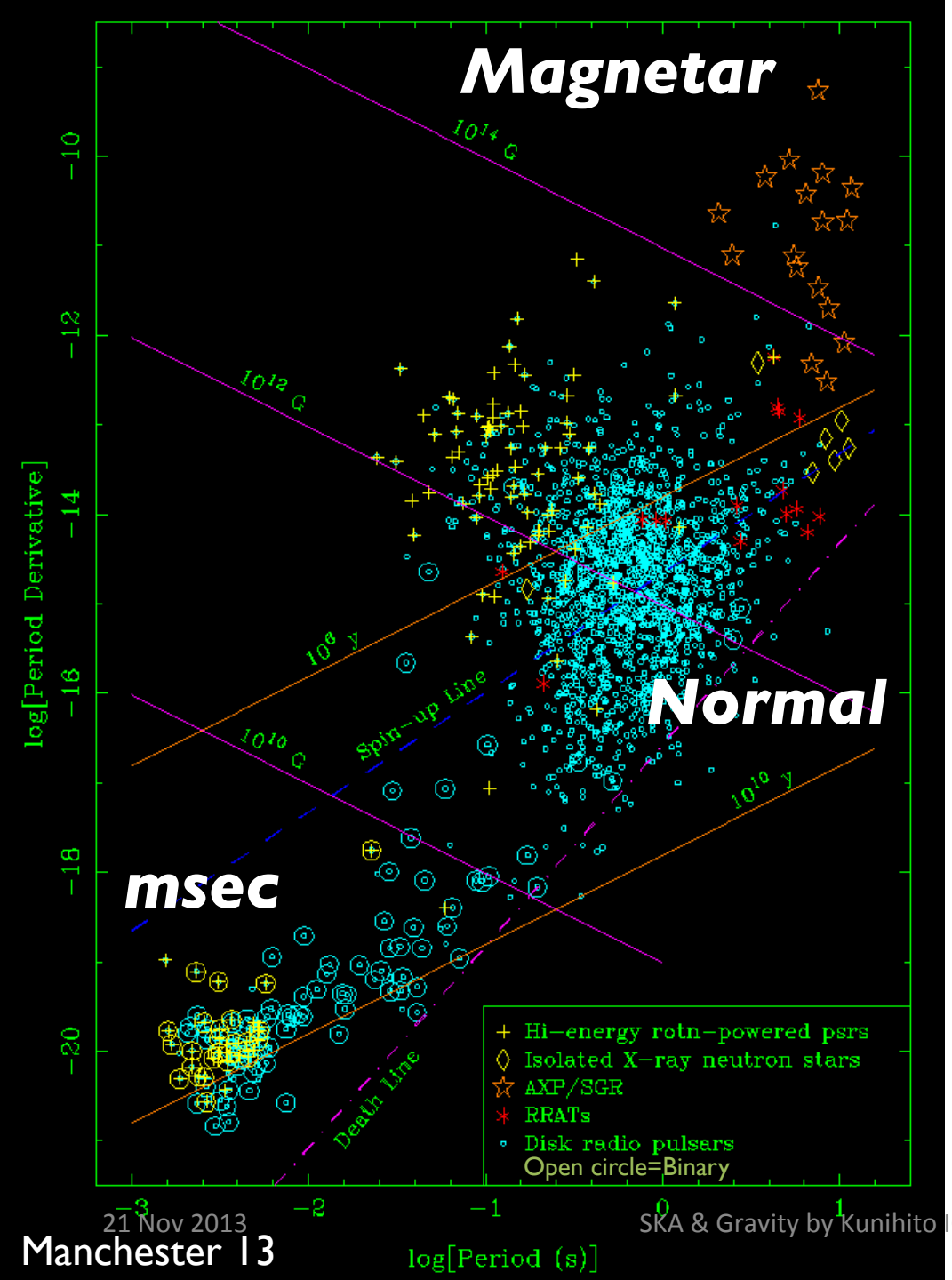

Age: $\tau_c = P/(2\dot{P})$

Magnetic field:

$$|\mathbf{m}| \approx \frac{B_p R^3}{2} \quad \text{(Mag. Dipole)}$$

$$\dot{E} = -\frac{2}{3c^3}|\ddot{\mathbf{m}}|^2 \approx -\frac{B_p^2 R^6 \Omega^4}{6c^3}$$

$$\dot{E} = I\Omega\dot{\Omega}, \ \Omega = \frac{2\pi}{P}$$

$$B_p = \sqrt{\frac{3c^3 I}{2\pi^2 R^6} P\dot{P}} \propto \sqrt{P\dot{P}}$$

Great diversity in the pulsar population!

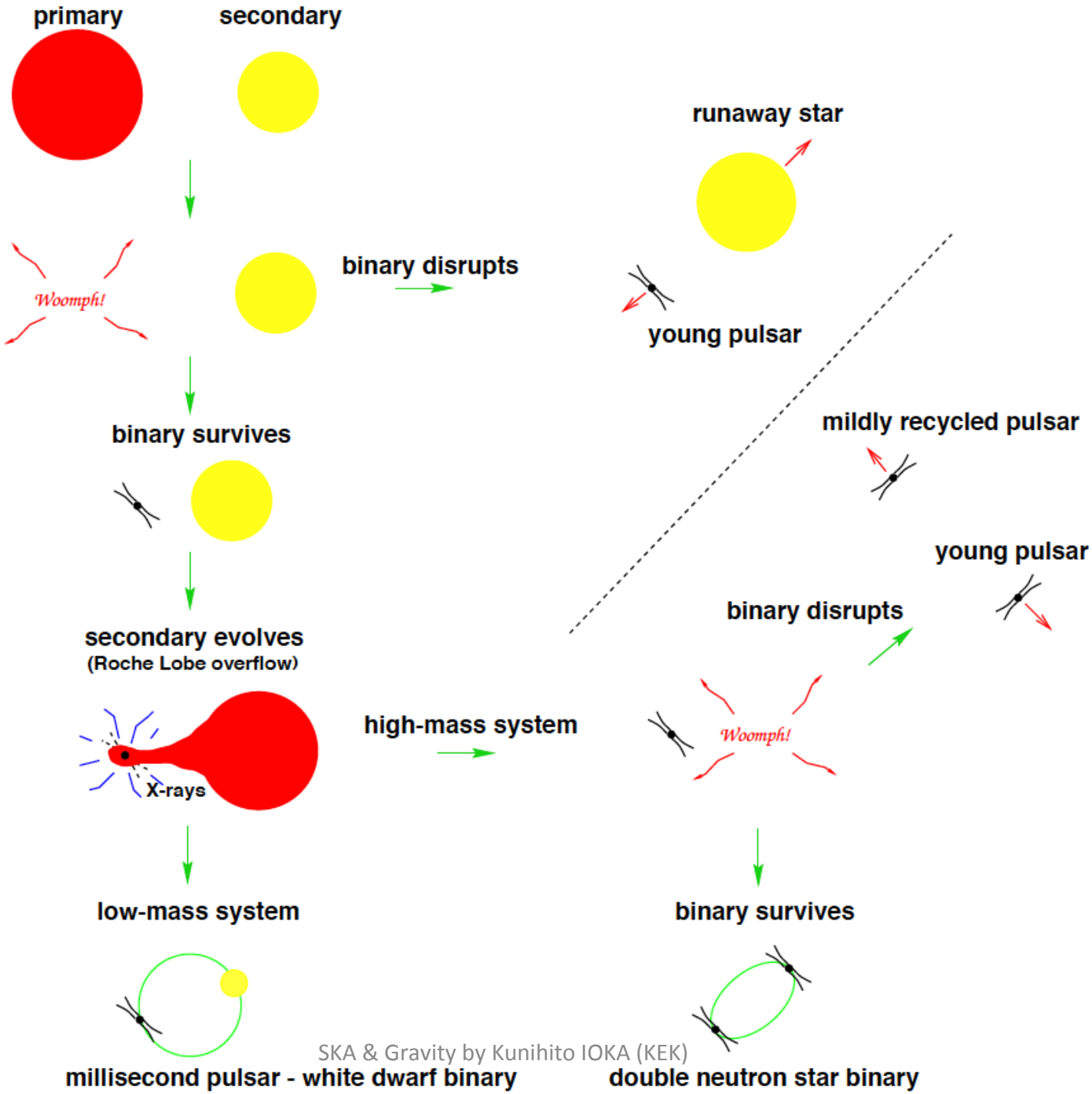
primary
secondary
Woomph!
binary disrupts
runaway star
young pulsar
binary survives
mildly recycled pulsar
young pulsar
binary disrupts
secondary evolves
(Roche Lobe overflow)
X-rays
high-mass system
Woomph!
low-mass system
binary survives
millisecond pulsar - white dwarf binary
double neutron star binary

Dispersion Measure

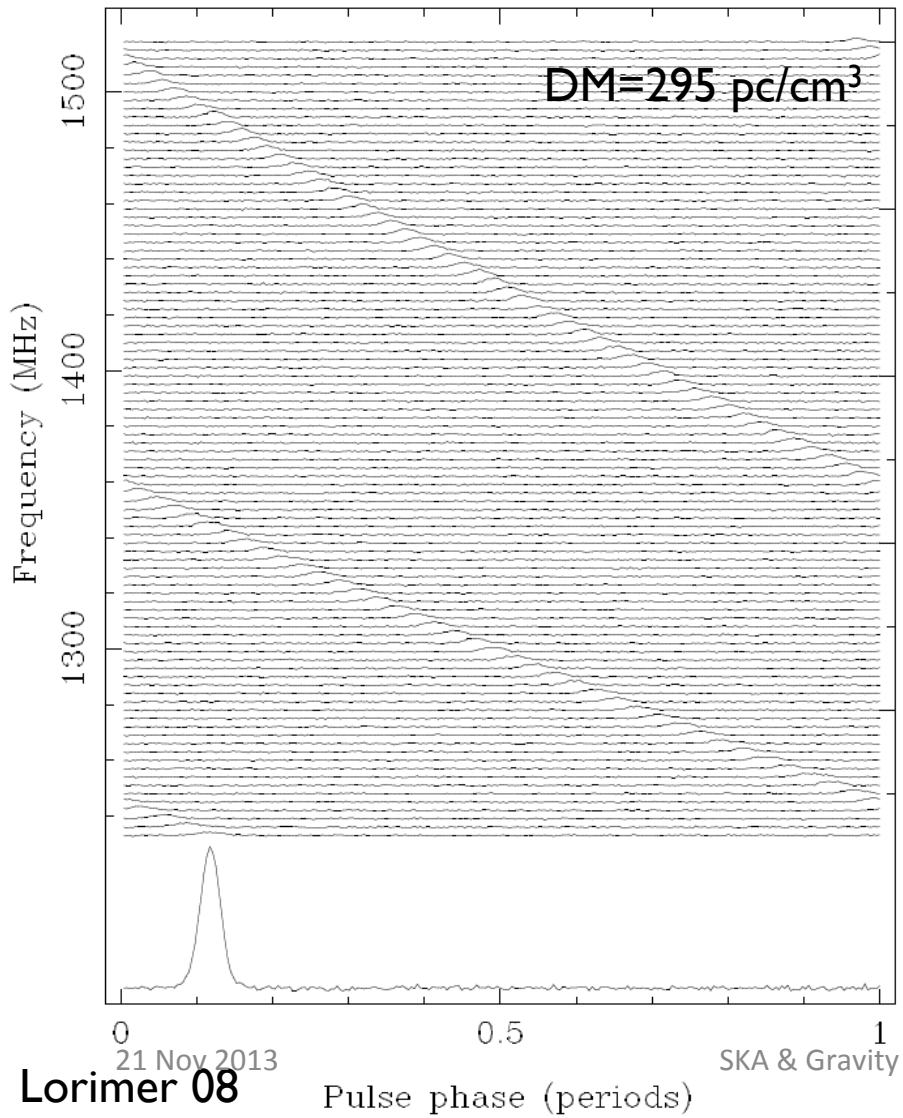

Lorimer 08

Photon is delayed in plasma

$$\omega^2 = k^2 c^2 + \omega_p^2$$

Plasma frequency

$$\omega_p = \sqrt{\frac{4\pi n_e e^2}{m}} = 5.63 \times 10^4 n_e^{1/2} \ \mathrm{s}^{-1}$$

$$\Delta t = 4.15 \ \mathrm{s} \left(\frac{\nu}{1 \ \mathrm{GHz}}\right)^{-2} \left(\frac{\mathrm{DM}}{10^3 \ \mathrm{pc \ cm^{-3}}}\right)$$

$$\mathrm{DM} \equiv \int_0^D ds \ n_e$$

Column density of free electrons

DM ⇒ Distance

Electron Distribution

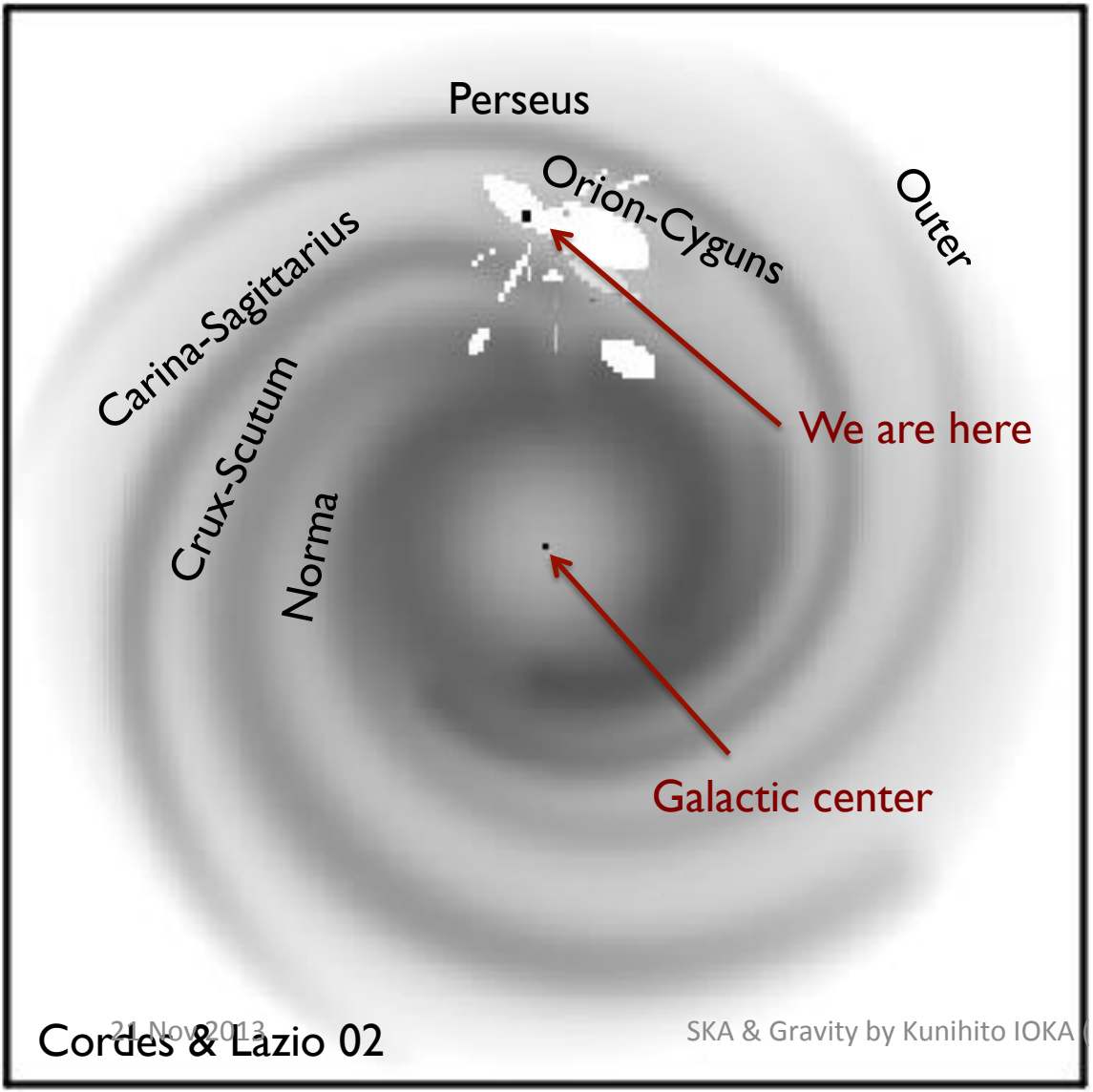

Cordes & Lazio 02

Greyscale with log levels
30 × 30kpc at z=0

Structure components

- Thick & thin disks
- Spiral arms (incl. molec. ring)
- Galactic center comp.
- Local ISM
- Individual clumps & voids

Propagation effects

- Dispersion measure
- Pulse/Angular broadening
- Scintillation bandwidth
- Emission measure

Distance estimates

- HI absorption
- Parallax (interfero. or timing)
- Associations w/ GC or SNR

Pulsar Distribution

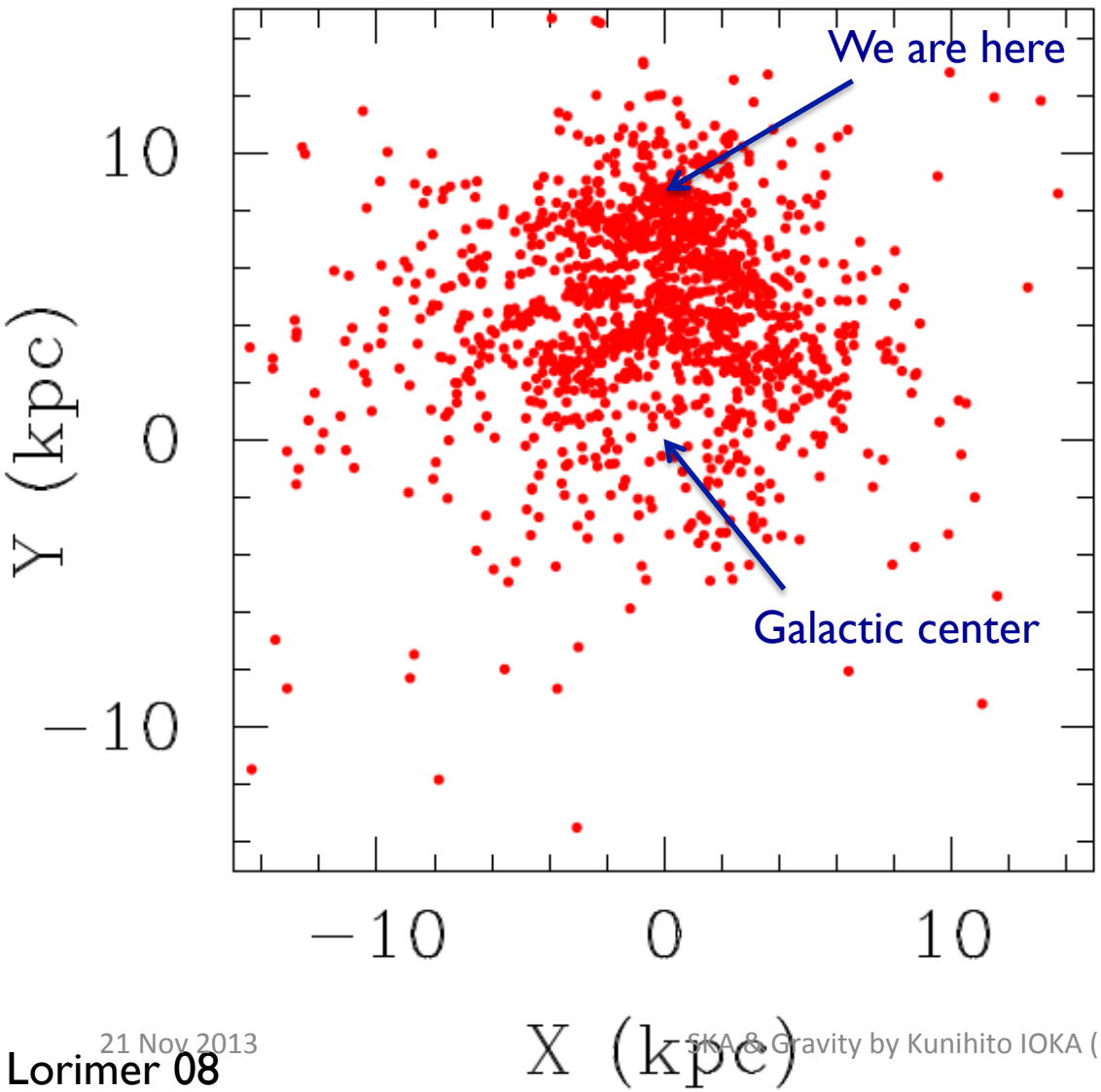

Lorimer 08

We know only nearby pulsars!

Pulsars in the Milky Way

~160,000 normal PSR

~40,000 MSP

160,000~10^7yr/60yr

[Life time/Birth time]

Observable pulsars

×Beaming 20%~30,000

SKA Pulsar Survey

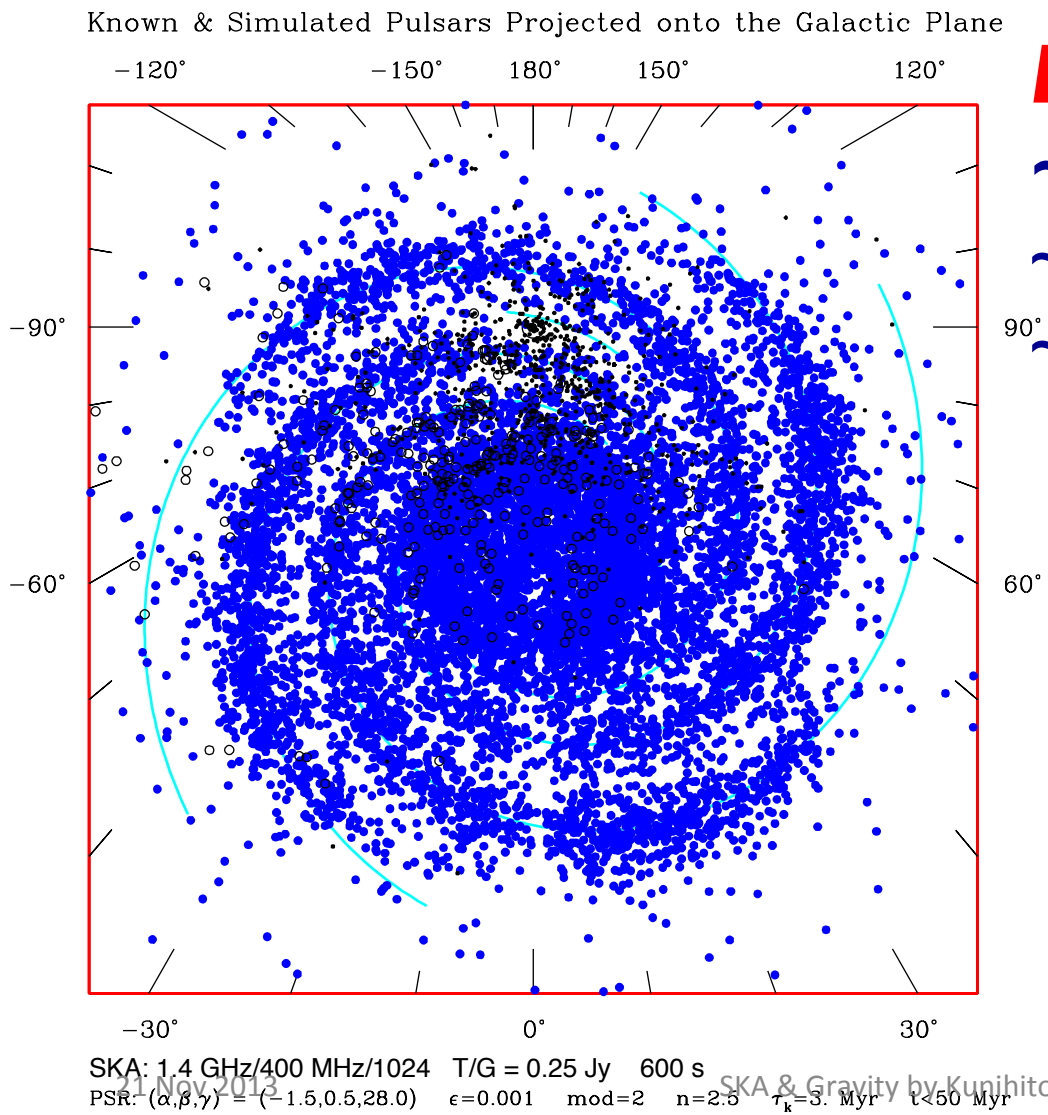

Finds all PSRs in MW

~30,000 normal PSR

~4,000 MSP [300/2200=14%]

~70 rela. NS^2 [5/2200=0.2%]

merging in Hubble time

Open circles: Parkes Multibeam PSR
Black dots: Princeton PSR Catalog
Blue dots: simulated SKA PSR
(400 MHz, 600 s, 1024 ch)
Assumed birth rate = 1 / (167 yr)
Distribute 30,000 PSR (w/ P, L, R, z)
Spectral index -1.6 ± 0.35
Sampling, dispersion smearing/scattering
No scintillation

Cordes+ 04, Kramer+ 04, Smits+ 08

SKA Sensitivity

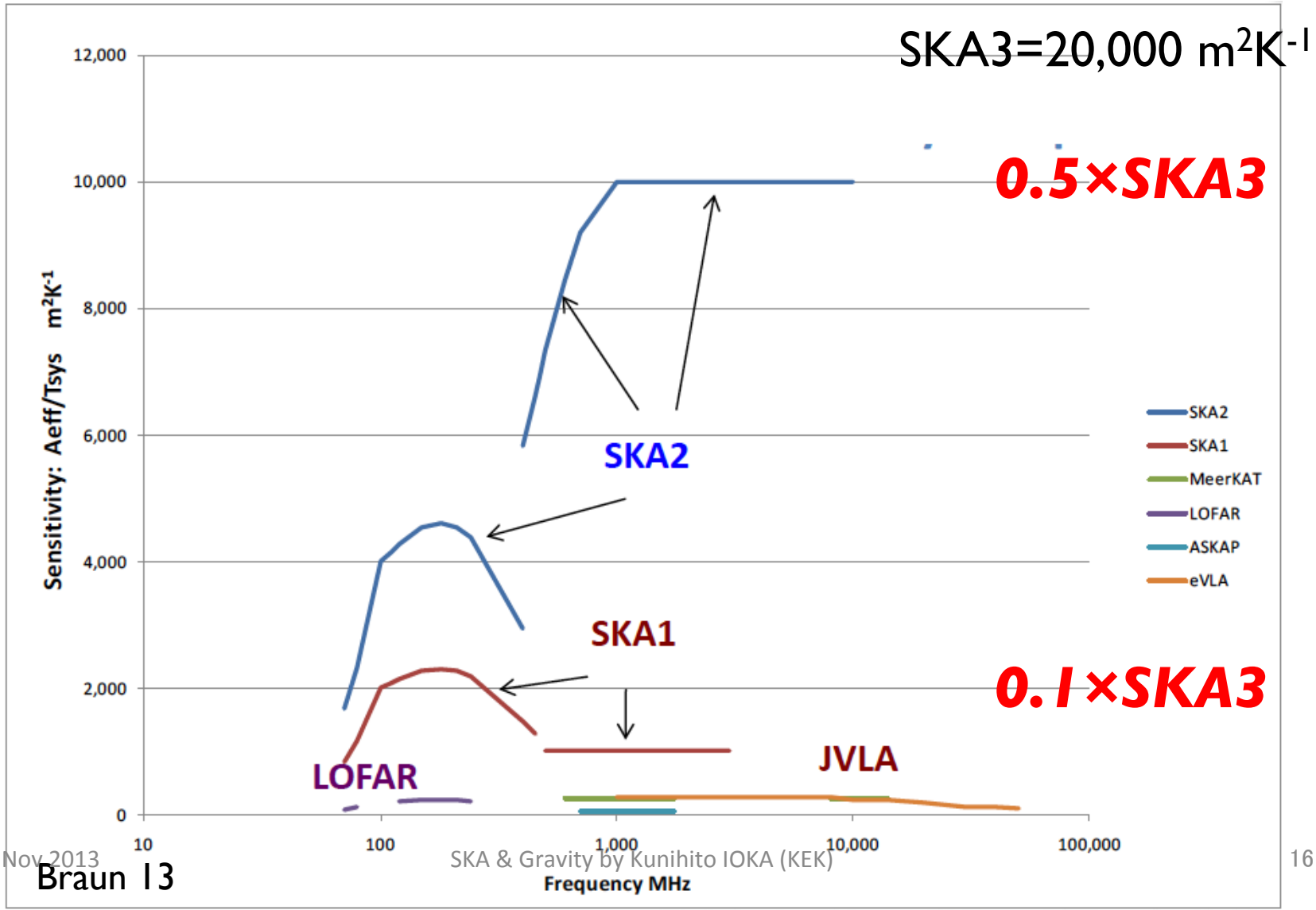

Braun 13

SKA Survey Speed

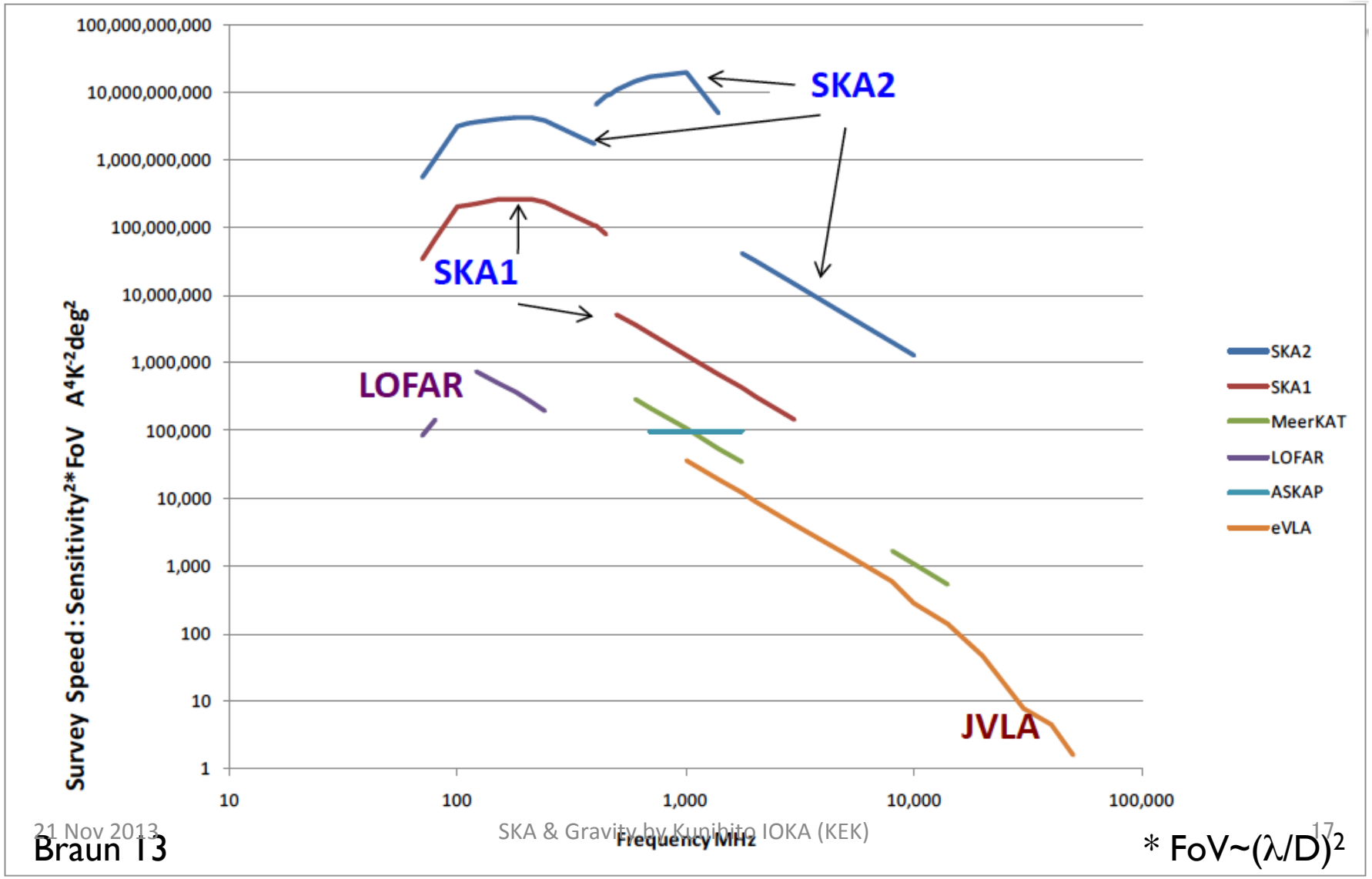

Braun 13

* FoV~$(\lambda/D)^2$

SKA1 & 2 Pulsar Survey

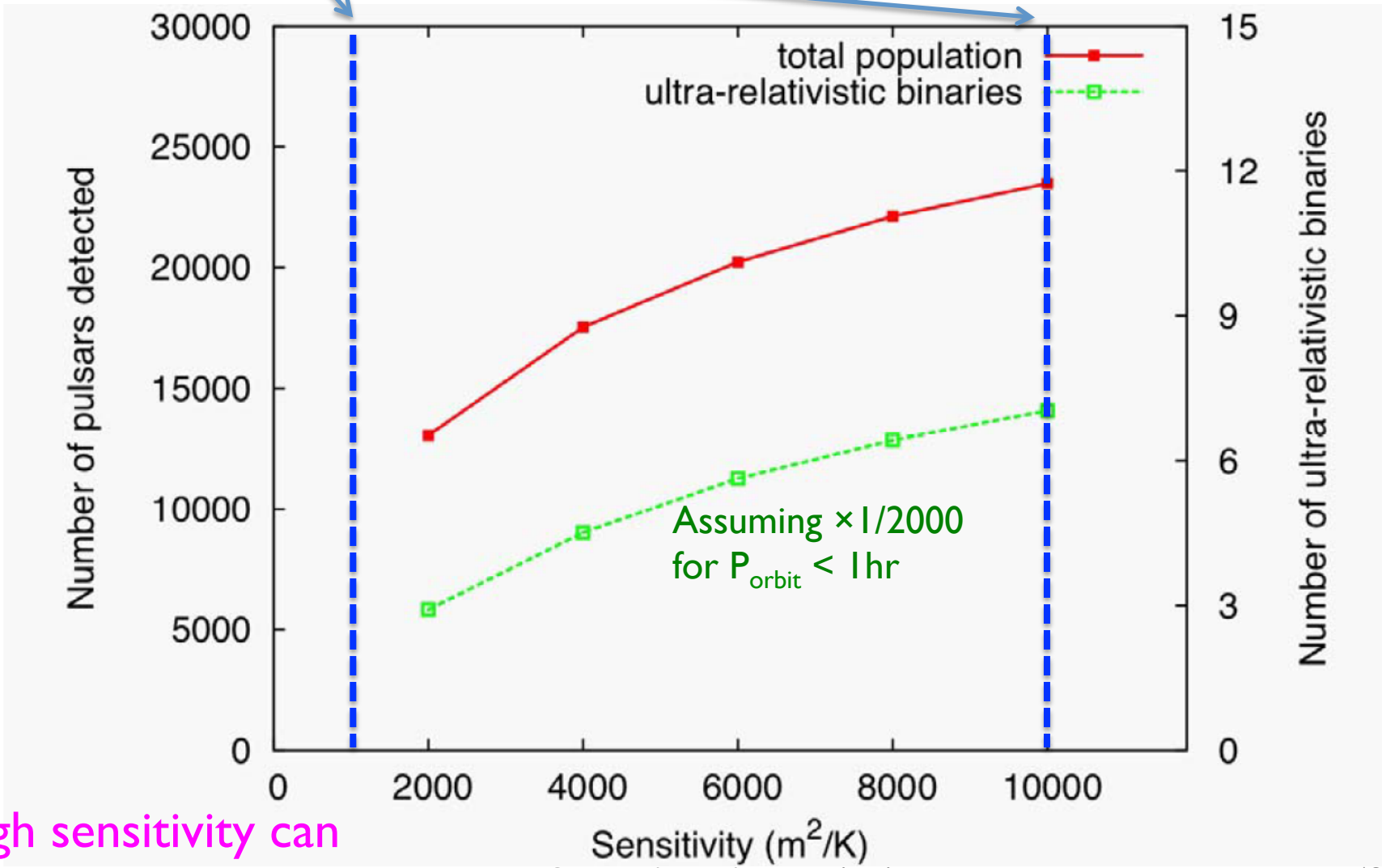

High sensitivity can probe P_{orbit}<1hr

Smits+ 09, SKA Design Reference Mission: SKA mid and SKA lo

Optimal Frequency

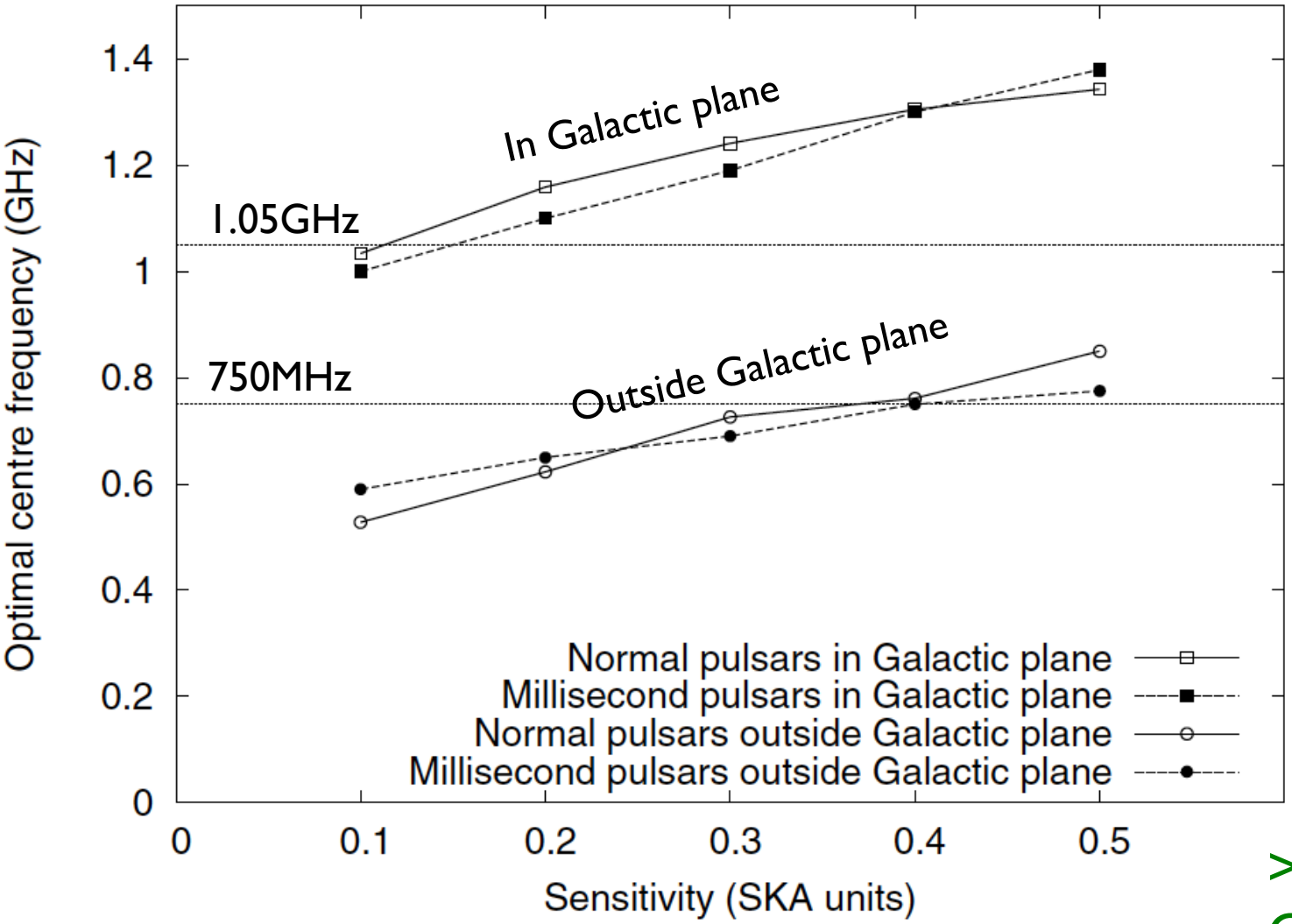

PSR spectra

$\propto \nu^{-1.6}$

⇒ Low freq.

Propagation

Dispersion ν^{-2}

Scattering ν^{-4}

⇒ High freq.

⇒ ~1GHz

>10GHz for the Galactic center?

Smits+ 09, SKA Design Reference Mission: SKA Phase 1

Pulse Scattering

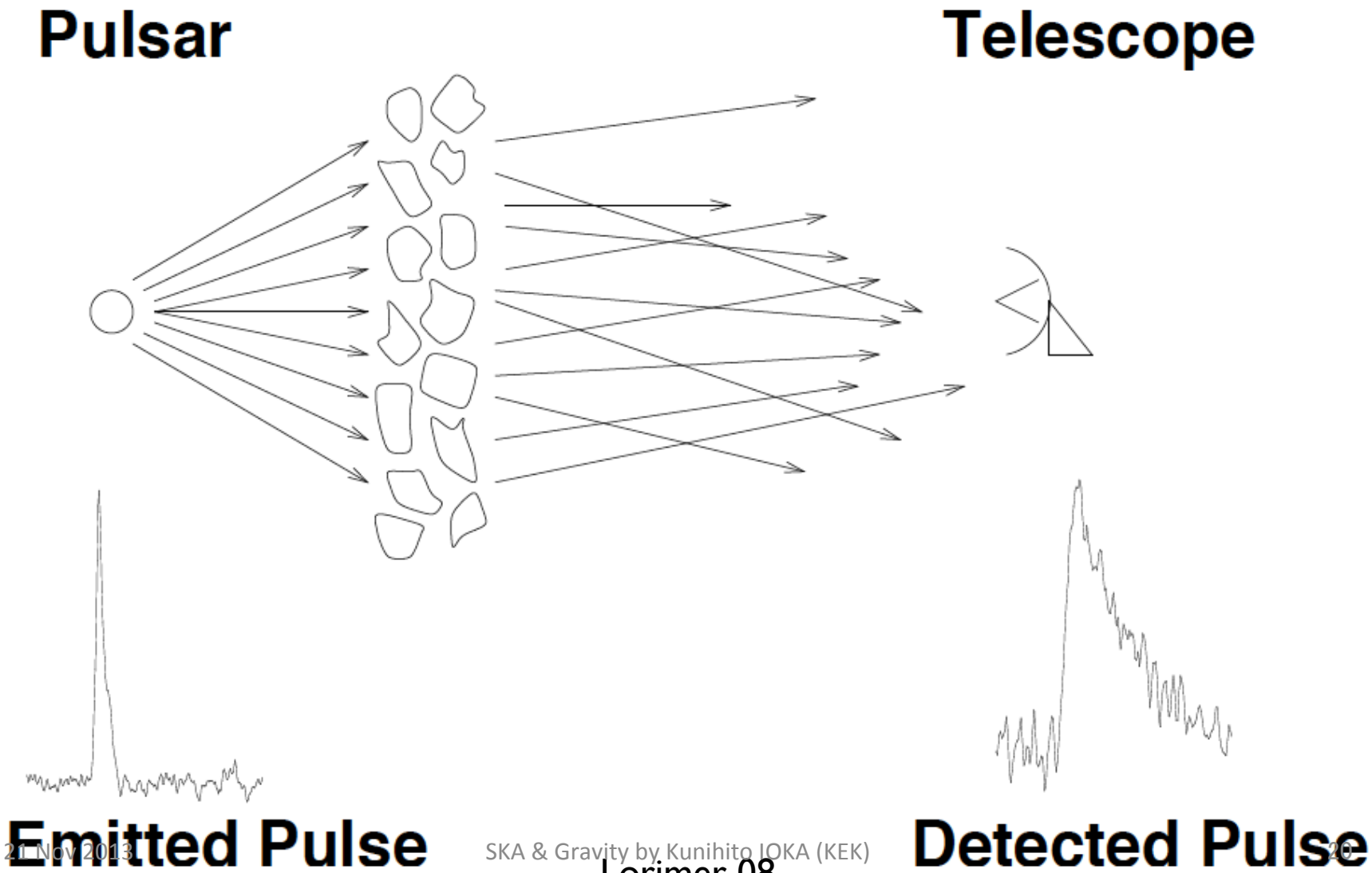

Lorimer 08

msec Pulsar Sky Distribution

Pulsar timing array: MSP

Gravity tests: Binary

Circle: Binary

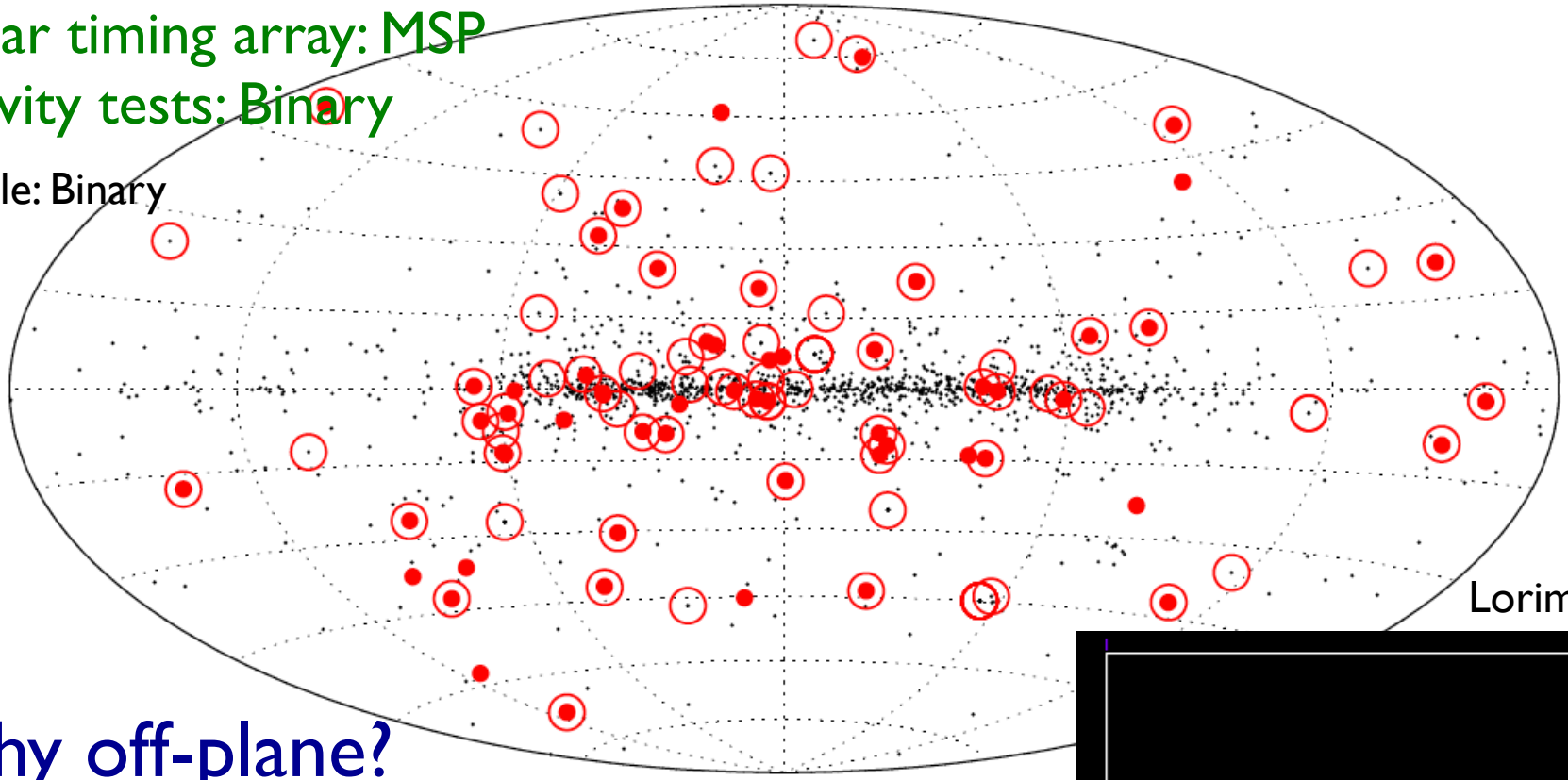

Lorimer 05

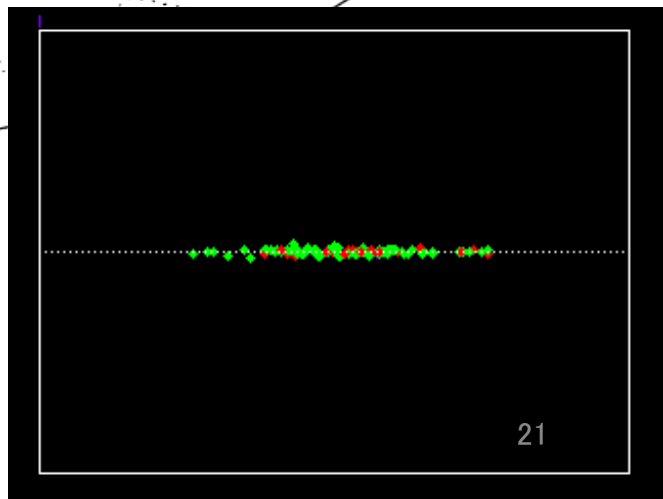

Why off-plane?

- Old age
- In globular cluster
- Nearby MSP

SKA Pulsar Timing

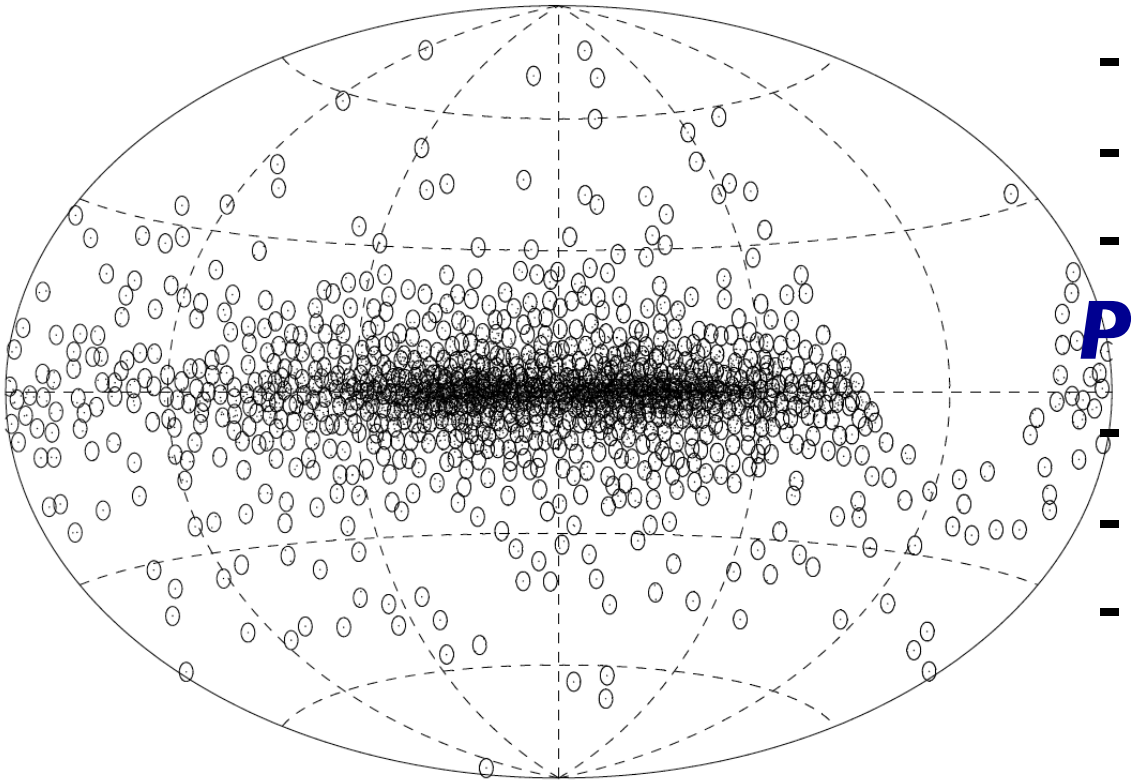

14,000 SKA1 pulsars
Circle: Optimized pointings (700) for timing with FoV of 20 deg2
Smits+ 09

Regular timing

- weekly for ~6 month
- SNR~9
- Optimized by grouping

Precise timing

- SNR>100
- Pulsar timing array: MSP
- Gravity tests: Binary

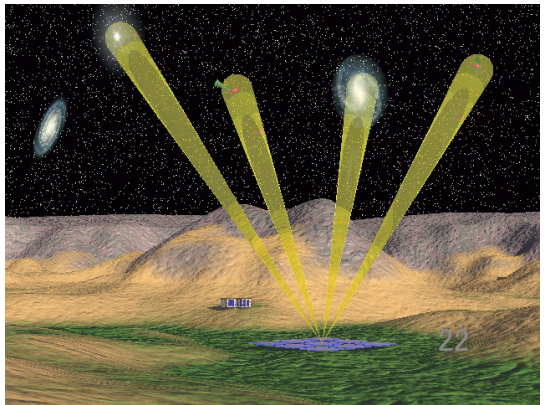

Pulsar Timing

Mean pulse profile

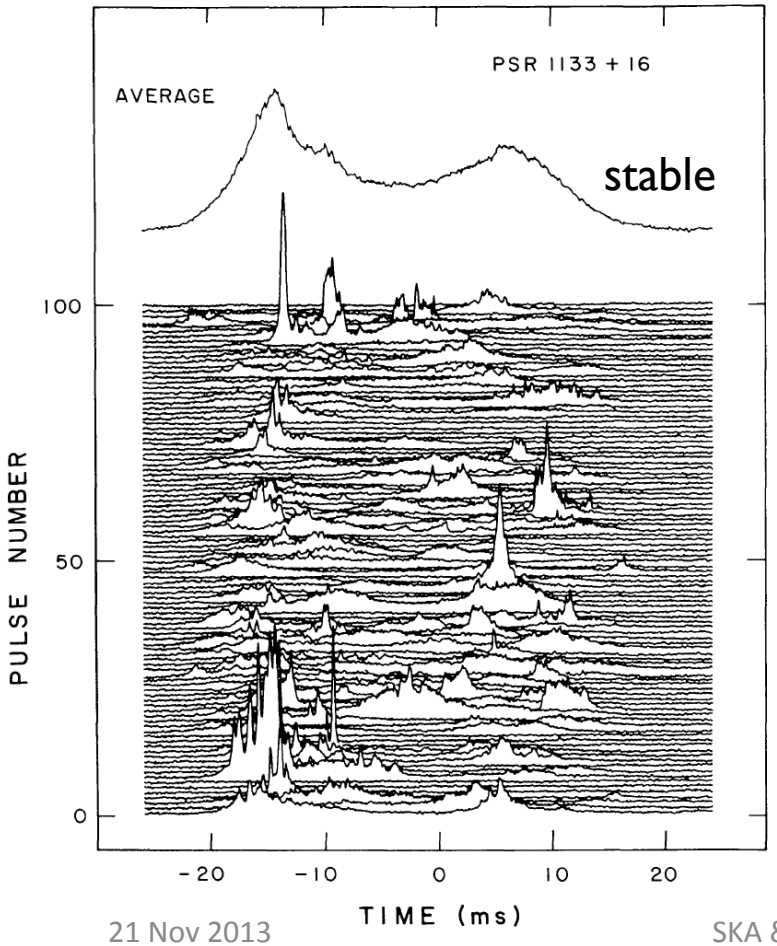

Time Of Arrival (TOA)

$$\phi(t) = \phi_0 + f(t - t_0) + \frac{1}{2}\dot{f}(t - t_0)^2 + \ldots$$

$$t = t_{\rm t} - t_{t_0} + \Delta_{\rm clock} - \Delta_{\rm DM} + \Delta_{\rm R\odot} + \Delta_{\rm E\odot} + \Delta_{\rm S\odot} + \Delta_{\rm R} + \Delta_{\rm E} + \Delta_{\rm S}$$

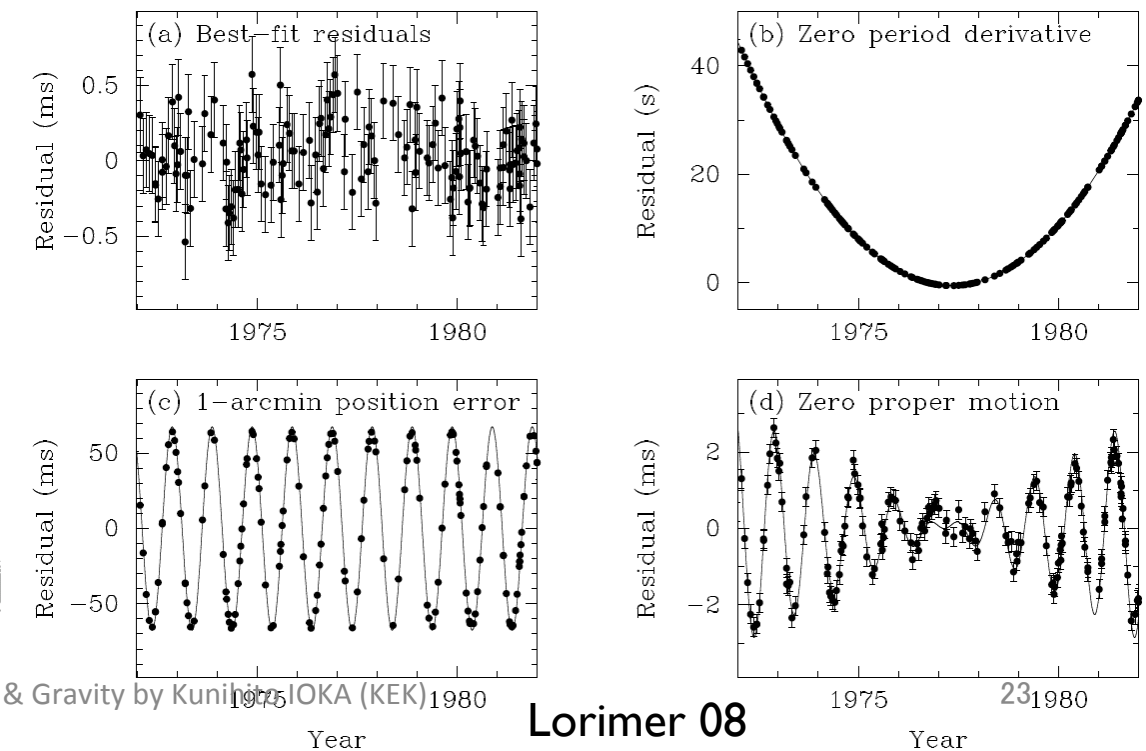

Lorimer 08

SKA Pulsar VLBI

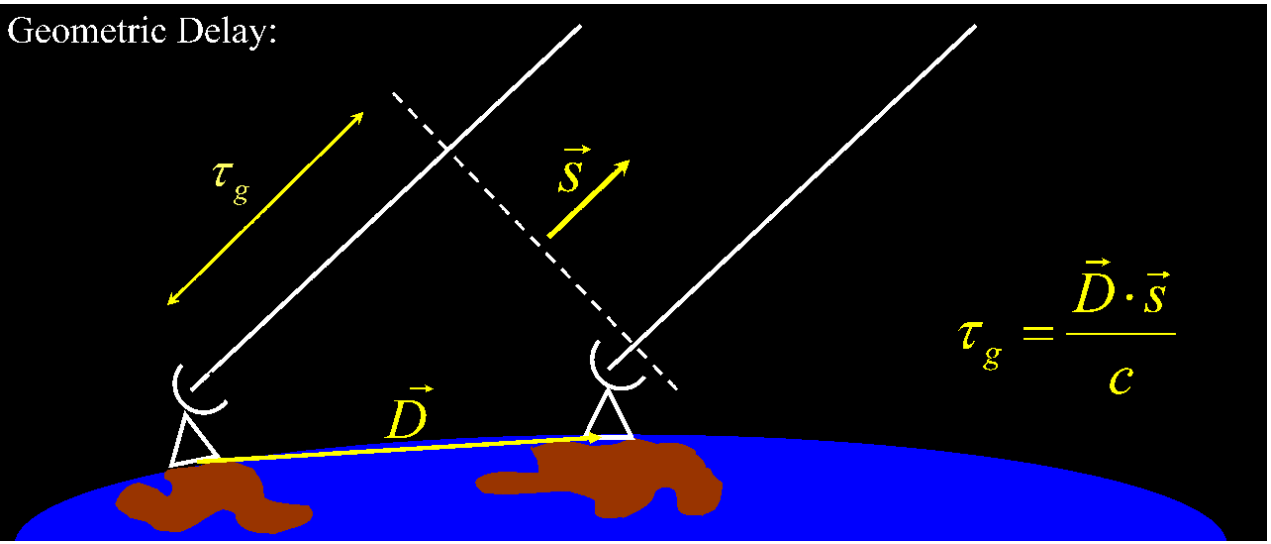

$$\Delta t \sim \frac{d\theta^2}{c}$$

$$\sim 0.02 \text{ ms } d_{10\,\mathrm{kpc}}\theta^2_{\mathrm{mas}}$$

Parallax (Distance) & Proper motion

1. Accurate timing
2. Formation site
3. Electron map
4. NS photosphere1 (EOS of NS)

$$\theta \sim \frac{\lambda}{b}\frac{1}{\mathrm{SNR}} \sim 3 \text{ mas } \frac{\lambda_{GHz}}{b_{200\,km}}\frac{100}{SNR}$$

Survey, Timing & VLBI

Pulsar Science with SKA

- Extreme dense matter physics
- Relativistic plasma physics
- Galactic probe
- Extragalactic pulsars
- “Holy grail” pulsars
- Gravitational physics

Pulsar Science with SKA

- ***Extreme dense matter physics***
- Relativistic plasma physics
- Galactic probe
- Extragalactic pulsars
- "Holy grail" pulsars
- Gravitational physics

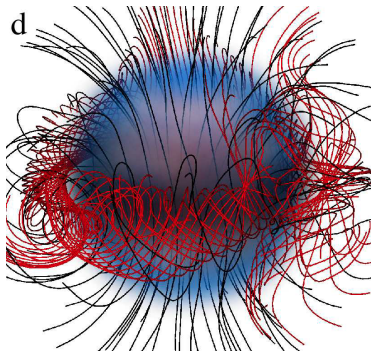

✓ Equation of State
✓ Super strong B
✓ Mass func. (⇒ Supernova)

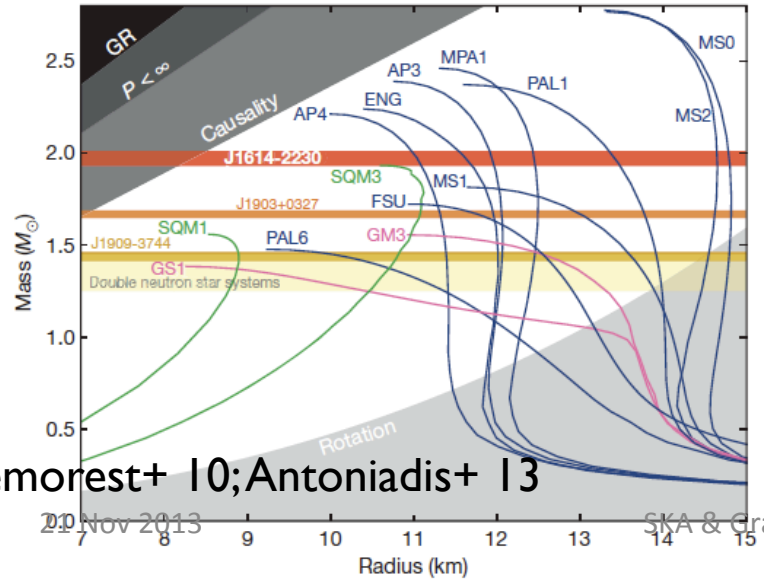

$2M_\odot$

TOV eq.

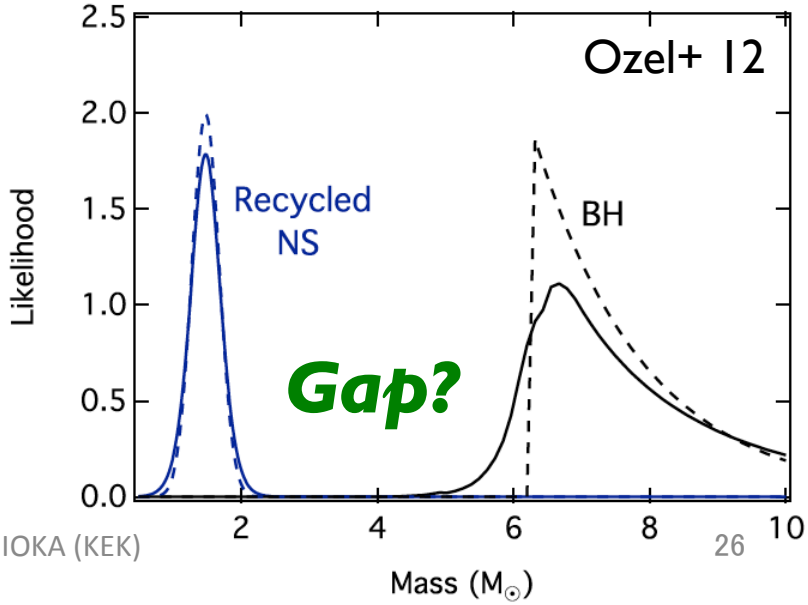

Demorest+ 10; Antoniadis+ 13

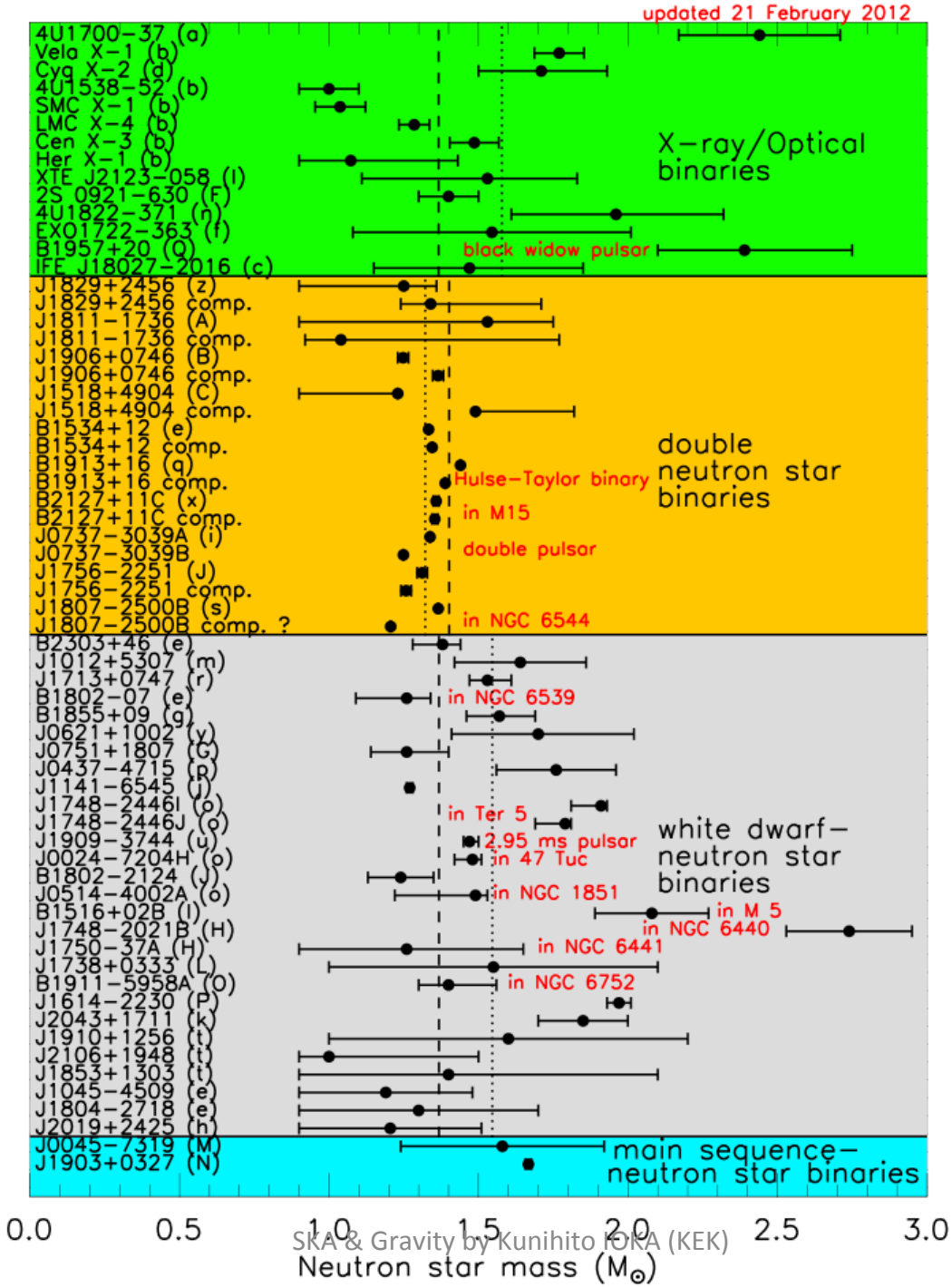
updated 21 February 2012
4U1700−37 (a)
Vela X−1 (b)
Cyg X−2 (d)
4U1538−52 (b)
SMC X−1 (b)
LMC X−4 (b)
Cen X−3 (b)
Her X−1 (b)
XTE J2123−058 (l)
2S 0921−630 (F)
4U1822−371 (n)
EXO1722−363 (f)
B1957+20 (Q)
IFE J18027−2016 (c)
black widow pulsar
X−ray/Optical binaries
J1829+2456 (z)
J1829+2456 comp.
J1811−1736 (A)
J1811−1736 comp.
J1906+0746 (B)
J1906+0746 comp.
J1518+4904 (C)
J1518+4904 comp.
B1534+12 (e)
B1534+12 comp.
B1913+16 (q)
B1913+16 comp.
Hulse−Taylor binary
B2127+11C (x)
B2127+11C comp.
in M15
J0737−3039A (i)
J0737−3039B
double pulsar
J1756−2251 (J)
J1756−2251 comp.
J1807−2500B (s)
J1807−2500B comp. ?
in NGC 6544
double neutron star binaries
B2303+46 (e)
J1012+5307 (m)
J1713+0747 (r)
B1802−07 (e)
in NGC 6539
B1855+09 (g)
J0621+1002 (y)
J0751+1807 (G)
J0437−4715 (R)
J1141−6545 (j)
J1748−2446I (o)
J1748−2446J (o)
in Ter 5
J1909−3744 (u)
2.95 ms pulsar
J0024−7204H (o)
in 47 Tuc
B1802−2124 (J)
J0514−4002A (o)
in NGC 1851
B1516+02B (I)
in M 5
J1748−2021B (H)
in NGC 6440
J1750−37A (H)
in NGC 6441
J1738+0333 (L)
B1911−5958A (O)
in NGC 6752
J1614−2230 (P)
J2043+1711 (k)
J1910+1256 (t)
J2106+1948 (t)
J1853+1303 (t)
J1045−4509 (e)
J1804−2718 (e)
J2019+2425 (h)
white dwarf−neutron star binaries
J0045−7319 (M)
J1903+0327 (N)
main sequence−neutron star binaries
0.0
0.5
1.0
1.5
2.0
2.5
3.0
Neutron star mass (M⊙)

Lattimer

Pulsar Science with SKA

- Extreme dense matter physics
- ***Relativistic plasma physics***
- Galactic
- Extragala
- "Holy gr
- Gravitati

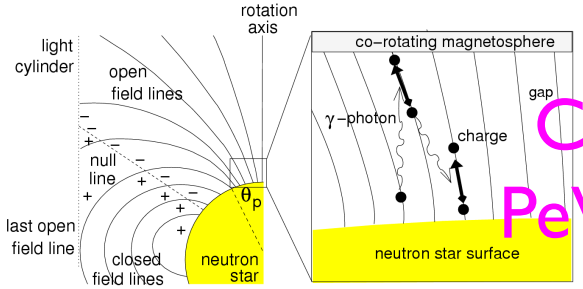

Cosmic PeVatron?

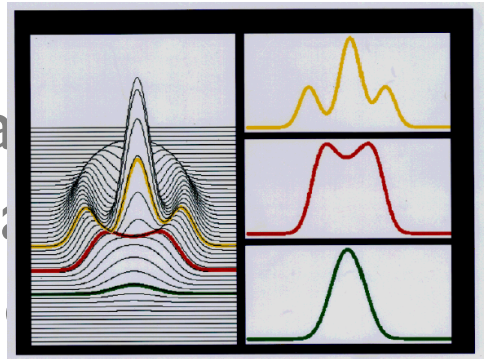

- ✓ Radio coherent emission
- ✓ High-energy emission
- ✓ Positron cosmic-ray

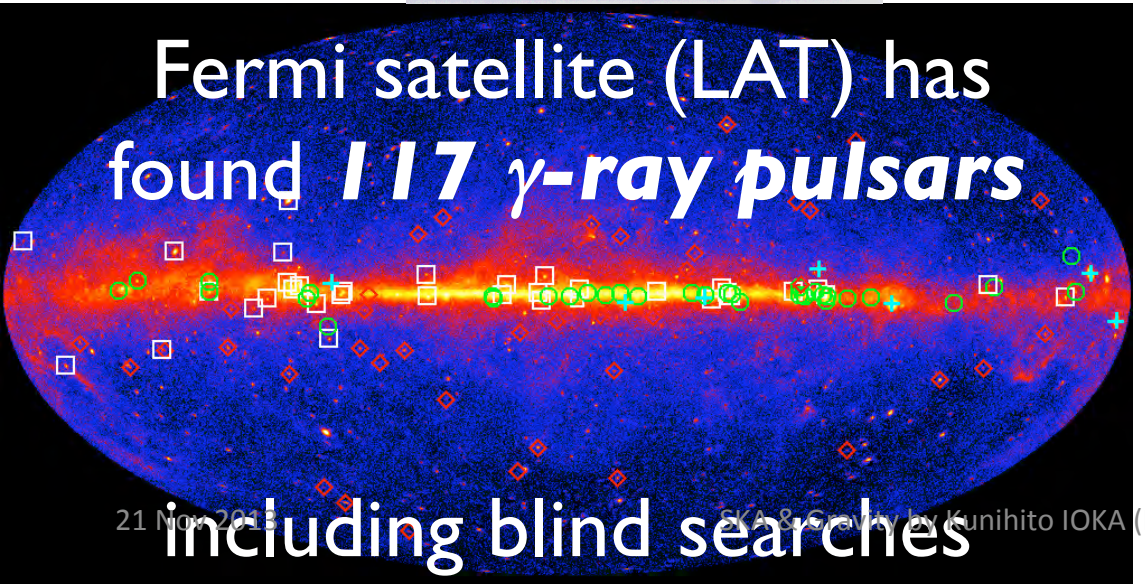

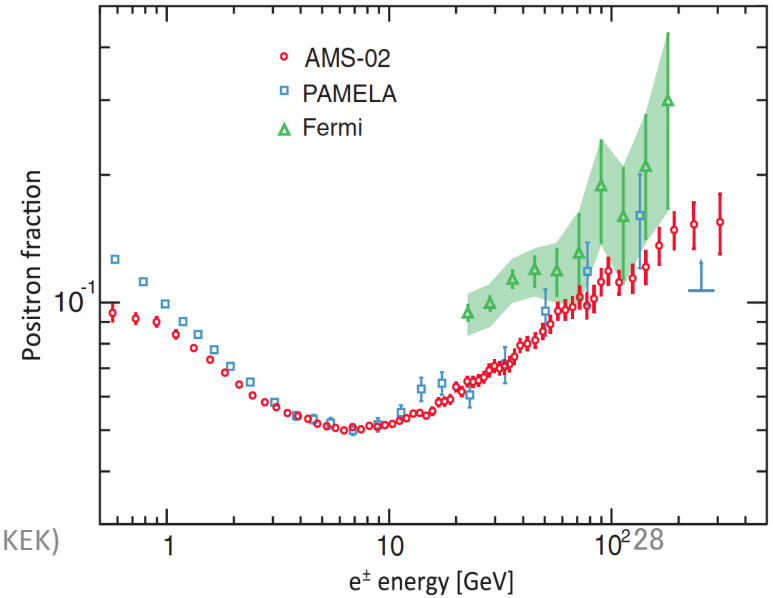

Pulsar Science with SKA

- Extreme dense matter physics
- Relativistic plasma physics
- ***Galactic probe***
- Extragalactic pulsars
- "Holy grail" pulsars
- Gravitational physics

✓ Interstellar e/B
✓ Star formation history
✓ Dynamics

Han+ 12

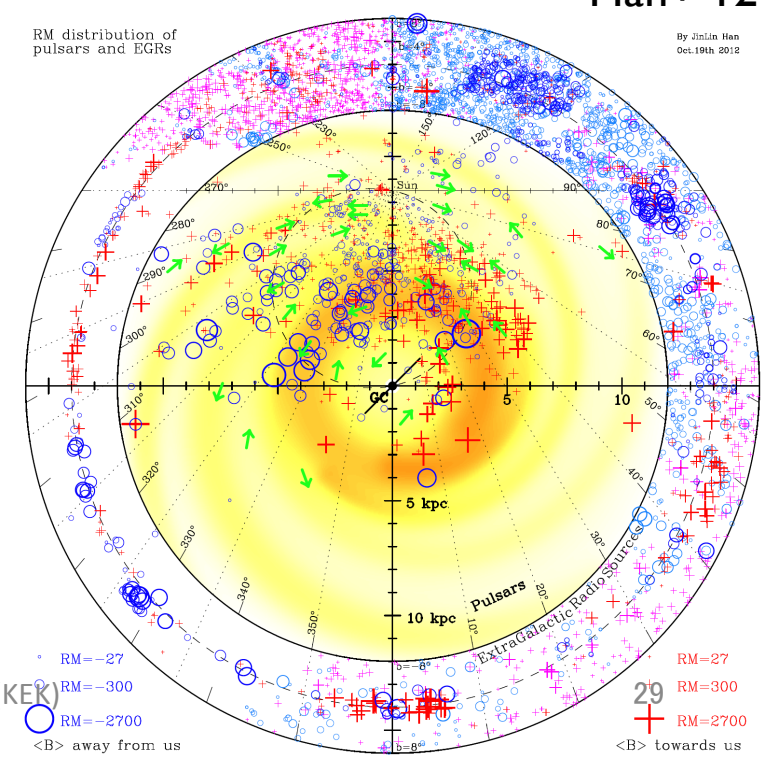

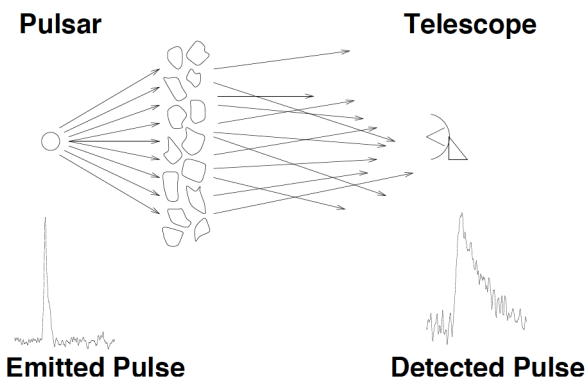

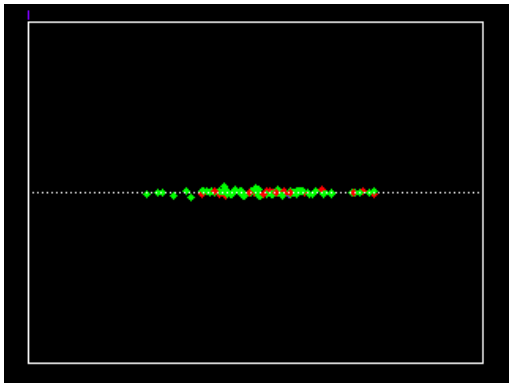

Pulsar Science with SKA

- Extreme dense matter physics
- Relativistic plasma physics
- Galactic probe
- ***Extragalactic pulsars***
- "Holy grail" pulsars
- Gravitational physics

✓ Formation & Population
✓ Turbulent magnetized IGM
✓ Missing baryon
✓ Dark Energy

KI 03
Kashiyama+ 13

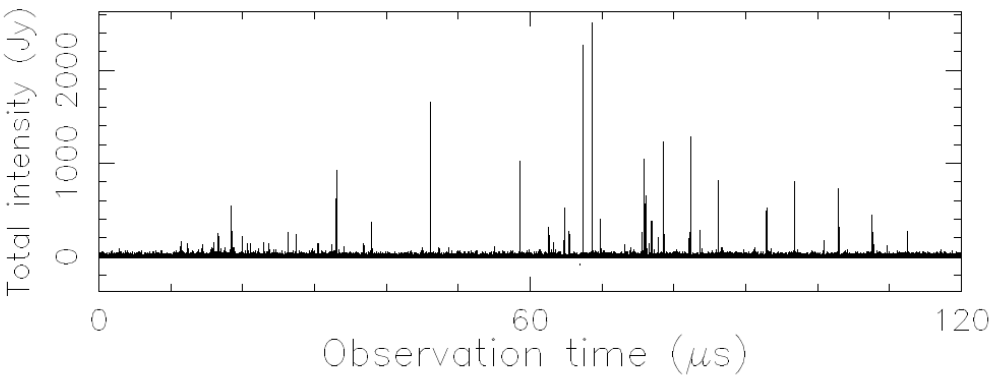

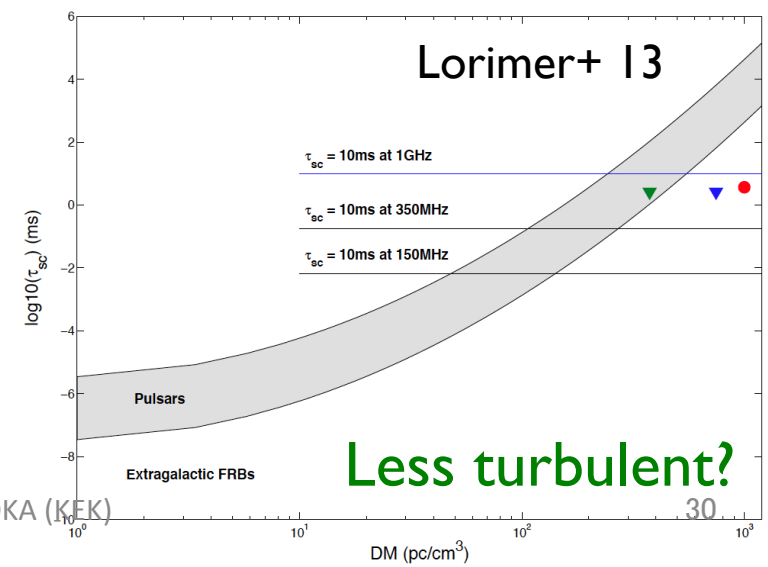

Less turbulent?

Giant pulse: $T_{bright} \sim 10^{35}$K

Fast radio burst: $T_{bright} > 10^{41}$K

Pulsar Science with SKA

- Extreme dense matter physics
- Relativistic plasma physics
- Galactic probe
- Extragalactic pulsars
- ***"Holy grail" pulsars***
- Gravitational physics

✓ Millisecond pulsars
✓ Relativistic binaries
✓ Double pulsars
✓ PSR-BH, PSR-Sgr A*
✓ Planet

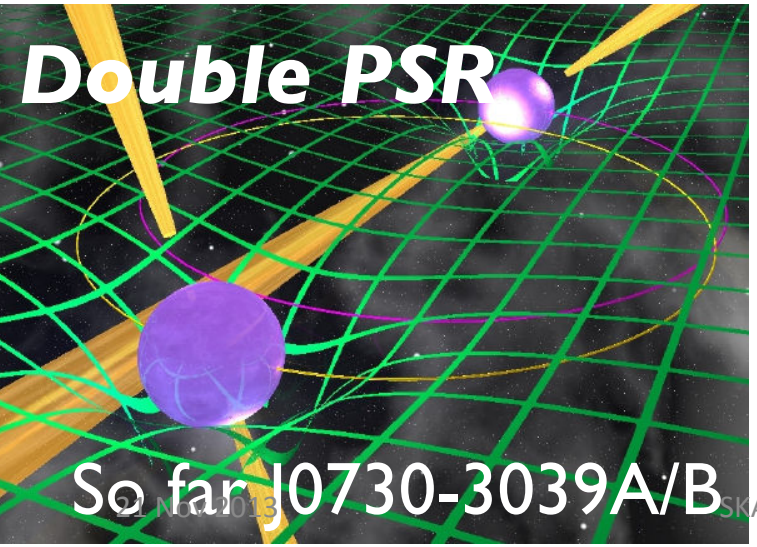

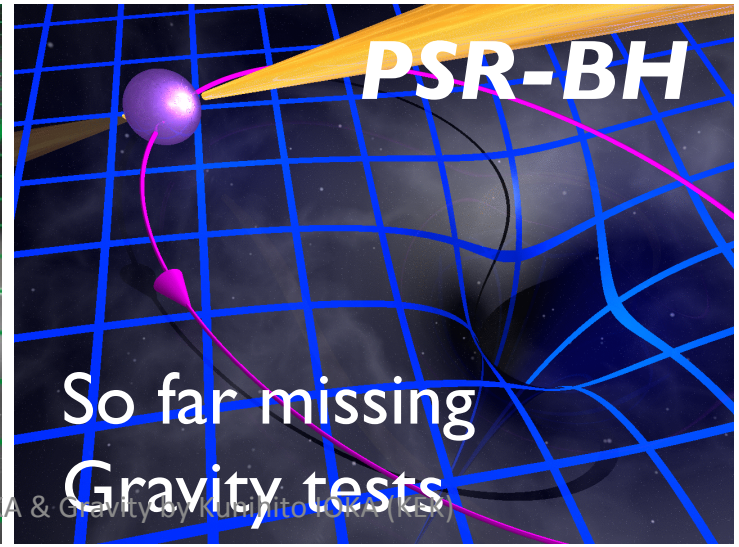

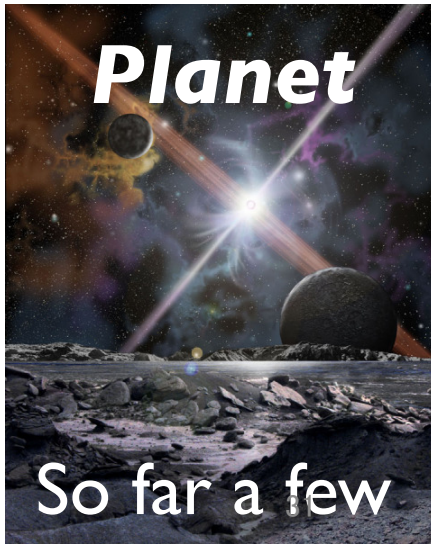

Pulsar Science with SKA

- Extreme dense matter physics
- Relativistic plasma physics
- Galactic probe
- Extragalactic pulsars
- "Holy grail" pulsars
- ***Gravitational physics***

✓ Tests of gravity
✓ Gravitational waves

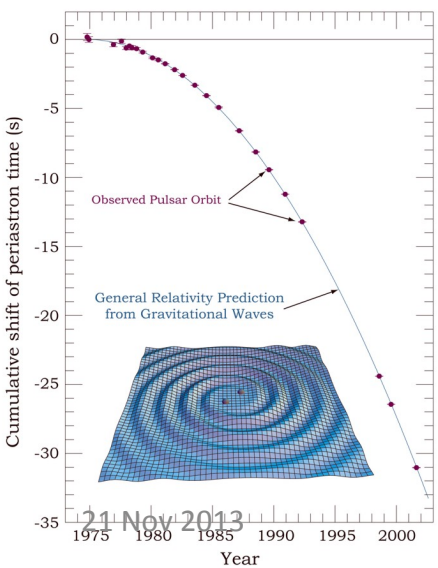

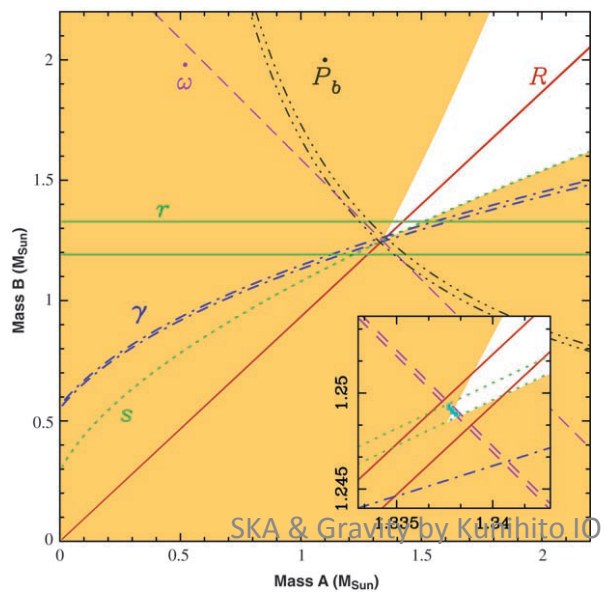

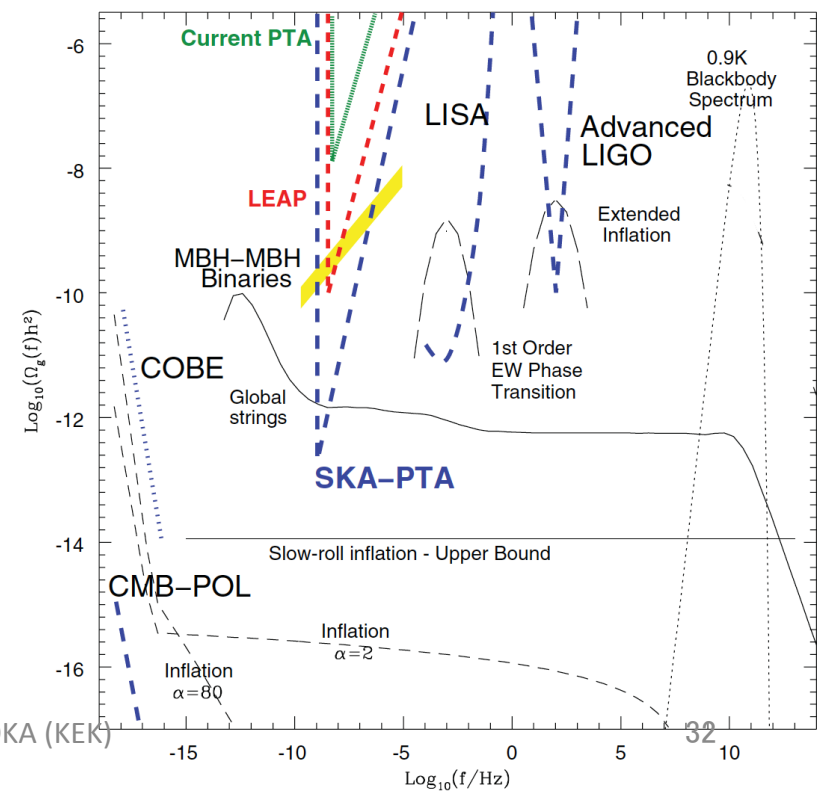

Outline

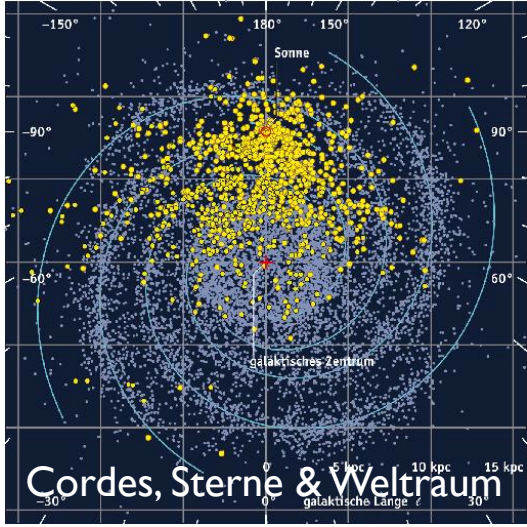

- Pulsar
  - Finding all pulsars in the Milky Way
  - Super dense matter physics, etc.
- Strong-field tests of gravity
- Gravitational wave astronomy
  - Complementary to AdvLIGO, KAGRA, eLISA, DECIGO, CMB-pol, LiteBIRD

Pulsars to Probe Gravity

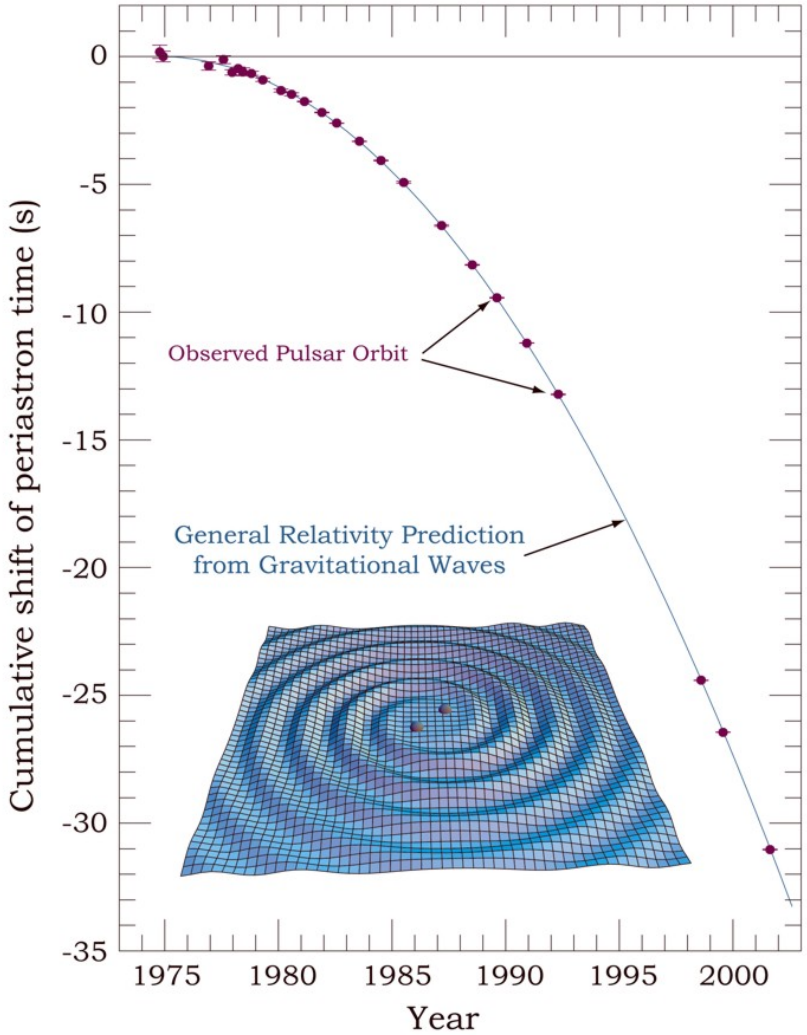

Binary PSR B1913+16

Orbit decay as predicted by General Relativity

First evidence of gravitational wave

Indirect detection

R. Hulse
J. Taylor
Arecibo in 74-75
Nobel prize1993

Hulse-Taylor Binary

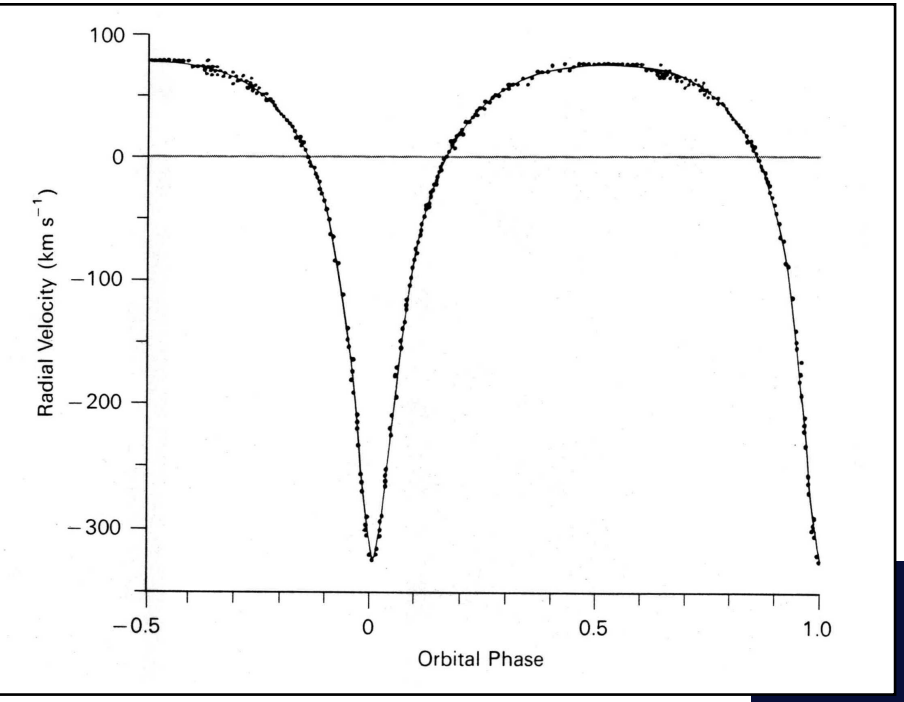

PSR B1913+16

We observe pulse TOA

⇒ Keplerian parameters except for M_p & M_c

P_b=7hr 45min

e=0.617

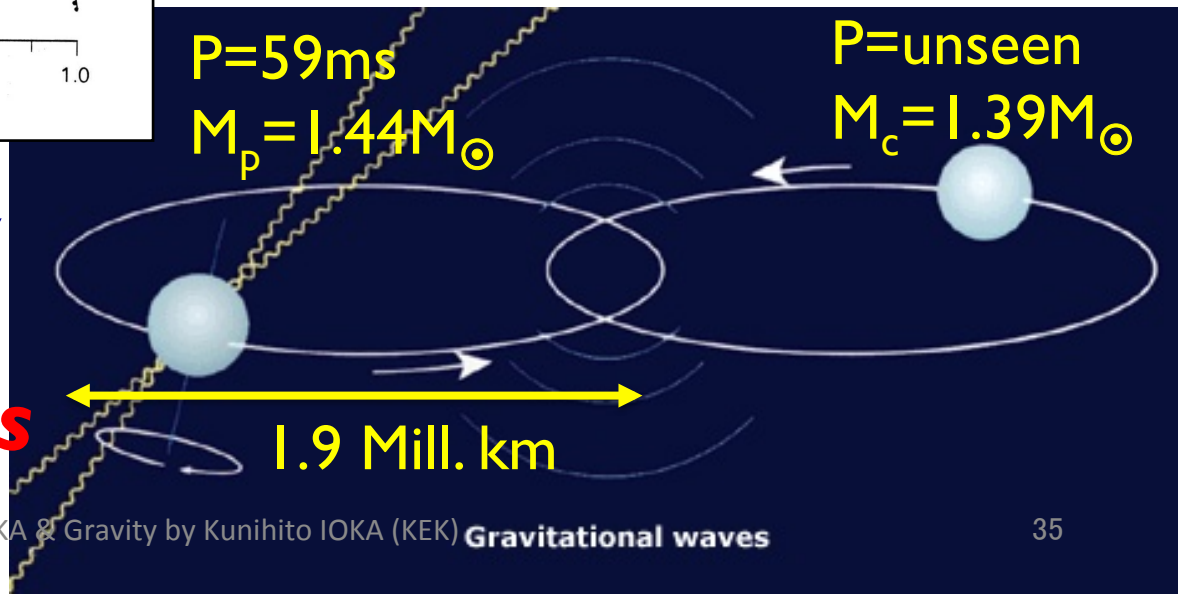

Max orbital velocity ~ 0.1% × c

Relativistic effects detectable!

Post-Keplerian

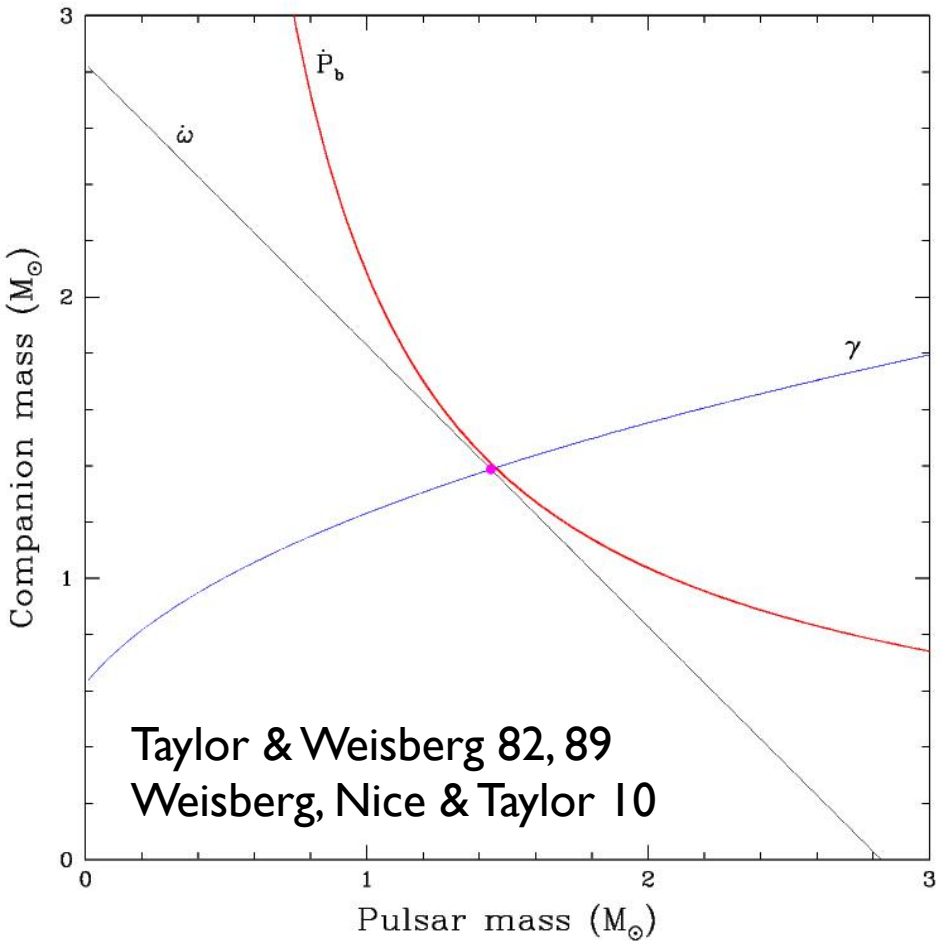

Taylor & Weisberg 82, 89
Weisberg, Nice & Taylor 10

M_p=1.4398±0.0002$M_\odot$
M_c=1.3886±0.0002$M_\odot$

Given Kepler orb. & GR

- Periastron advance

~4.2deg/yr

$$\dot{\omega} = 3\left(\frac{P_b}{2\pi}\right)^{-5/3}\left(\frac{GM_\odot}{c^3}M\right)^{2/3}(1-e^2)^{-1}$$

- Gravitational redshift + transverse Doppler

~4.3ms

$$\gamma = e\left(\frac{P_b}{2\pi}\right)^{1/3}\left(\frac{GM_\odot}{c^3}\right)^{2/3} M^{-4/3}\, m_2\,(m_1+2m_2)$$

- Orbital period decay

~-2.4e-12

$$\dot{P}_b = -\frac{192\pi}{5}\left(\frac{P_b}{2\pi}\right)^{-5/3}\left(1+\frac{73}{24}e^2+\frac{37}{96}e^4\right)(1-e^2)^{-7/2}\left(\frac{GM_\odot}{c^3}\right)^{5/3} m_1\, m_2\, M^{-1/3}$$

Orbital Decay

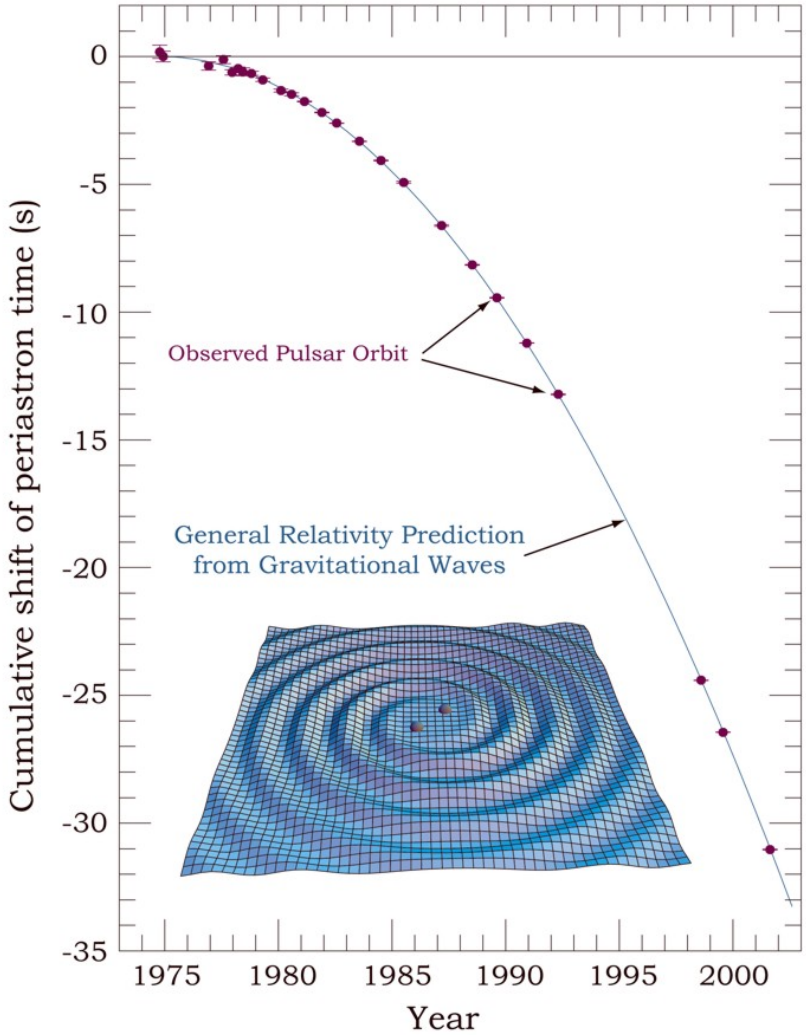

Binary PSR B1913+16

Test of General Rela.

~0.997±0.002

First evidence of gravitational wave

Orbit decay by ~1cm/day

Indirect detection

Taylor & Weisberg 82, 89
Weisberg, Nice & Taylor 10

Double Pulsar

PSR J0737-3039A/B

First double pulsar (by Parkes 03)

Most relativistic & Most constrained

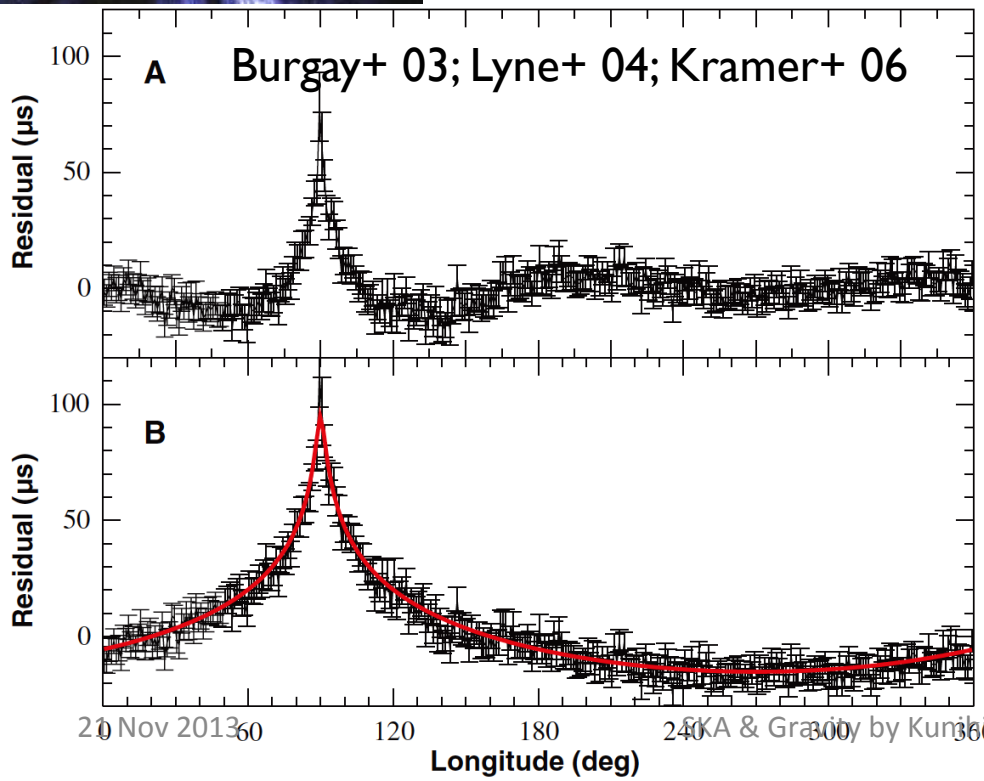

P_A=22ms, P_B=2.7s,

P_b=2.7hr

Periastron adv. 16.9deg/yr

Shapiro time delay

5 Post Keplerian parameters

GR Test ~0.05% level

Now ~0.02%

(non-GW test ≠ B1913+16 test)

Shapiro Time Delay

Irwin Shapiro 64

$$\Delta t \approx \int \frac{2GM}{c^3 r} ds$$

$$\approx \frac{2GM}{c^3} \ln\left(\frac{4 r_E r_p}{d^2}\right)$$

$$\frac{2GM_\odot}{c^3} = 10\mu s$$

$$r_E >> d,\ r_p >> d$$

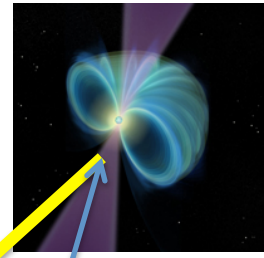

Orbital phase

Longitude of periastron

Binary pulsar case

$$\Delta t \approx \frac{2GM}{c^3} \ln\left(\frac{1 + e\cos\varphi}{1 - \sin i \sin(\omega + \varphi)}\right)$$

r s

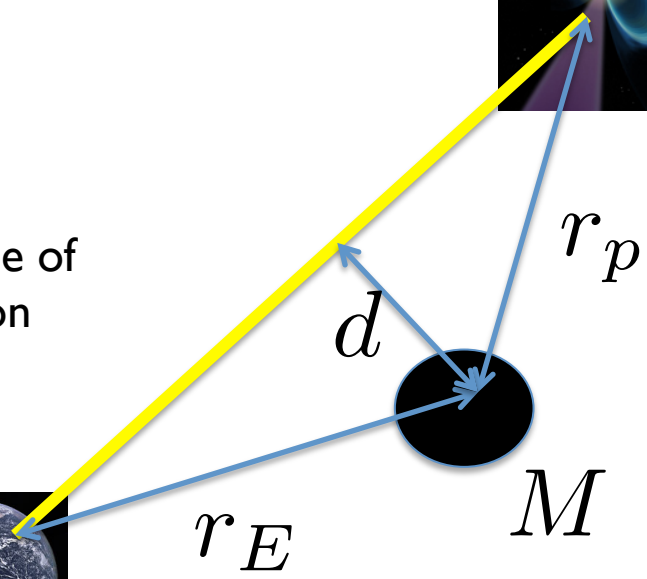

Double Pulsar: Test of GR

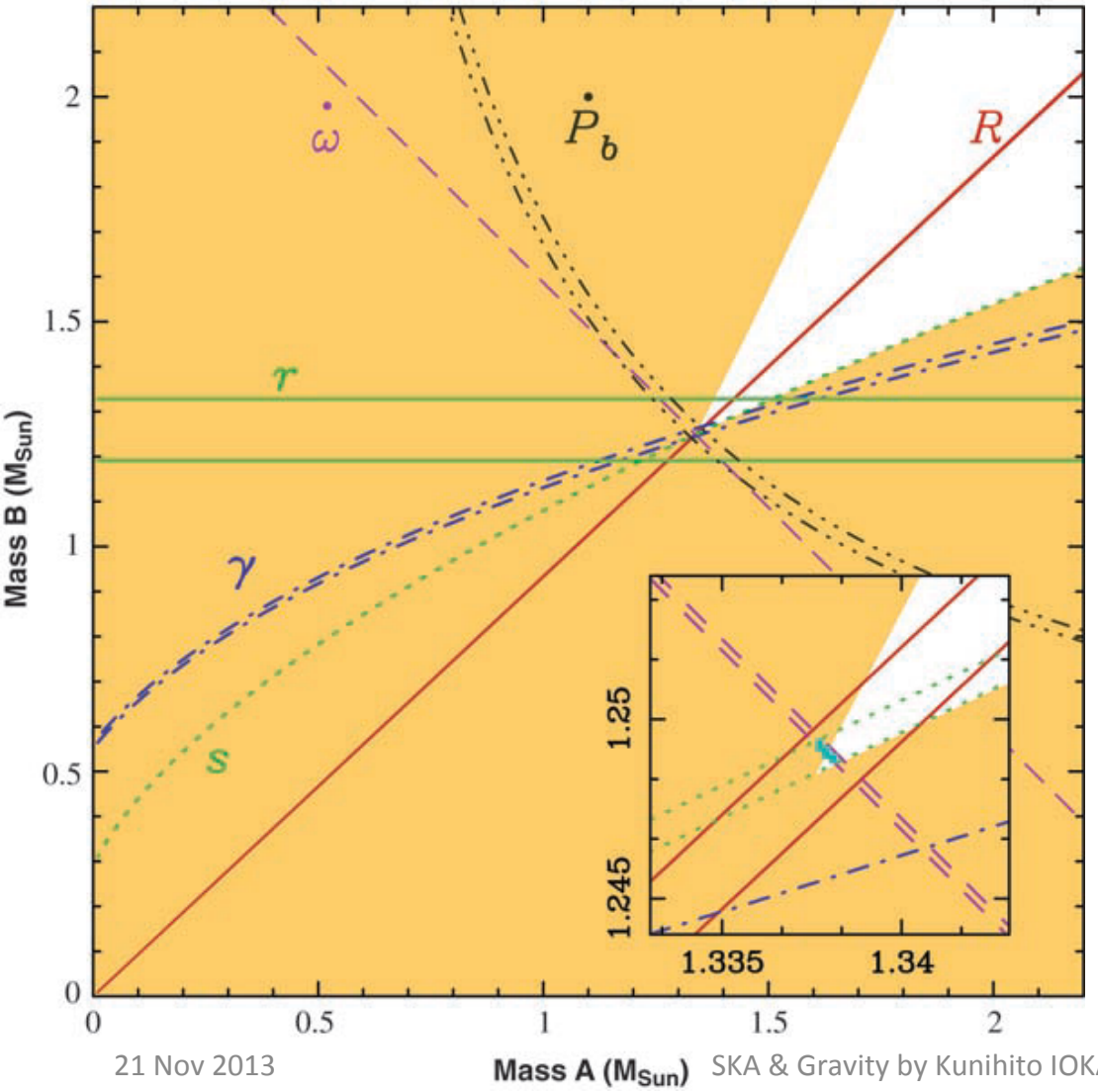

- Shapiro delay para. r

$$r = \left(\frac{GM_\odot}{c^3}\right) m_2$$

- Shapiro delay para. s

$$s = x\left(\frac{P_b}{2\pi}\right)^{-2/3}\left(\frac{GM_\odot}{c^3}\right)^{-1/3} M^{2/3}\, m_2^{-1}$$

- Mass ratio R

s = sin i=0.9997±0.0002

PSR B has disappeared by geodesic precession

2PN, e.g., spin-orbit?

Moment of inertia⇒EOS?

Table 1. Parameters for PSR J0737-3039A (A) and PSR J0737-3039B (B). The values were derived from pulse timing observations using the DD (*11*) and DDS (*19*) models of the timing analysis program Tempo and the Jet Propulsion Laboratory DE405 planetary ephemeris (*41*). Estimated uncertainties, given in parentheses after the values, refer to the least significant digit of the tabulated value and are twice the formal 1σ values given by Tempo. The positional parameters are in the DE405 reference frame, which is close to that of the International Celestial Reference System. Pulsar spin frequencies $\nu \equiv 1/P$ are in barycentric dynamical time (TDB) units at the timing epoch quoted in modified Julian days (MJD). The five Keplerian binary parameters (P_b, e, ω, T_0, and x) are derived for pulsar A. The first four of these (with an offset of 180° added to ω) and the position parameters were assumed when fitting for B's parameters. Five post-Keplerian parameters have now been measured. An independent fit of $\dot{\omega}$ for B yielded a value (shown in square brackets) that is consistent with the much more precise result for A. The value derived for A was adopted in the final analysis (*16*). The dispersion-based distance is based on a model for the interstellar electron density (*26*).

Timing parameter	PSR J0737-3039A	PSR J0737-3039B
Right ascension α	$07^h37^m51^s.24927(3)$	—
Declination δ	$-30°39'40''.7195(5)$	—
Proper motion in the RA direction (mas year^{-1})	−3.3(4)	—
Proper motion in declination (mas year^{-1})	2.6(5)	—
Parallax π (mas)	3(2)	—
Spin frequency ν (Hz)	44.054069392744(2)	0.36056035506(1)
Spin frequency derivative $\dot{\nu}$ (s^{-2})	$-3.4156(1) \times 10^{-15}$	$-0.116(1) \times 10^{-15}$
Timing epoch (MJD)	53,156.0	53,156.0
Dispersion measure DM (cm^{-3} pc)	48.920(5)	—
Orbital period P_b (day)	0.10225156248(5)	—
Eccentricity e	0.0877775(9)	—
Projected semimajor axis $x = (a/c)\sin i$ (s)	1.415032(1)	1.5161(16)
Longitude of periastron ω (°)	87.0331(8)	87.0331 + 180.0
Epoch of periastron T_0 (MJD)	53,155.9074280(2)	—
Advance of periastron $\dot{\omega}$ (°/year)	16.89947(68)	[16.96(5)]
Gravitational redshift parameter γ (ms)	0.3856(26)	—
Shapiro delay parameter s	0.99974(−39,+16)	—
Shapiro delay parameter r (μs)	6.21(33)	—
Orbital period derivative $\dot{P}_b$	$-1.252(17) \times 10^{-12}$	—
Timing data span (MJD)	52,760 to 53,736	52,760 to 53,736
Number of time offsets fitted	10	12
RMS timing residual σ (μs)	54	2169
Total proper motion (mas year^{-1})	4.2(4)	
Distance d(DM) (pc)	~500	
Distance $d(\pi)$ (pc)	200 to 1,000	
Transverse velocity (d = 500 pc) (km s^{-1})	10(1)	
Orbital inclination angle (°)	88.69(−76,+50)	
Mass function ($M_\odot$)	0.29096571(87)	0.3579(11)
Mass ratio R	1.0714(11)	
Total system mass ($M_\odot$)	2.58708(16)	
Neutron star mass ($m_\odot$)	1.3381(7)	1.2489(7)

$2M_\odot$ PSR - White Dwarf Binary

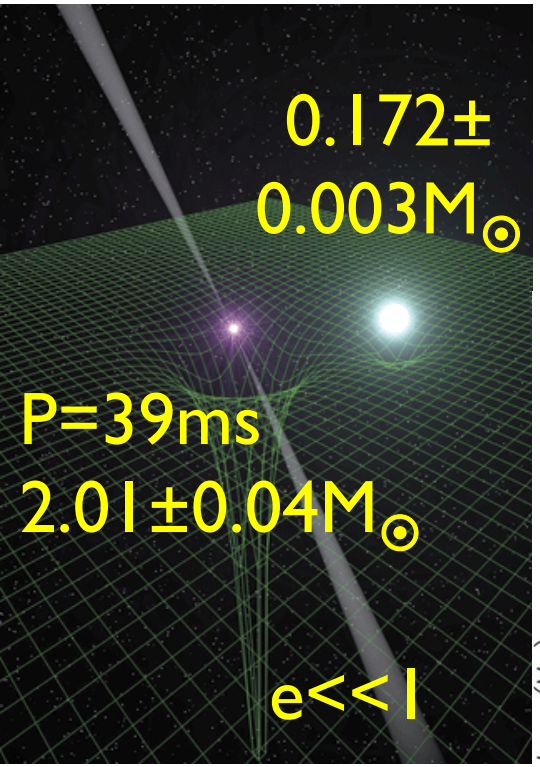

PSR J0348+0432

P_b=2.46hr

dP_b/dt=-(2.73±0.45)e-13

GR test @ 1.05±0.18

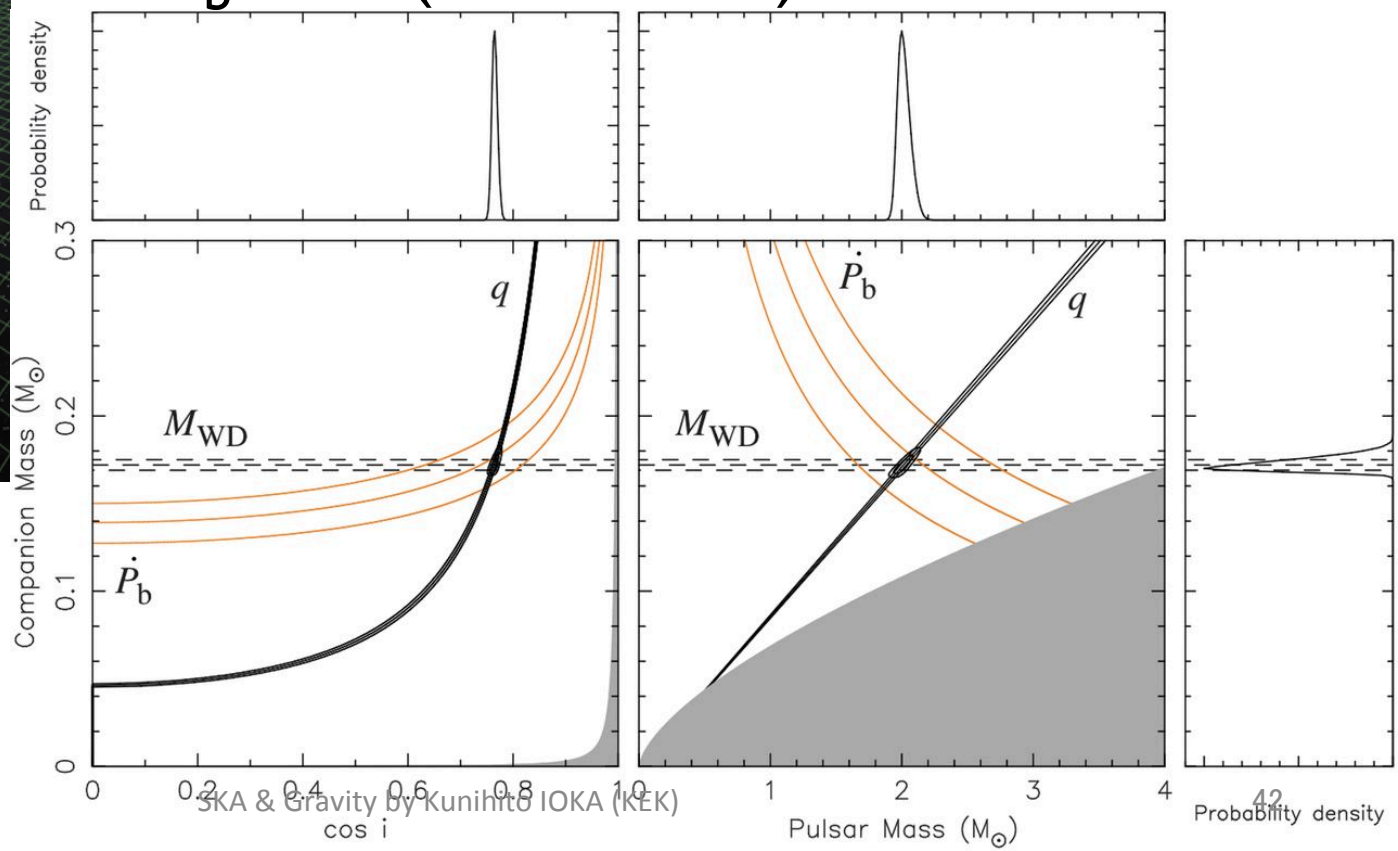

2nd $2M_\odot$ neutron star

Antoniadis+ 13
Demorest+ 10

Test Scalar-Tensor Theory

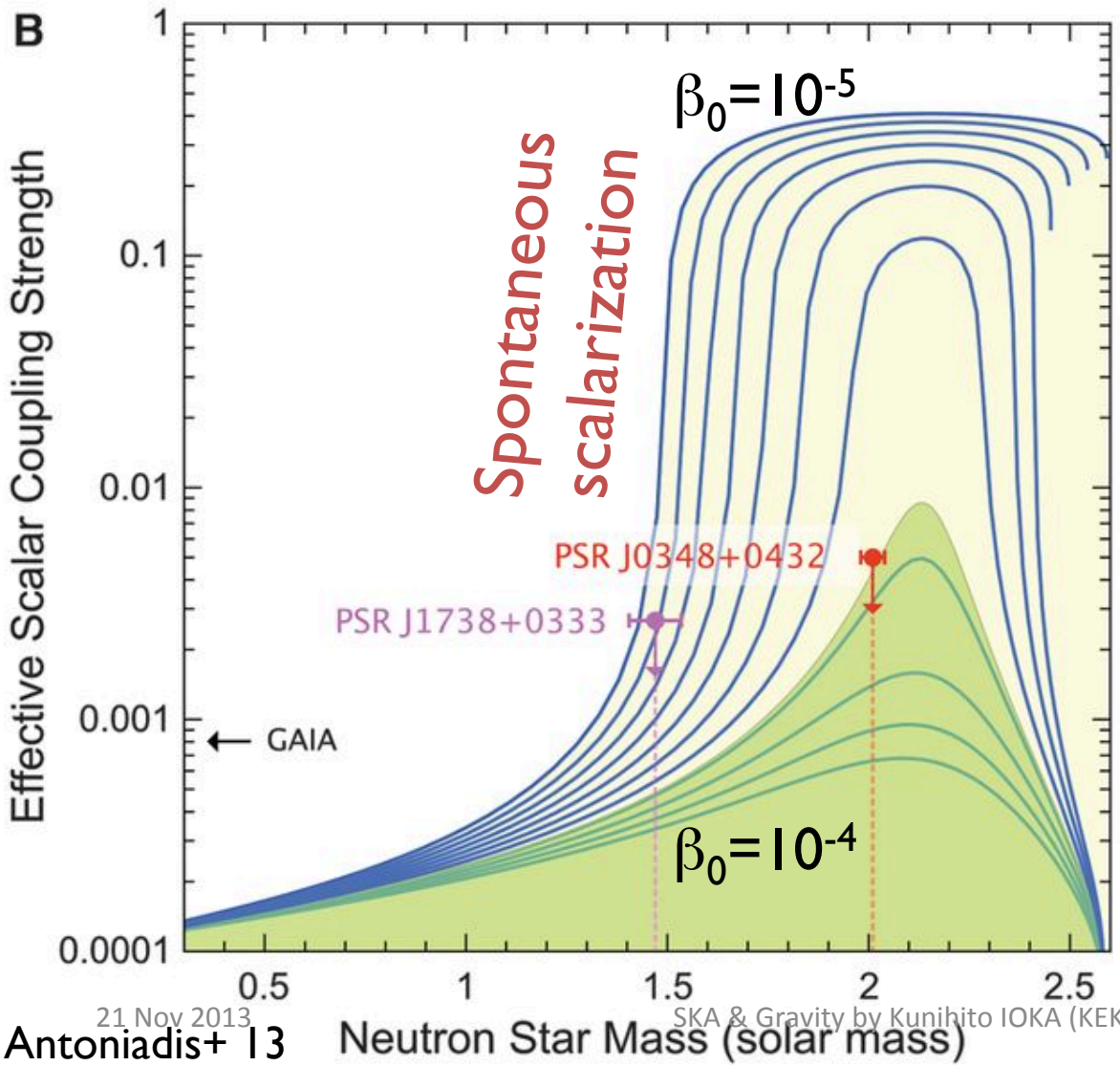

Antoniadis+ 13

Action

Damour+ 96

$$S=\frac{c^4}{16\pi G_*}\int\frac{d^4x}{c}g_*^{1/2}(R_*-2g_*^{\mu\nu}\partial_\mu\varphi\partial_\nu\varphi)$$
$$+S_m[\psi_m;\underline{A^2(\varphi)g^*_{\mu\nu}}].$$

physical metric

Coupling strength

$$\alpha(\varphi)\equiv\frac{\partial\ln A(\varphi)}{\partial\varphi}$$

$\alpha_0=10^{-4}$ here

$$\beta_0\equiv\frac{\partial^2\ln A(\varphi_0)}{\partial\varphi_0^2}$$

Dipole radiation

$$\dot{P}_b^{\rm dipolar}\simeq-\frac{4\pi^2G}{c^3P_b}\frac{M_{\rm PSR}M_{\rm WD}}{M_{\rm PSR}+M_{\rm WD}}(\underline{\alpha_{\rm PSR}-\alpha_{\rm WD}})^2$$

PSR-BH: WANTED

Table 1. Observed and derived parameters for the PSR J0348+0432 system. Timing parameters for the PSR J0348+0432 system, indicated with their 1-σ uncertainties as derived by tempo2 where appropriate (numbers in parentheses refer to errors on the last digits). The timing parameters are calculated for the reference epoch modified Julian date (MJD) 56000 and are derived from TOAs in the range MJD 54872 to 56208.

Optical parameters	
Effective temperature, T_{eff} (K)	$10120 \pm 47_{stat} \pm 90_{sys}$
Surface gravity, $\log_{10}[g(\mathrm{cm\ s^{-1}})]$	$6.035 \pm 0.032_{stat} \pm 0.060_{sys}$
Semiamplitude of orbital radial velocity, K_{WD} (km s^{-1})	351 ± 4
Systemic radial velocity relative to the Sun, γ (km s^{-1})	−1 ± 20
Timing parameters	
Right ascension, α (J2000)	$03^h\ 48^m\ 43^s.639000(4)$
Declination, δ (J2000)	+04° 32′ 11.″4580(2)
Proper motion in right ascension, μ_α (mas $year^{-1}$)	+4.04(16)
Proper motion in declination, μ_δ (mas $year^{-1}$)	+3.5(6)
Parallax, π_d (mas)	0.47*
Spin frequency, ν (Hz)	25.5606361937675(4)
First derivative of ν, $\dot{\nu}$ (10^{-15} Hz s^{-1})	−0.15729(3)
Dispersion measure, DM (cm^{-3} pc)	40.46313(11)
First derivative of DM, DM1 (cm^{-3} pc $year^{-1}$)	−0.00069(14)
Orbital period, P_b (day)	0.102424062722(7)
Time of ascending node, T_{asc} (MJD)	56000.084771047(11)
Projected semimajor axis of the pulsar orbit, x (lt-s)	0.14097938(7)
$\eta \equiv e\sin\omega$	$+1.9 \times 10^{-6} \pm 1.0 \times 10^{-6}$
$\kappa \equiv e\cos\omega$	$+1.4 \times 10^{-6} \pm 1.0 \times 10^{-6}$
First derivative of P_b, $\dot{P}_b$ (10^{-12} s s^{-1})	−0.273(45)
Derived parameters	
Galactic longitude, l	183.°3368
Galactic latitude, b	−36.°7736
Distance, d (kpc)	2.1(2)
Total proper motion, μ (mas $year^{-1}$)	5.3(4)
Spin period, P (ms)	39.1226569017806(5)
First derivative of P, $\dot{P}$ (10^{-18} s s^{-1})	0.24073(4)
Characteristic age, τ_c (Gy)	2.6
Transverse magnetic field at the poles, B_0 (10^9 G)	~2
Rate or rotational energy loss, $\dot{E}$ (10^{32} erg s^{-1})	~1.6
Mass function, f ($M_\odot$)	0.000286778(4)
Mass ratio, $q \equiv M_{PSR}/M_{WD}$	11.70(13)
White dwarf mass, M_{WD} ($M_\odot$)	0.172(3)
Pulsar mass, M_{PSR} ($M_\odot$)	2.01(4)
"Range" parameter of Shapiro delay, r (μs)	0.84718*
"Shape" parameter of Shapiro delay, $s \equiv \sin i$	0.64546*
White dwarf radius, R_{WD} ($R_\odot$)	0.065(5)
Orbital separation, a (10^9 m)	0.832
Orbital separation, a ($R_\odot$)	1.20
Orbital inclination, i	40.°2(6)
$\dot{P}_b$ predicted by GR, $\dot{P}_b^{GR}$ (10^{-12} s s^{-1})	$-0.258^{+0.008}_{-0.011}$
$\dot{P}_b/\dot{P}_b^{GR}$	1.05 ± 0.18
Time until coalescence, τ_m (My)	~400

*For these timing parameters, we adopted the optically derived parameters (see text for details).

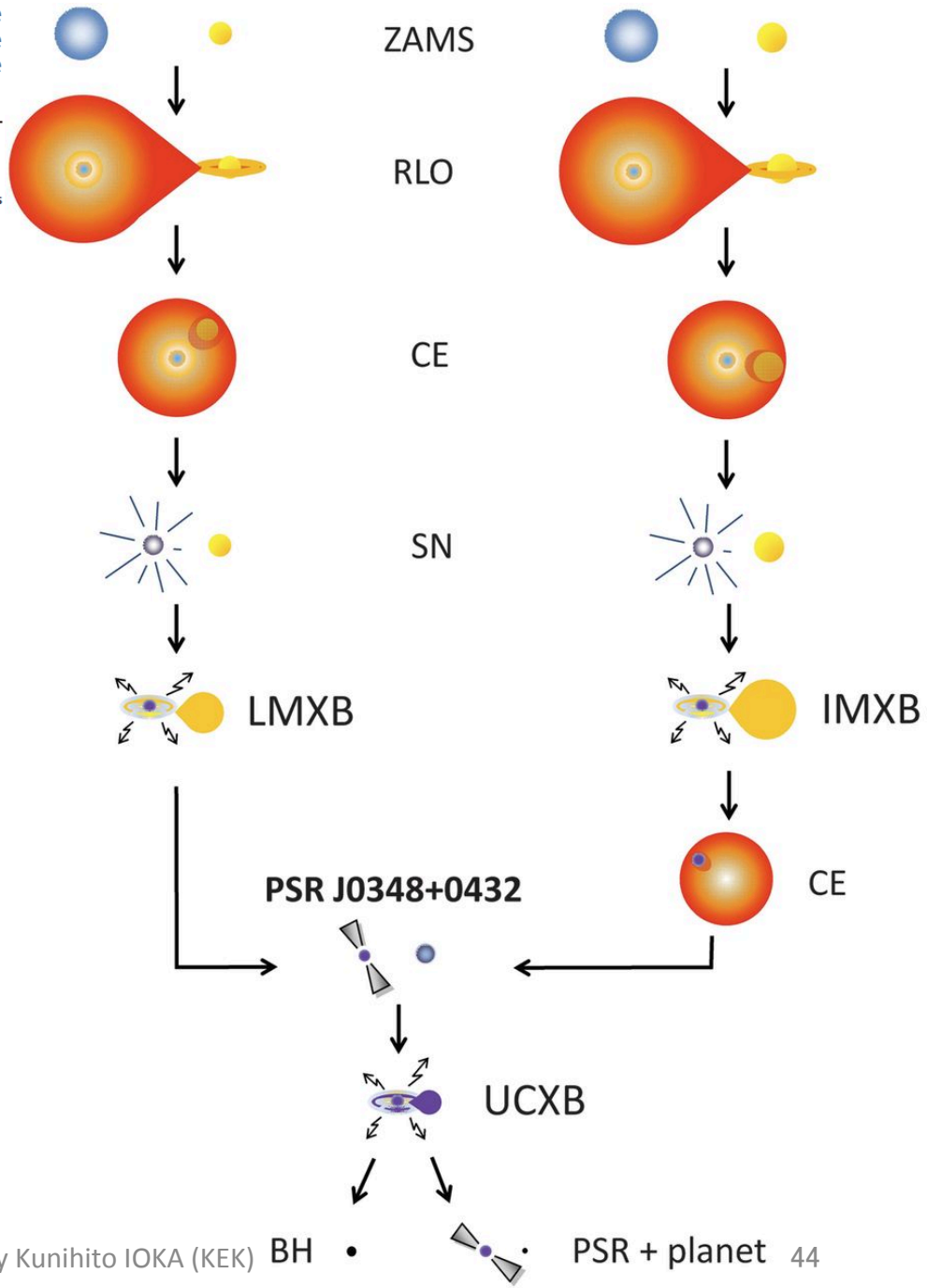

Parametrized Post Newtonian

Parameter	Effect	Limit	Remarks
$\gamma - 1$	(i) time delay	2.3×10^{-5}	Cassini tracking
Curvature per mass	(ii) light deflection	4×10^{-4}	VLBI
$\beta - 1$	(i) perihelion shift	3×10^{-3}	assumes $J_2 = 10^{-7}$ from helioseismology
Superposition law nonlinearity	(ii) Nordtvedt effect	2.3×10^{-4}	$\eta = 4\beta - \gamma - 3$ assumed
Preferred location ξ	Earth tides	10^{-3}	gravimeter data
α_1	orbital polarization	10^{-4}	Lunar laser ranging PSR J2317+1439
Preferred frame; Orbital Preferred frame; Spin α_2	solar spin precession	4×10^{-7}	alignment of Sun and ecliptic
Preferred frame; Momentum conservation α_3	pulsar acceleration	2×10^{-20}	pulsar $\dot{P}$ statistics
η^a	Nordtvedt effect	9×10^{-4}	Lunar laser ranging
ζ_1	–	2×10^{-2}	combined PPN bounds
ζ_2	binary motion	4×10^{-5}	$\ddot{P}_p$ for PSR 1913+16
ζ_3	Newton's 3rd law	10^{-8}	Lunar acceleration
ζ_4	–	–	not independent

[a] Here $\eta = 4\beta - \gamma - 3 - 10\xi/3 - \alpha_1 - 2\alpha_2/3 - 2\zeta_1/3 - \zeta_2/3$

Tests of gravity

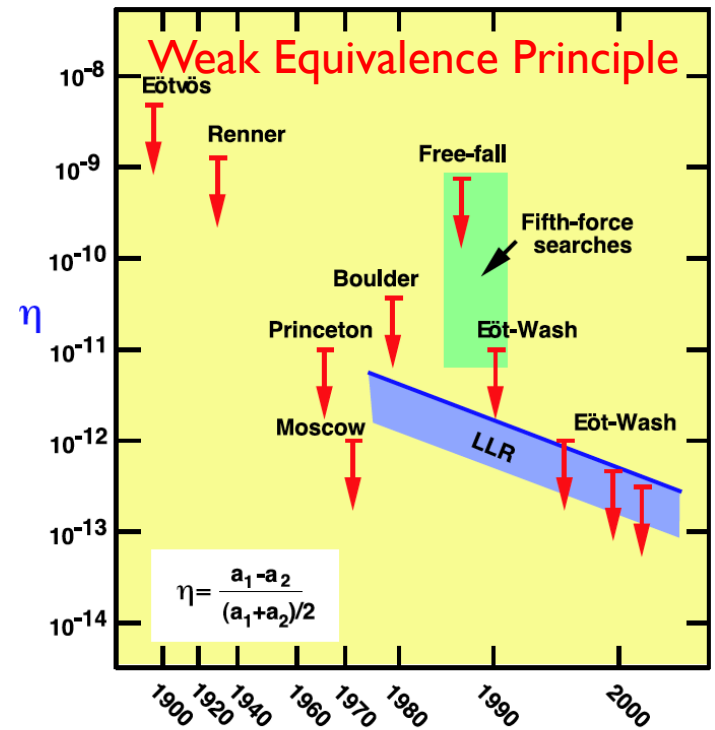

+LLI
+LPI

Will 93, 06, 09

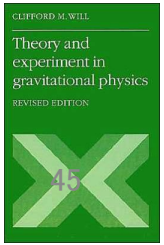

Strong-Field Tests

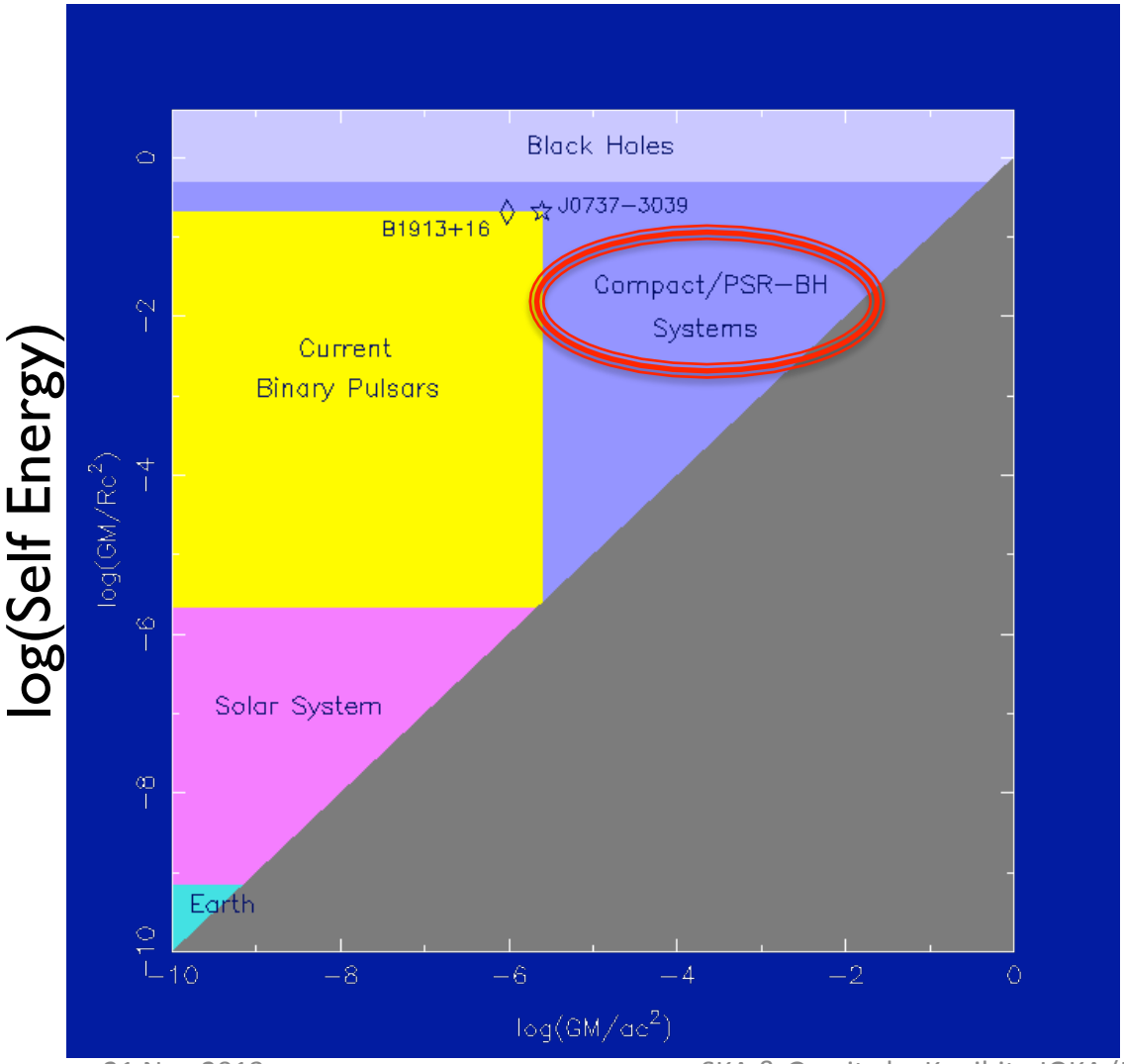

log(Self Energy)

log(Orbital Energy)

Kramer+ 04

Solar system:
weak & slow field

Neutron star surface
X-ray emission
BH Disk emission
but model-depend.

Ultrarelativistic binary
PSR-BH: WANTED

BH Uniqueness Theorem

Kerr-Newman solutions are the only stationary, axisymmetric electrovac solutions

No hair theorem

Israel, Carter, Hawking, Robinson in ~1967-1975

$$ds^2 = -\frac{\Delta}{\Sigma}\left(dt - a\sin^2\theta\, d\phi\right)^2 + \frac{\sin^2\theta}{\Sigma}\left[\left(r^2+a^2\right)d\phi - a dt\right]^2 + \frac{\Sigma}{\Delta}dr^2 + \Sigma d\theta^2$$

$$a \equiv \frac{J}{M}, \quad \Delta \equiv r^2 - 2Mr + a^2 + Q^2, \quad \Sigma \equiv r^2 + a^2\cos^2\theta$$

Only Mass M, Angular momentum J, Charge Q

Other properties are radiated away by gravitational waves

$qQ/m_pM \sim 10^{18}Q/M \Rightarrow$ Kerr BH in astrophysics

Horizon $\Delta=0$

$$r_+ = M + \left(M^2 - a^2\right)^{1/2}$$

If $M<a \Rightarrow$ Naked singularity $\Sigma=0$

Probing No Hair

Spinning black holes are oblate

Black hole quadrupole moment Q_2

No hair ⇒ Q_2 is a function of M & J

$$q \equiv \frac{c^4}{G^2}\frac{Q_2}{M^3} = -\chi^2$$

But if we measure $q \neq -\chi^2$

Then, either GR is wrong,

or a new kind of object

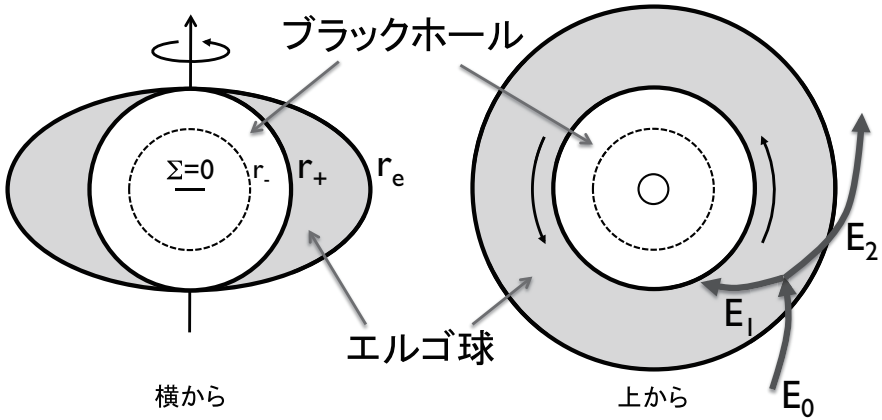

Cosmic Censorship Conjecture

Penrose 69

The complete gravitational collapse of a body always results in a black hole rather than a naked singularity; i.e., all singularities of gravitational collapse are "hidden" within black holes, where they cannot be "seen" by distant observers.

$$\chi \equiv \frac{c}{G}\frac{J}{M^2} \leq 1$$

But if we measure $\chi>1$

$\Rightarrow$ Event horizon vanished $\Rightarrow$ Naked singularity

Then, either GR is wrong, or CCC is violated

PSR-BH Sgr A* by SKA

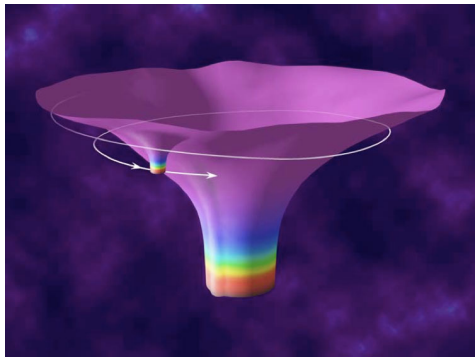

- ***Mass***
  - Fundamental quantity
  - Precision <0.0001% level ($\Delta M \sim 1 M_\odot$!)
- ***Spin***
  - Cosmic Censorship Conjecture
  - Precision ~0.1% level
- ***Quadrupole moment***
  - No hair theorem
  - Precision ~1% level

High precision tests of gravity by SKA!

PSR-Sgr A*: Mass

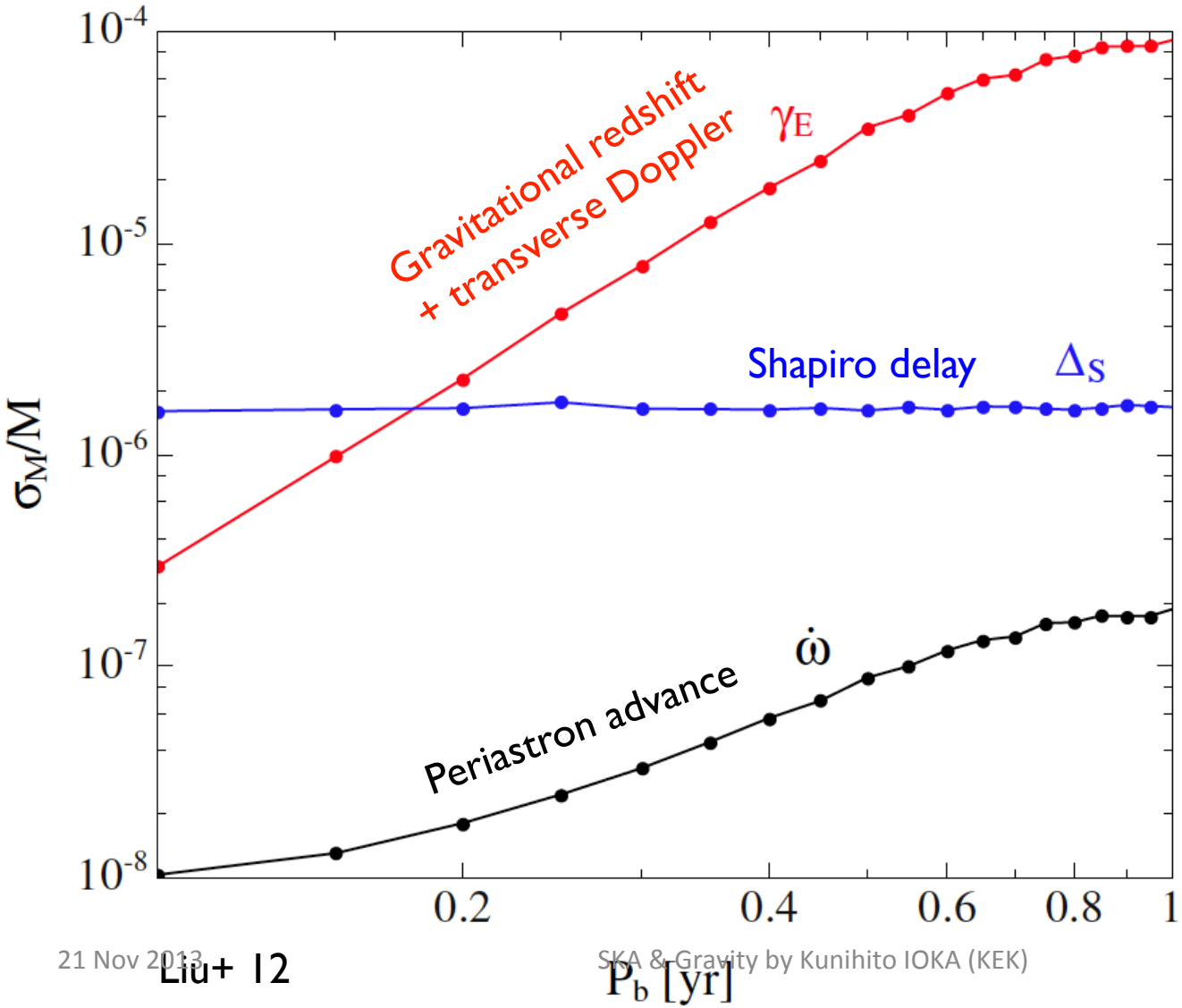

Liu+ 12

Pulsar timing near Sgr A*

⇒ Precision ~10^{-6}

Simulation
Weekly TOA
σ_{TOA}=100μs
over 5yr
e=0.5
i=60deg
No BH spin

Puslar Timing near Sgr A*

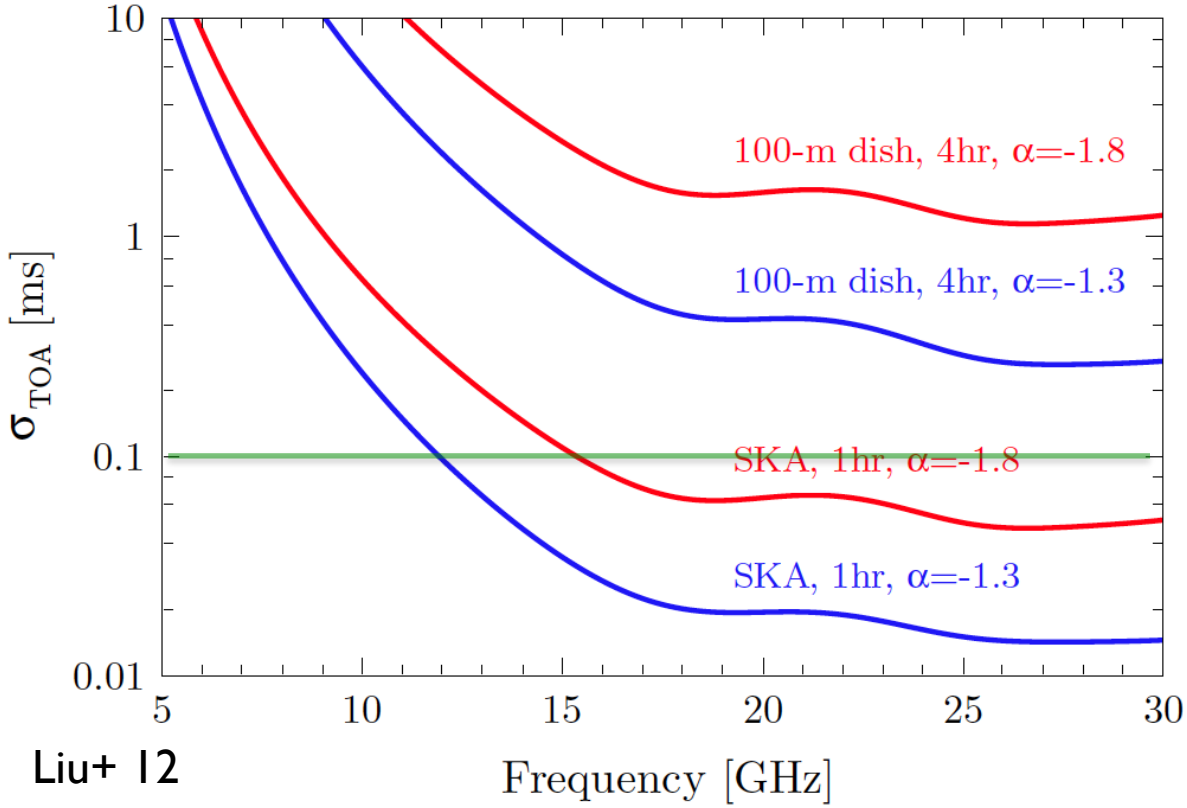

Liu+ 12

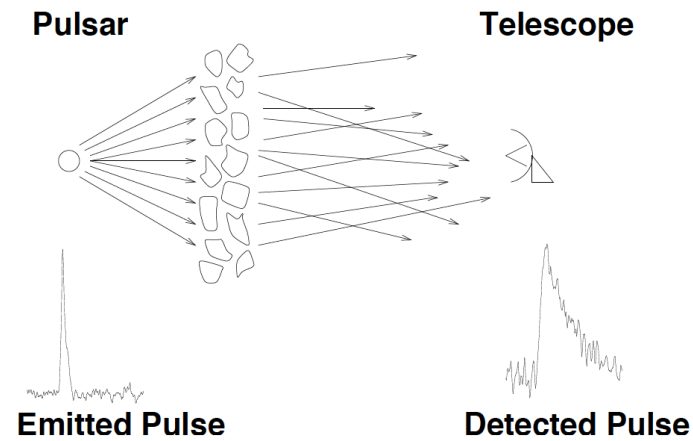

P=0.5s, W=10ms

S_{1400}=1mJy @1.4GHz

t_{scat}~2.3e3s(f/1GHz)$^{-4}$

100m dish: 2K/Jy, 4hr

SKA: 100K/Jy, 1hr

PSR J1745-2900 @~0.1pc

DM=1778±3pc/cm^3, t_{scat}~1.3s(f/GHz)$^{-4}$

Magnetar

Consistent with 1000 PSR @<1pc?

Mori+ 13; Eatough+ 13; Spitler+ 14

Chennamangalam & Lorimer 13

PSR-10M$_\odot$ BH: Mass

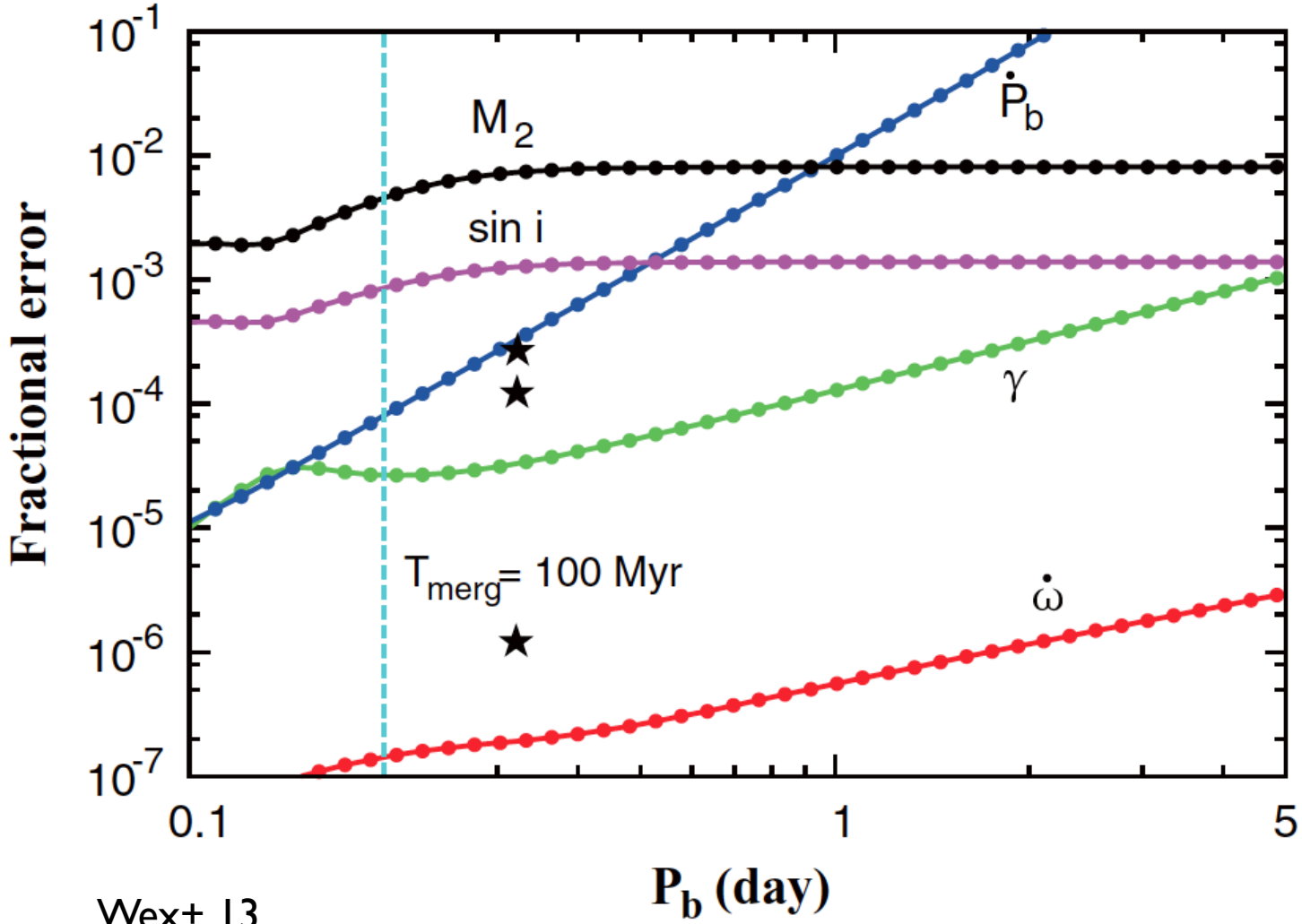

~1% level

Simulation
Weekly TOA
100m dish
over 5yr
e=0.1
★:Hulse-Taylor

Wex+ 13

Spin & Quadrupole

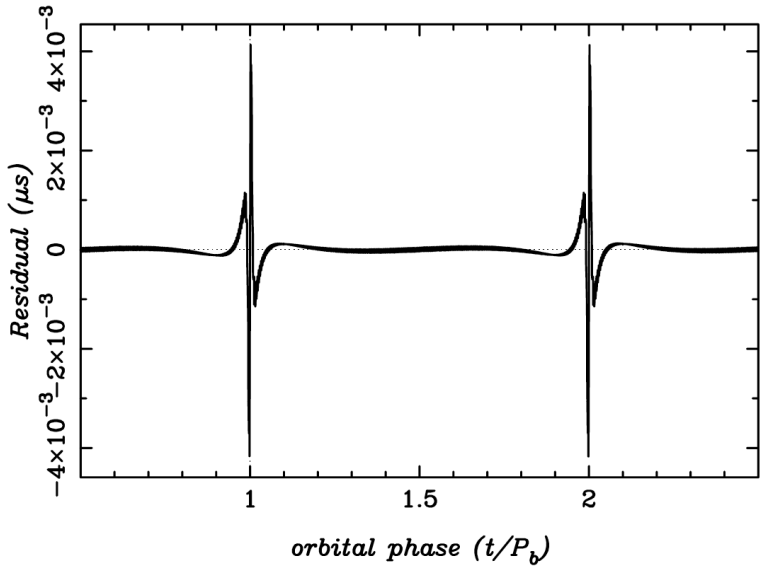

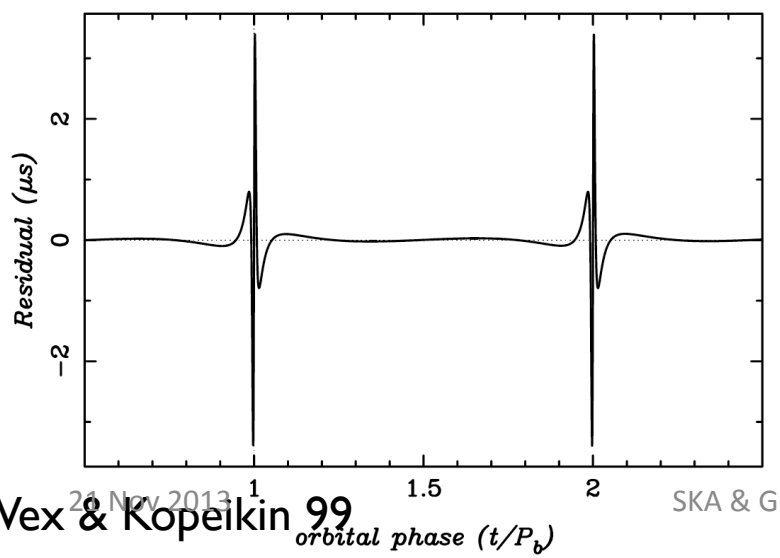

Wex & Kopeikin 99

Lense-Thirring precession by BH spin-orbit coupling

Quadrupole also affect orbit

⇒ Features in TOA of pulses

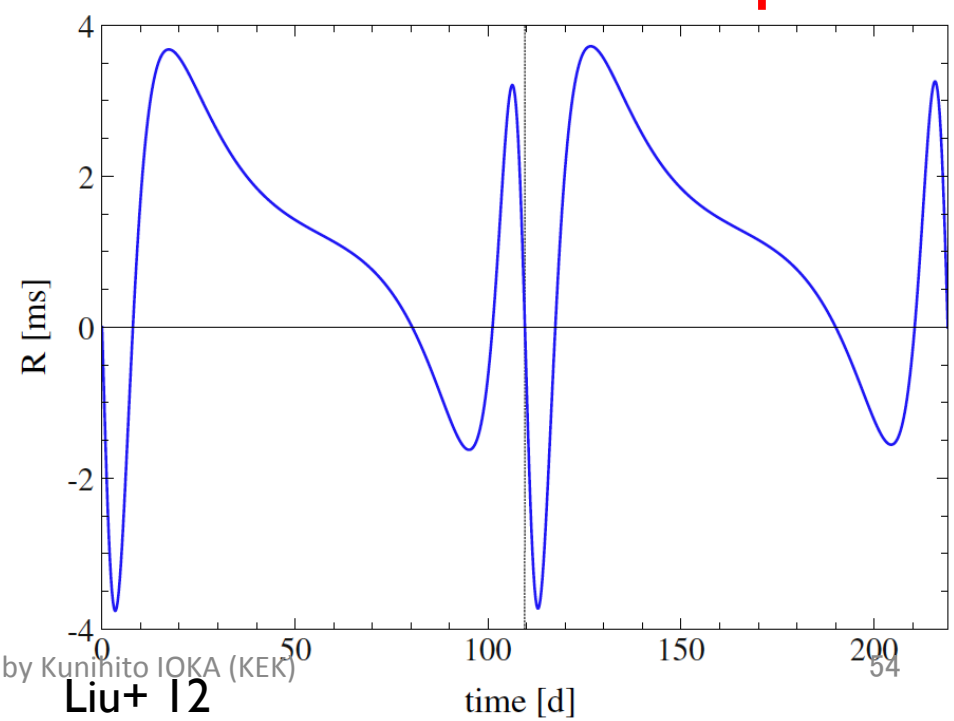

Liu+ 12

Sgr A*: Spin & Quadrupole

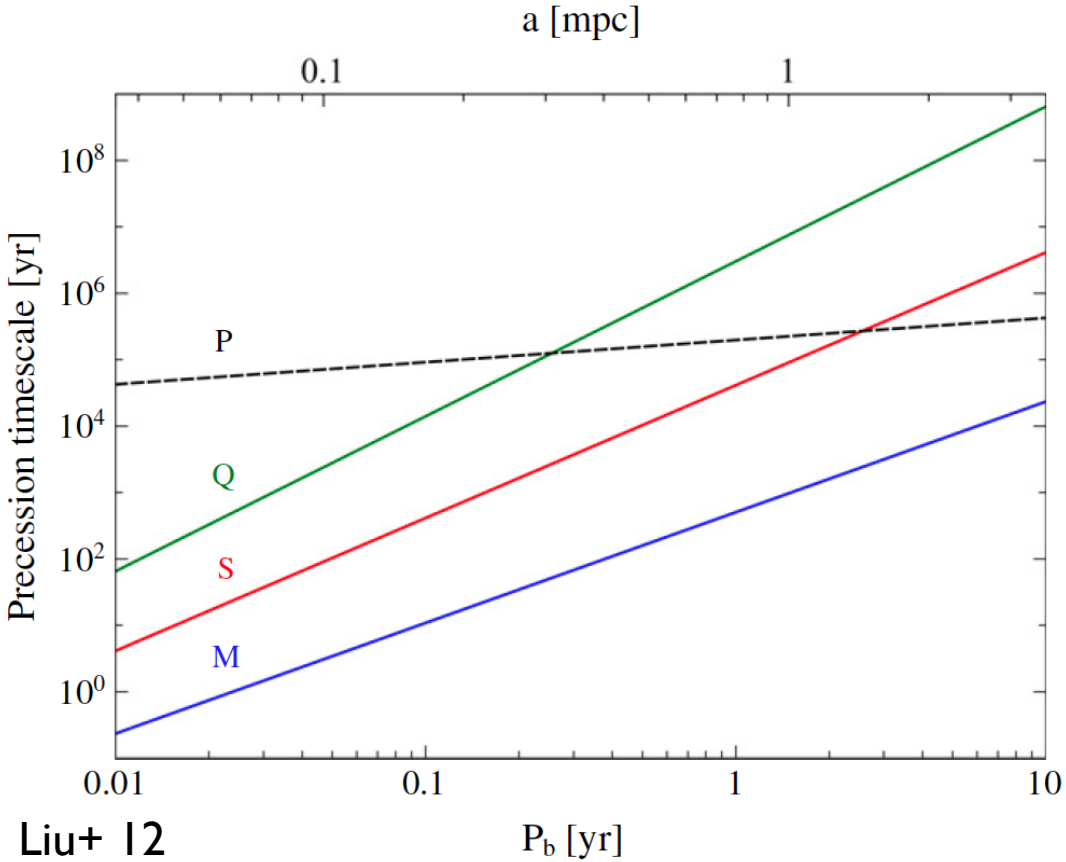

Liu+ 12

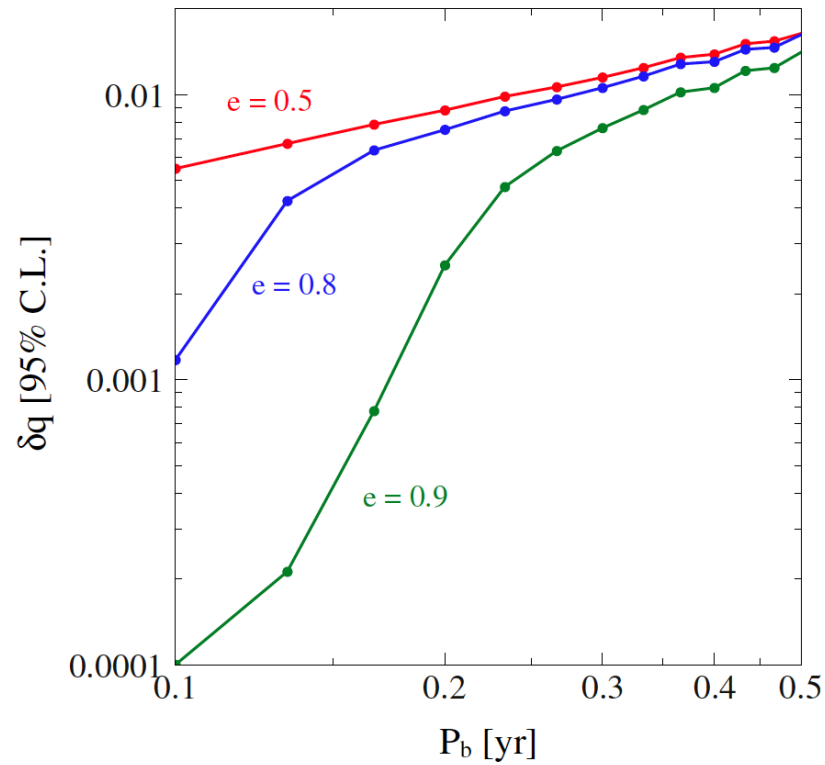

Spin (Cosmic Censorship) ~ 0.1%

Quadrupole (No hair) ~ 1%

PSR-10M$_\odot$ BH: Spin

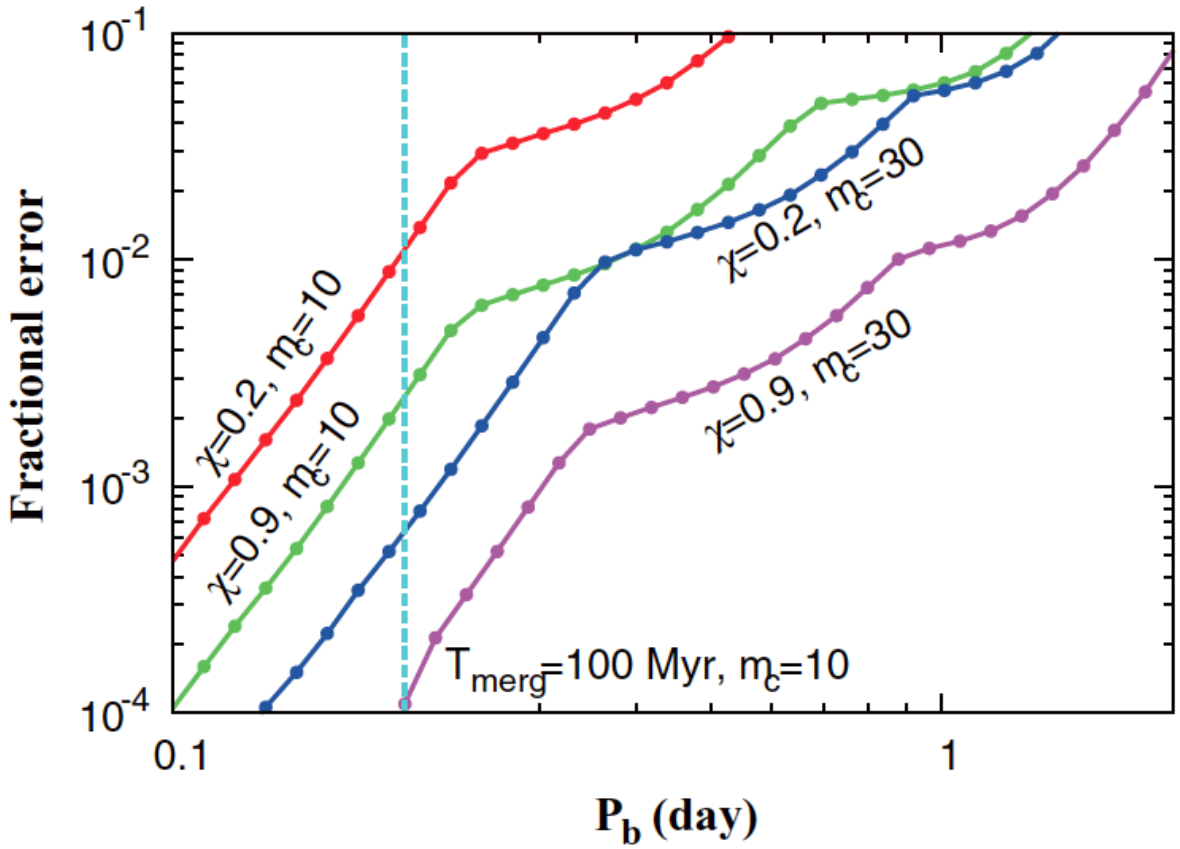

Wex+ 13

Figure 2. Fractional error in the BH spin, as a function of the orbital period. The figure is based on mock data simulations for weekly observations over 5 years with SKA, assuming a recycled PSR in a mildly eccentric ($e = 0.1$) orbit. m_c denotes the BH mass.

Scalar-Tensor Theory

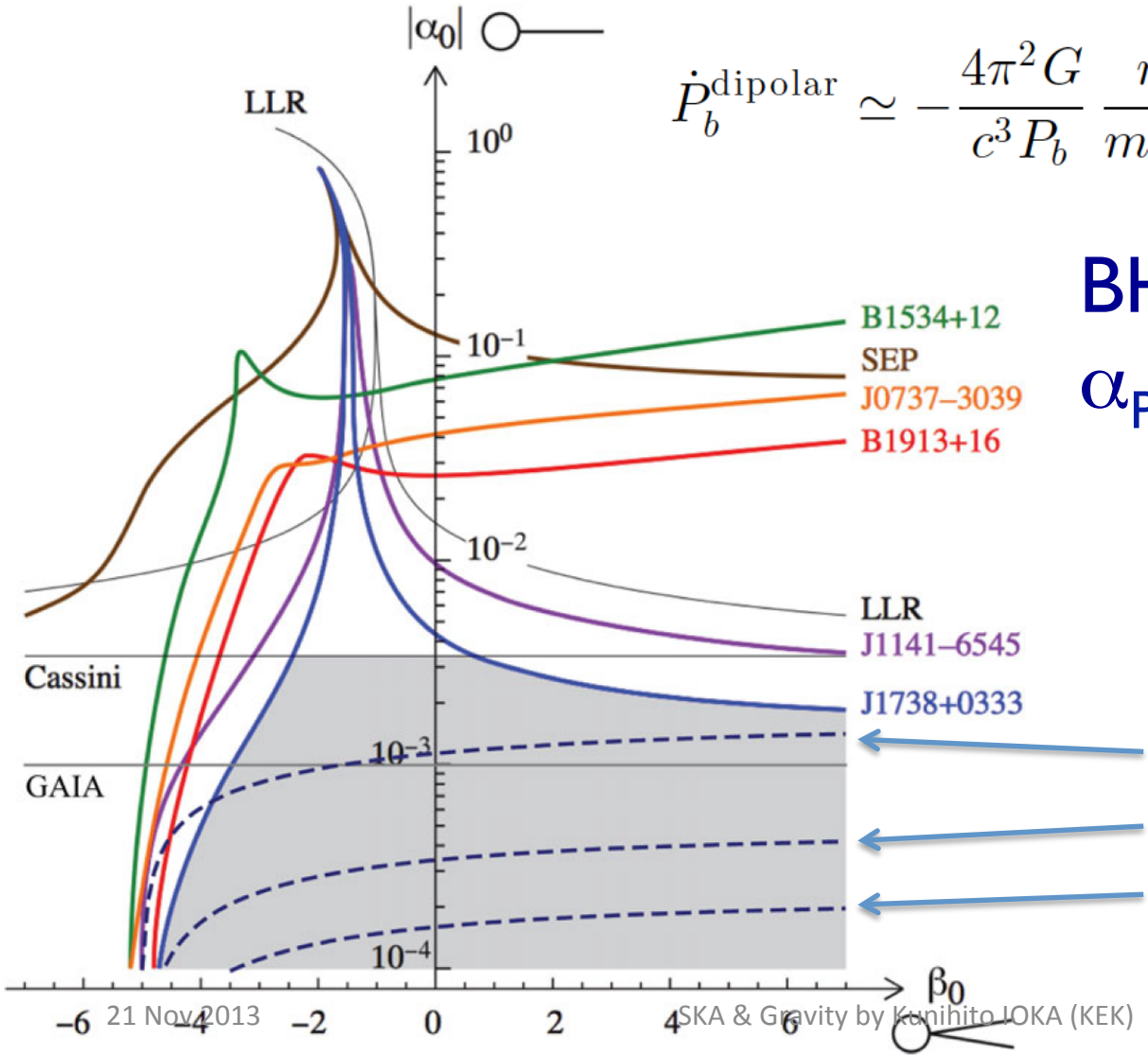

$$\dot{P}_b^{\rm dipolar} \simeq -\frac{4\pi^2 G}{c^3 P_b}\frac{m_{\rm PSR} m_{\rm BH}}{m_{\rm PSR}+m_{\rm BH}}\frac{1+e^2/2}{(1-e^2)^{5/2}}\alpha_{\rm PSR}^2$$

BH has no hair $\alpha_{BH}=0$

$\alpha_{PSR}-\alpha_{BH}=\alpha_{PSR}$

MSP-10$M_\odot$ BH

P_b=5d, e=0.8

Weekly timing

100m dish 10yr

FAST 5yr

SKA 5yr

Wex+ 13; Liu+

Variation of G

$$\left|\frac{\Delta \dot{P}}{P}\right| \sim \frac{0.3\% \times 10^{-20}}{m\,\mathrm{sec}} \sim 3 \times 10^{-20}\,\mathrm{s}^{-1} \sim 10^{-12}\,\mathrm{yr}^{-1}$$

$$\Rightarrow \quad \left|\frac{\dot{G}}{G}\right| = (9 \pm 12) \times 10^{-13}\ \mathrm{yr}^{-1}$$

Zhu+ in prep.

Dirac's large number hypothesis: $G \propto 1/t$

Scalar-tensor theory, Kalza-Klein, Superstring: $L = \varphi R + \ldots$

Lunar laser ranging: $(4 \pm 9) \times 10^{-13}$/yr

Variation of the Astronomical Unit (AU)

なぜαの時間変化を考えるか

Date
No.

Dirac theory. (large number hypothesis)

$$\frac{e^2}{G m_p m_e} \simeq 0.23 \times 10^{40}$$: electronとprotonの間の重力とクーロン力の比

大きな数はなんらかの説明がいる。Diracは時間変化していると考えた

$$\left(\frac{\hbar c}{G m_p^2} \simeq 1.5 \times 10^{38} \right.$$: protonのComptonwavelengthとSchwarzschild radiusの比 $\left. \right)$

$$\frac{c H_0^{-1}}{e^2/m_e c^2} \simeq 3.7 \times 10^{40}$$: cosmological horizonとelectron radiusの比

にたものに

$$\left(\frac{1}{m_\pi} \left(\frac{\hbar^2 H_0}{G c} \right)^{1/3} \simeq \frac{1}{m_e} \left(\frac{e^4 H_0}{G c^3} \right)^{1/3} \simeq 1 \right)$$

宇宙論的な量とミクロスケールの量の関係

たまたま一致 or 深い意味

↓ 何か関係があってorder 1の量になる

(星が進化するための Dicke時間)

$$\frac{e^2}{G m_p m_e} \Big/ \frac{c H_0^{-1}}{e^2/m_e c^2} = \frac{e^4 H_0}{G m_p m_e^2 c^3} \simeq 1$$

この関係が保たれるには

Gが変わるか $G(t) \propto H(t) \Rightarrow \frac{\dot{a}}{a}$, 一方 $G(t) a^{-3} \propto H^2$

$\rho \propto a^{-3}$ より

$$\Rightarrow \frac{\dot{a}}{a} \propto a^{-3}$$

$$a = a_0 \left(\frac{t}{t_0} \right)^{1/3}, \quad G(t) = G_0 \left(\frac{t}{t_0} \right)^{-1}$$

その他 eが変わってもよい

Outline

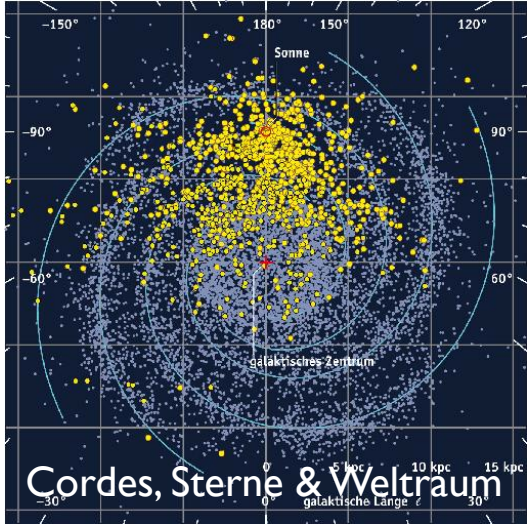

- Pulsar
  - Finding all pulsars in the Milky Way
  - Super dense matter physics, etc.
- Strong-field tests of gravity
- Gravitational wave astronomy
  - Complementary to AdvLIGO, KAGRA, eLISA, DECIGO, CMB-pol, LiteBIRD

Mass ~10^{-6}
No hair ~0.1%
CCC ~1%

Gravitational Wave

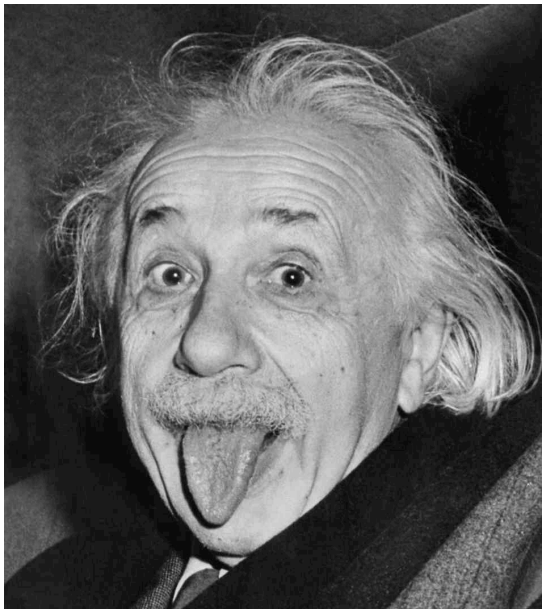

- ***Einstein equation***

$$R_{\mu\nu} - \frac{1}{2} g_{\mu\nu} R = \frac{8\pi G}{c^4} T_{\mu\nu}$$

- ***Wave solution***

$$g_{\mu\nu} = \eta_{\mu\nu} + h_{\mu\nu}$$

$$\left(\nabla^2 - \frac{1}{c^2} \frac{\partial^2}{\partial t^2} \right) h_{\mu\nu} = 0$$

$v_{GW}=c$

GW = Tidal Force

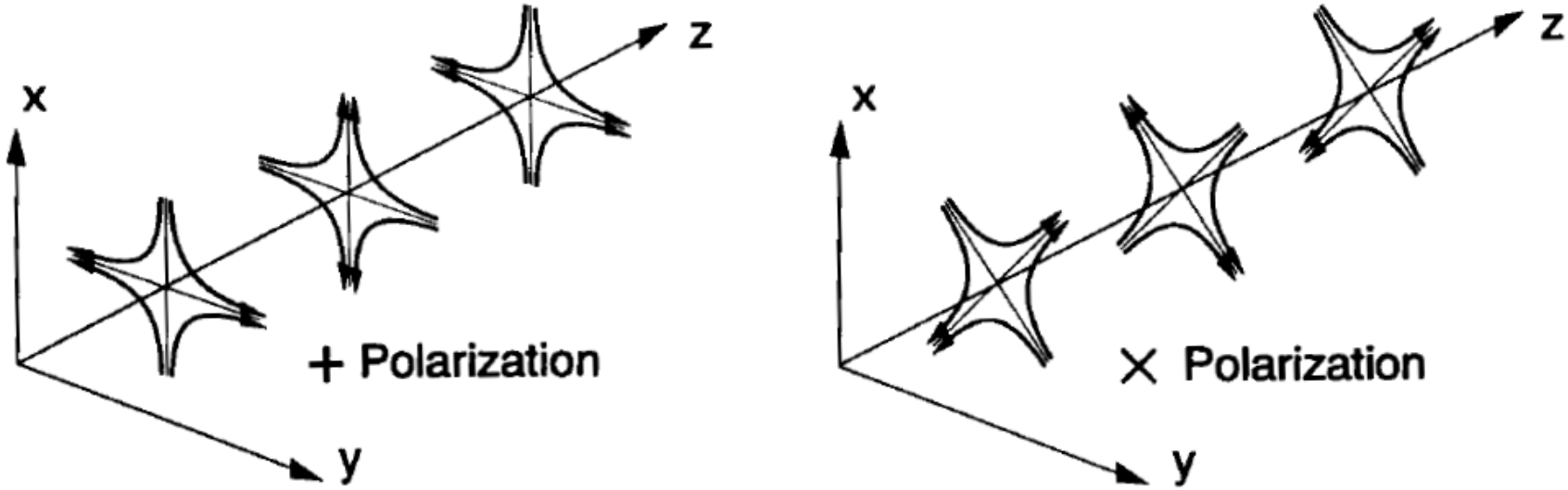

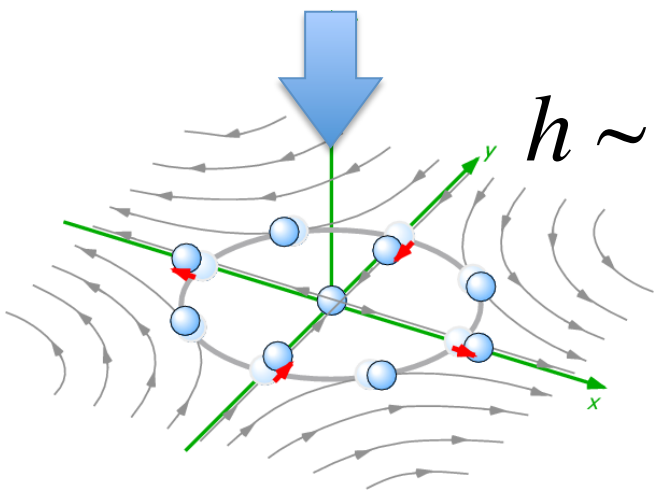

$$h \sim \frac{\Delta x}{x}$$

Laser Interferometer

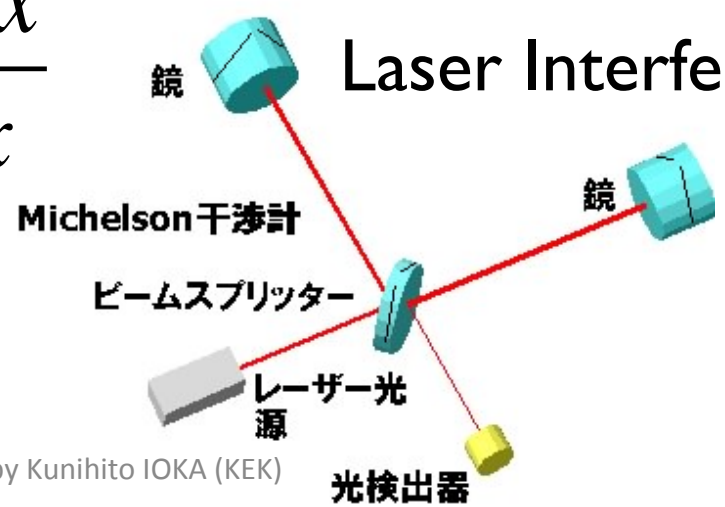

Tidal force on test mass

Penetration Power

More than Neutrino

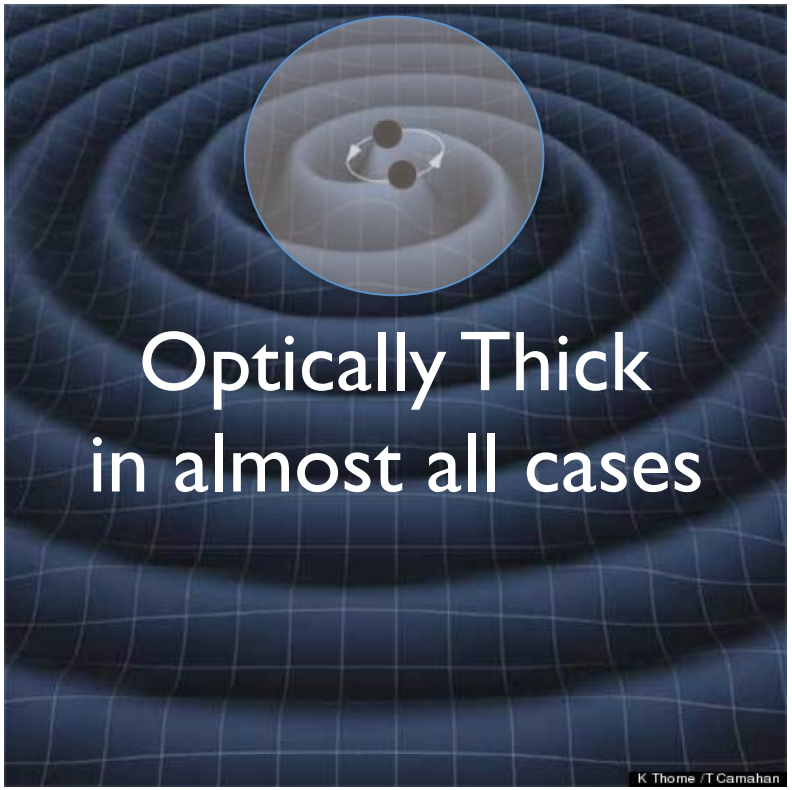

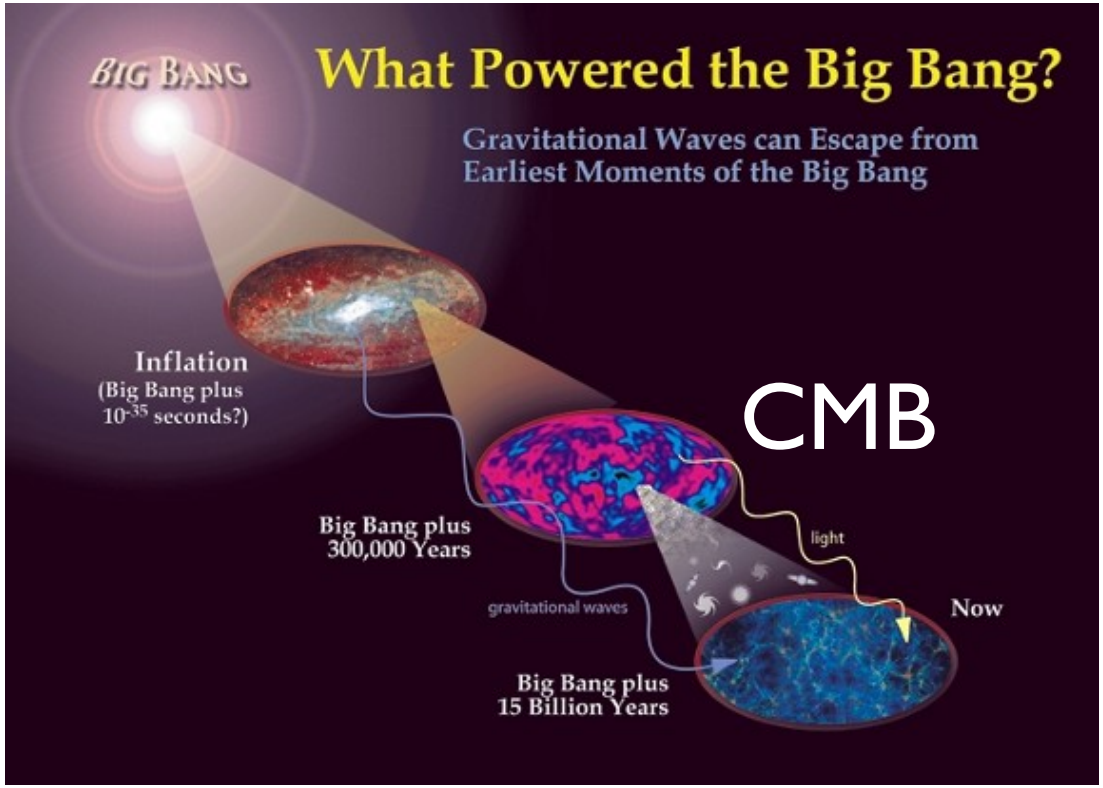

Astrophysical GW

Inflation GW

GW Generation

- Electromagnetic wave: Electric charge
- Gravitational wave: Mass
- No monopole, No dipole radiation
- Quadrupole formula

$$h \sim \frac{2G}{c^4 d}\frac{d^2 I_{ij}}{dt^2} \sim \frac{4GM\epsilon}{c^2 d}\left(\frac{v}{c}\right)^2 \qquad \frac{\text{BH size}}{\text{Distance}}$$

$$\sim 10^{-21}\epsilon\left(\frac{v}{c}\right)^2\left(\frac{M}{M_\odot}\right)\left(\frac{d}{100\,\mathrm{Mpc}}\right)^{-1}$$

$$\sim \frac{\Delta x}{x}$$

For x=1km, $\Delta x \sim 10^{-16}$cm < Atomic Nuclei

2nd Generation of GW Observatories

©Ando

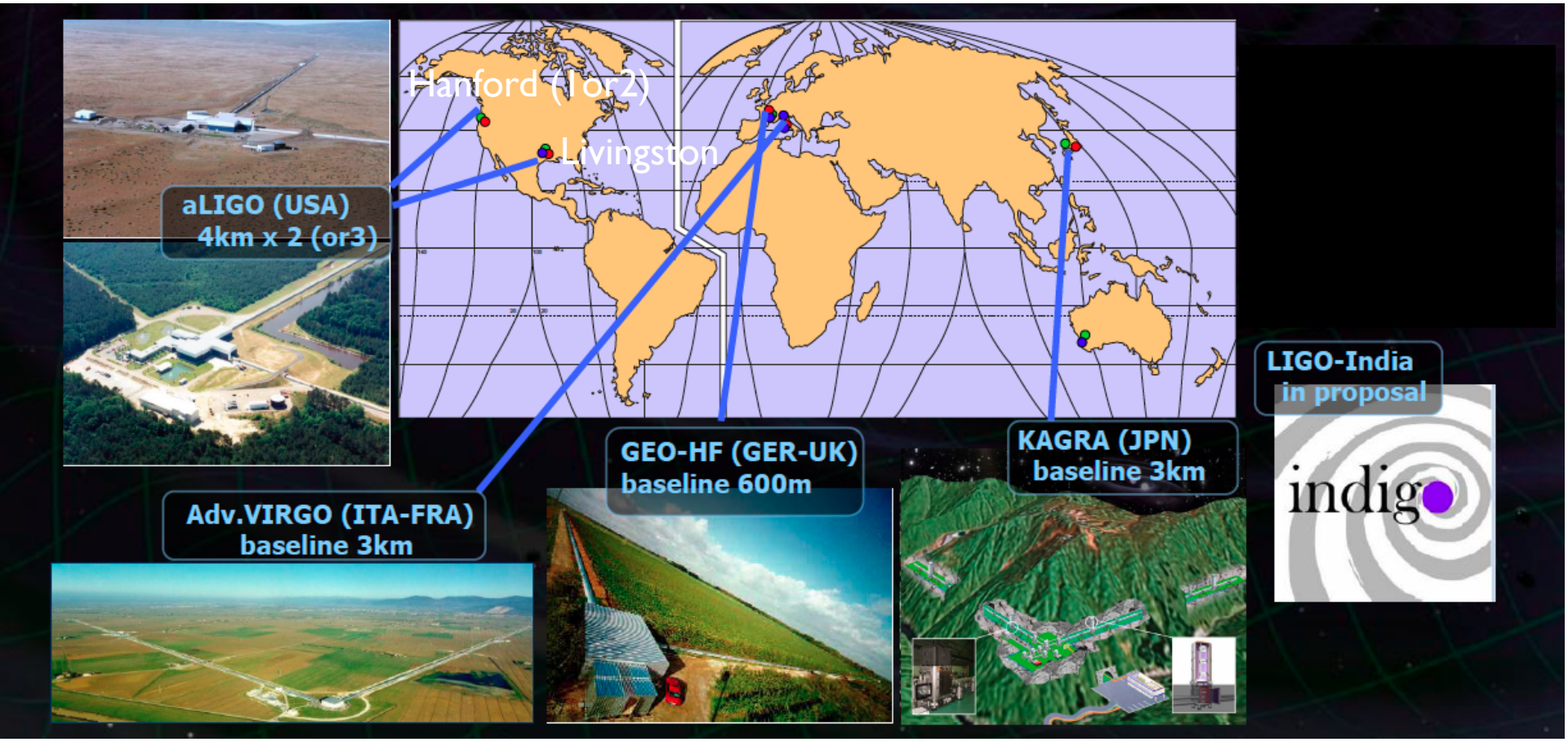

GW will be directly detected within ~5 yr

Sensitivities

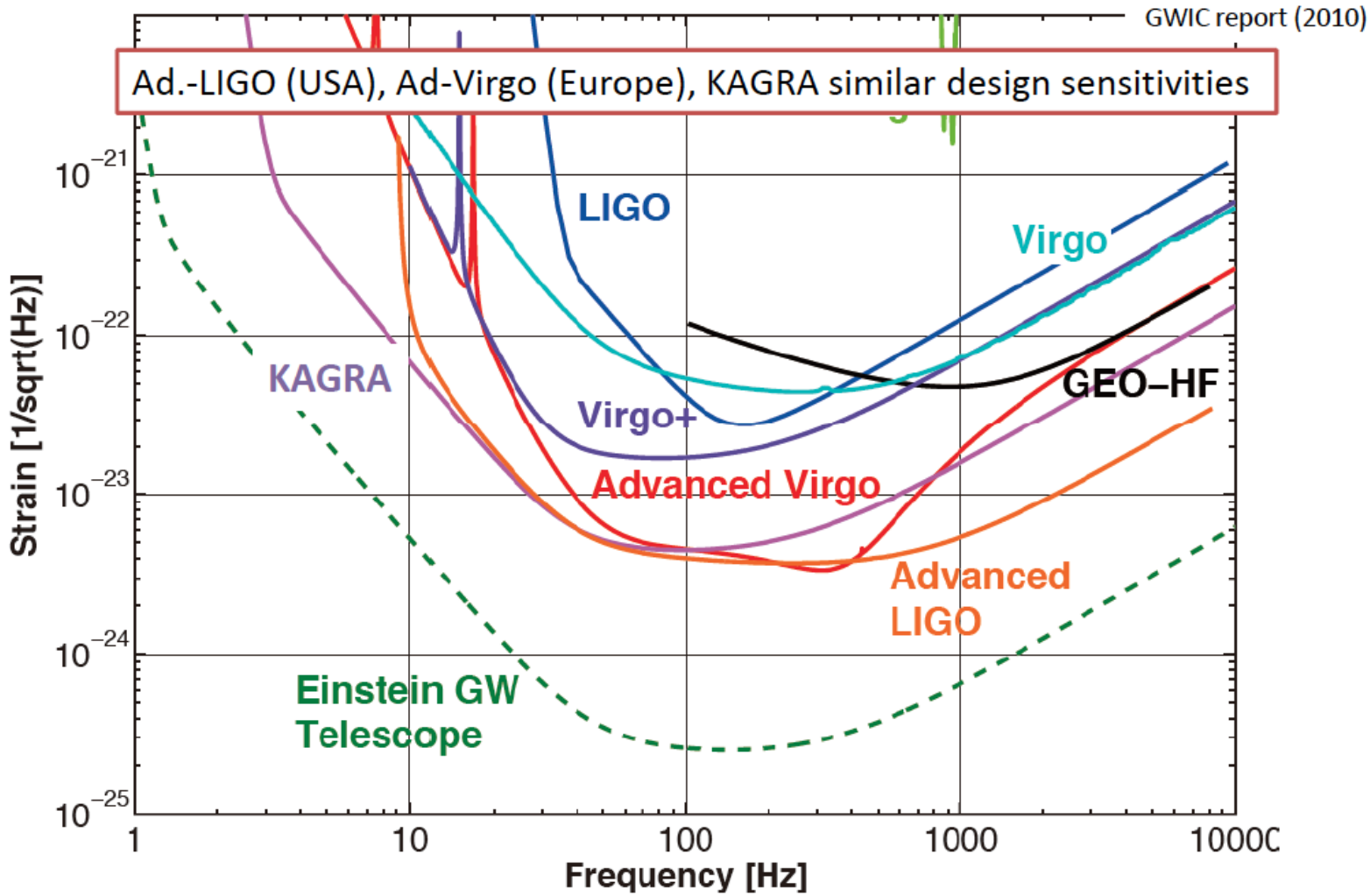

Budget and revised schedule

Dec. 2013

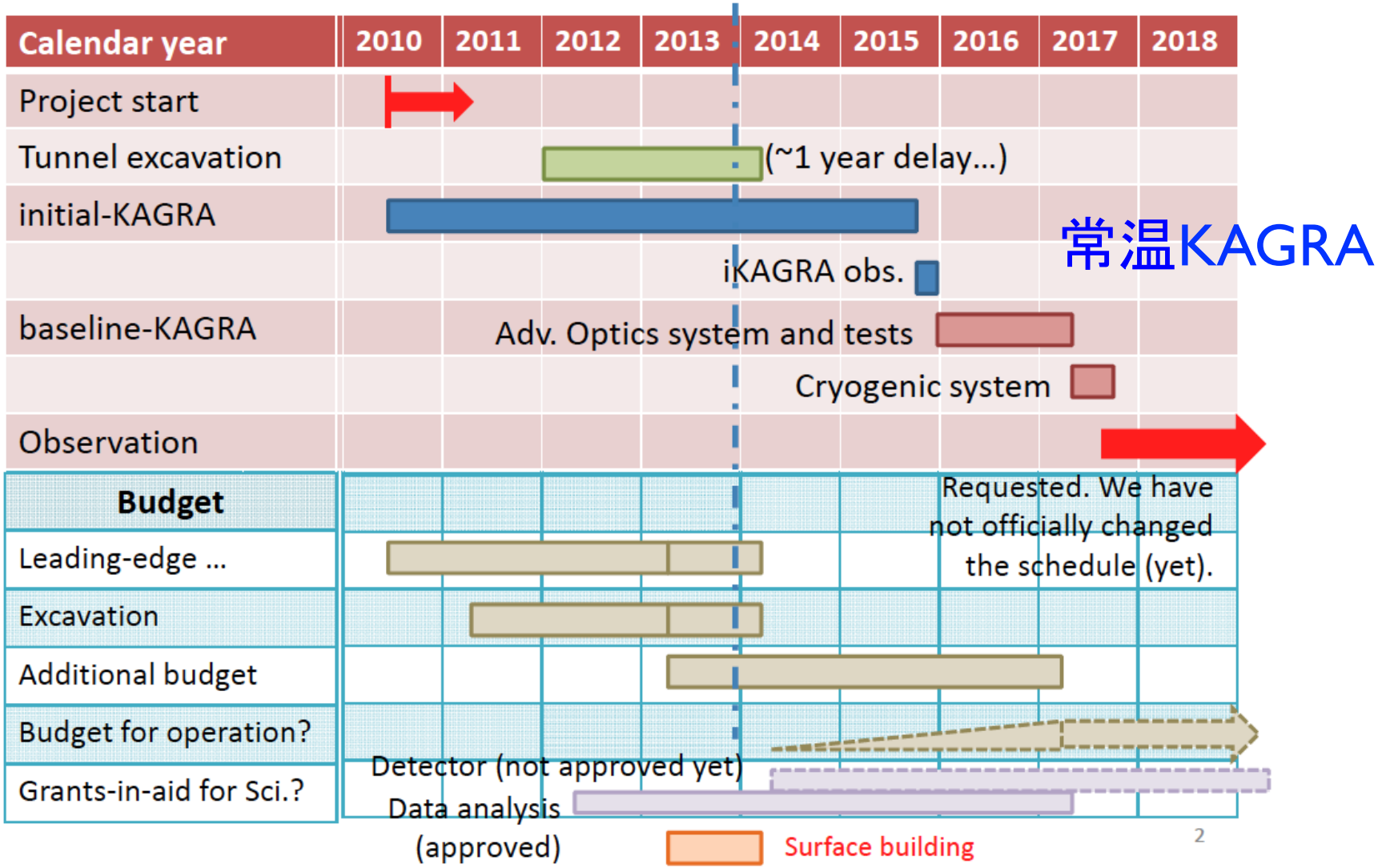

©Kajita

Expected Sources

$$f \simeq \frac{1}{\pi}\sqrt{\frac{GM}{R^3}} \sim 20\ \mathrm{Hz}\left(\frac{M}{3M_\odot}\right)^{1/2}\left(\frac{R}{500\,\mathrm{km}}\right)^{-2/3}$$

1/free fall time

Ground interferometers ⇒ Solar mass BH or NS

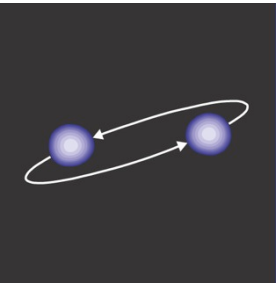

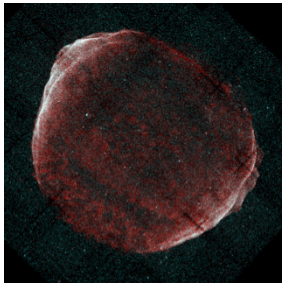

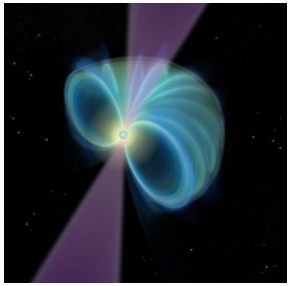

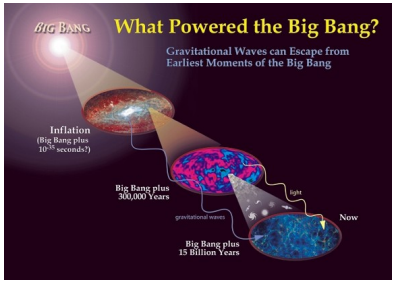

Binary	***Burst***	***Oscillation***	***Pulsar***	***Stochastic***
NS-NS	Supernova	BH ringdown		Inflation
NS-BH	GRB	NS r-mode		Phase transition
BH-BH	String	Magnetar flare		Superposition

Compact Star Merger

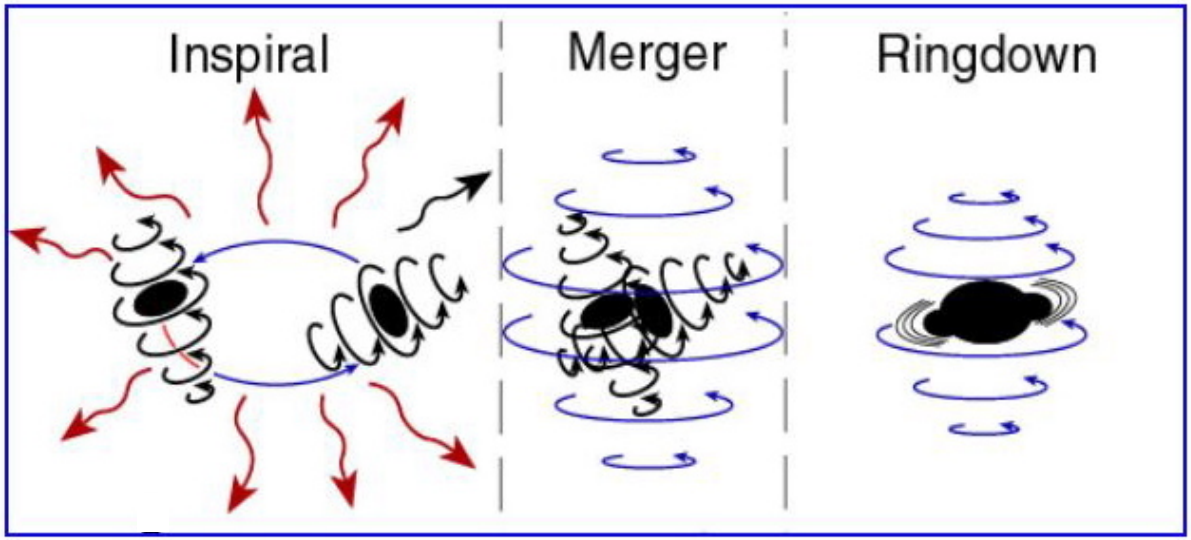

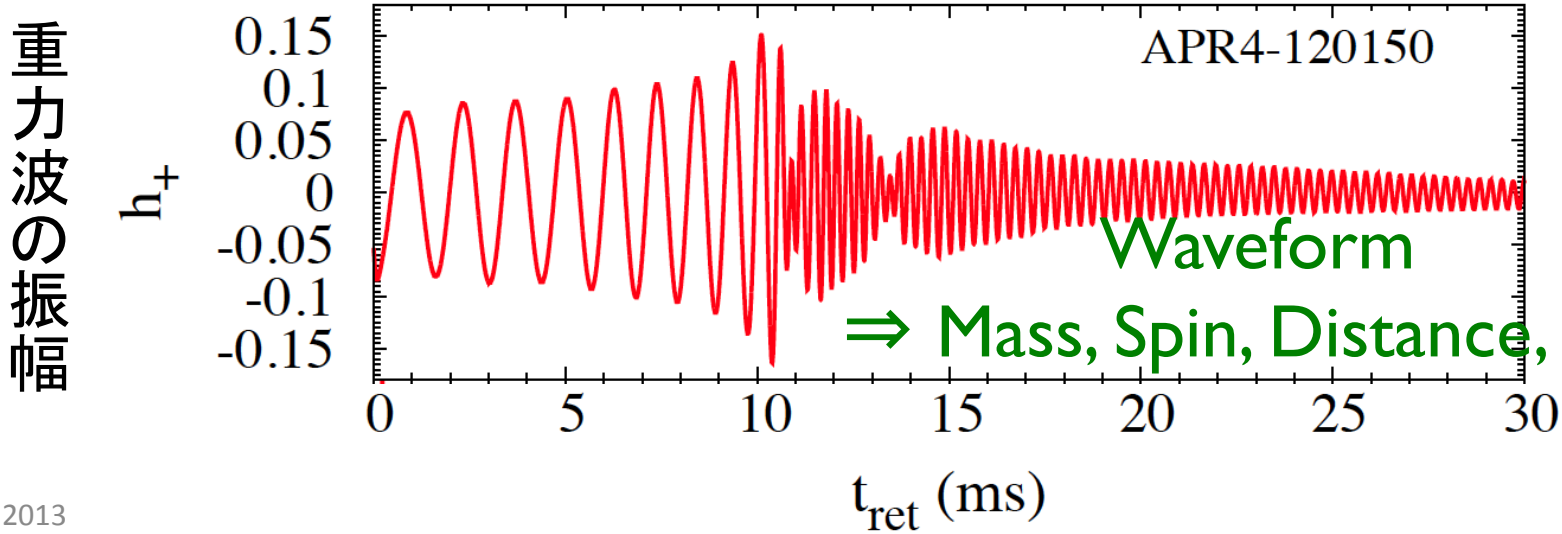

Waveform

⇒ Mass, Spin, Distance, etc.

Event Rate

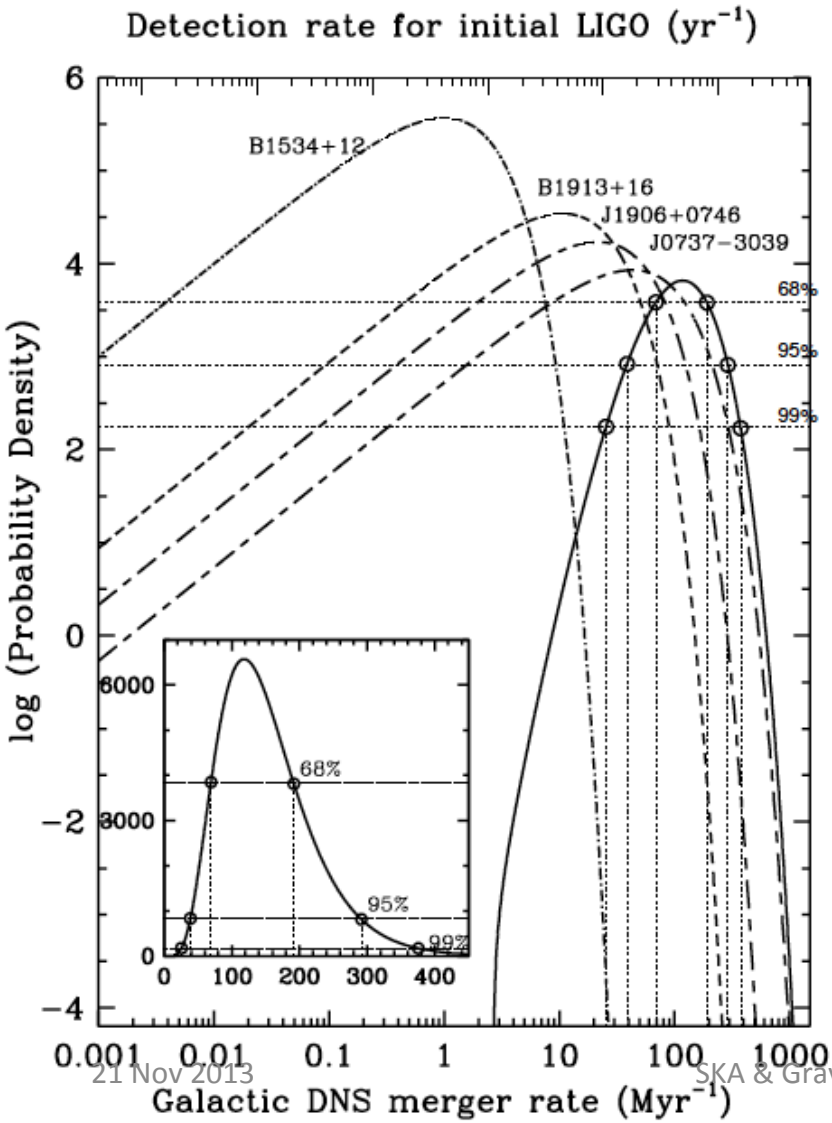

Based on ~5 Galactic NS[2]

⇒ R_{merger}~100/Myr/galaxy

× ~0.01galaxy/Mpc^3

× (~200Mpc)^3

~10 events/yr

by KAGRA, advLIGO

Kalogera+ 04, Abadie+ 10

Table 5. Detection rates for compact binary coalescence sources.

IFO	Source[a]	$\dot{N}_{\rm low}$ yr^{-1}	$\dot{N}_{\rm re}$ yr^{-1}	$\dot{N}_{\rm high}$ yr^{-1}	$\dot{N}_{\rm max}$ yr^{-1}
	NS–NS	2×10^{-4}	0.02	0.2	0.6
	NS–BH	7×10^{-5}	0.004	0.1	
Initial	BH–BH	2×10^{-4}	0.007	0.5	
	IMRI into IMBH			<0.001[b]	0.01[c]
	IMBH-IMBH			10^{-4}[d]	10^{-3}[e]
	NS–NS	0.4	40	400	1000
	NS–BH	0.2	10	300	
Advanced	BH–BH	0.4	20	1000	
	IMRI into IMBH			10[b]	300[c]
	IMBH-IMBH			0.1[d]	1[e]

[a] To convert the rates per MWEG in table 2 into detection rates, optimal horizon distances of 33 Mpc/445 Mpc are assumed for NS–NS inspirals in the Initial/Advanced LIGO–Virgo networks. For NS–BH inspirals, horizon distances of 70 Mpc/927 Mpc are assumed. For BH–BH inspirals, horizon distances of 161 Mpc/2187 Mpc are assumed. These distances correspond to a choice of 1.4 $M_\odot$ for NS mass and 10 $M_\odot$ for BH mass. Rates for IMRIs into IMBHs and IMBH–IMBH coalescences are quoted directly from the relevant papers without conversion. See section 3 for more details.
[b] Rate taken from the estimate of BH–IMBH IMRI rates quoted in [19] for the scenario of BH–IMBH binary hardening via three-body interactions; the fraction of globular clusters containing suitable IMBHs is taken to be 10%, and no interferometer optimizations are assumed.
[c] Rate taken from the optimistic upper limit rate quoted in [19] with the assumption that all globular clusters contain suitable IMBHs; for the advanced network rate, the interferometer is assumed to be optimized for IMRI detections.
[d] Rate taken from the estimate of IMBH-IMBH ringdown rates quoted in [20] assuming 10% of all young star clusters have sufficient mass, a sufficiently high binary fraction, and a short enough core collapse time to form a pair of IMBHs.
[e] Rate taken from the estimate of IMBH-IMBH ringdown rates quoted in [20] assuming all young star clusters have sufficient mass, a sufficiently high binary fraction, and a short enough core collapse time to form a pair of IMBHs.

Abadie+ 10

Table 2
LIGO/VIRGO Detection Rates (yr^{-1})

Sensitivity ($d_{0,nsns}$ =)	Type	$Z_\odot$ (100%)	0.1 $Z_\odot$ (100%)	$Z_\odot$ + 0.1 $Z_\odot$ (50% + 50%)
4*18 Mpc	NS–NS	0.01 (0.003)	0.01 (0.001)	0.01 (0.002)
	BH–NS	0.007 (0.00002)	0.04 (0.02)	0.02 (0.01)
	BH–BH	0.02 (0.00005)	9.9 (0.1)	4.9 (0.05)
	Total	0.03 (0.003)	10.0 (0.1)	5.0 (0.06)
4*45 Mpc	NS–NS	0.2 (0.05)	0.2 (0.01)	0.2 (0.03)
	BH–NS	0.1 (0.0003)	0.5 (0.3)	0.3 (0.15)
	BH–BH	0.3 (0.0007)	145.4 (1.6)	72.8 (0.82)
	Total	0.6 (0.05)	146.1 (1.9)	73.3 (1.0)
4*97 Mpc	NS–NS	1.5 (0.5)	1.6 (0.1)	1.5 (0.3)
	BH–NS	1.0 (0.003)	4.8 (2.9)	2.9 (1.5)
	BH–BH	2.8 (0.007)	1454.6 (16.4)	728.7 (8.2)
	Total	5.3 (0.5)	1461.0 (19.5)	733.2 (10.0)
4*300 Mpc	NS–NS	44.3 (15.1)	45.9 (4.0)	45.1 (9.5)
	BH–NS	29.7 (0.1)	141.9 (85.4)	85.8 (42.8)
	BH–BH	82.4 (0.21)	42768.0 (483.3)	21425.2 (241.7)
	Total	156.4 (15.2)	42955.8 (572.7)	21556.0 (294.0)

Notes. Detection rates for model A (B) as a function of sensitivity of a given instrument. Sensitivity is defined as the sky and angle averaged distance horizon for detection of a double neutron star inspiral. The rates are given for a local universe consisting of only solar composition stars (unrealistically high), 0.1 $Z_\odot$ stars (unrealistically low), and for a 50–50 mixture of the above (realistic local universe; Panter et al. 2008). The sensitivity of $d_{0,nsns}$ = 18 Mpc and 300 Mpc corresponds to the current and advanced (2015) LIGO detectors, respectively. $d_{0,nsns}$ = 45 Mpc and 97 Mpc were chosen such that our pessimistic model (B) results in 1 and 10 detections, respectively.

Belczynski+ 10

Magnetar Flare

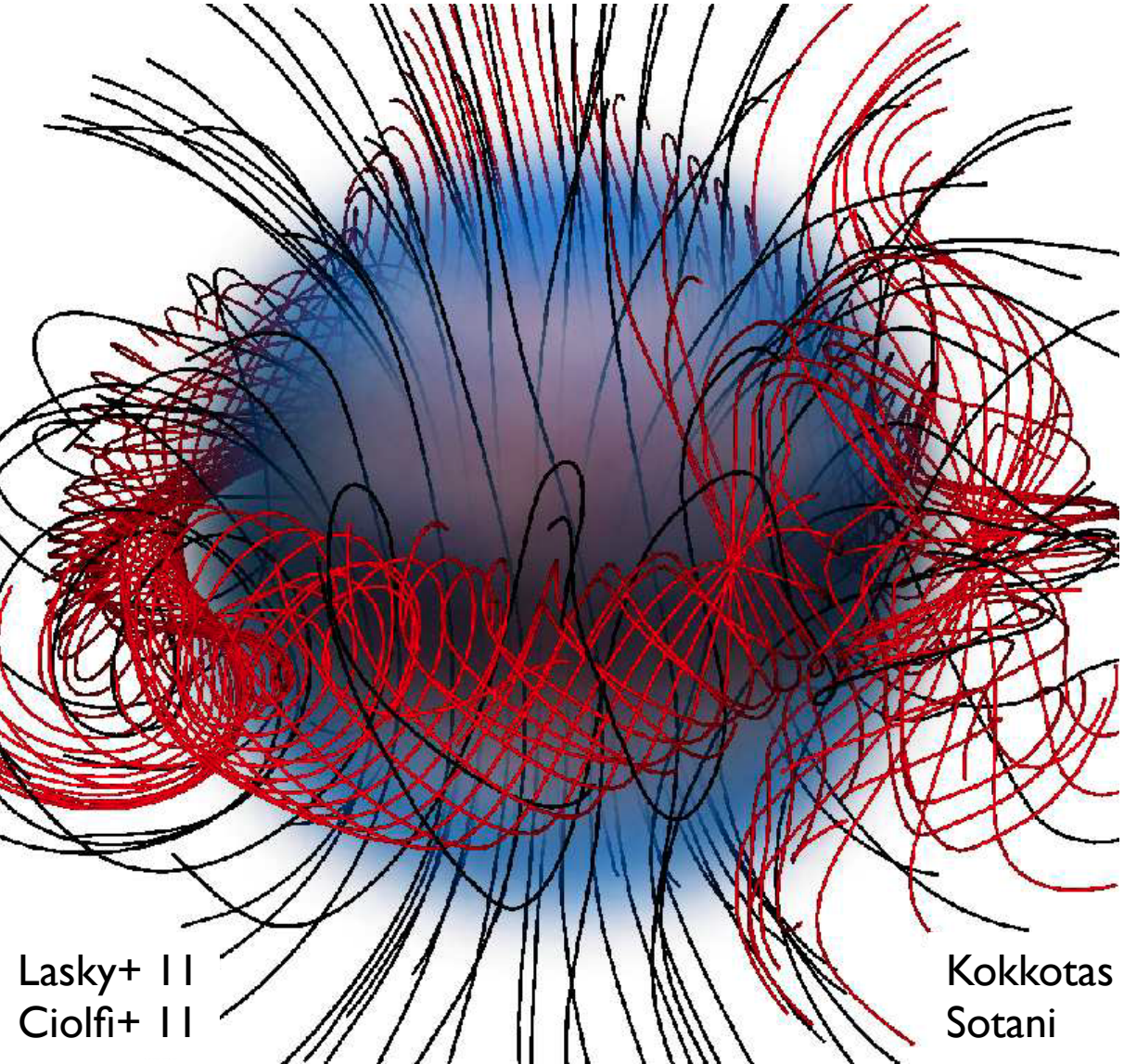

Lasky+ 11
Ciolfi+ 11

Kokkotas
Sotani

Magnetar

NS w/ B >10^{14} G

Flares

E_{Giant}>$10^{44\text{-}46}$ erg

Oscillations

⇒ GW?

KI 01
Kashiyama
& KI 11

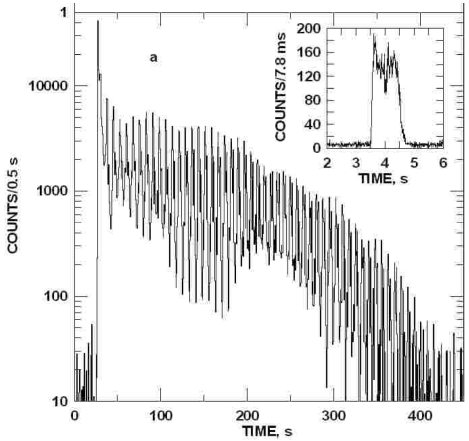

GW from Magnetar Flare

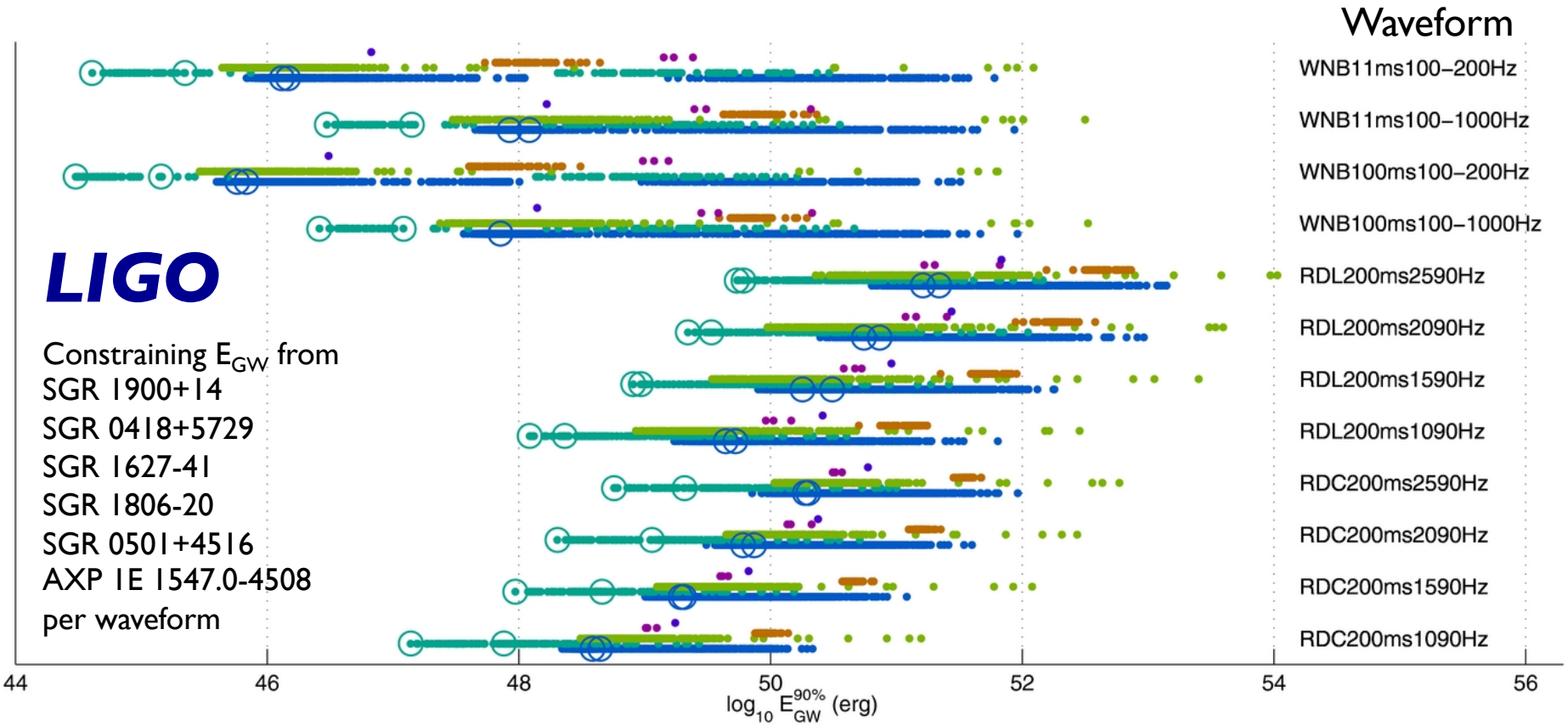

Fluid polar mode

$$f_s \approx \frac{c_s}{R} \approx \text{kHz}$$

$$\tau_{GW} \approx 0.1 \text{ sec}$$

But search only for $t_{GW} < 10^3$ sec

Pulsar Timing Array

$$f \simeq \frac{1}{\pi}\sqrt{\frac{GM}{R^3}} \sim 20\ \mathrm{Hz}\left(\frac{M}{3M_\odot}\right)^{1/2}\left(\frac{R}{500\,\mathrm{km}}\right)^{-2/3}$$

Massive BH merger
⇒ f<10Hz
⇒ Seismic noise

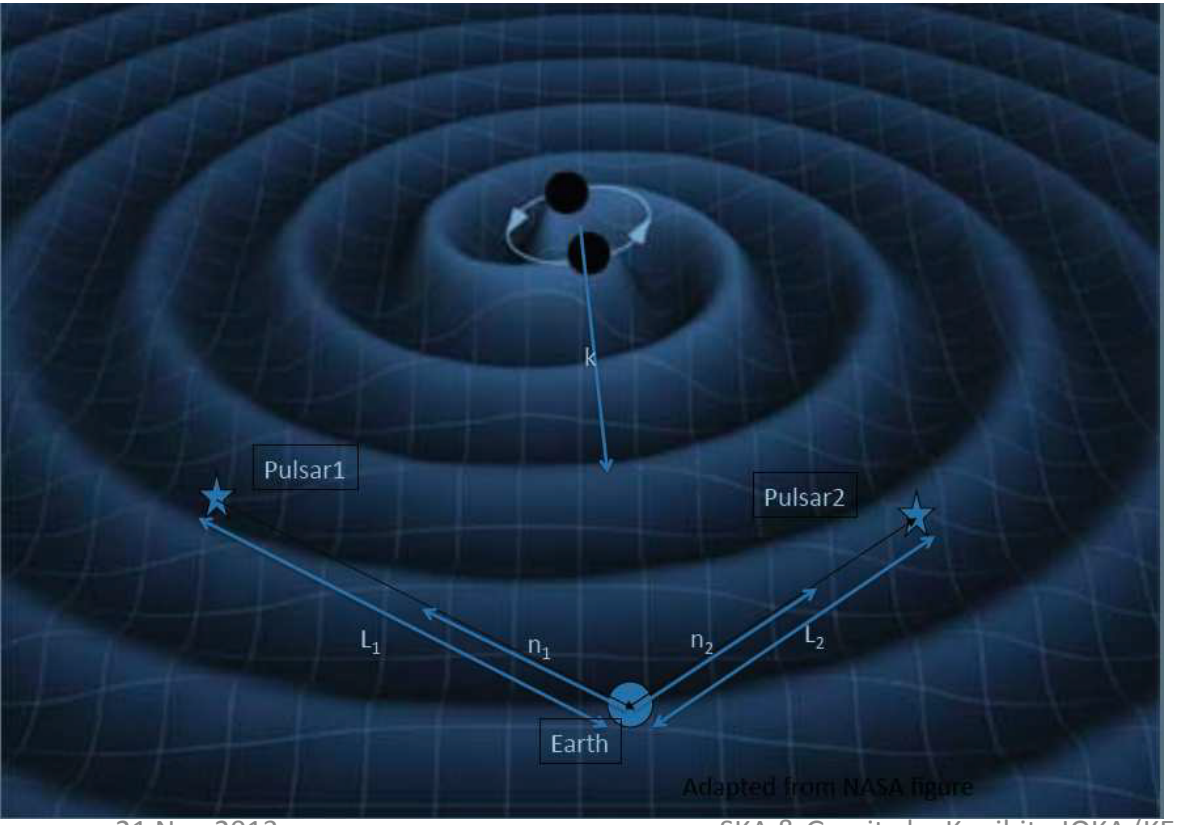

Earth term correlate
Quadrupole signal
f~1/T~1/10yr~nHz
h~σ_{rms}/T
~100ns/10yr~10^{-15}
λ_{gw}~1-10 lyr
d_{PSR}~1000 lyr

Lommen 12

GW Background

Hierarchical galaxy merger ⇒ SMBH binary

GW signal overlap ⇒ Stochastic background

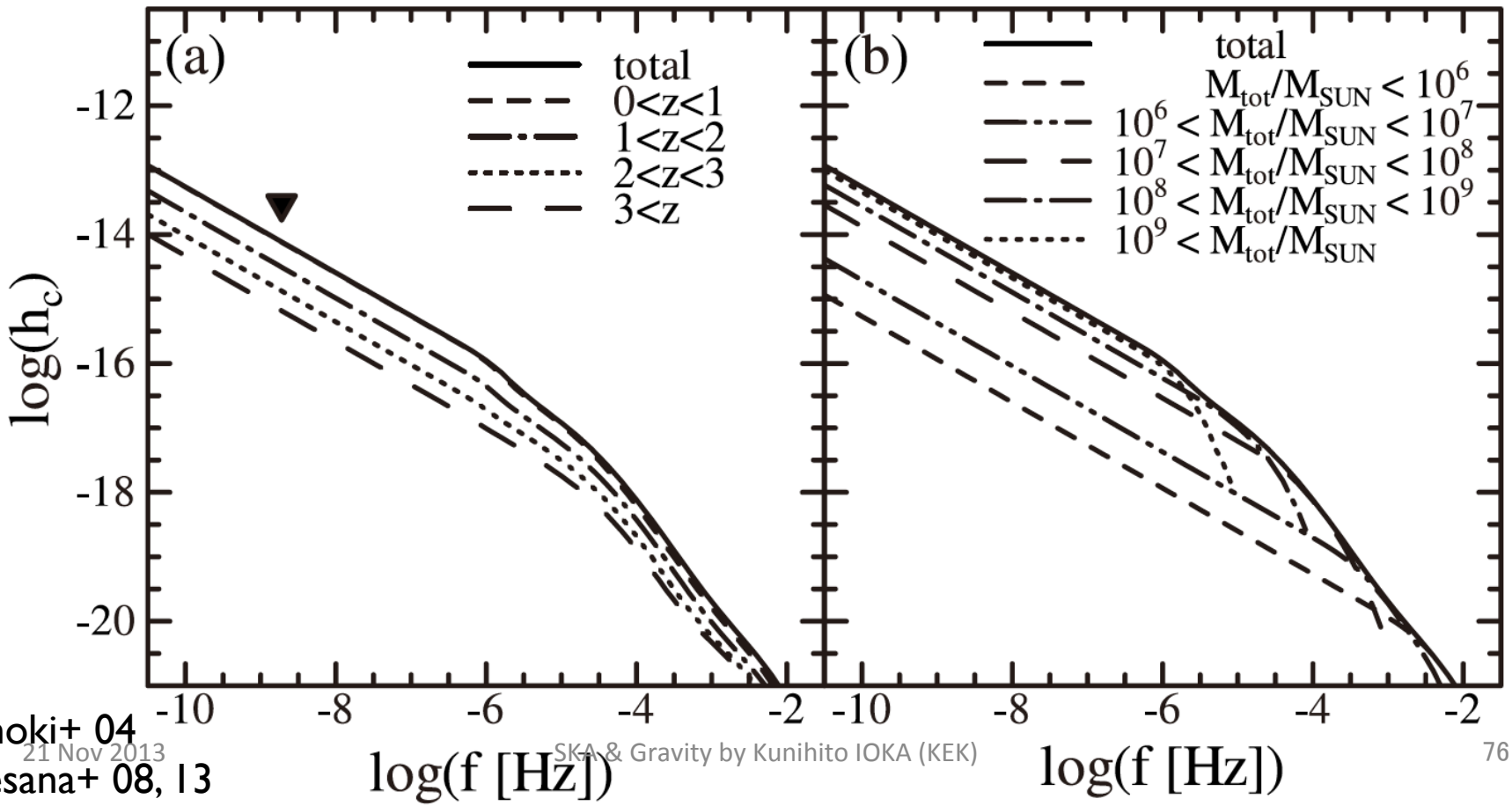

Enoki+ 04
Sesana+ 08, 13

PTA Constraints

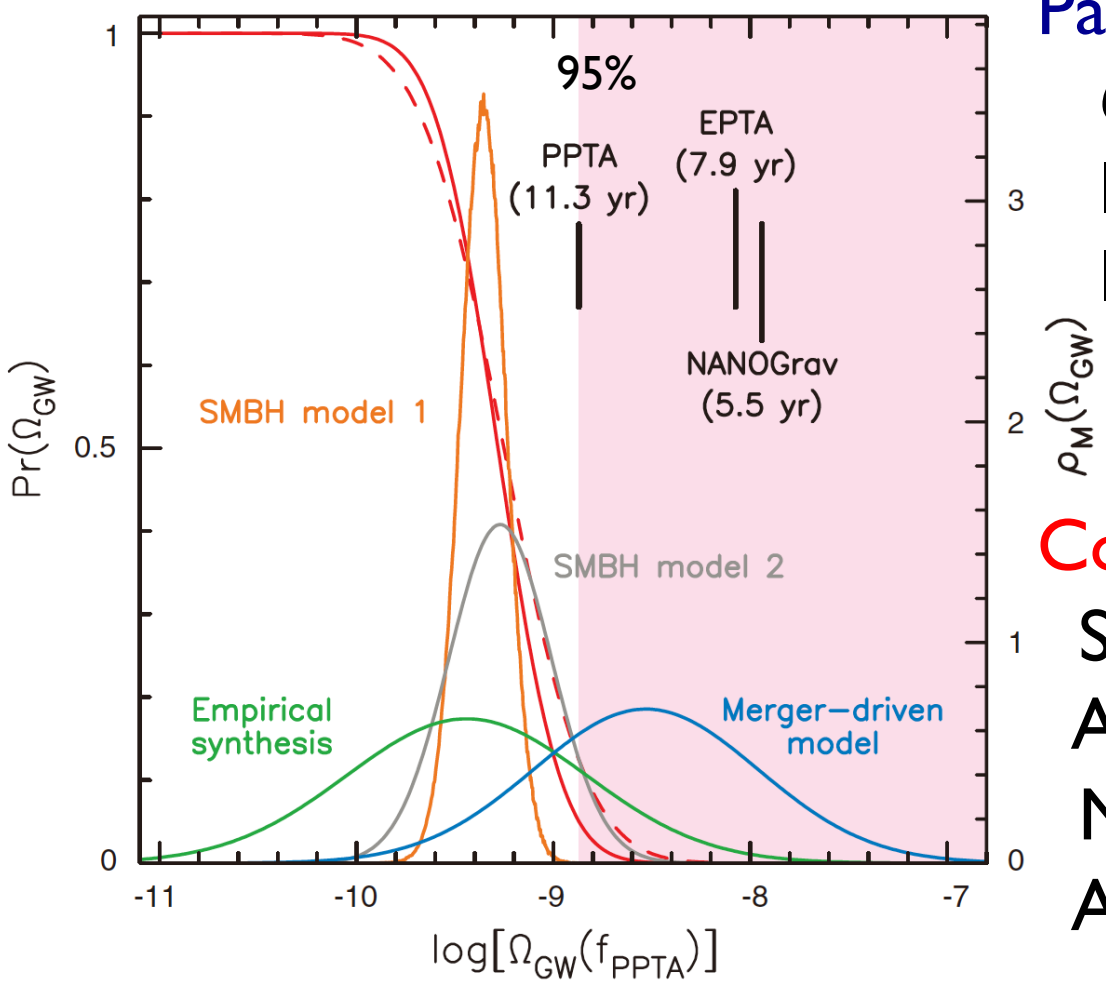

Shannon+13

Parkes Pulsar Timing Array

- 6 pulsars
- lowest noise
- longest obs.

Constrain SMBH models

- Satisfy M-σ relation
- Assume circular orbits
- Millennium Simulation 50%
- A_{95}<2e-15

PTA with SKA

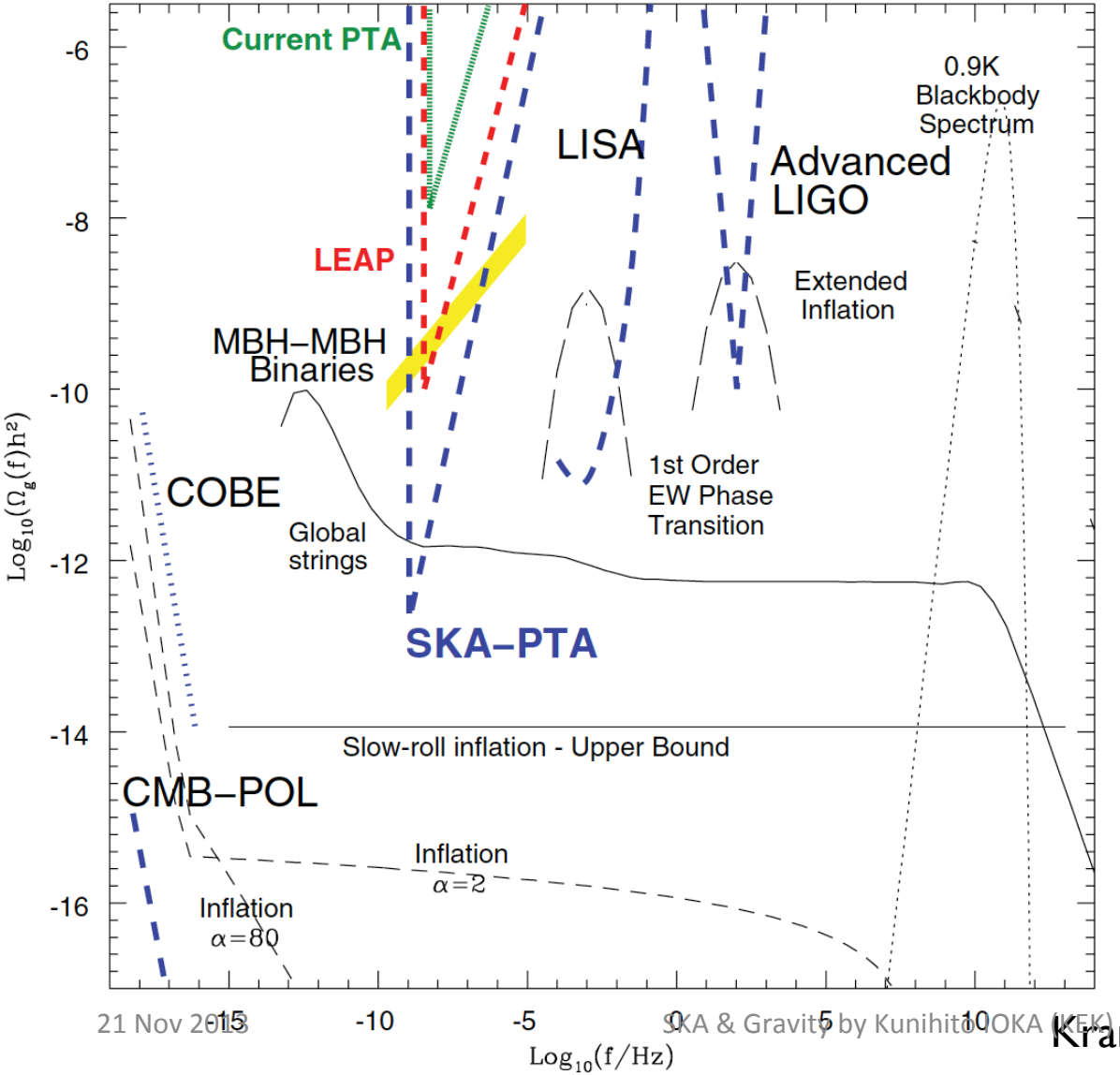

SMBH binary
Cosmic string
Inflation
Phase transition

Large European Array for Pulsars
SKA

Kramer+ 04, 11

Future PTA

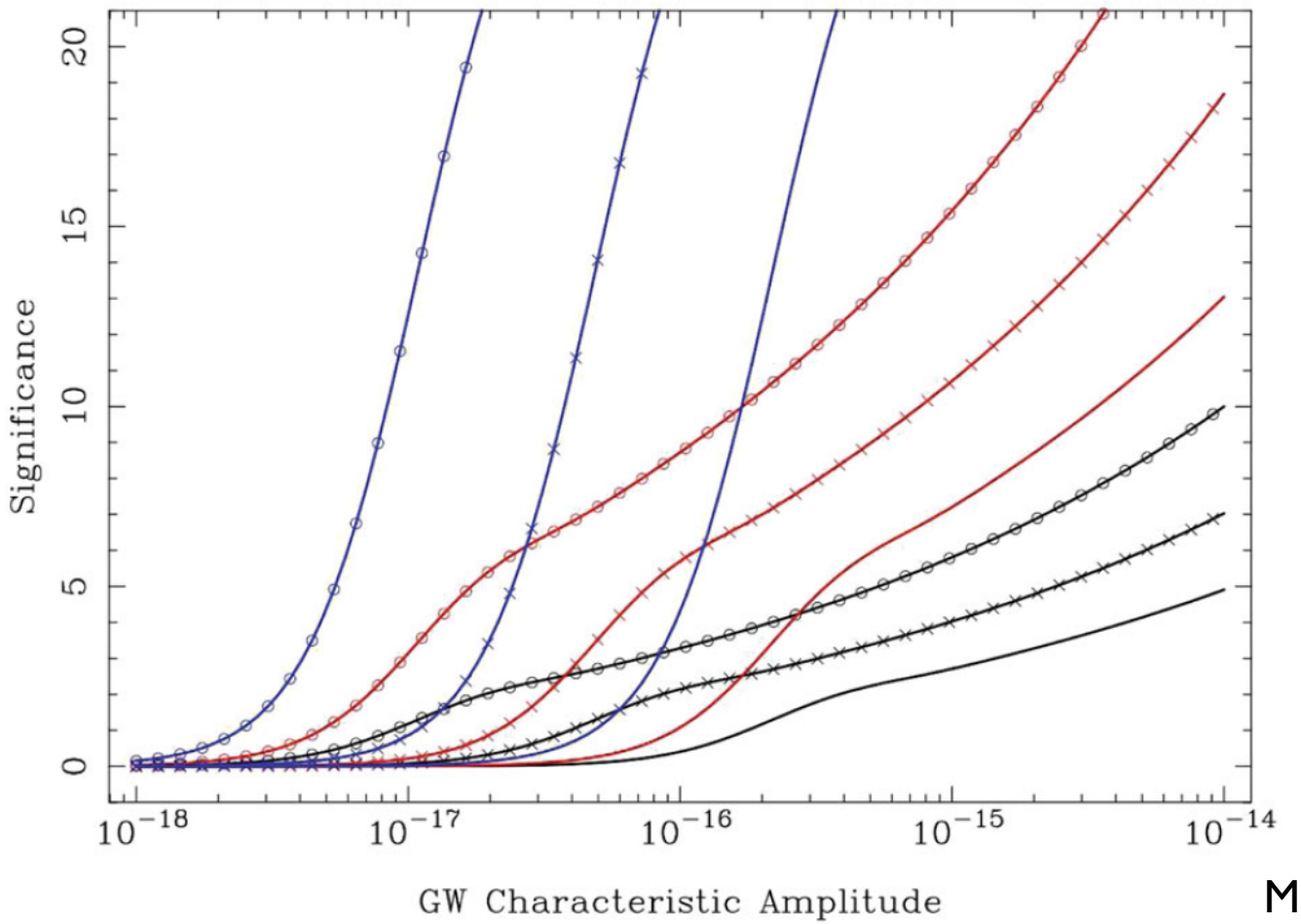

Manchester+ 13

Figure 12. Sensitivity of a PTA to a stochastic background of GWs as a function of total data span T_{obs}, number of pulsars N in the PTA, and assuming 100-ns rms timing residuals. Black lines are for $N_{psr} = 20$ and T_{obs} of 5 yr (unmarked), 10 yr (×), and 20 yr (○), respectively. Red lines are similar for $N_{psr} = 50$ and blue lines for $N_{psr} = 200$.

GW Astronomy by PTA

- We may expect a single strong source
  - Direction within possibly ~arcmin
  - Waveform
  - Time machines (Earth term & Pulsar term)
  - Luminosity distance
- First detection of GW memory
  - Sensitive to mergers far higher than nHz
- Tests of gravity

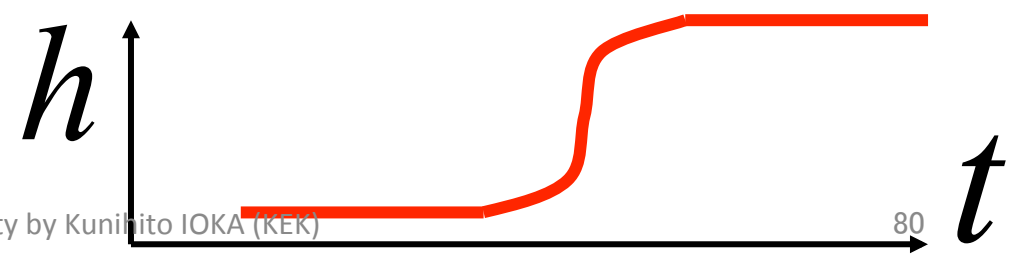

Graviton Mass

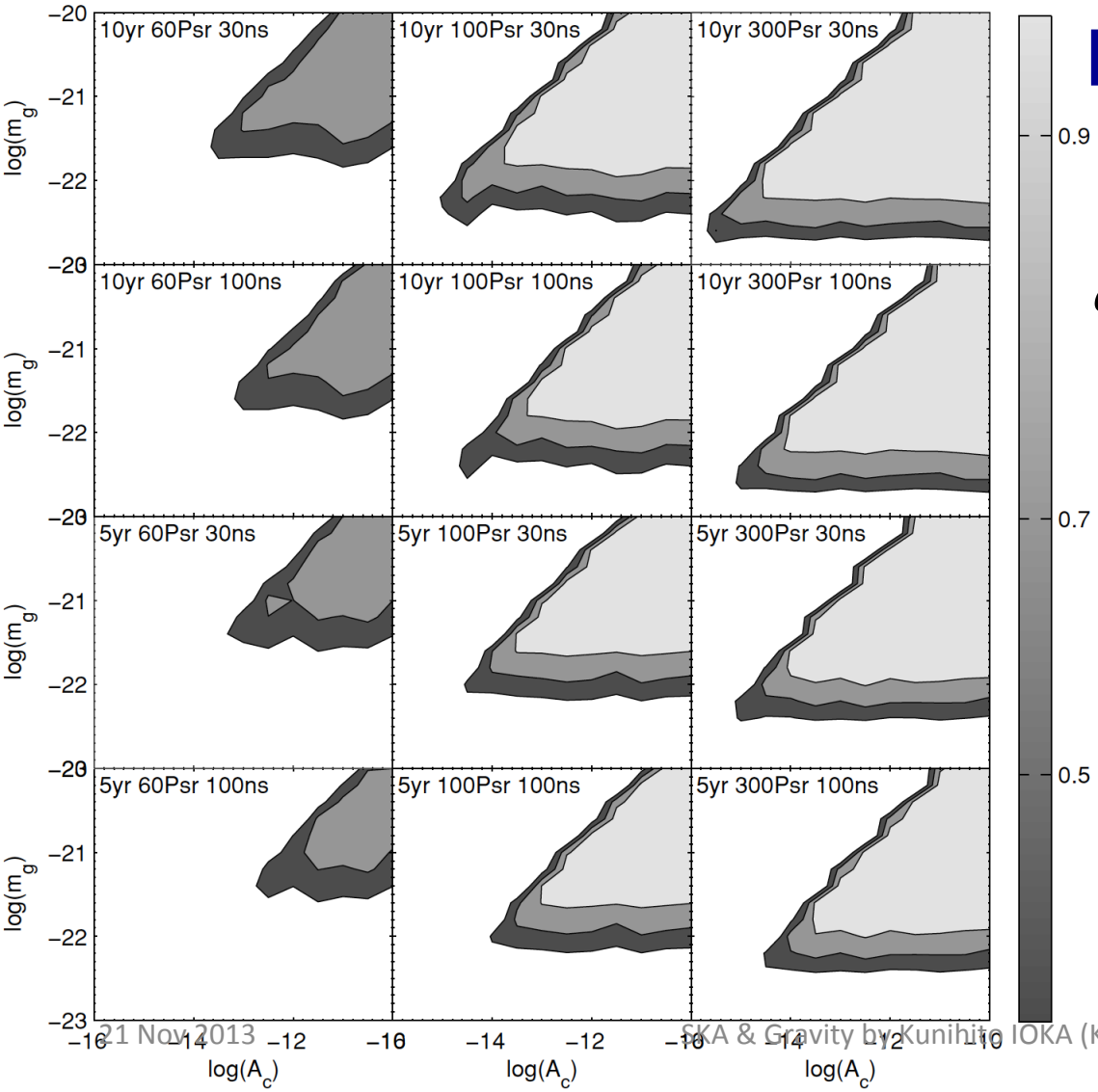

Dispersion relation of gravitational waves

$$\omega_{cut} \equiv \frac{m_g c^2}{\hbar} = 3 \text{ rad yr}^{-1} \left(\frac{m_g}{10^{-23} \text{eV}} \right)$$

Pulsar Timing Array Gravitational waves

T_{obs} ~ day-year

$\Rightarrow \omega_g \sim 1/T$

$\Rightarrow m_g < 10^{-22}$eV

Also polarization

Lee+ 08, 10

TABLE I. A list of the most significant mass limits of various types for the photon and graviton.

Description of method	$\lambda_C \gtrsim$ (m)	$\mu \lesssim$ (eV)	$\mu \lesssim$ (kg)	Comments
1. Secure photon mass limits:				
Dispersion in the ionosphere (Kroll, 1971a)	8×10^{5}	3×10^{-13}	10^{-49}	
Coulomb's law (Williams, Faller, and Hill, 1971)	2×10^{7}	10^{-14}	2×10^{-50}	
Jupiter's magnetic field (Davis, Goldhaber, and Nieto, 1975)	5×10^{8}	4×10^{-16}	7×10^{-52}	
Solar wind magnetic field (Ryutov, 2007)	2×10^{11} (1.3 AU)	10^{-18}	2×10^{-54}	
2. Speculative photon-mass limits:				
Extended Lakes method (Lakes, 1998; Luo, Tu, Hu, and Luan, 2003a, 2003b; Goldhaber and Nieto, 2003)	3×10^{9} $\Leftrightarrow 3\times10^{12}$	7×10^{-7} $\Leftrightarrow 7\times10^{-20}$	10^{-52} $\Leftrightarrow 10^{-55}$	$\lambda_C \sim 4R_\odot$ to 20 AU, depending on **B** speculations
Higgs mass for photon (Adelberger, Dvali, and Gruzinov, 2007)	No limit feasible			Strong constraints on 3D Higgs parameter space
Cosmic magnetic fields (Yamaguchi, 1959; Chibisov, 1976; Adelberger, Dvali, and Gruzinov, 2007)	3×10^{19} (10^{3} pc)	6×10^{-27}	10^{-62}	Needs const **B** in galaxy regions
3. Graviton mass limits:				
Gravitation wave dispersion (Finn and Sutton, 2002)	3×10^{12}	8×10^{-20}	10^{-55}	Question mark for scalar graviton
Pulsar timing (Baskaran *et al.*, 2008)	2×10^{16}	9×10^{-24}	2×10^{-59}	Fluctuations due to graviton phase velocity
Gravity over cluster sizes (Goldhaber and Nieto, 1974)	2×10^{22}	10^{-29}	2×10^{-65}	
Near field constraints (Gruzinov, 2005)	3×10^{24} (10^{8} pc)	6×10^{-32}	10^{-67}	For DGP model
Far field constraints (Dvali, Gruzinov, and Zaldarriaga, 2003)	3×10^{26} (10^{10} pc)	6×10^{-34}	10^{-69}	For DGP model

Goldhaber & Nieto 10

LISA ⇒ eLISA

No seismic noise

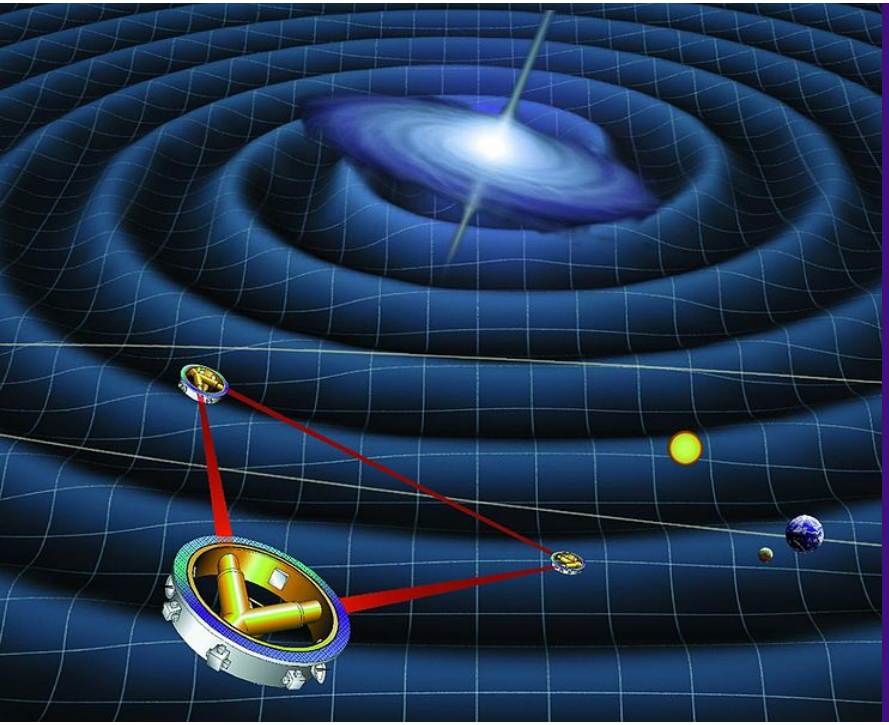

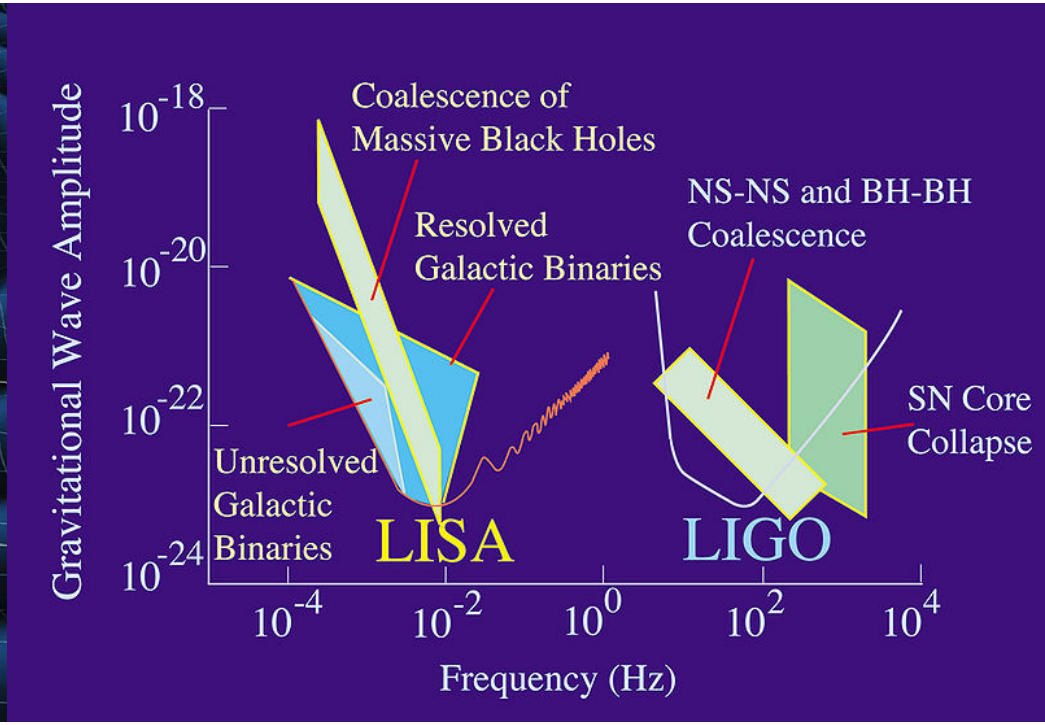

Arm length: 5×10^{9}m ⇒ 10^{9}m

Orbit may be drifting away from Earth

2 yr lifetime (up to 5 yr)

LISA pathfinder

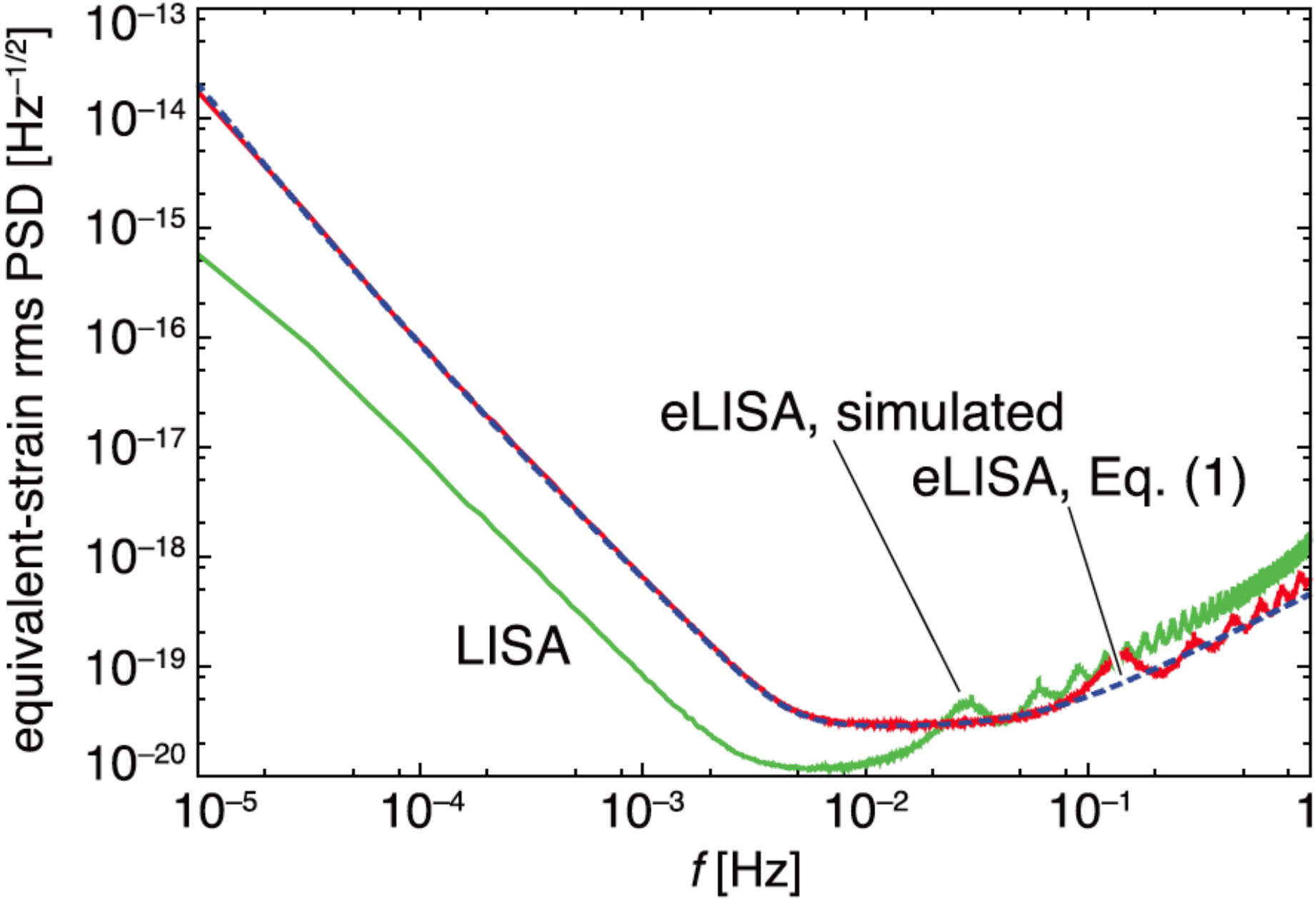

Amaro-Seoane+ 12

スペース重力波アンテナDECIGO

Deci-hertz Interferometer Gravitational Wave Observatory

アーム長：1000 km
ミラー直径：1 m
レーザー波長：532 nm

レーザーパワー：10 W
ミラー質量：100 kg

干渉計3台で1クラスター

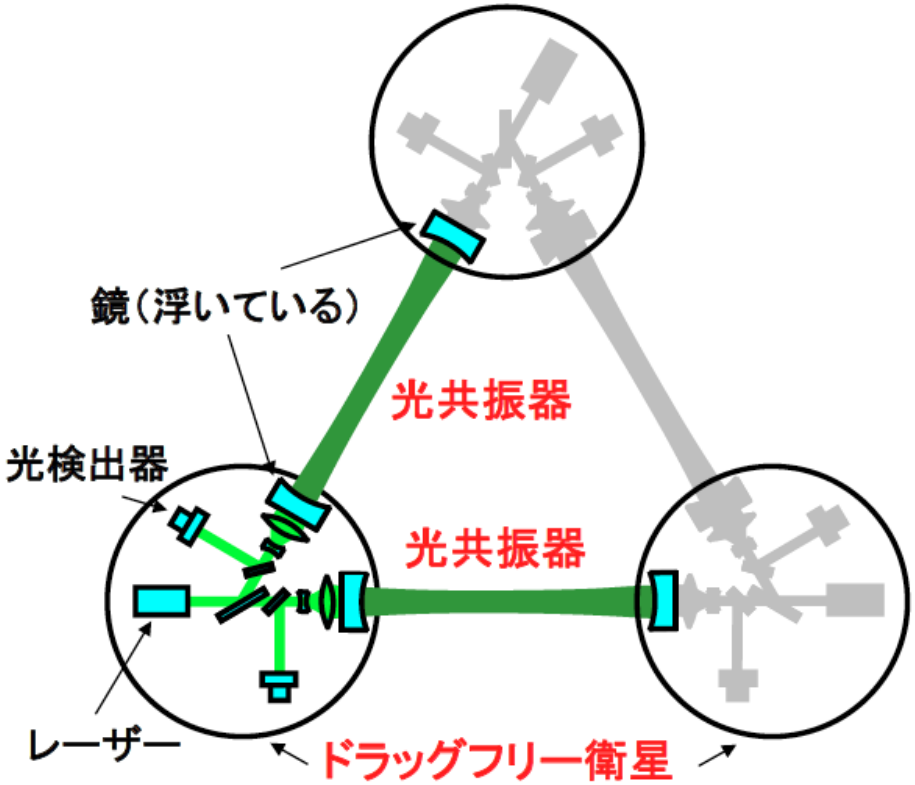

©Kawamura

軌道とコンステレーション（案）

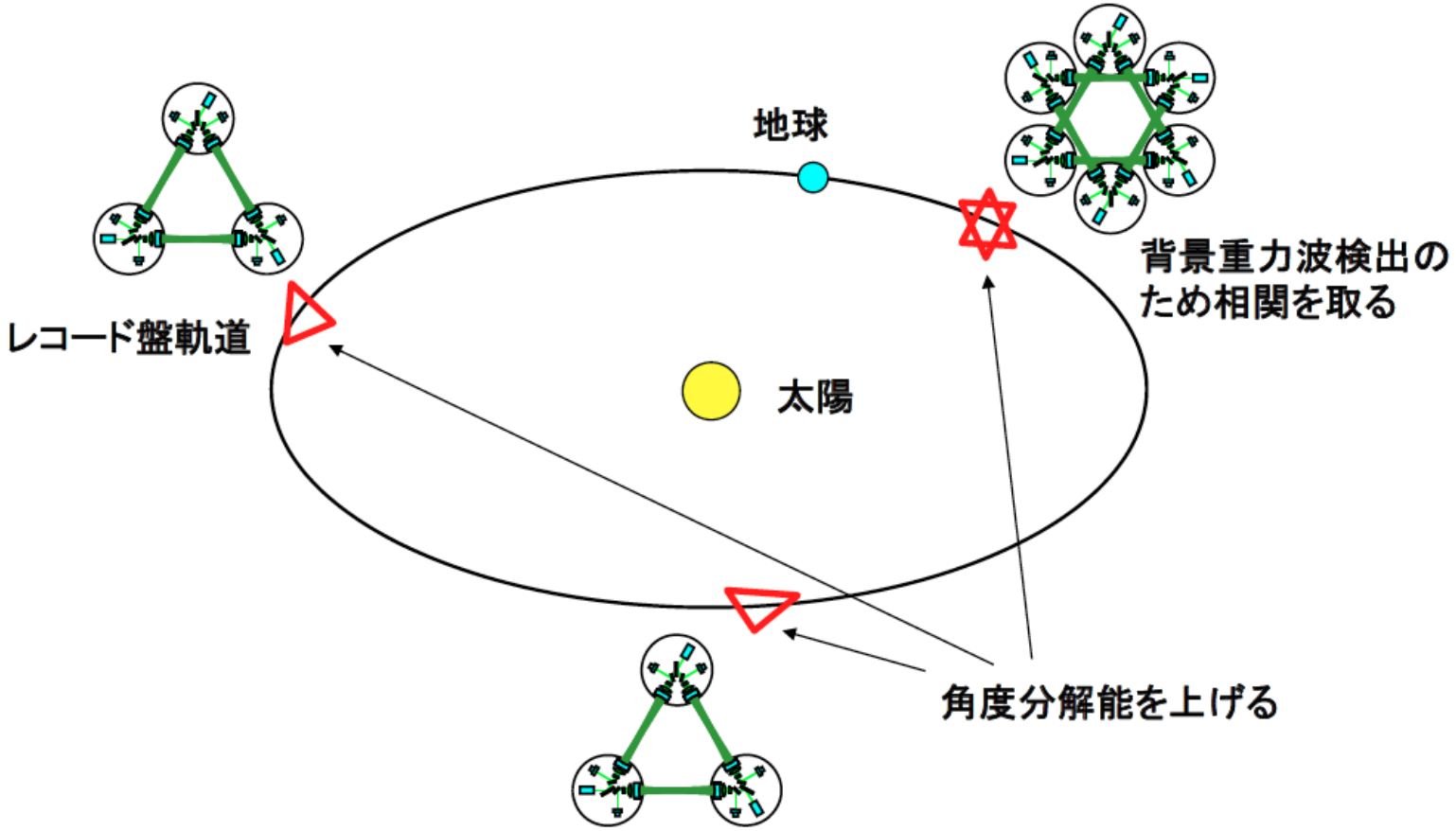

©Kawamura

DECIGOの目標感度と得られるサイエンス

巨大ブラックホール形成のメカニズム解明

ダークマターの探索

一般相対性理論の検証

インフレーションの検証

宇宙膨張加速度の計測

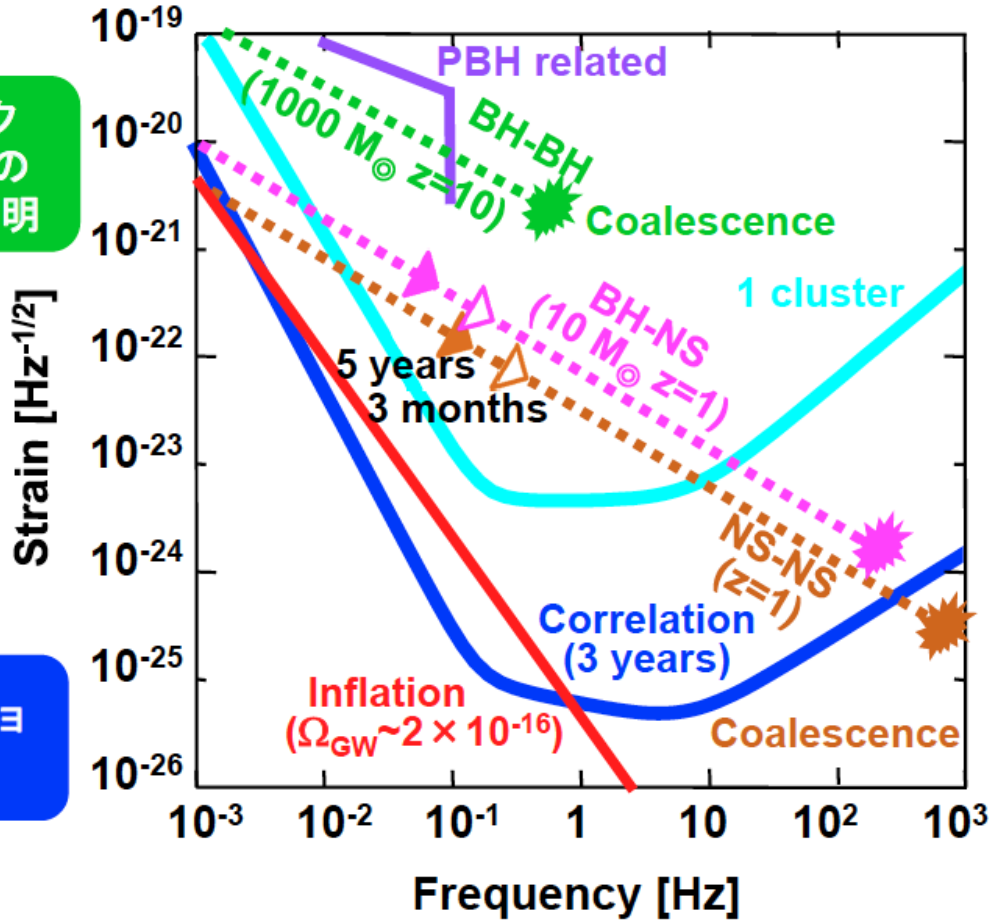

©Kawamura

宇宙の膨張加速度の直接計測

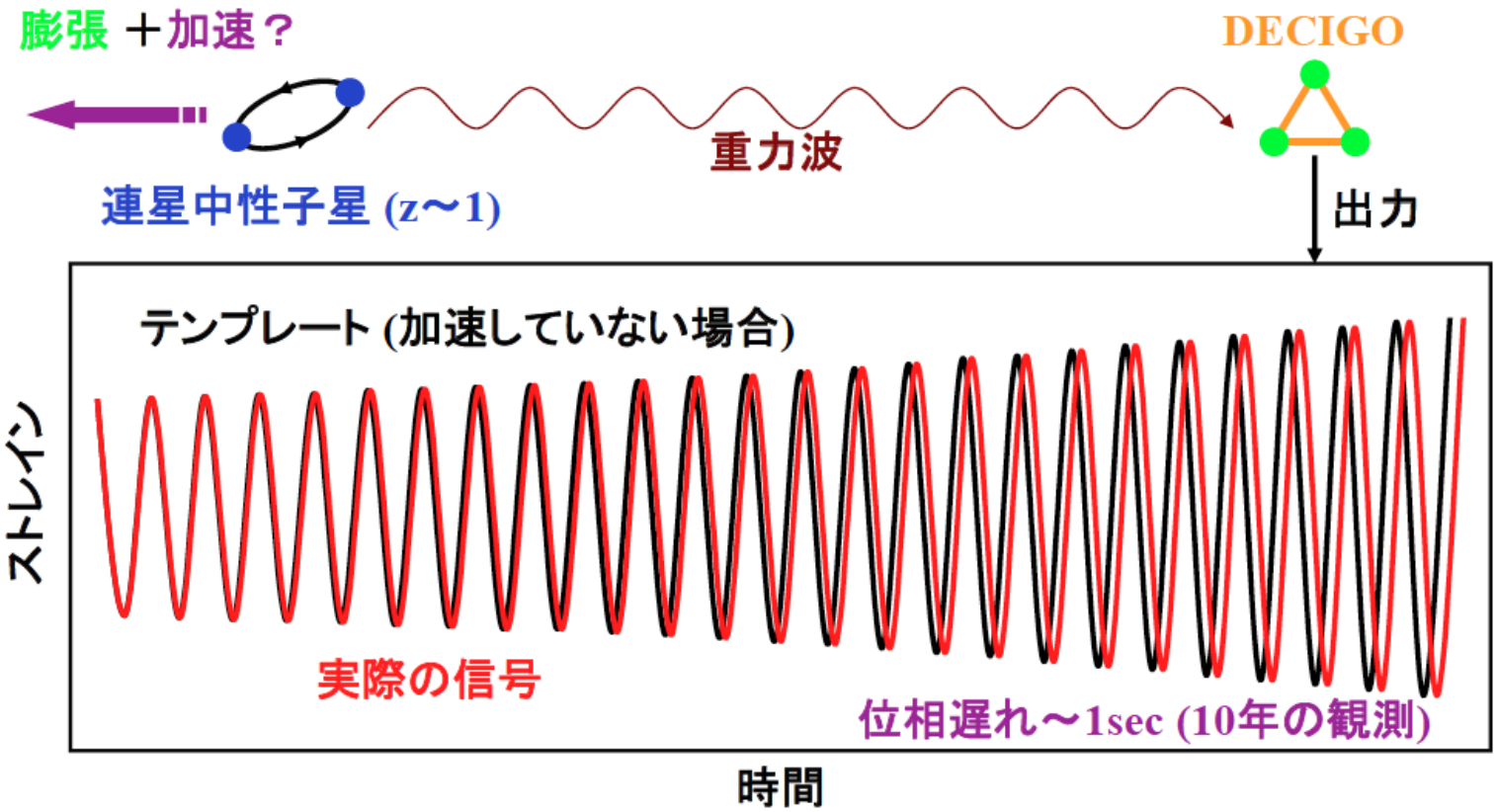

Seto, Kawamura, Nakamura, PRL 87, 221103 (2001)

©Kawamura

Einstein Telescope

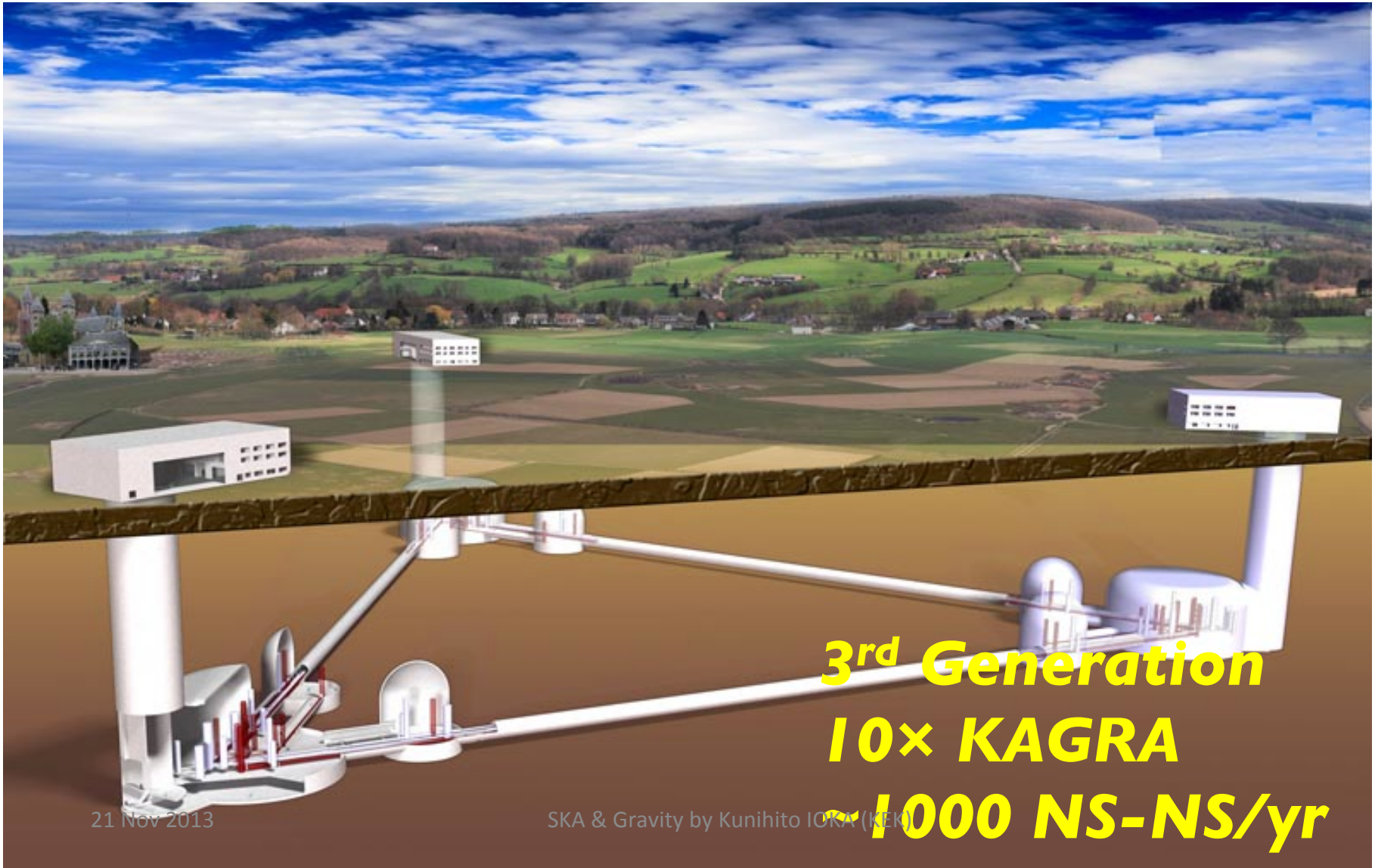

The Gravitational Wave Spectrum

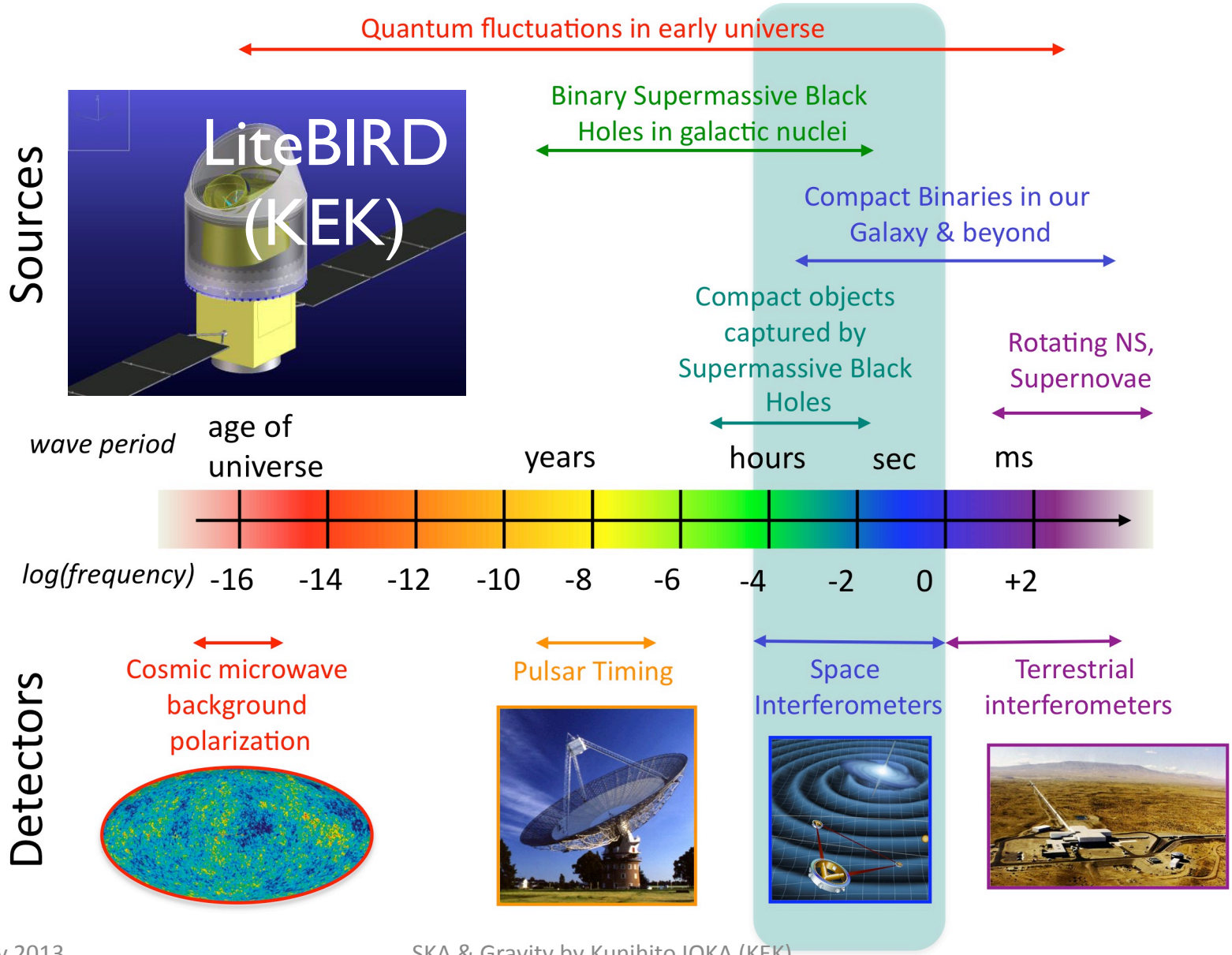

©NASA

Multi-Wavelength

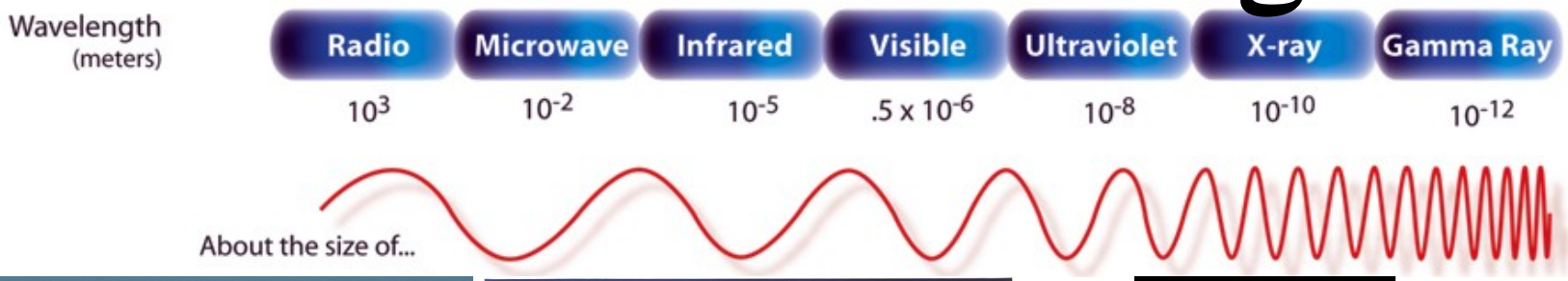

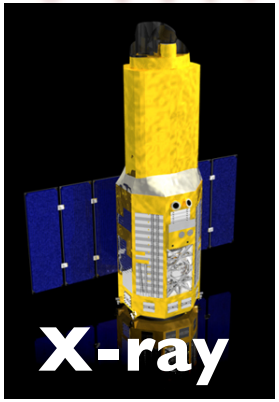

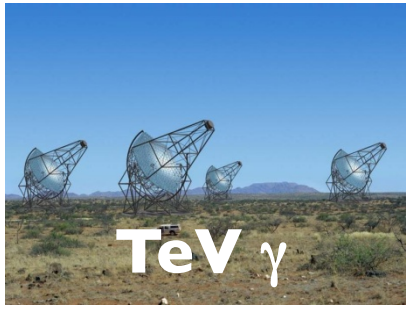

TeV= 10^{12}eV

GeV= 10^{9}eV

20th century observations:

In particular, X-γ-VHE γ

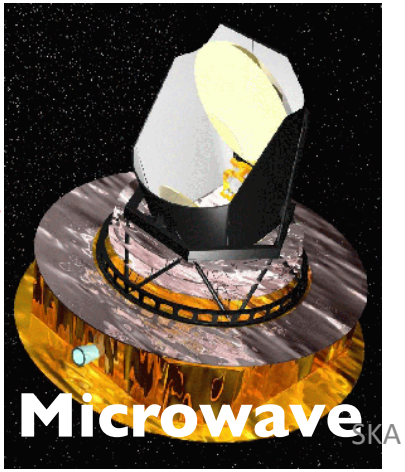

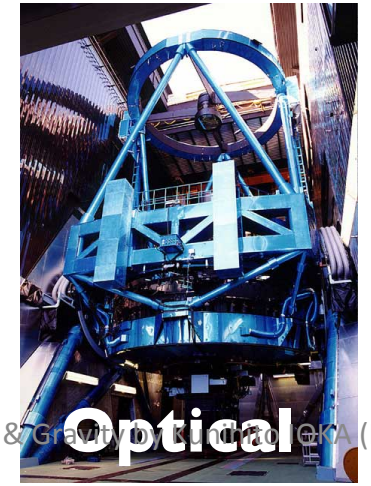

Multi-Messenger

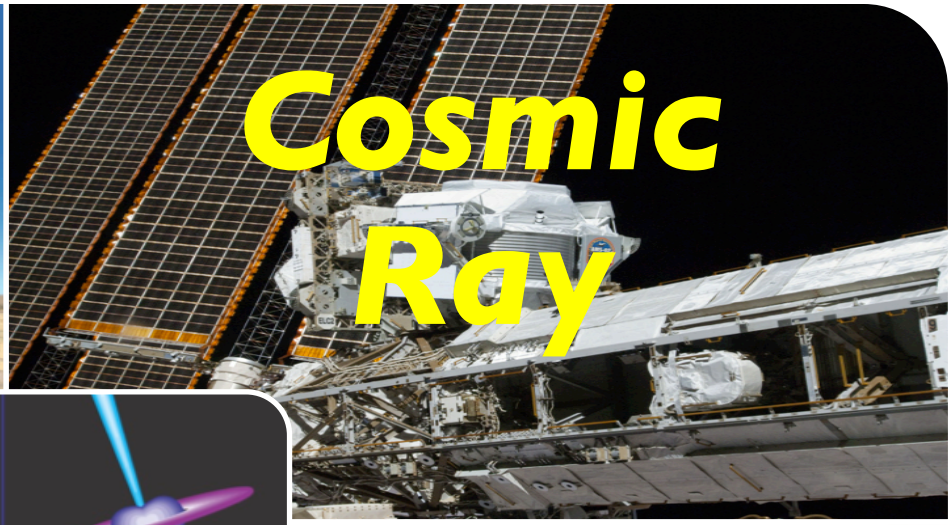

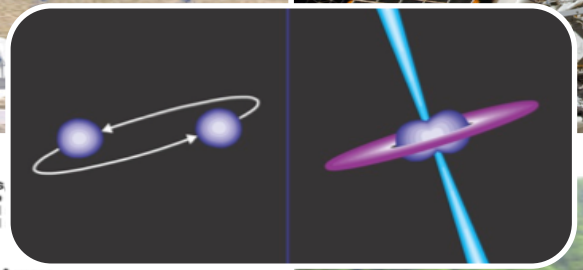

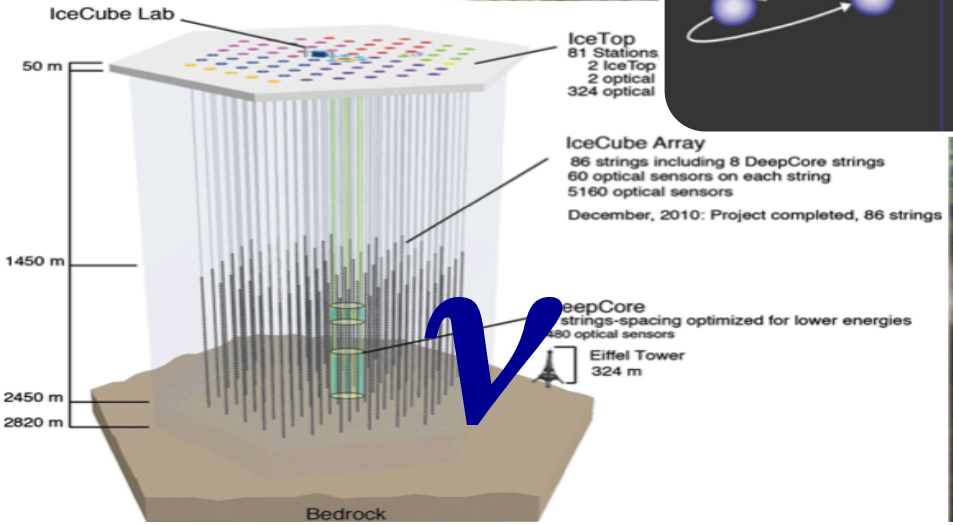

21 Century: Multi-Messenger Era

Counterparts to GW

Gravitational Wave Sources

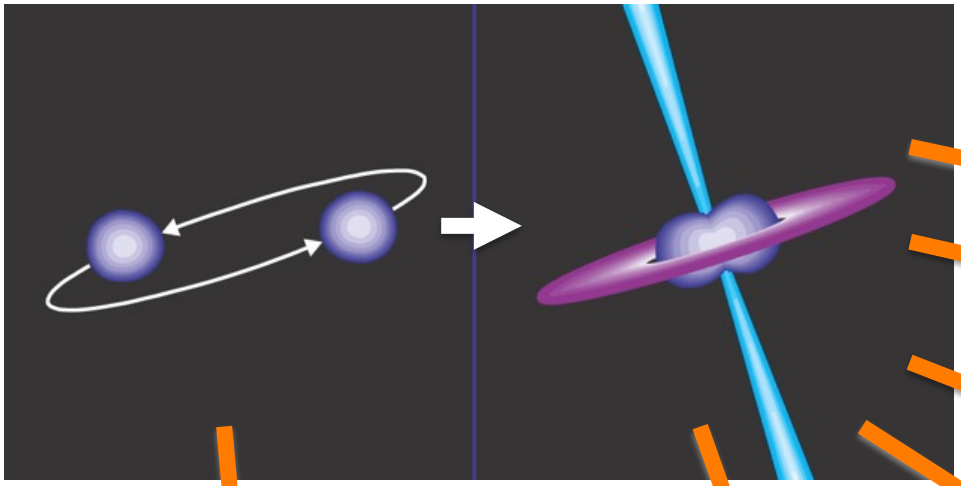

Neutrino

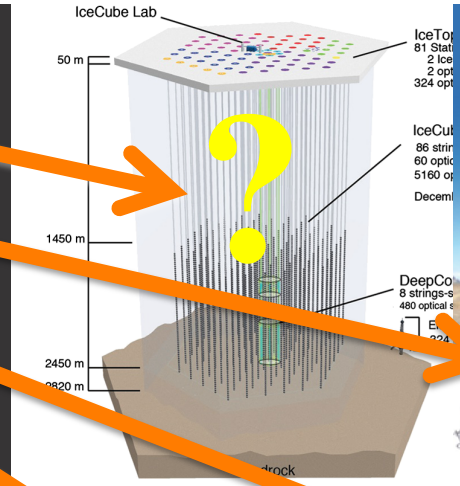

Gamma-ray

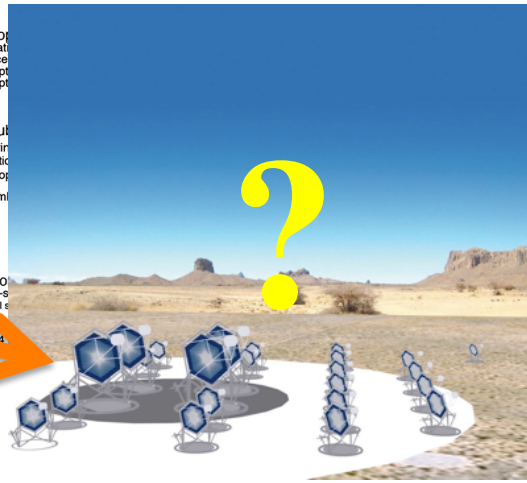

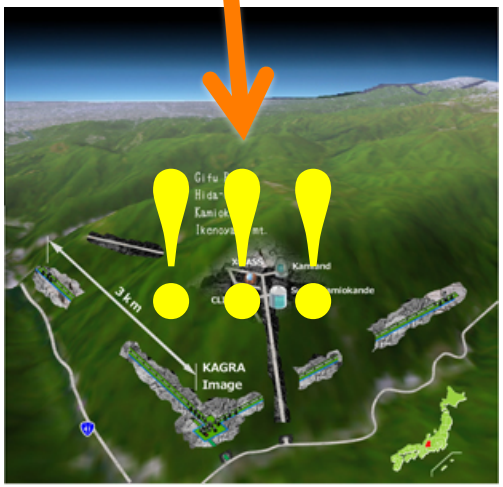

Gravitational wave

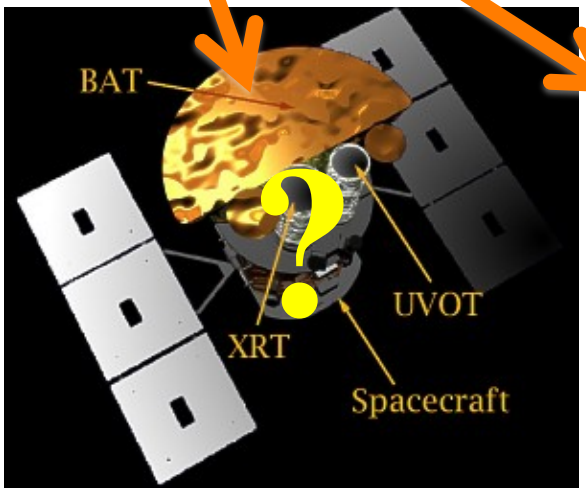

X-ray

IR-Opt

Radio

Counterparts to GW

Gravitational Wave Sources | Neutrino | Gamma-ray

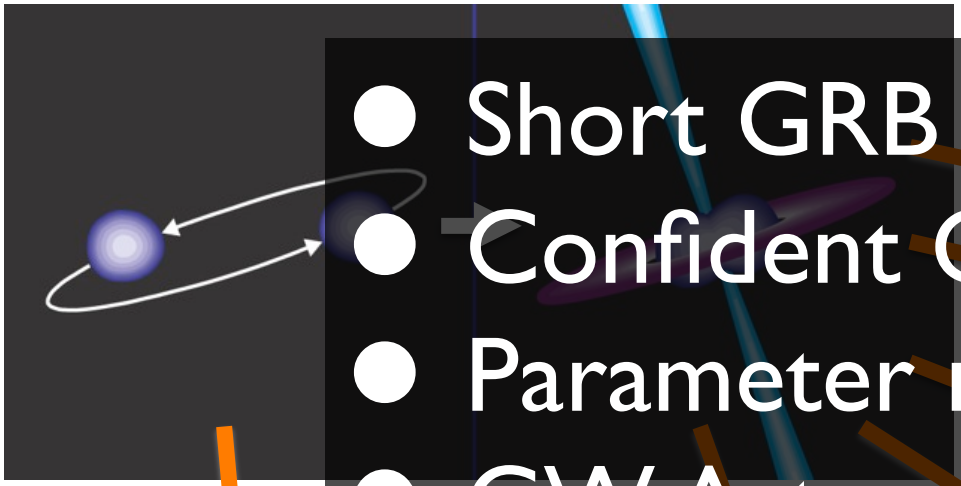

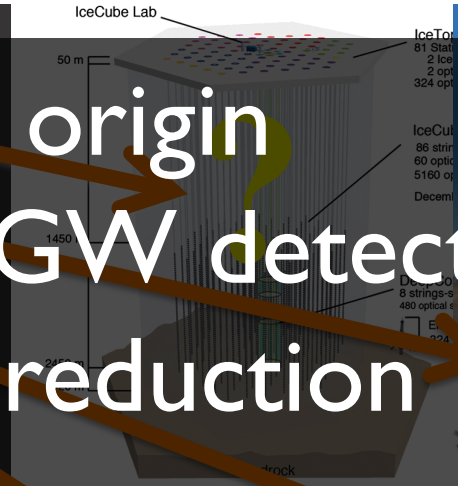

- Short GRB origin
- Confident GW detection
- Parameter reduction
- GW Astronomy
- GW Cosmology
- r-process elements
- Hadron physics

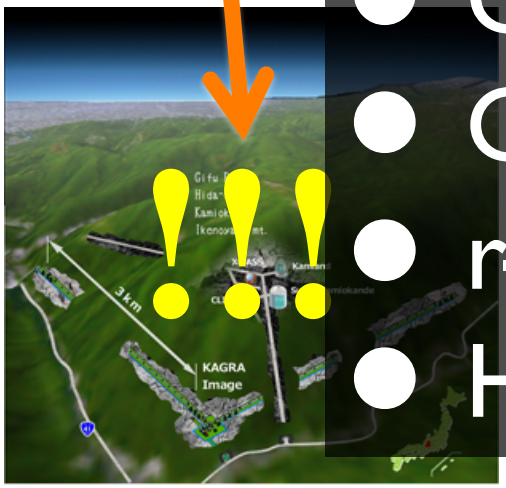

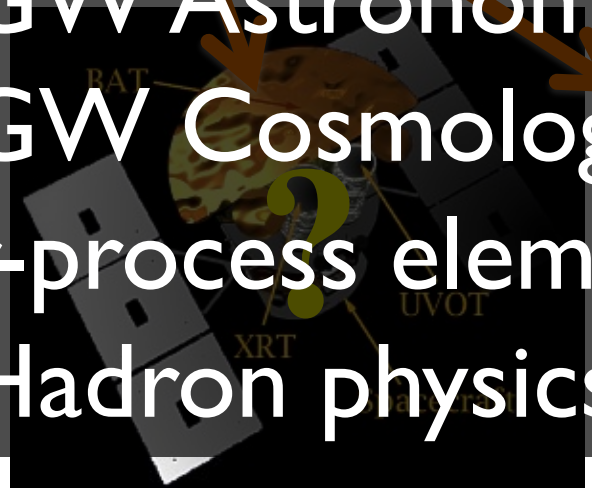

Gravitational wave | X-ray | IR-Opt | Radio

Short GRB = NS Merger?

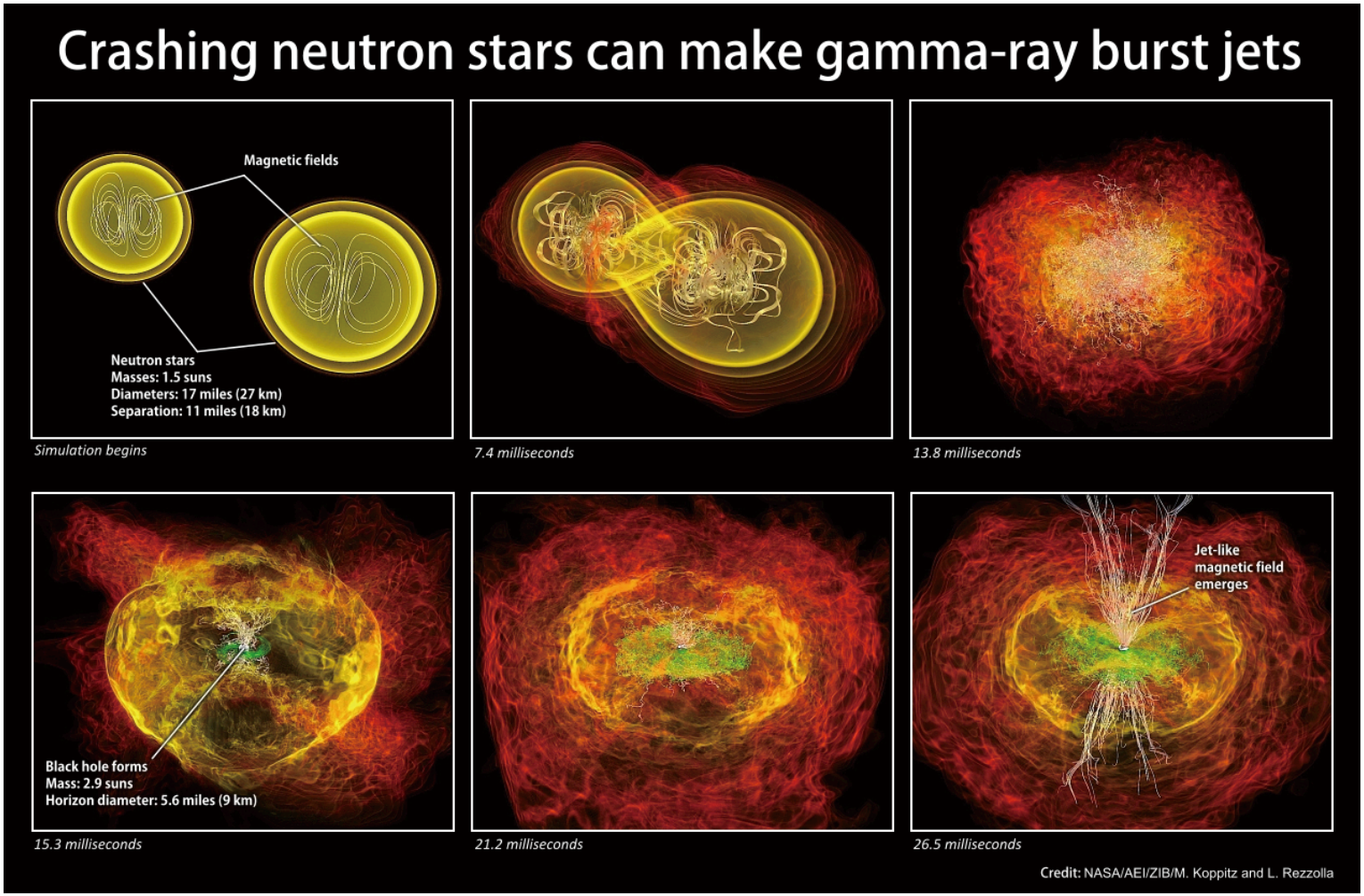

Eichler+ 89
Rezzolla+ 11

Most GRB Jets are Off-Axis ⇒ Faint

©Shibata, Hotokezaka

Merger of 1.3-1.4 M_{sun} NS:

EOS=APR4; stiff but relatively soft

ρ (g/cm^3)

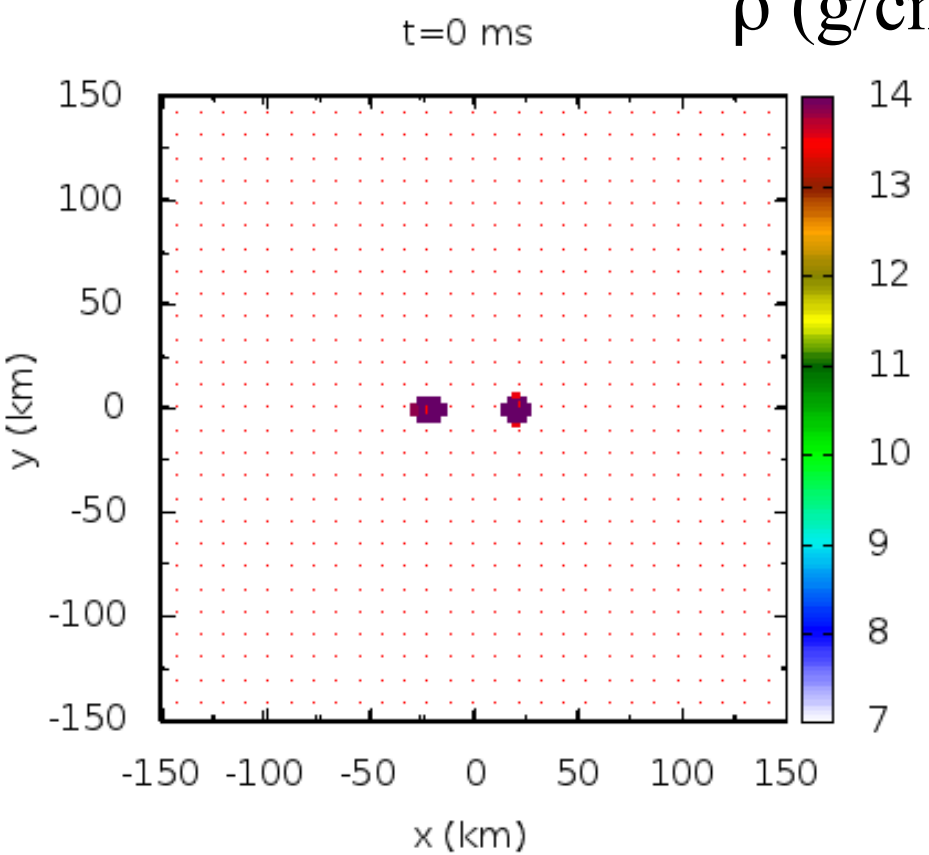

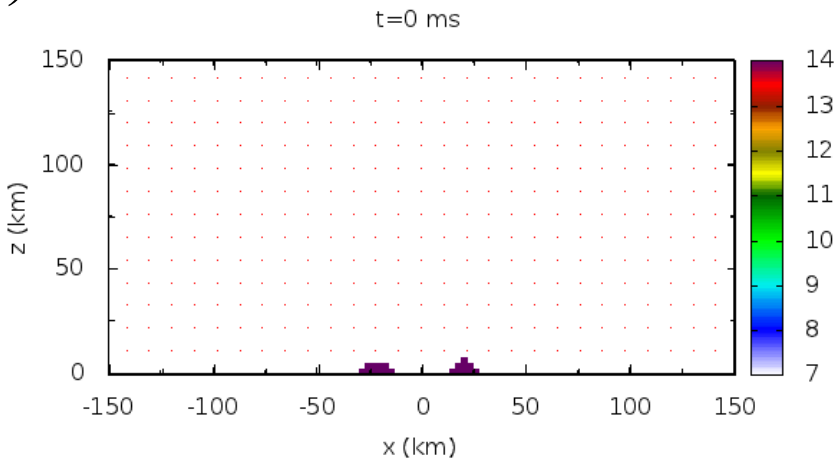

Relatively wider view

Orbital plane

***X-Z* plane**

r-Process

Neutron-rich Ejecta ⇒ n-capture>β decay

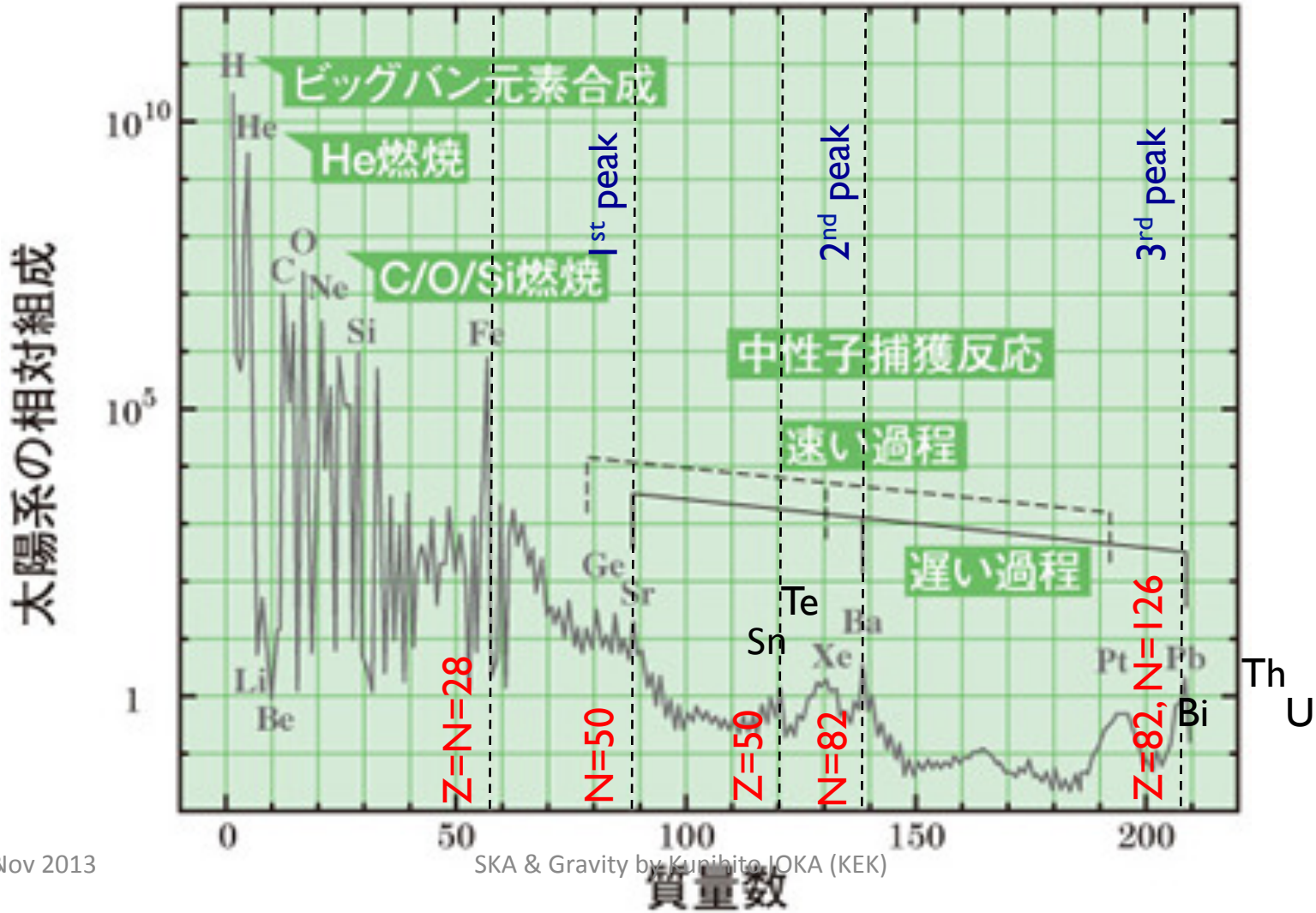

Macro/Kilo-nova

Radioactivity (r-process → β-decay, fission, neutron)

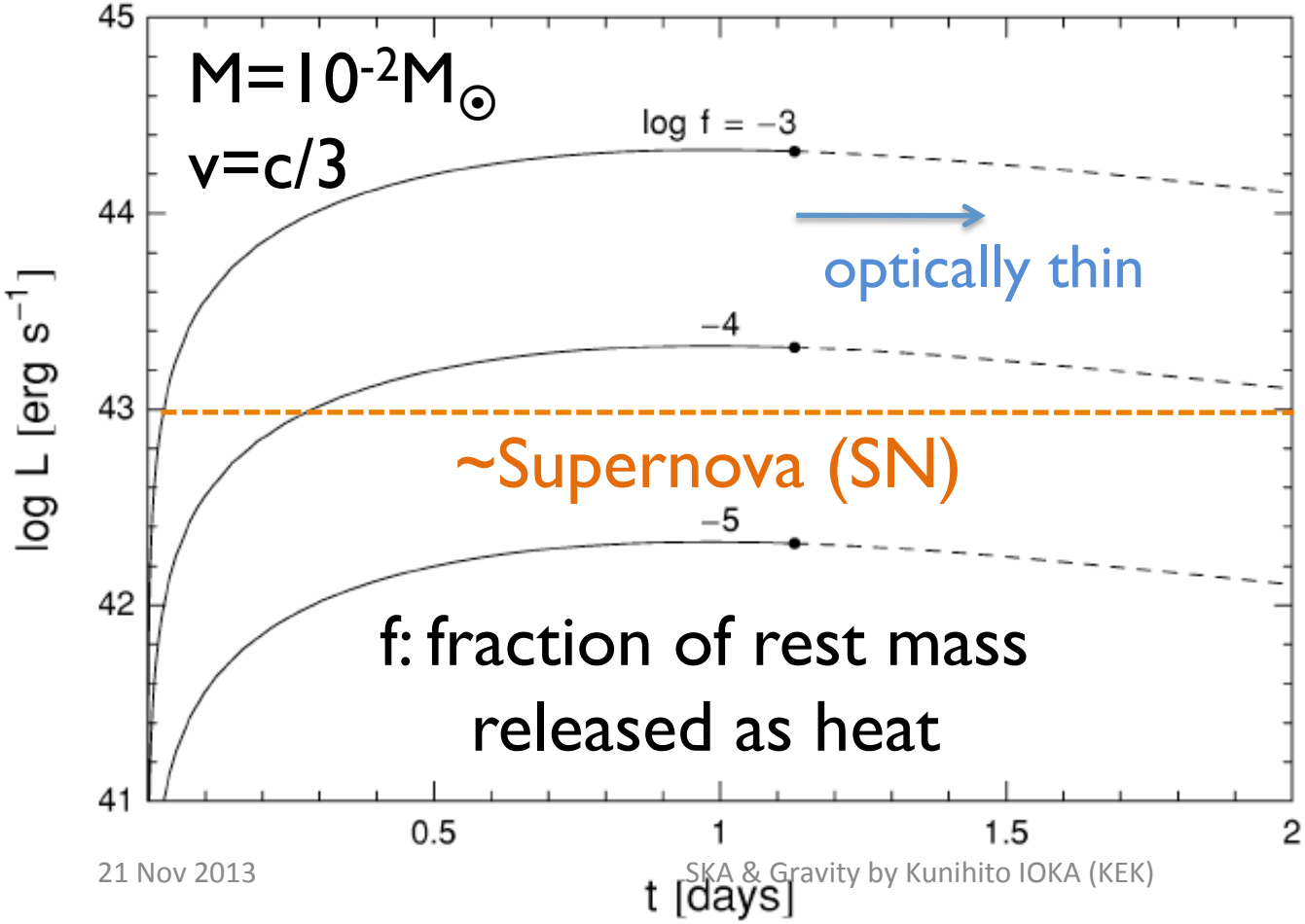

- 超新星-like
- Duration $\propto (M/v)^{1/2}$
- $T \propto (f^2/Mv)^{1/8}$ **~ IR-Opt**
- $f \sim 3\times10^{-6}$

⇒ 暗い超新星

Li & Paczynski 98
Kulkarni 05

Discovery of Macro/Kilo-nova?

Tanvir+ 13
Berger+ 13

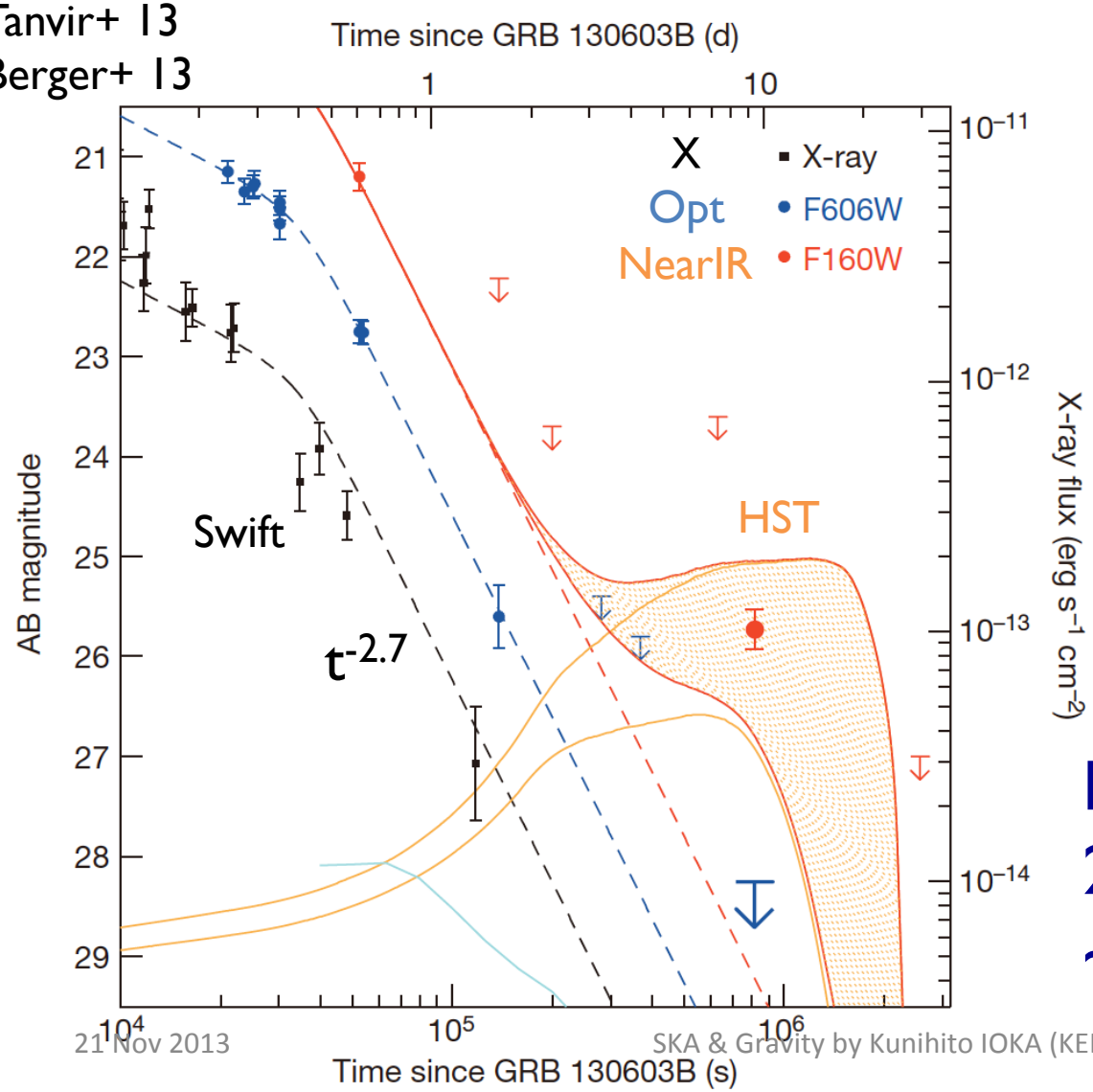

Ejecta with
~0.01-0.1M$_\odot$
~0.1-0.3c
~10^{50}-10^{52}erg

L~10^{41}erg/s @z~0.356
22-23 mag if @200Mpc
~10 days

BH-NS Merger

©Kyutoku

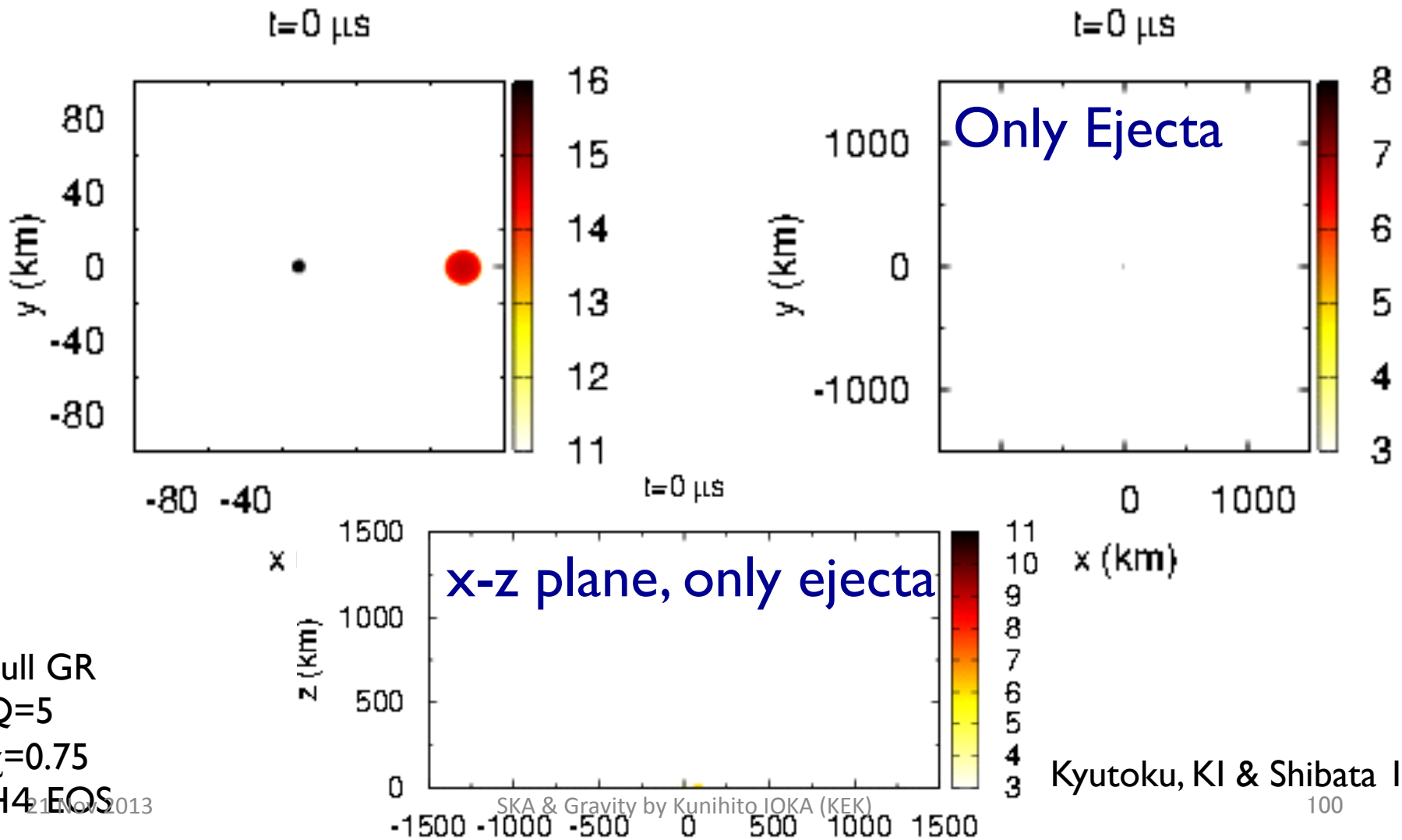

Full GR
Q=5
χ=0.75
H4 EOS

Kyutoku, KI & Shibata 13

Anisotropic Mass Ejection

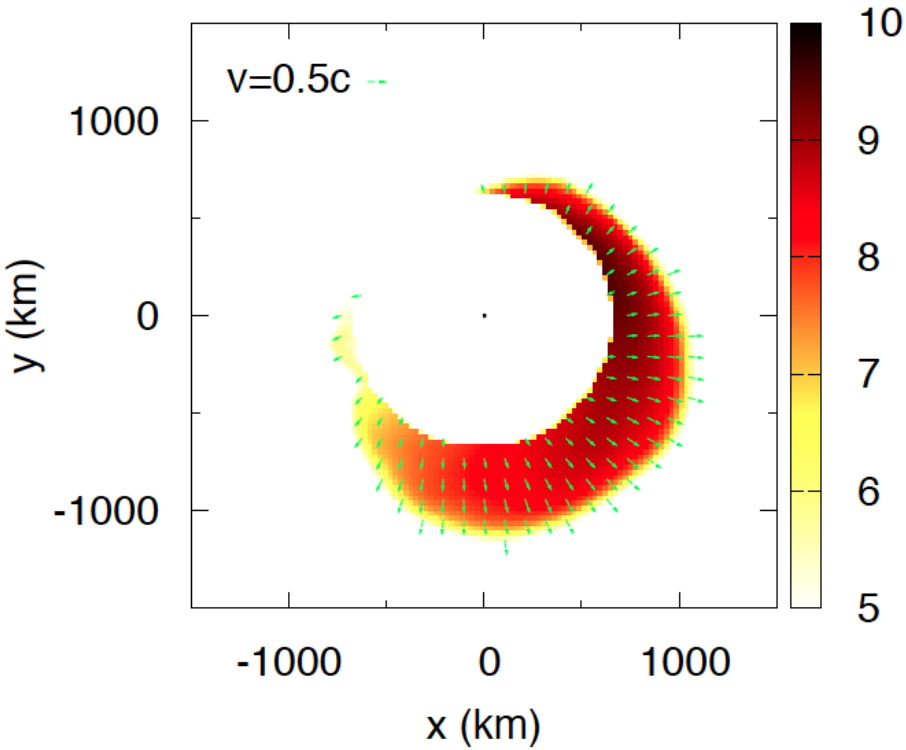

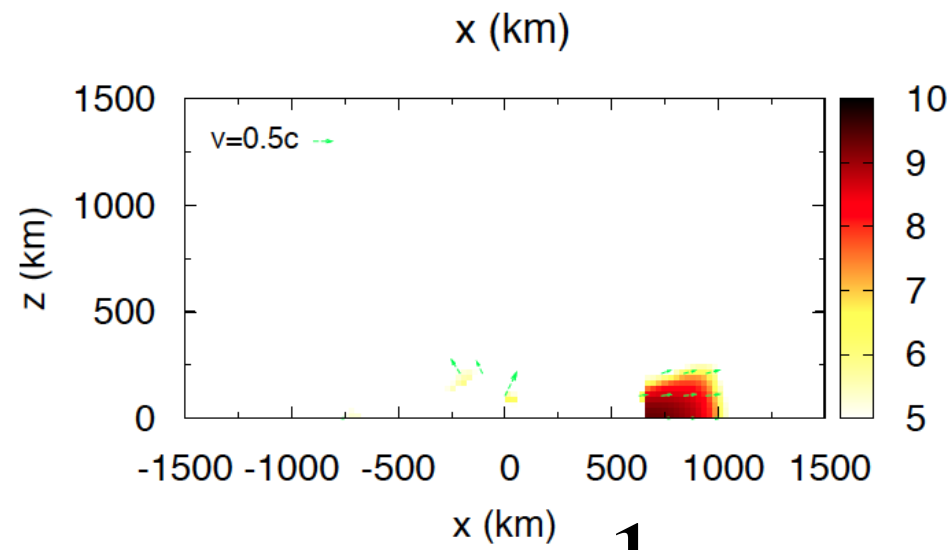

$$\theta_{ej} \approx \frac{1}{5}$$

$$\varphi_{ej} \approx \pi$$

Kyutoku, KI & Shibata 13

Viewing angle diversity
Polarization
Proper motion

Like Supernova Remnant?

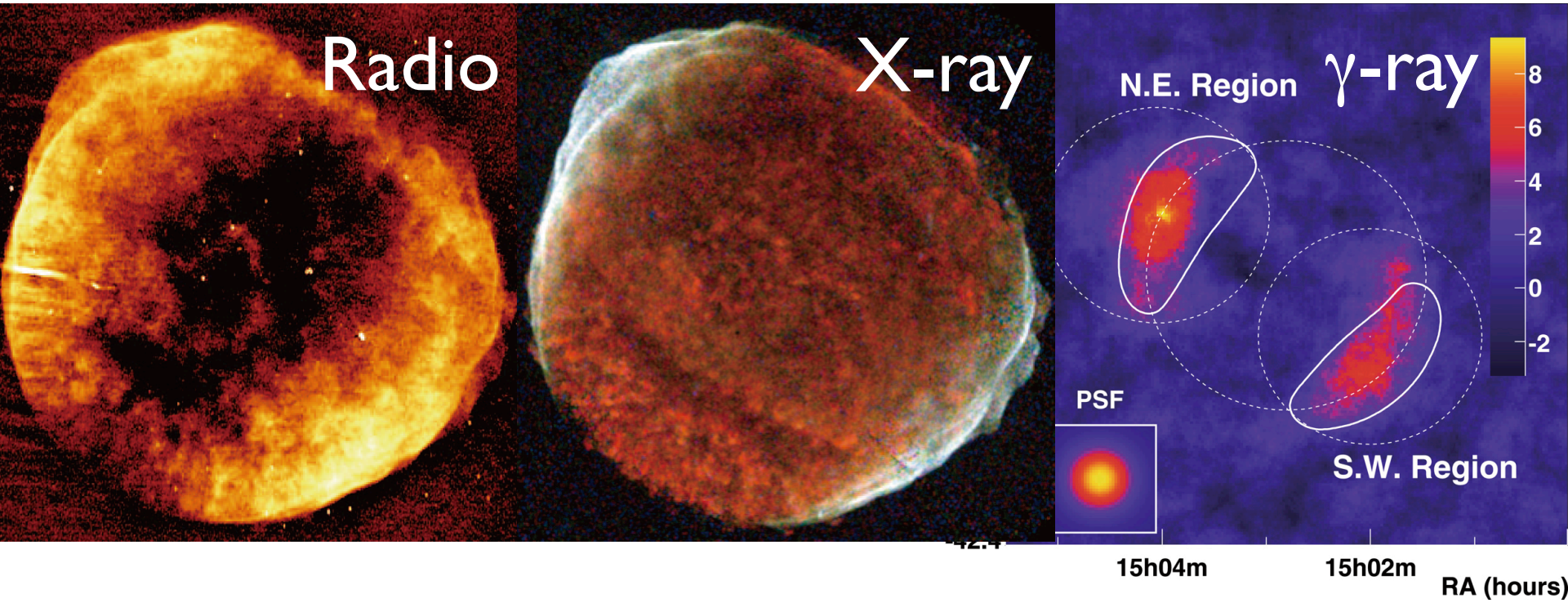

NS merger remnant ~ Supernova remnant

⇒ ***NS merger remnant?***

Only @t_{Sedov}~5yr

Nakar & Piran 11
Takami, Kyutoku & KI 13

Radio Flare

Piran+ 12

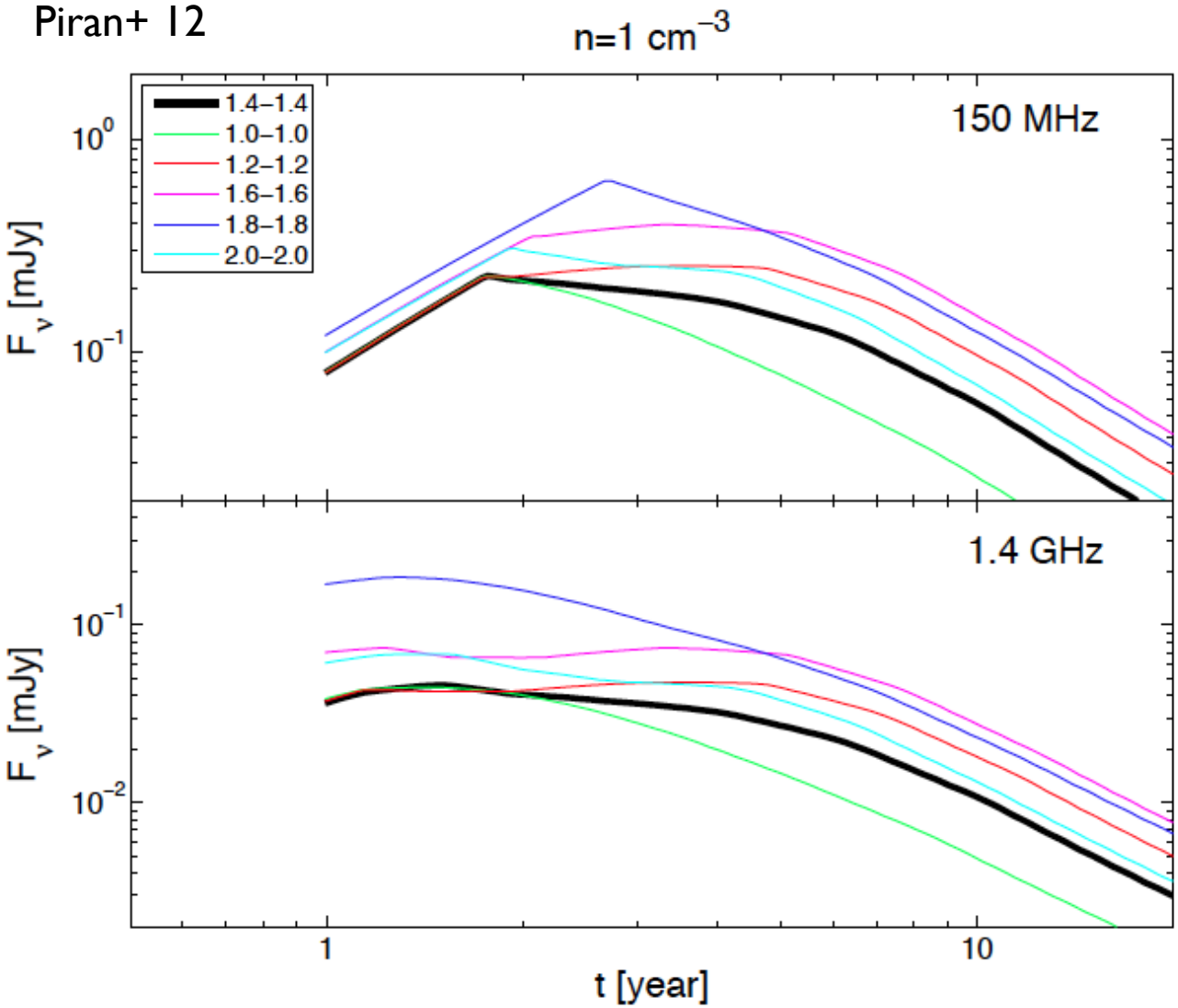

~GRB afterglow

Shock ⇒

1. Electron acc.
2. Magnetic amp.

⇒ Synchrotron

t~year

F_ν~0.1mJy

Merger Remnant

Optimistic case

@t_{Sedov}~5yr

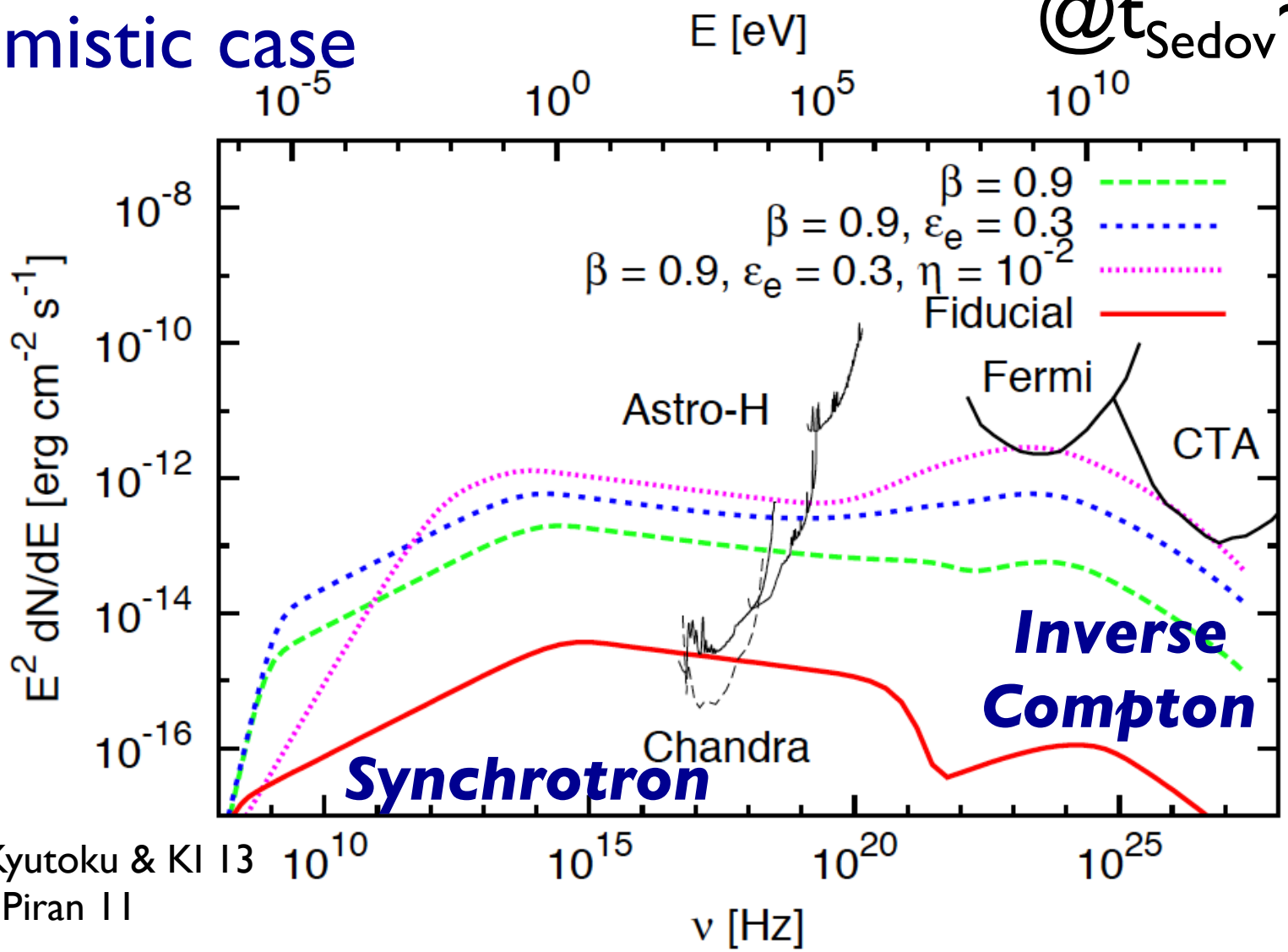

Takami, Kyutoku & KI 13
Nakar & Piran 11

Relativistic Shock Breakout

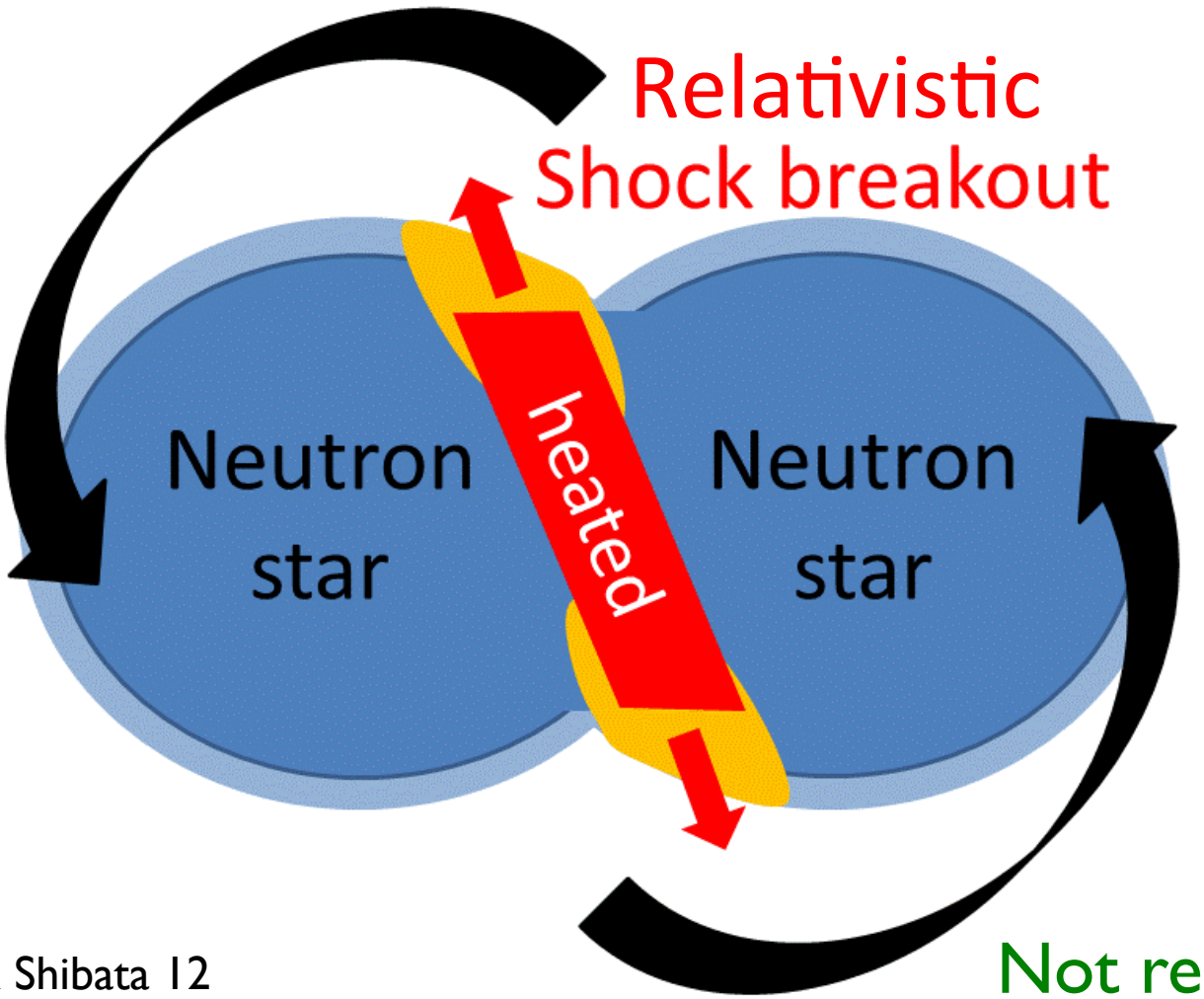

Kyutoku, KI & Shibata 12

Not resolved yet
by numerical simulation

Relativistic Shock Acceleration

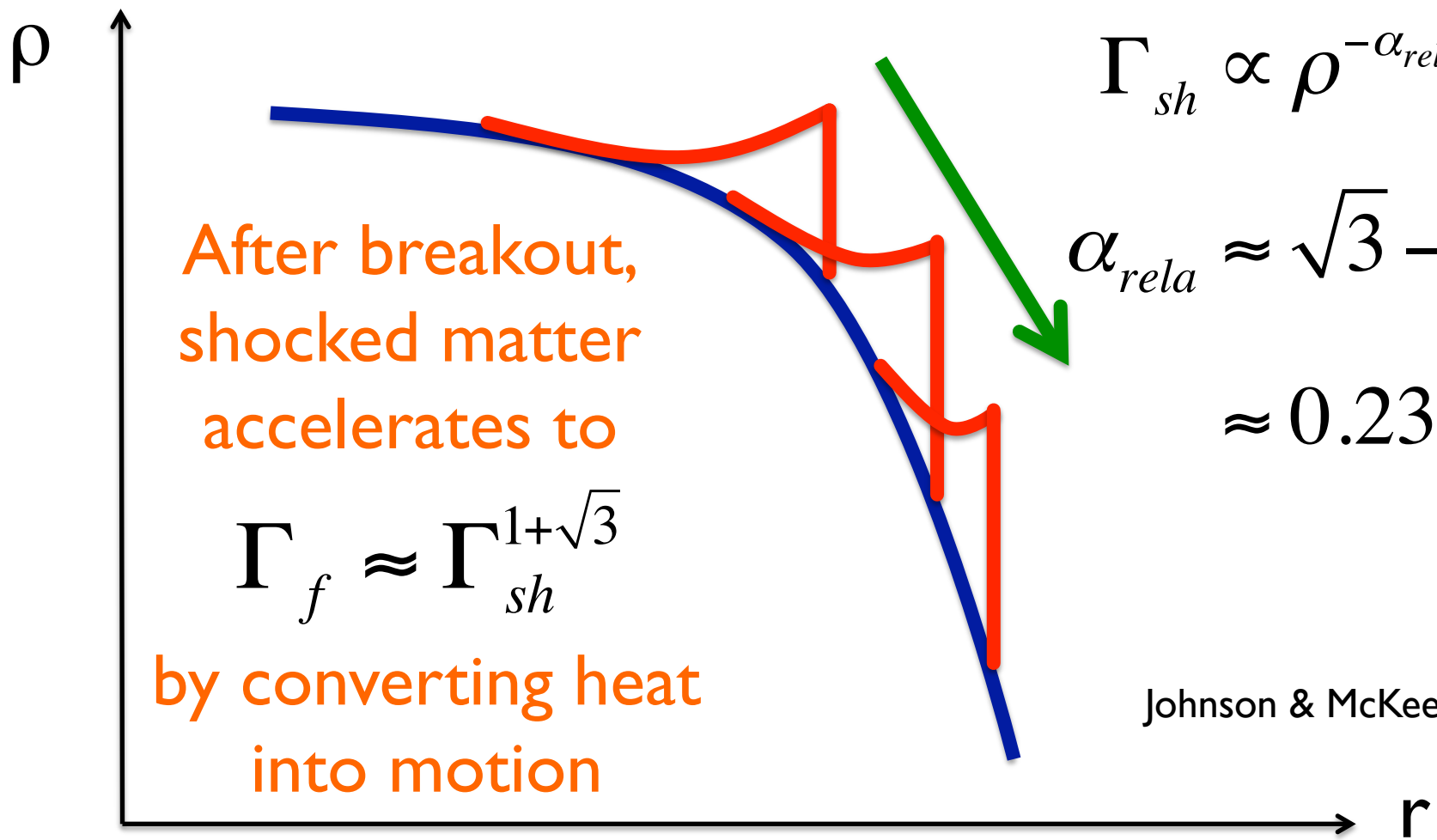

$$\Gamma_{sh} \propto \rho^{-\alpha_{rela}}$$

$$\alpha_{rela} \approx \sqrt{3} - \frac{3}{2}$$

$$\approx 0.232$$

After breakout, shocked matter accelerates to

$$\Gamma_f \approx \Gamma_{sh}^{1+\sqrt{3}}$$

by converting heat into motion

Johnson & McKee 71

Relativistic Outflow

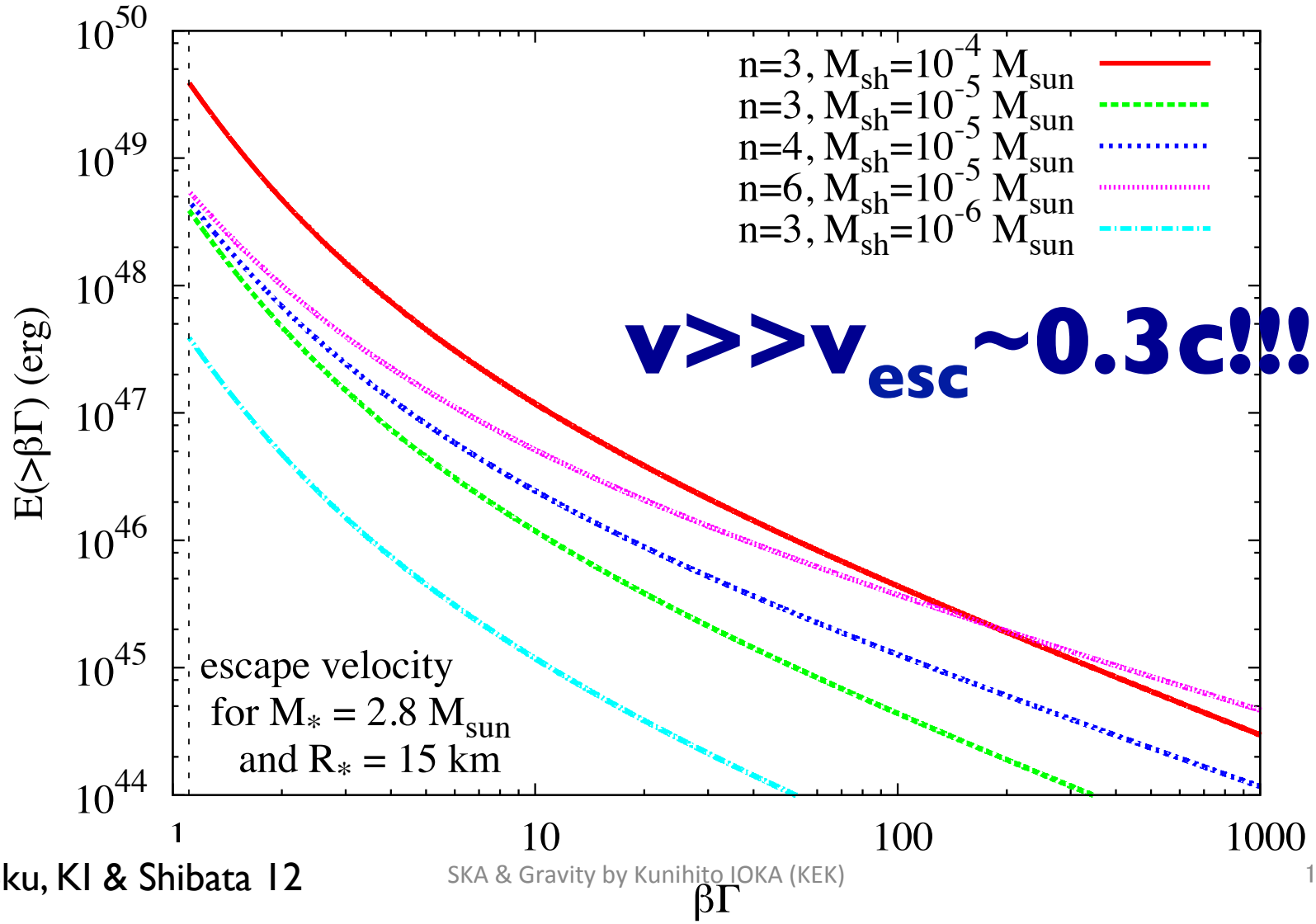

Kyutoku, KI & Shibata 12

Early & High-Energy Emission

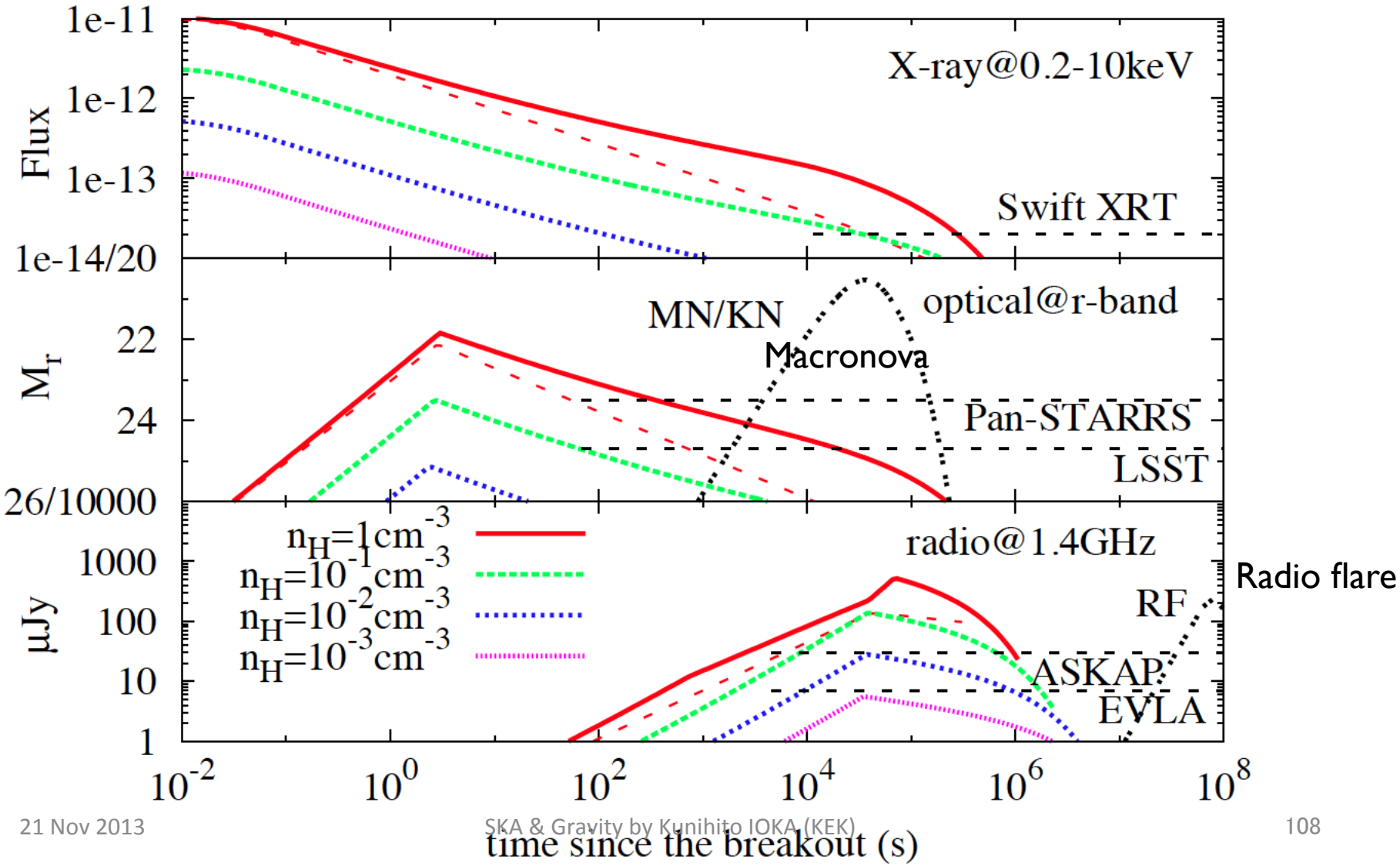

SKA2 Key Science Drivers

- ORIGINS
  - Neutral Hydrogen in the Universe from the Epoch of Re-ionisation to now [SKA1]
    - When did the first stars and galaxies form?
    - How did galaxies evolve?
    - Dark Energy, Dark Matter
  - Astro-biology
- FUNDAMENTAL FORCES
  - Pulsars, General Relativity and gravitational waves [SKA1]
  - Origin and evolution of cosmic magnetism
- TRANSIENTS (new phenomenon)

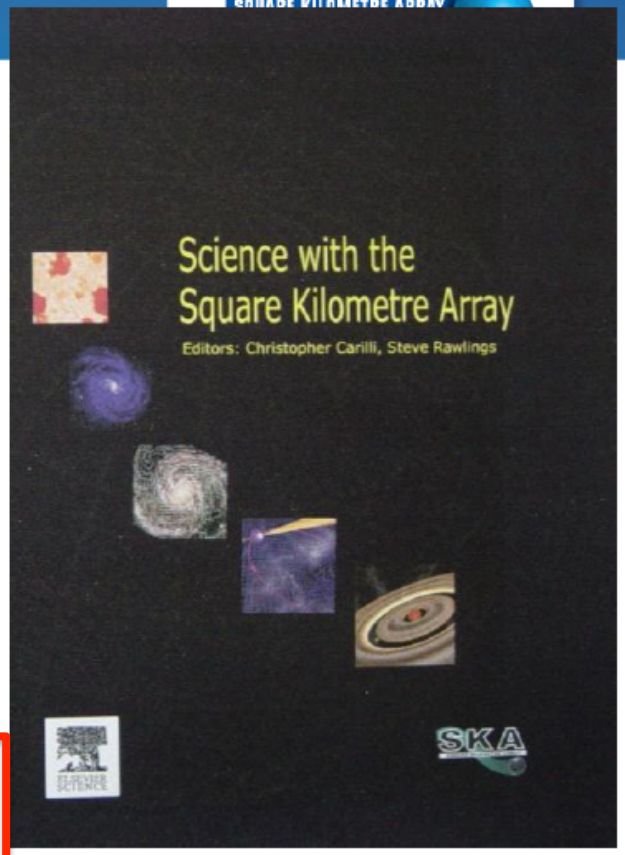

Science with the Square Kilometre Array
(2004, eds. C. Carilli & S. Rawlings, *New Astron. Rev.*, **48**)

Super-Massive Pop III Star?

Present Day Massive Star ~20M$_\odot$

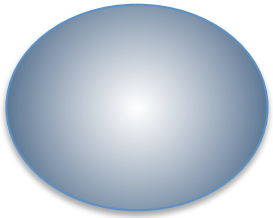

Omukai & Nishi 98;
Abel+ 02; Bromm+ 02;
Omukai+ 03; Yoshida+ 08;

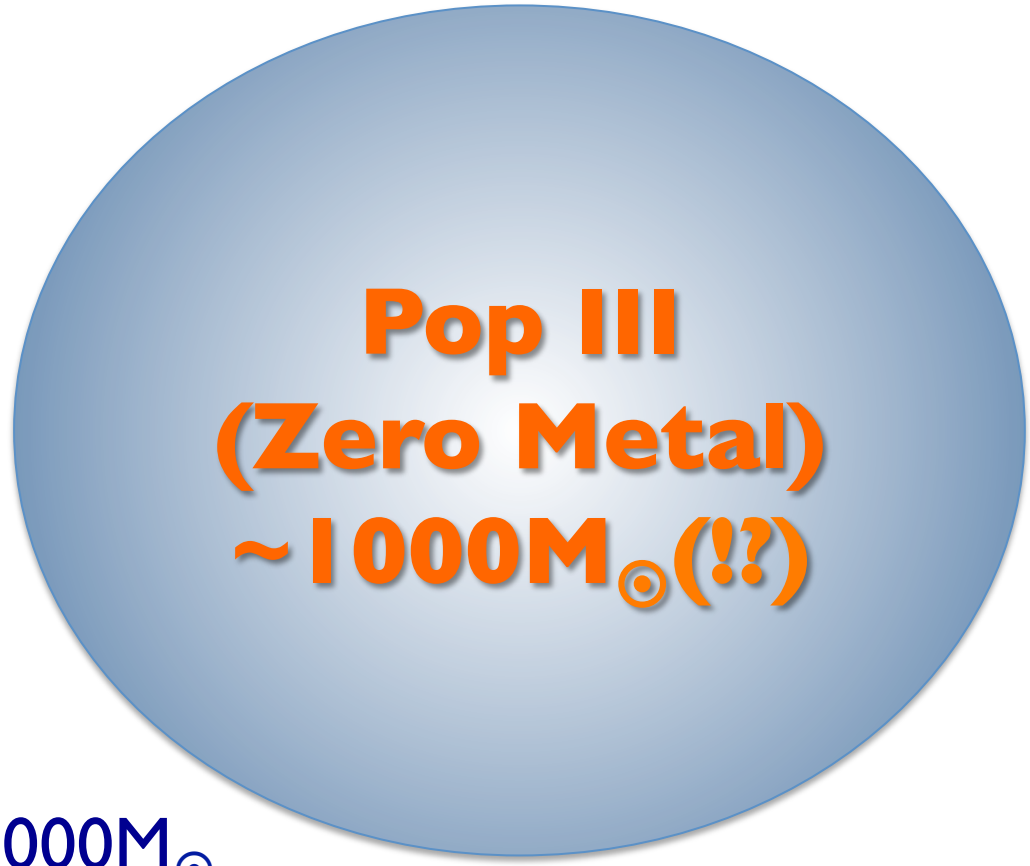

Mini halo (first object): ~1000M$_\odot$
If all the mass is accreted to a proto-star,

First stars are very MASSIVE?

Pop III GRB?

Present Day GRB

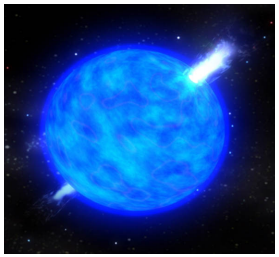

Komissarov & Barkov 10
Meszaros & Rees 10
Suwa & KI 11
Nagakura+ 11
de Souza, Yoshida & KI 11
Toma+ 11

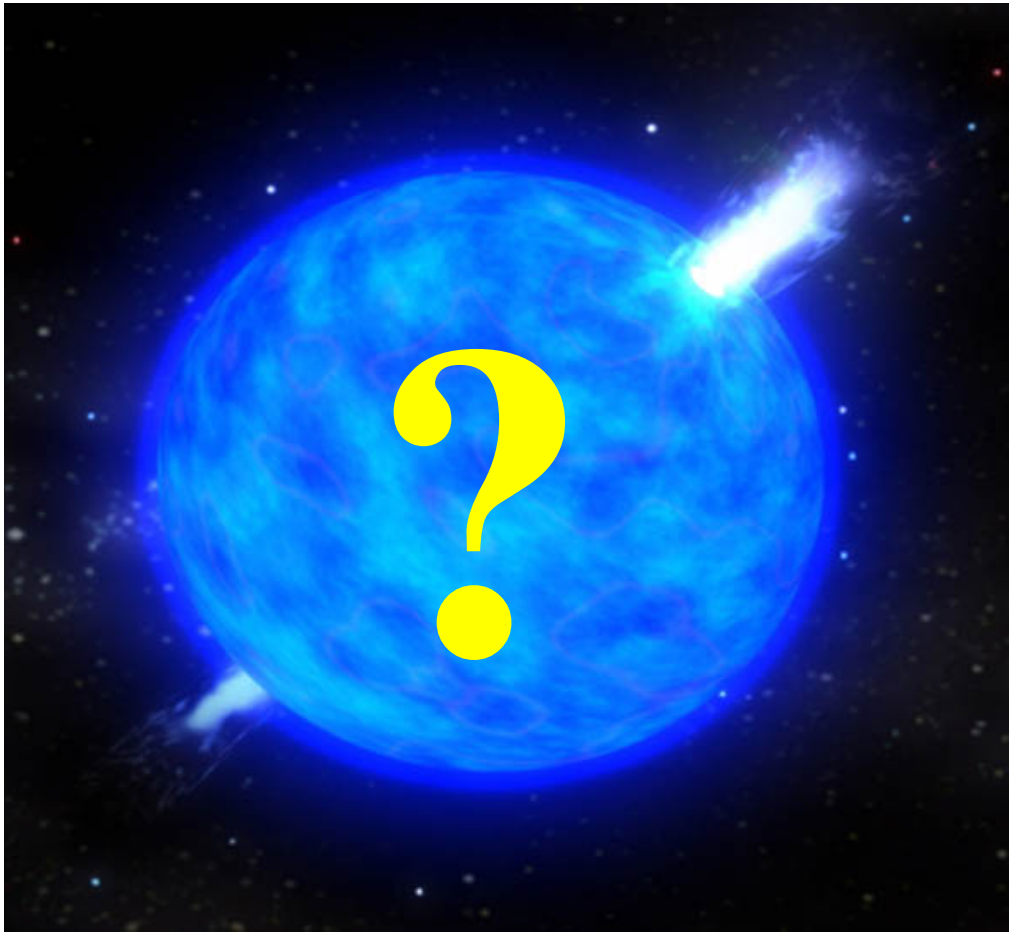

Gigantic (x100) GRB @ z~10-30???

Radio Afterglow

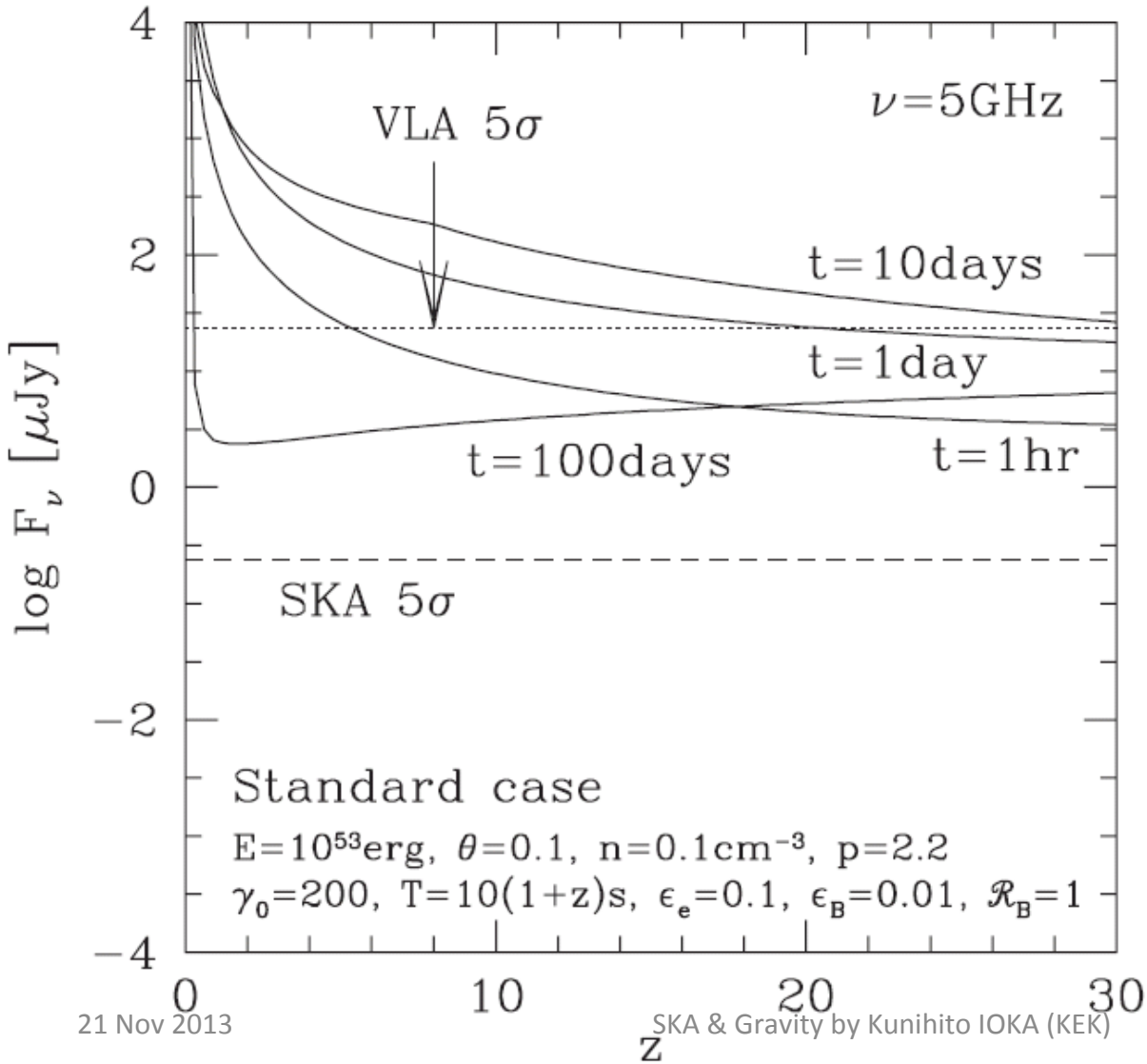

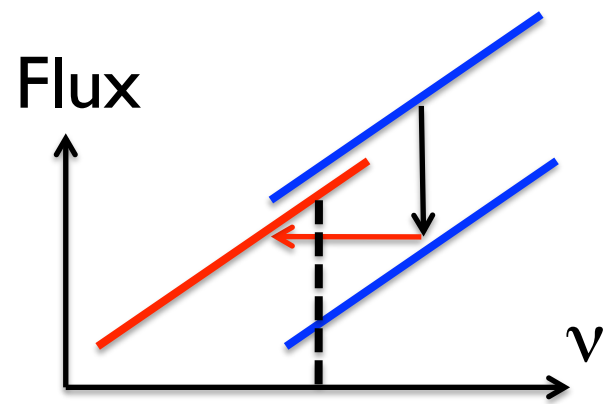

K-correction ⇒
Not dim @high-z

Spherical after jet break

KI & Meszaros 05
Inoue+ 07, Toma+ 10

Future Radio Transient

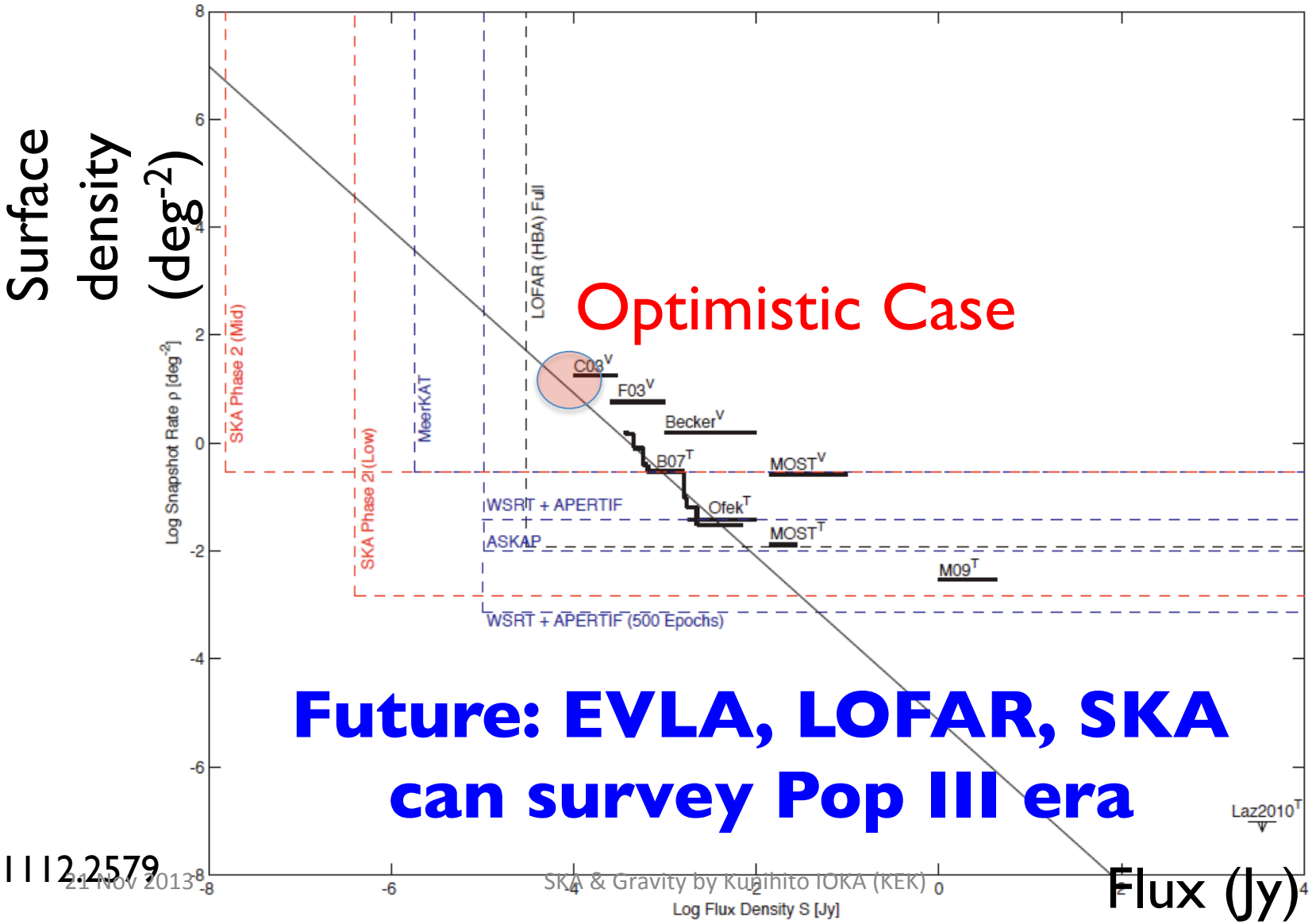

1112.2579

Fast Radio Bursts

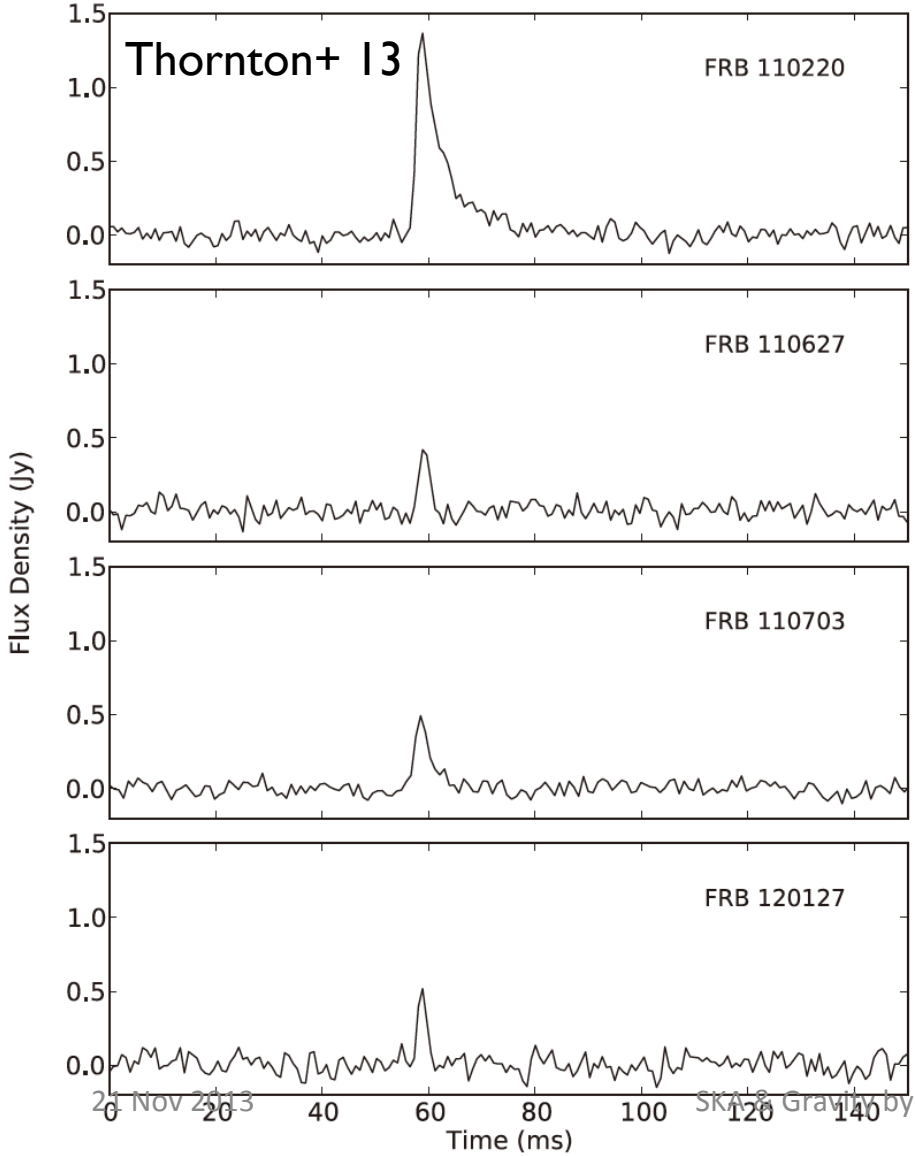

F=0.6-8.0 Jy ms !!!

Most luminous radio transients if cosmological

Dispersion Measure

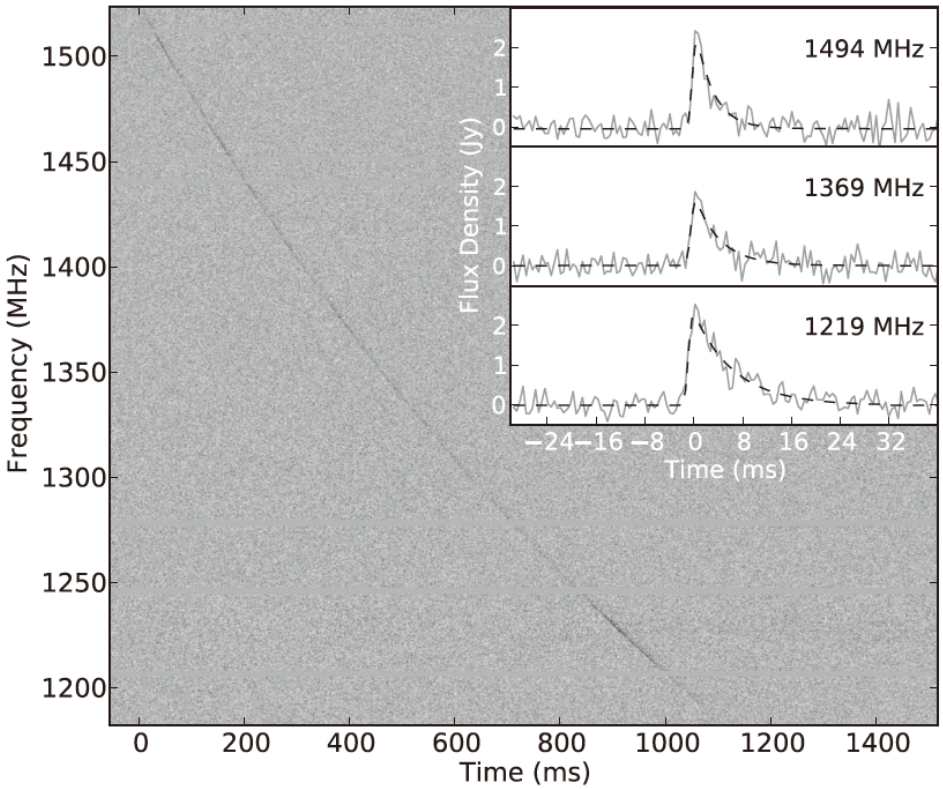

Thornton+ 13

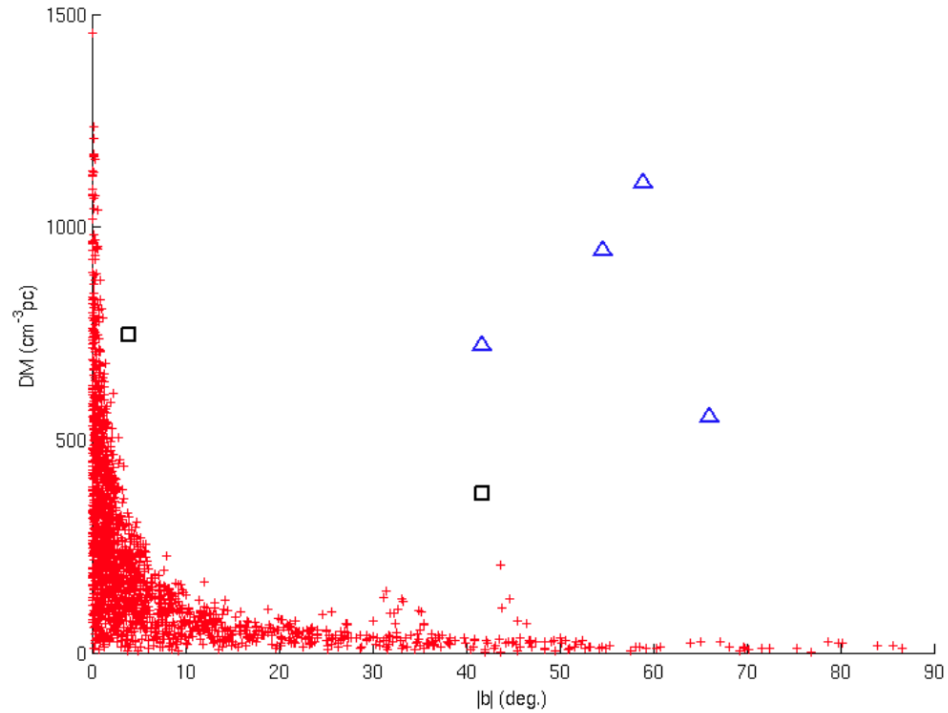

Galactic latitude

$\delta t \propto DM \cdot \nu^{-2}$

DM=500-1000 cm^{-3} pc

Intergalactic DM

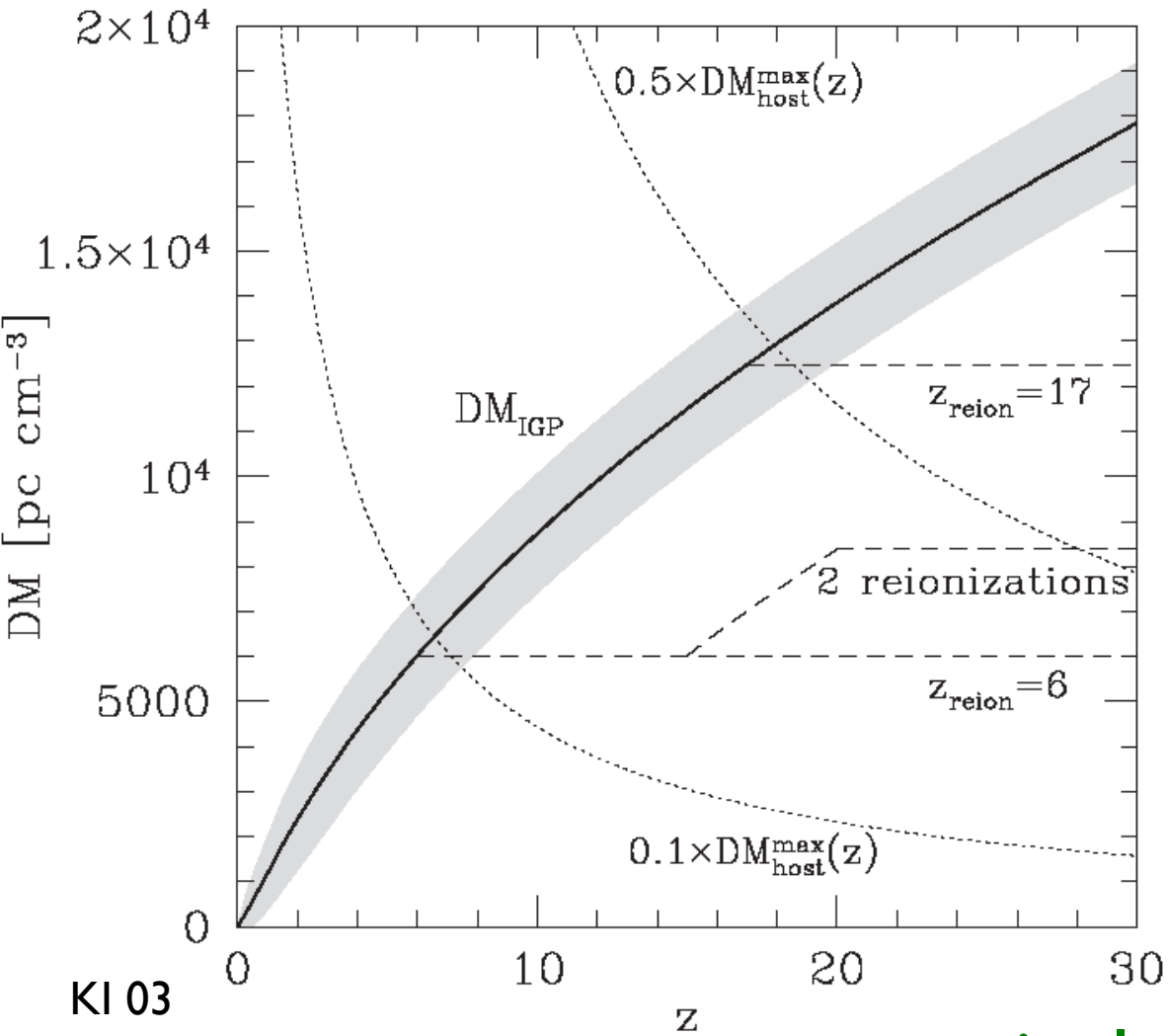

KI 03

$$\Delta t = \int_0^z dz \frac{dt}{dz} \frac{1}{2} \frac{(1+z)\nu_p^2}{\left[(1+z)\nu\right]^2}$$

$$= \frac{e^2}{2\pi m_e c} \frac{1}{\nu^2} \times$$

$$\frac{cn_0}{H_0} \int_0^z \frac{(1+z)\,dz}{\left[\Omega_m (1+z)^3 + \Omega_\Lambda\right]^{1/2}}$$

DM_{IGP}

DM~500-1000 cm^{-3} pc

⇒ ***z~0.5-1***

including missing baryon

Summary of FRB Obs.

- DM=500-1000 cm^{-3} pc (z=0.5-1)
- S_ν~Jy ⇒ E_{iso}~$10^{38\text{-}40}$ erg
- δt=5.6ms,<4.3,1.4,1.1ms
  ⇒ $c\delta t(1+z)^{-1} < 1500(1+z)^{-1}$ km
- Rate~$(1\pm0.5)\times10^4$/sky/day~10^{-3}/yr/galaxy
  ⇔ Supernova rate 10^{-2}/yr/galaxy
- No repeated bursts so far
- No counterparts so far

Expected Rate

Hassall+ 13
Lorimer+ 13
Trott+ 13

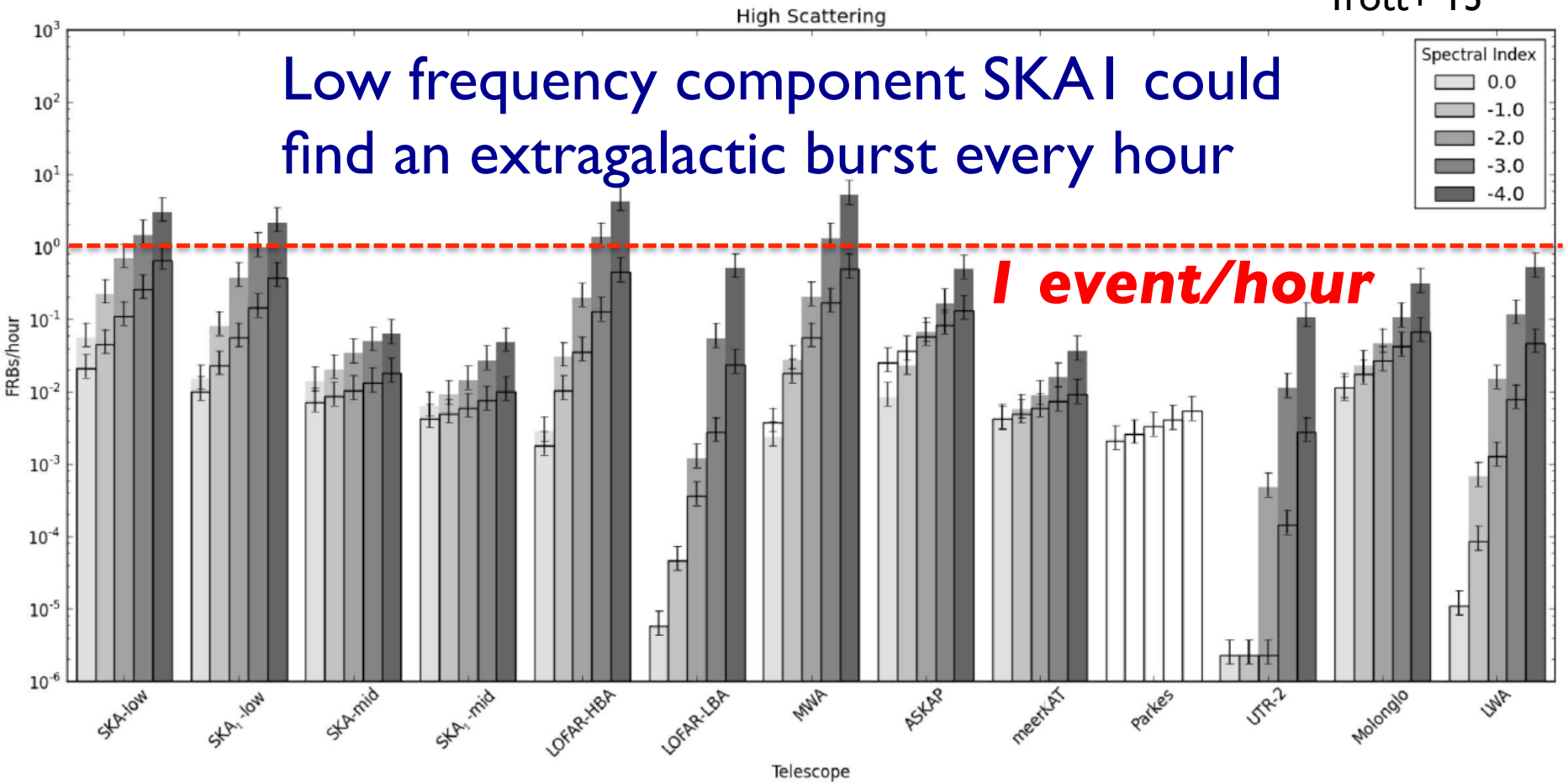

Figure 2. Expected number of FRBs per hour for various observatories in the high-scattering simulations. The solid bars show the number of FRBs detectable in imaging surveys, assuming different spectral indices of: 0.0 (white), -1.0, -2.0, -3.0 and -4.0 (darkest grey). The number of FRBs detectable in beamformed surveys are indicated by the corresponding transparent bars. The DM range used was $0 - 6000$ pc cm^{-3}.

Possible Origins

- RRAT (Rotating Radio Transient; intermittent pulsar)
- Giant pulse from a msec/young pulsar
- Evaporation of BH — Rees 77; Blandford 77; Kavic+ 08; Keane+ 12
- SN into a nearby star — Colgate+ 71,75; Egorov & Postnov 09
- Magnetar giant flare — Popov & Postnov 07; Thornton+ 13
- Collapse of hypermassive NS — Falcke & Rezzolla 13; Zhang 13
- Binary NS mergers — Hansen & Lyutikov 01; Totani 13
- Superconducting cosmic strings — Cai+ 12
- Nearby flaring stars — Loeb+ 12

Binary White Dwarf Mergers?

Kashiyama, KI & Meszaros 13

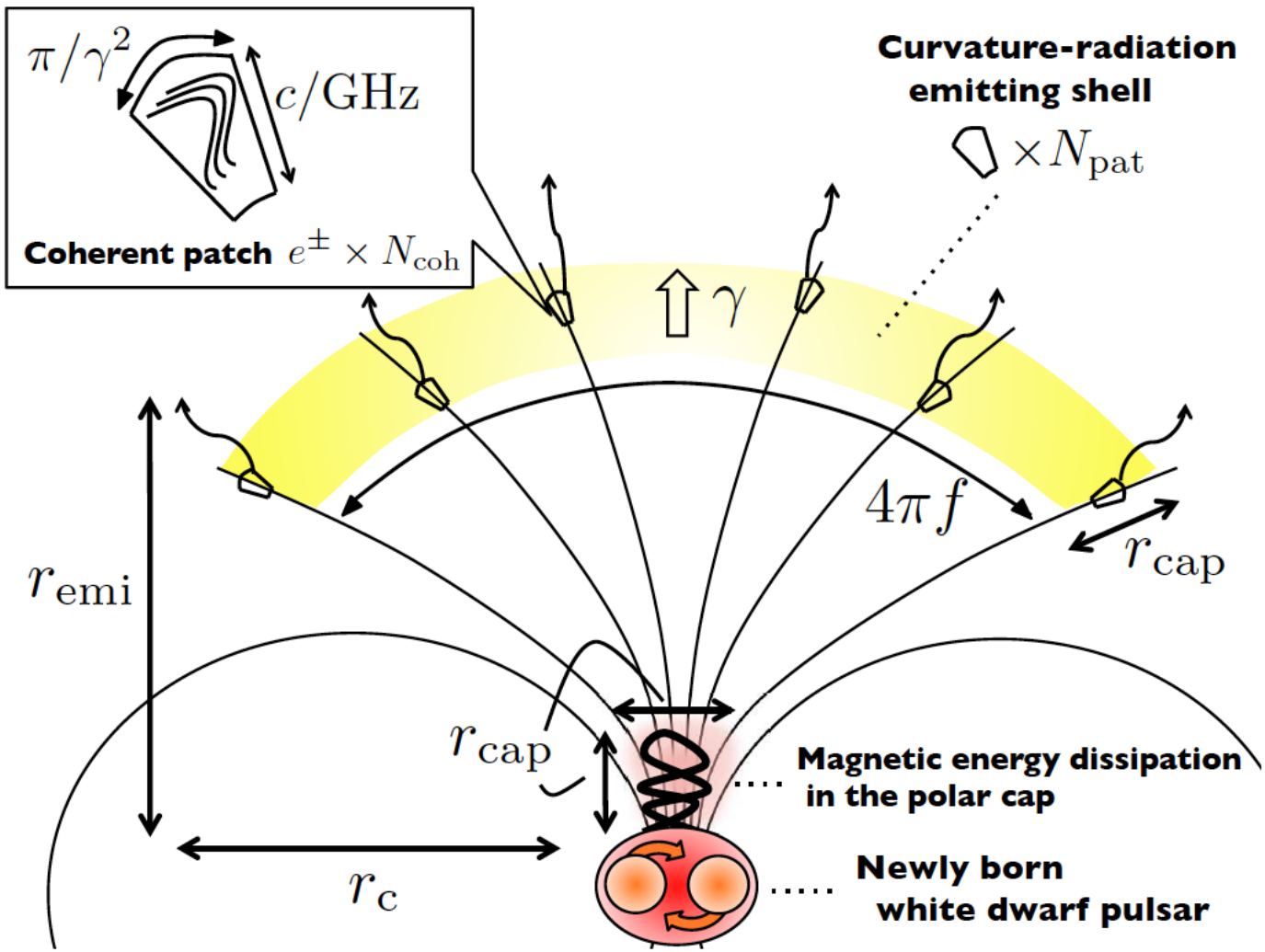

- Energetics $E_B \sim 10^{40}$erg
- Timescale $r_{cap}/c \sim$ms
- Event rate ~SN Ia
- SN Ia as a counterpart?

Brightness Temperature

$$F_\nu = \frac{\pi r_\perp^2}{d^2}\frac{2\nu^2}{c^2}kT$$

$$T \sim 3\times10^{41}\,\mathrm{K}\; L_{43} r_{emi,10}^{-2}$$

⇒ Coherent emission

$P \sim |E|^2 \sim |E_1+E_2+E_3+\ldots+E_N|^2$

$\sim N|E_1|^2$ (incoherent)

$\sim N^2|E_1|^2$ (coherent)

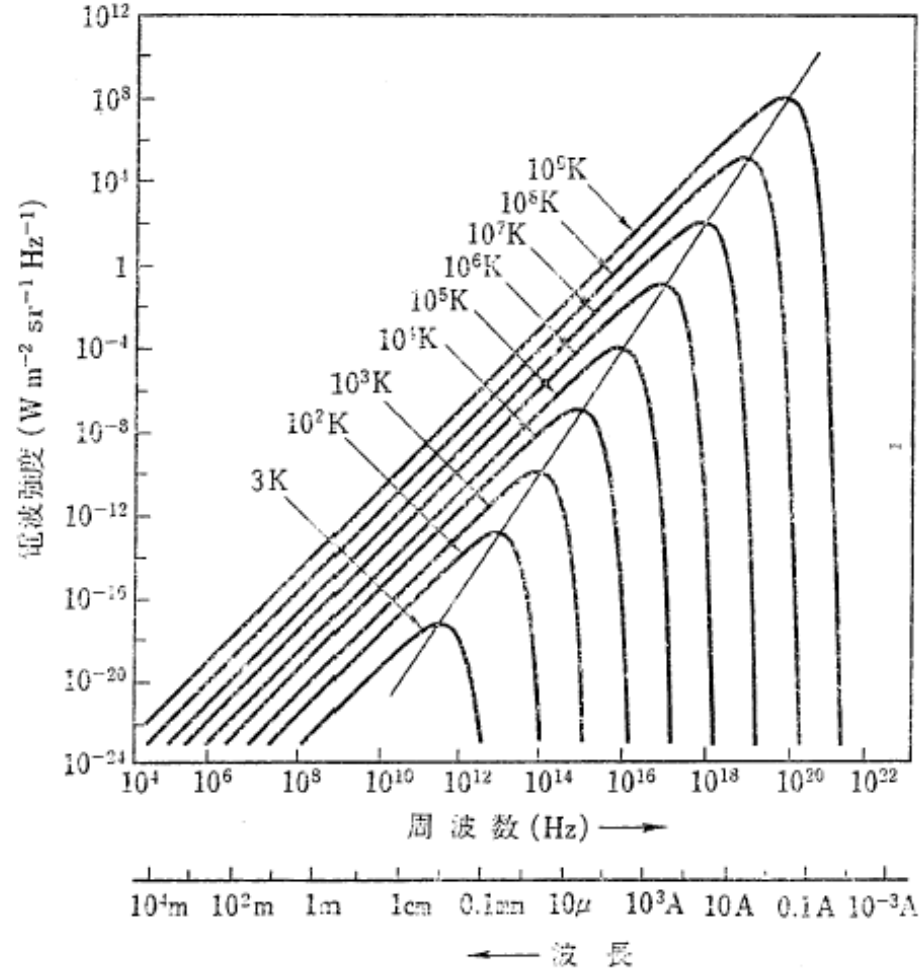

図 2·6 熱放射（プランク放射）の強度スペクトル

FRB Cosmology

- Reionization
- Missing baryon
- Dark energy, cosmological parameters

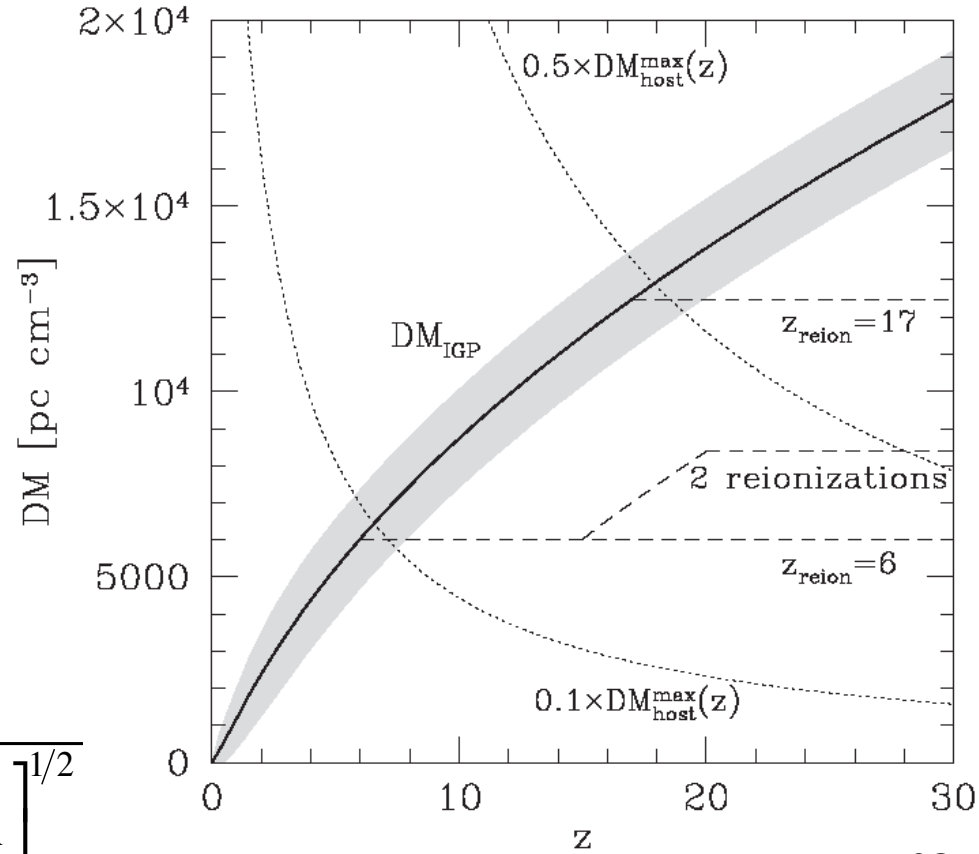

KI 03

$$\mathrm{DM}_{\mathrm{IGP}} = \frac{3cH_0\Omega_b}{8\pi G m_p}\int_0^z \frac{(1+z)\,dz}{\left[\Omega_m(1+z)^3+\Omega_\Lambda\right]^{1/2}}$$

$$d_L = \frac{c(1+z)}{H_0}\int_0^z \frac{dz}{\left[\Omega_m(1+z)^3+\Omega_\Lambda\right]^{1/2}}$$

Fast radio bursts as cosmological tools

New frontier?

Summary

+ Transients

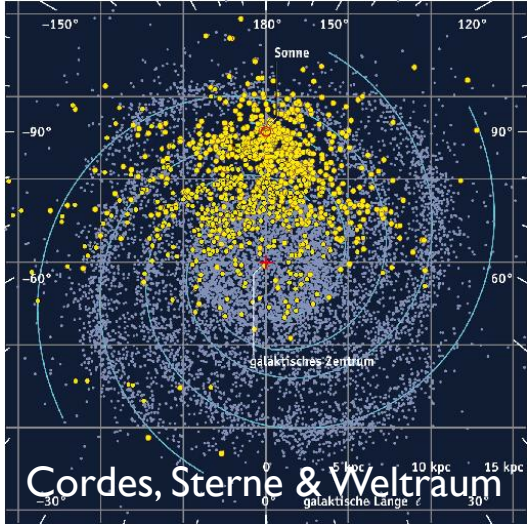

- Pulsar
  - Finding all pulsars in the Milky Way
  - Super dense matter physics, etc.
- Strong-field tests of gravity
- Gravitational wave astronomy
  - Complementary to AdvLIGO, KAGRA, eLISA, DECIGO, CMB-pol, LiteBIRD

Mass ~10^{-6}

No hair ~0.1%

CGC ~1%

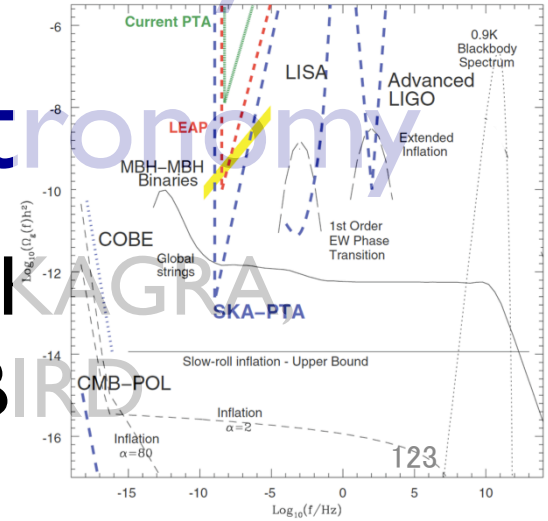

重力波検出のインパクト

- **一般相対論の検証**
  - 重力波の生成と伝搬
  - 高次元重力を含む修正重力理論
- **重力波源の解明**
  - Short GRBの起源、距離
  - 超新星、マグネターフレア等
- **基礎物理**
  - 超高密度物質の状態方程式
  - ニュートリノ物理

重力理論

宇宙論

天体物理

天文学

原子核

素粒子

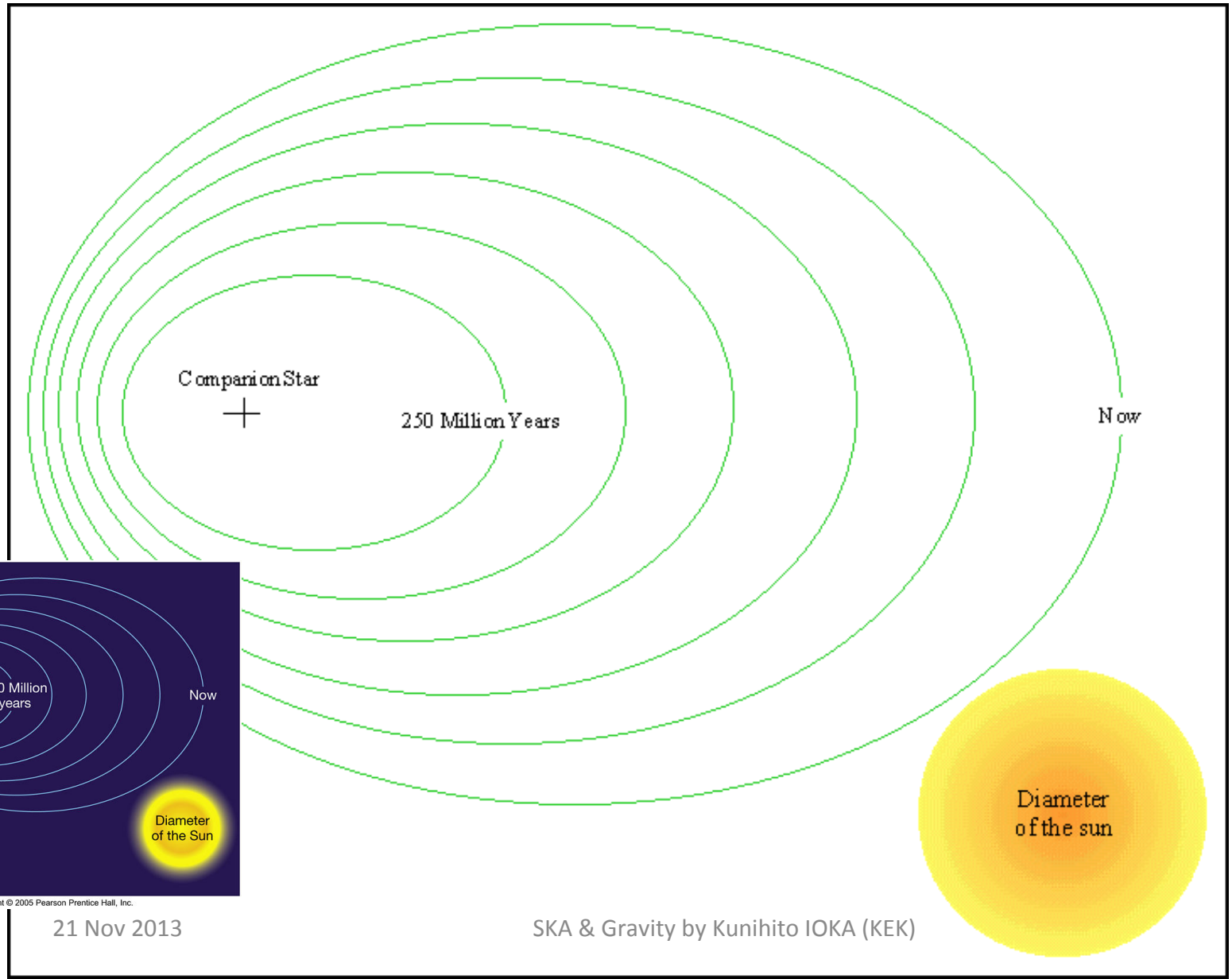

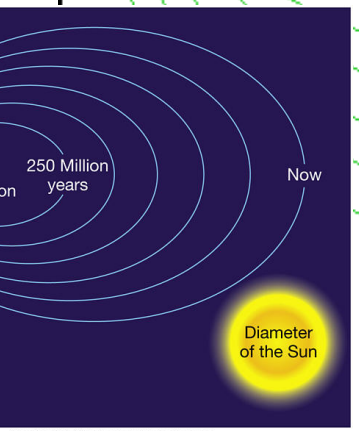

Weisberg+ 81

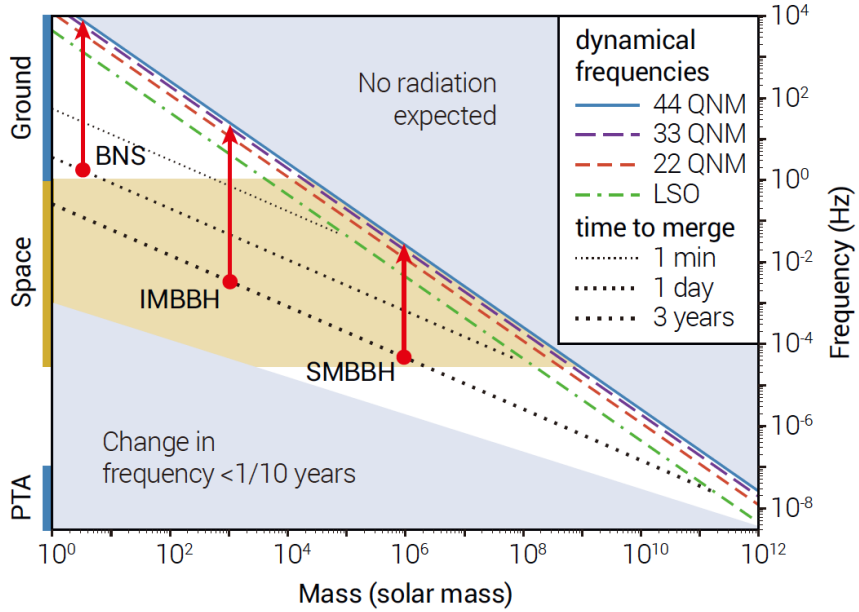

Figure 15: Measurement capabilities of ET, eLISA, and PTAs. The horizontal axis is the total mass of the binary system. The vertical axis is the frequency of the gravitational waves. The left side shows the frequency bands of the different instruments. The grey shaded region at the top is inaccessible because no system of a given mass can radiate at such high frequencies. The shaded region at the bottom is less interesting, because the chirp mass cannot be measured in an observation lasting less than 10 years, so the mass and distance of the source cannot be independently determined. Sloping dotted lines show the three-year, one-day, and one-minute time-to-merger lines. Sloping dashed lines are relevant dynamical frequencies: last stable orbit and the frequencies of ringdown modes of the merged black hole. Vertical lines indicate evolutionary tracks of systems of various masses as their orbits shrink and they move to higher frequencies. There is some overlap in the mass-range of sources that can be studied between ground and space detectors, but whether this translates into real science depends on the instruments' sensitivities and the source populations. Among the most interesting, would be the observation of an intermediate-mass binary black hole (IMBBH) system (if such systems exist) of around 1000 $M_\odot$ during inspiral and coalescence with both eLISA and ET. This track is shown in the diagram as (IMBBH). With such a source at redshift 0.5, both instruments might have an SNR around 20 (see Figure 16), but most of the science-including the direction to the source-would come from the eLISA measurement. Additionally, tracks for binary neutron stars (BNS) and super massive binary black holes (SMBBHs) are shown.

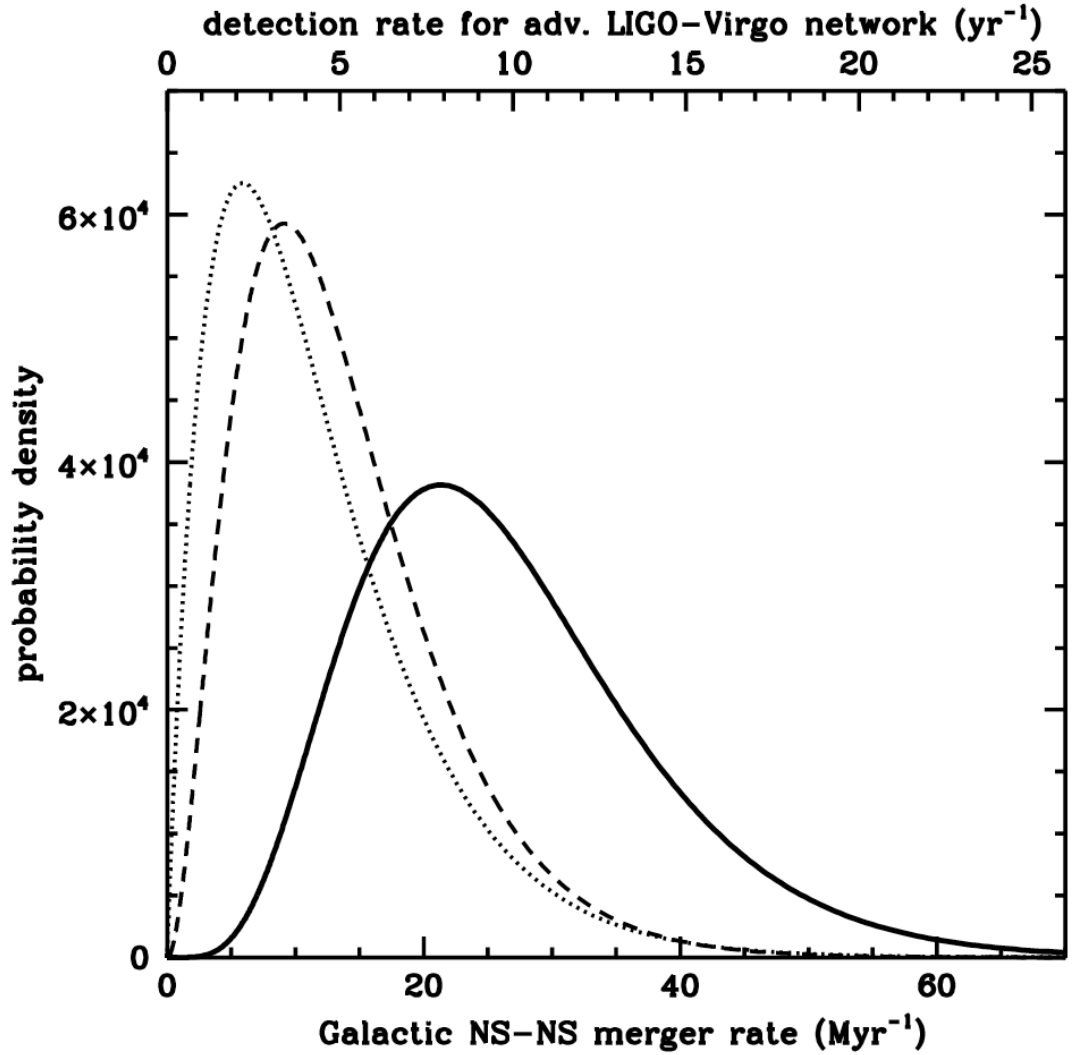

Figure 6. $\mathcal{P}_{\rm g}(\mathcal{R}_{\rm g})$ (solid) is overlaid with individual $\mathcal{P}(\mathcal{R})$ obtained from PSR B1916+13 (dotted) and the Double Pulsar (short dashed). Based on our reference model, the Galactic NS-NS merger rate is most likely to be 21 Myr^{-1}. The corresponding GW detection rate for the advanced ground-based GW detectors is ~ 8 yr^{-1}.

Kim+ 13

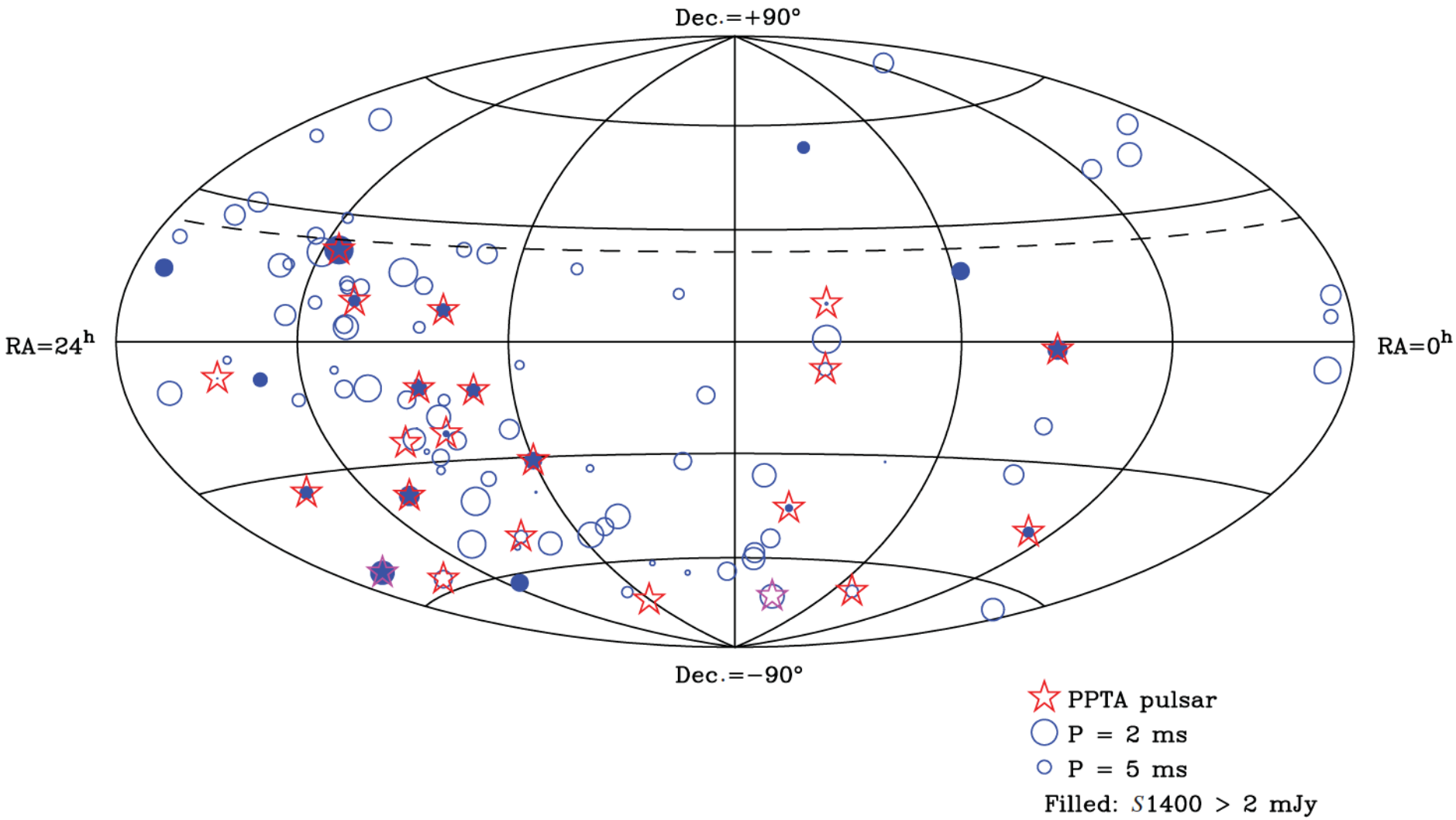

Figure 6. Distribution in celestial coordinates of pulsars suitable for pulsar timing array observations. All are radio-emitting MSPs (with P<20 ms) in the Galactic disc except PSR J1824−2452A which is an MSP located in the globular cluster M28 (see text). The area of the plotted circle is inversely proportional to the pulsar period and the circles are filled for pulsars with mean flux density above 2 mJy. The dashed line is the northern declination limit of the Parkes radio telescope. Pulsars selected for the PPTA are marked with a star, red for the original 20 pulsars and mauve for the two pulsars recently added to the PPTA sample (see text).

Manchester+ 13

SKA Layout

Dishes (high, d=15m, several thousand, 3000km in Africa)
Aperture Array (mid, low, more, 200km in Africa & Australia)

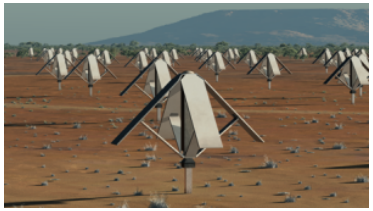

Spiral configuration
Many different baselines and angles
Random is better but more expensive

SKA Phase 1 (SKA1)
Cost €650M, construction start 2018

Southern Africa

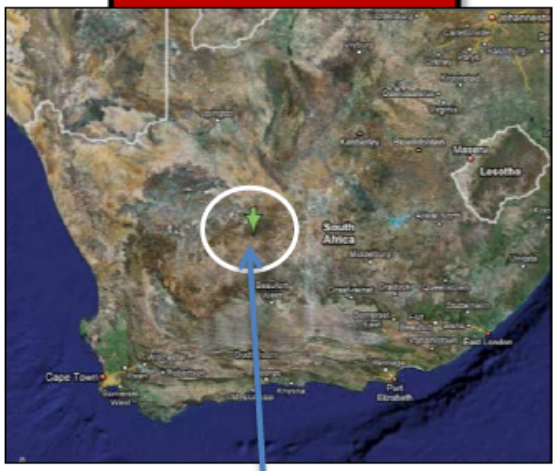

SKA1_MID
254 Dishes including:
64 x MeerKAT dishes
190 x SKA dishes

Australia

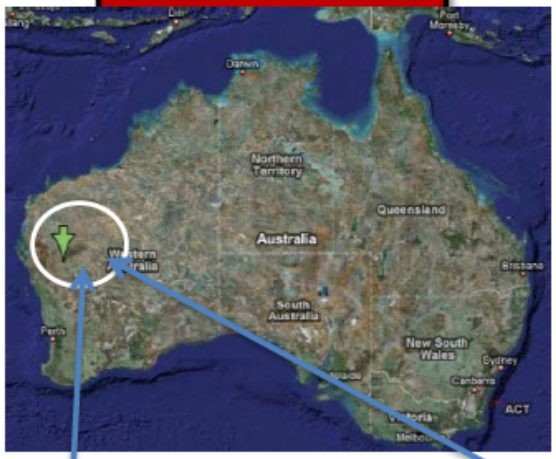

SKA1_LOW
Low Frequency Aperture Array Stations

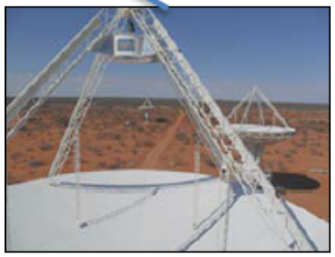

SKA1_SURVEY
96 Dishes including:
36 x ASKAP
60 x SKA dishes

Ref. MWA (Murchison Widefield Array)

d=15m

Exploring the Universe with the world's largest radio telescope

SKA Phase 2 (SKA2)
Cost > €1.5B; construction start 2022

Southern Africa

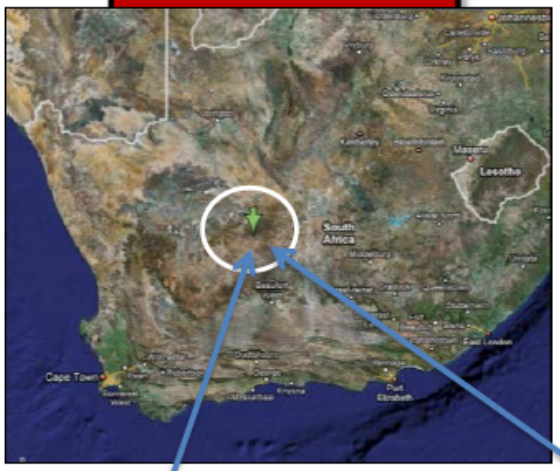

Australia

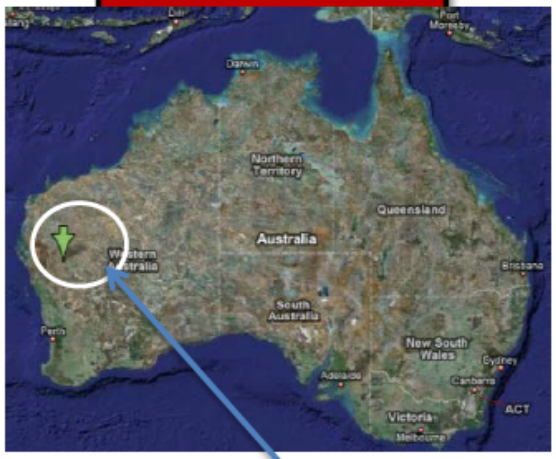

SKA2_MID
2500 Dishes

SKA2_AA
Mid Frequency Aperture Array Stations

SKA2_LOW
Low Frequency Aperture Array Stations

Several million antennas

How does SKA1 baseline redefine state-of-art?

		JVLA	MeerKAT	SKA1-mid	ASKAP	SKA1-survey	LOFAR-NL	SKA1-low
Aeff/Tsys	m^2/K	265	321	1630	65	391	61	1000
Survey FoV	deg^2	0.14	0.48	0.39	30	18	6	6
Survey Speed FoM	$deg^2\ m^4\ K^{-2}$	0.98×10^4	5.0×10^4	1.0×10^6	1.3×10^5	2.8×10^6	2.2×10^4	6.0×10^6
Resolution	arcsec	1.4	11	0.22	7	0.9	5	11

A_{eff}/T_{sys}:	6xJVLA	6xASKAP	16xLOFAR
Survey Speed:	100x	22x	270x

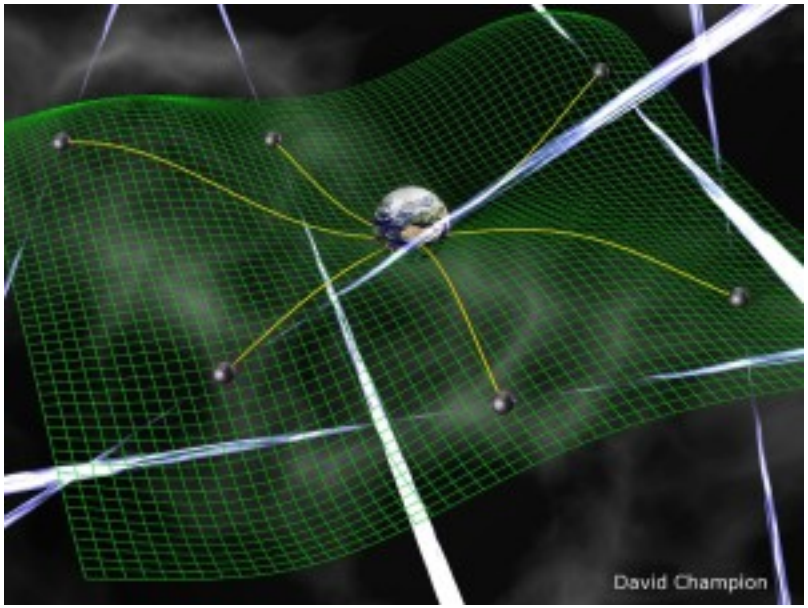
David Champion

Timeline

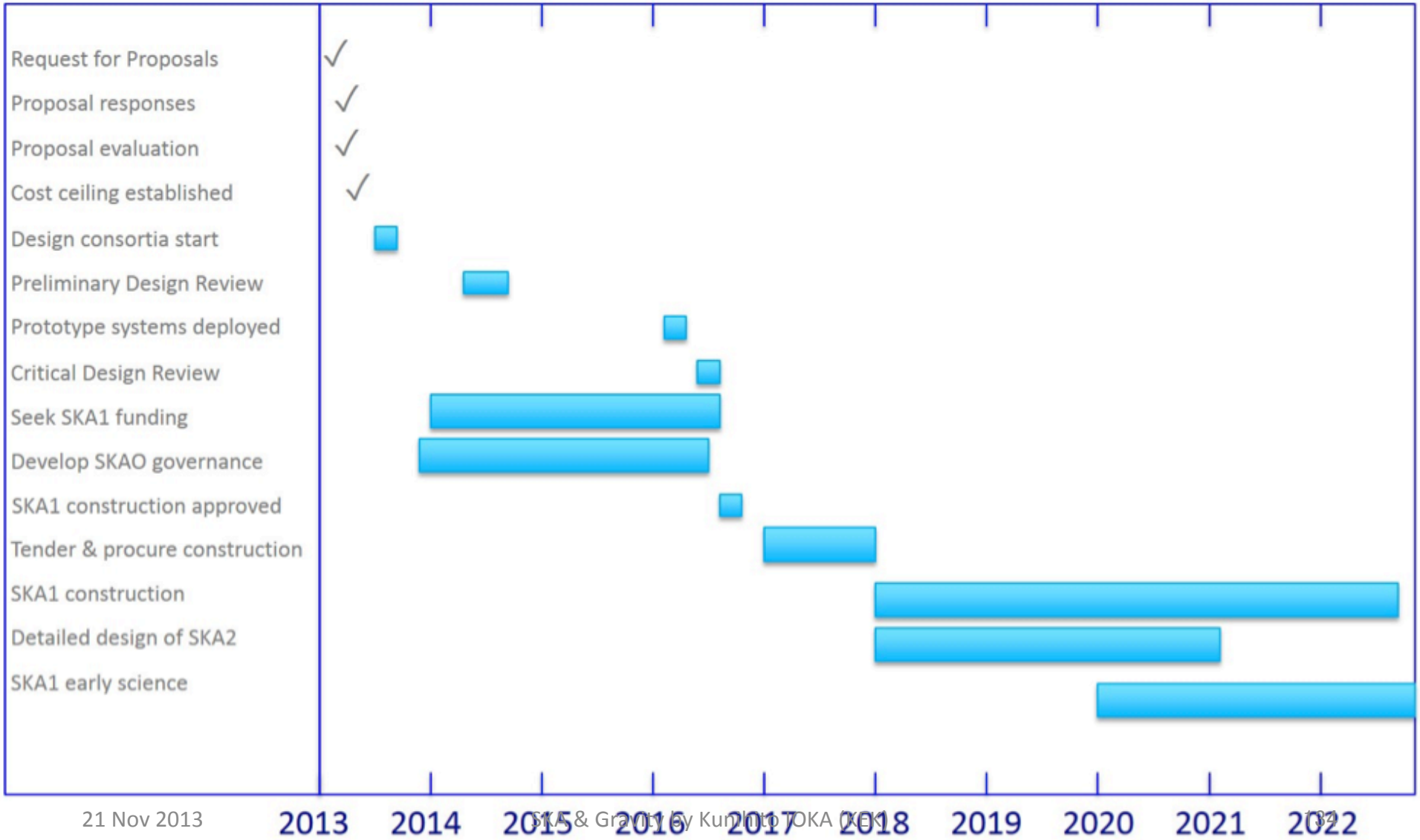
Request for Proposals
Proposal responses
Proposal evaluation
Cost ceiling established
Design consortia start
Preliminary Design Review
Prototype systems deployed
Critical Design Review
Seek SKA1 funding
Develop SKAO governance
SKA1 construction approved
Tender & procure construction
SKA1 construction
Detailed design of SKA2
SKA1 early science
2013
2014
2015
2016
2017
2018
2019
2020
2021
2022

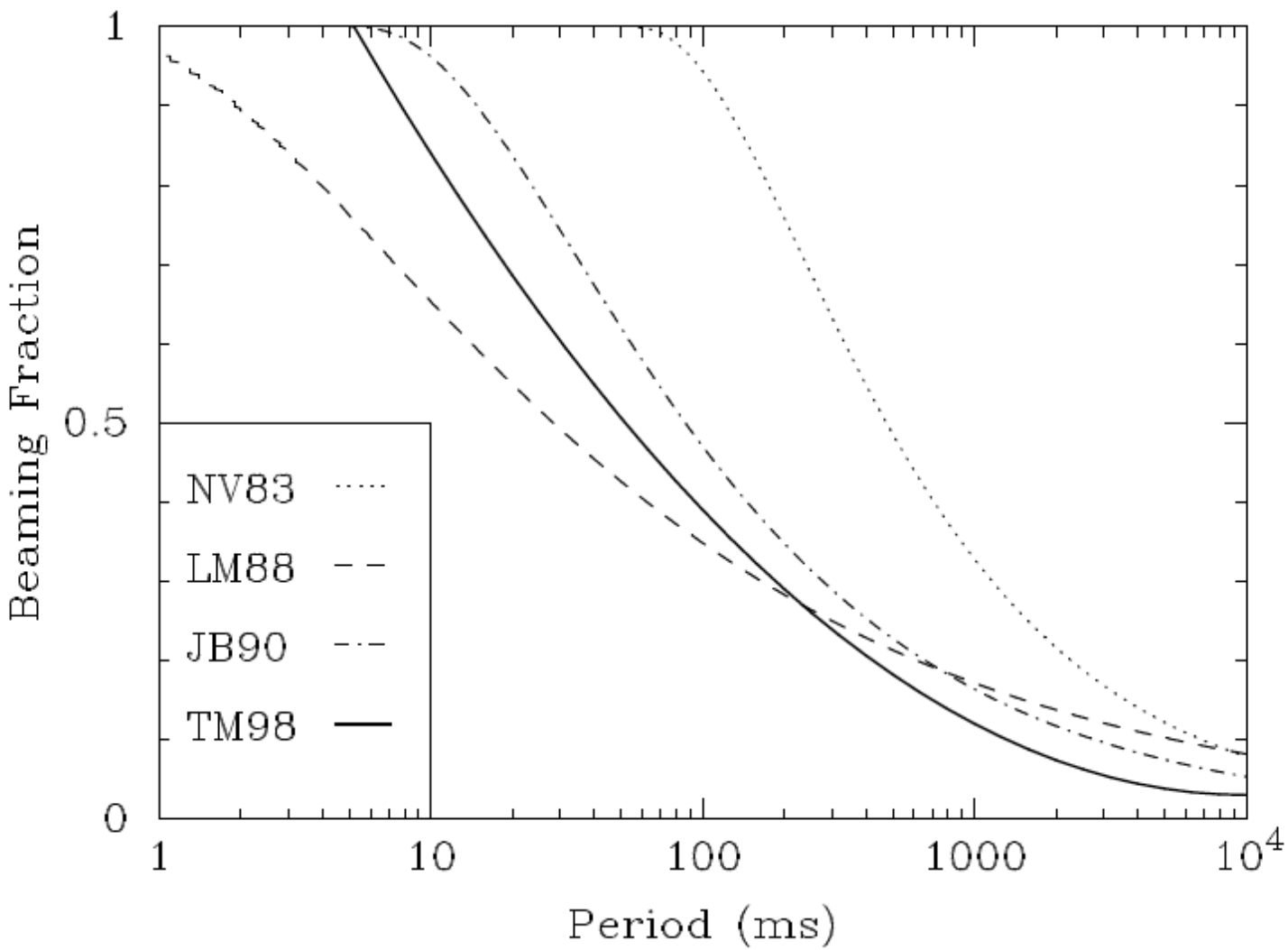

Figure 16: Beaming fraction plotted against pulse period for four different beaming models: Narayan & Vivekanand 1983 (NV83) [269], Lyne & Manchester 1988 (LM88) [243], Biggs 1990 (JDB90) [37] and Tauris & Manchester 1998 (TM98) [360].

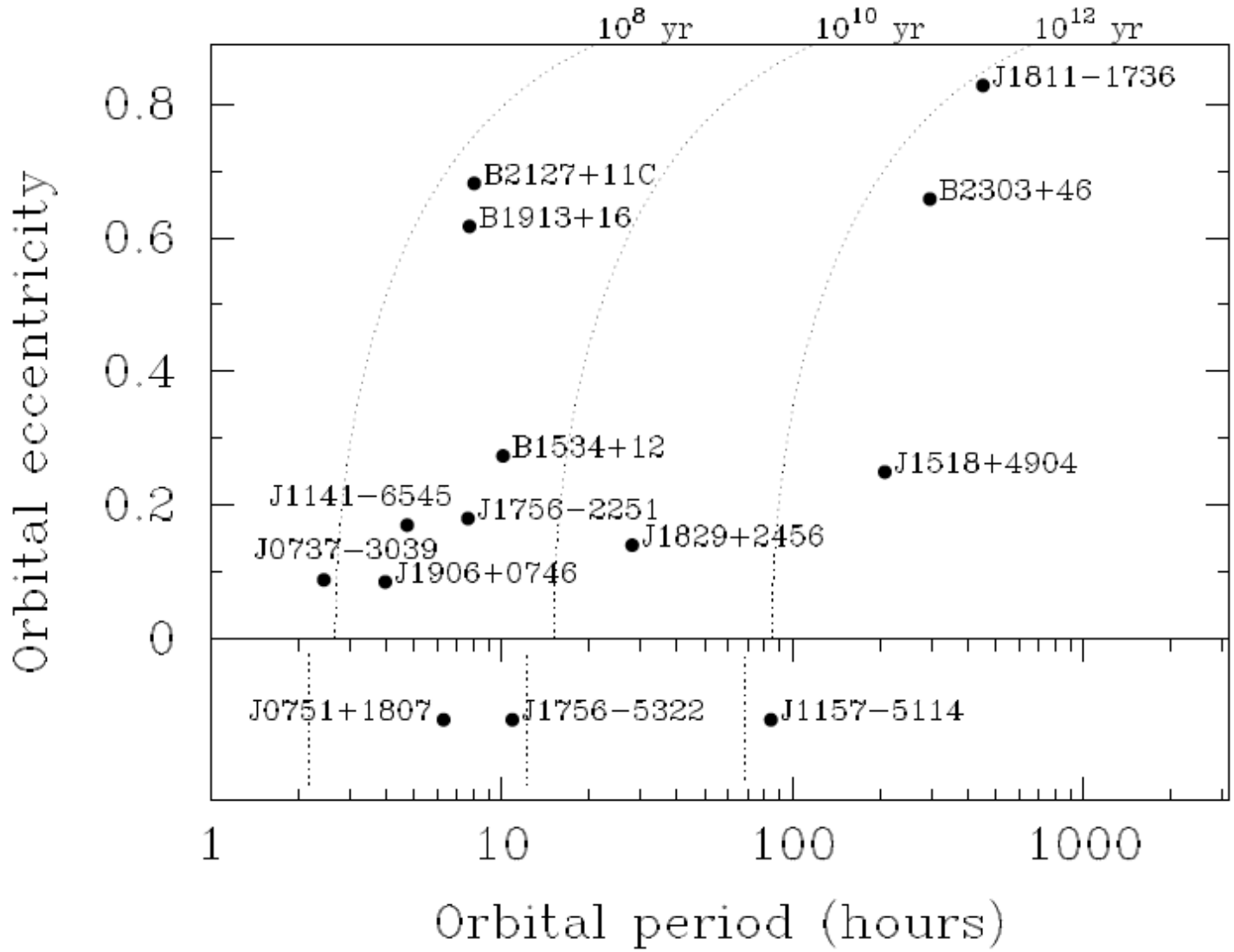

Figure 18: The relativistic binary merging plane. Top: Orbital eccentricity versus period for eccentric binary systems involving neutron stars. Bottom: Orbital period distribution for the massive white dwarf–pulsar binaries. Isocrones show coalescence times assuming neutron stars of $1.4\,M_\odot$ and white dwarfs of $0.3\,M_\odot$.

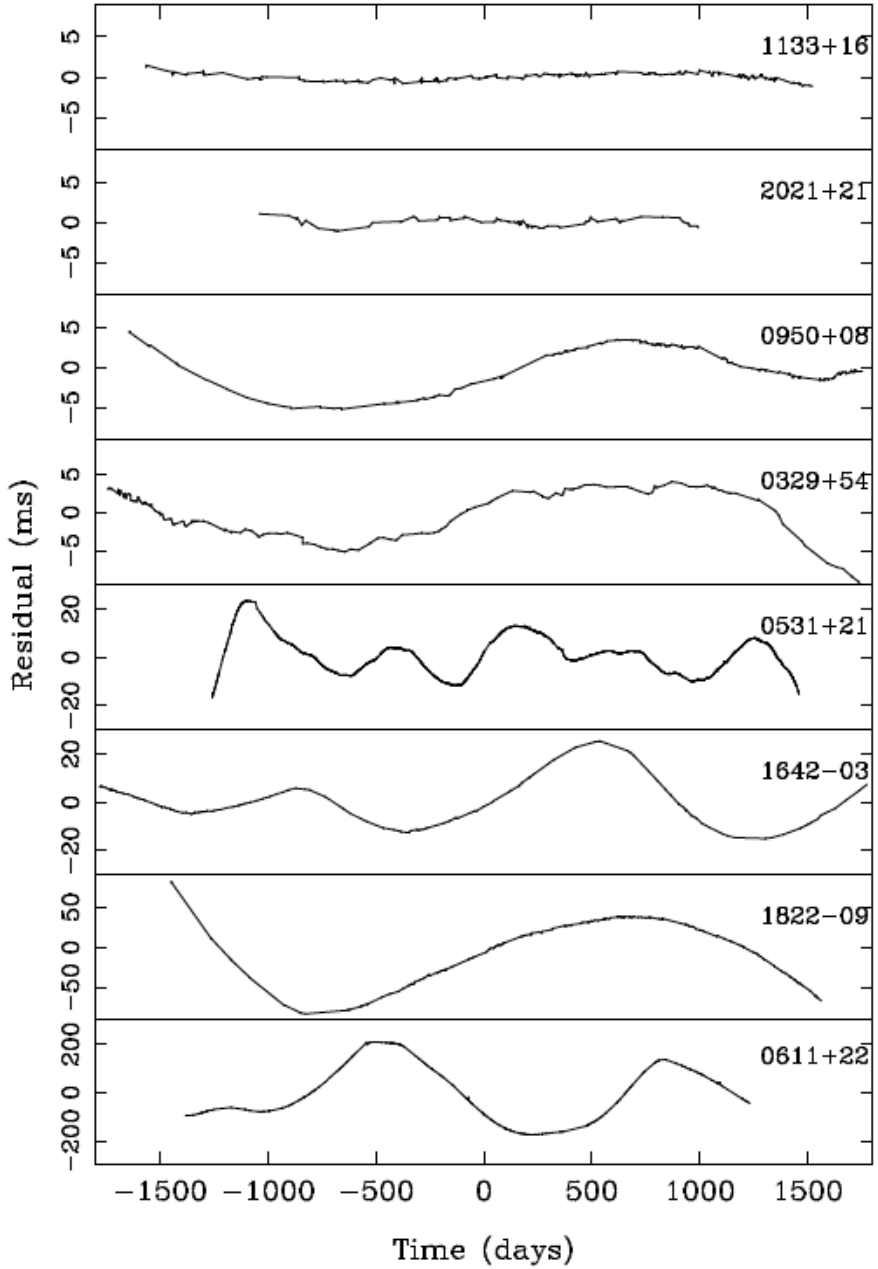

Figure 23: Examples of timing residuals for a number of normal pulsars. Note the varying scale on the ordinate axis, the pulsars being ranked in increasing order of timing "activity". Data taken from the Jodrell Bank timing program [335, 146]. Figure provided by Andrew Lyne.

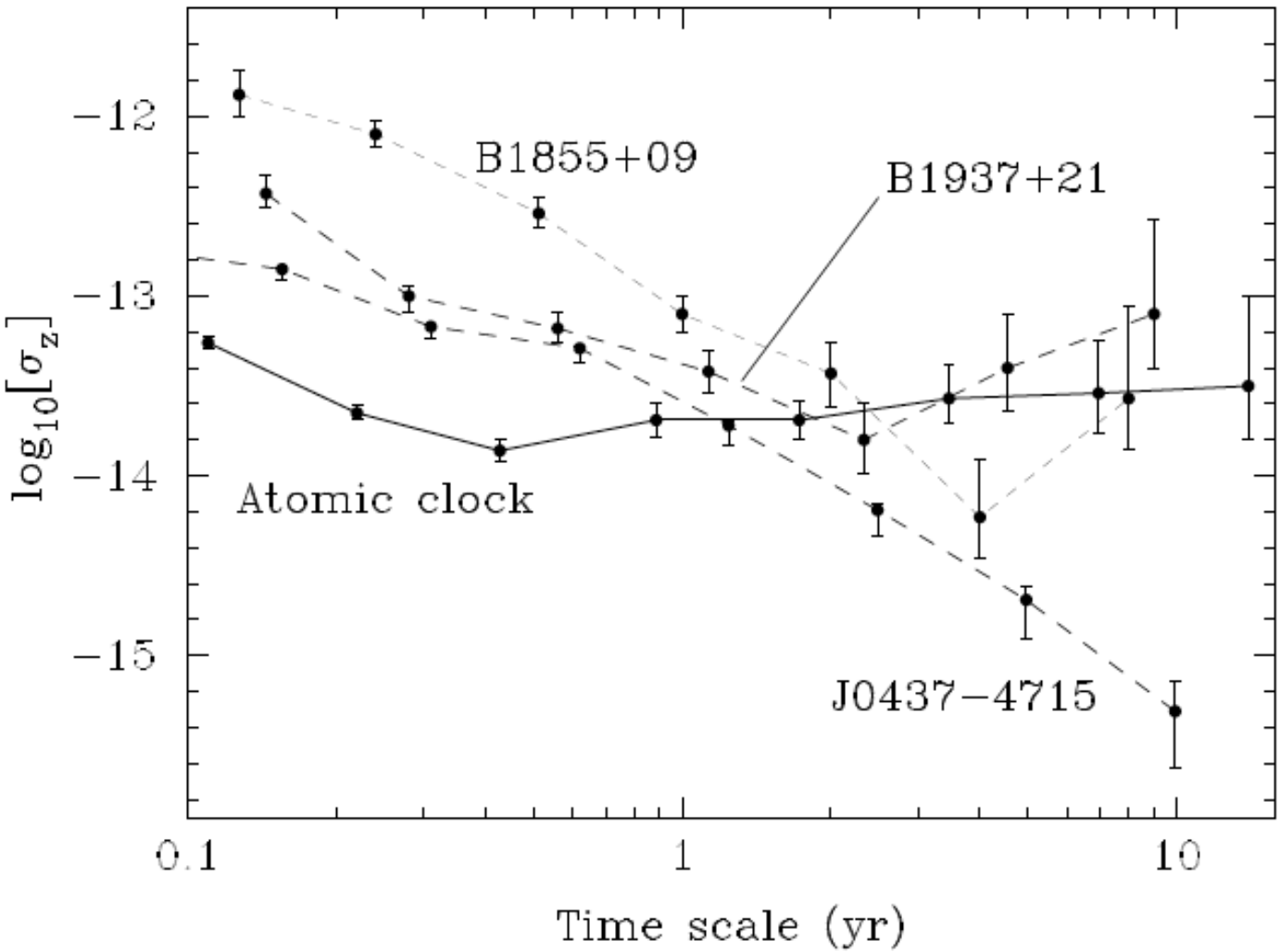

Figure 24: The fractional stability of three millisecond pulsars compared to an atomic clock. Both PSRs B1855+09 and B1937+21 are comparable, or just slightly worse than, the atomic clock behaviour over timescales of a few years [254]. More recent timing of the millisecond pulsar J0437−4715 [388] indicates that it is inherently a very stable clock. Data for the latter pulsar provided by Joris Verbiest.

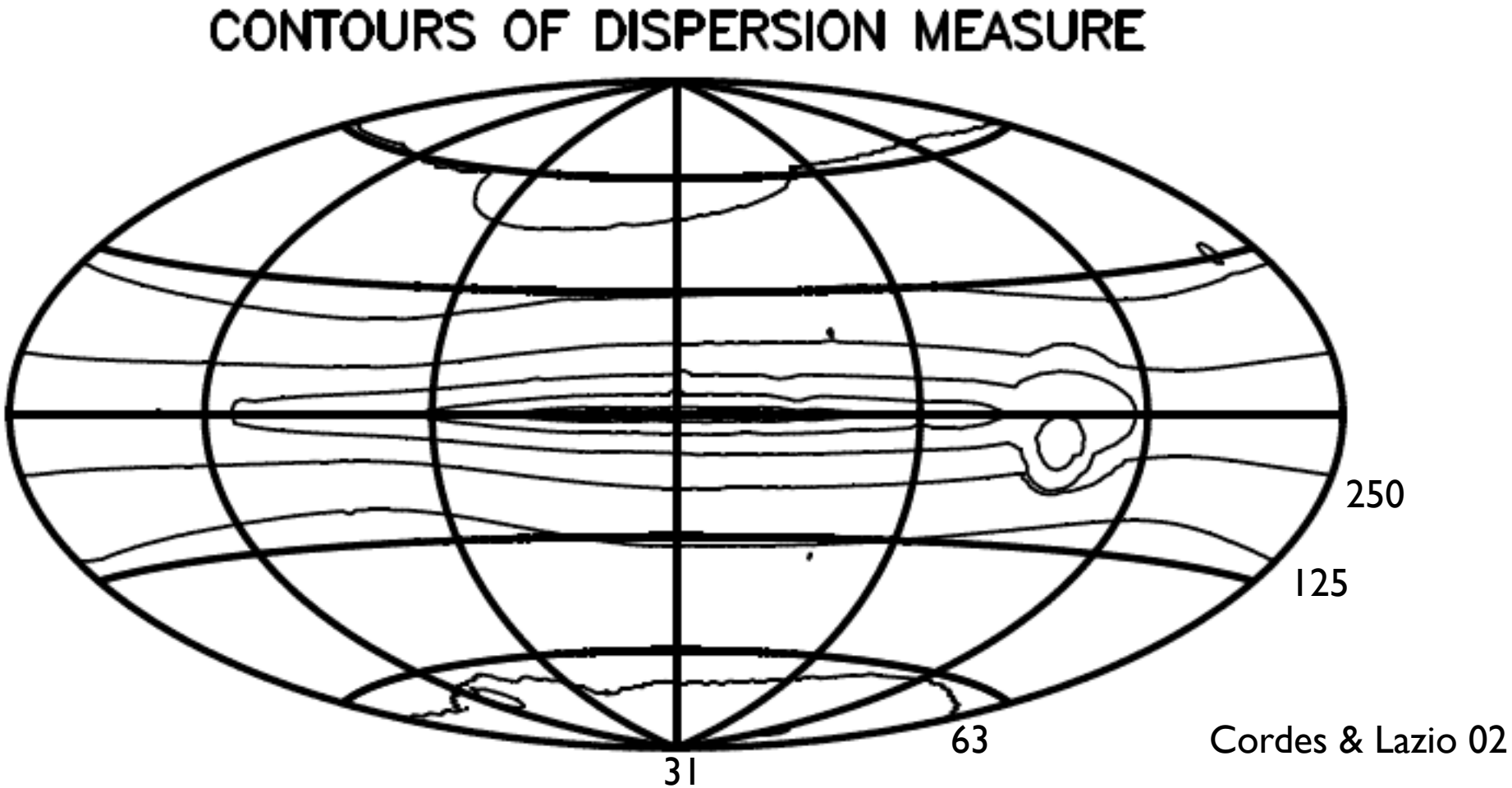

FIG. 15.— Contours of DM integrated to infinite distance and plotted against Galactic latitude and longitude on an Aitoff projection with the Galactic center in the middle and negative longitudes to the right. Contours are at $4000/2^n$ pc cm^{-3} for $n = 0, 1, \ldots, 7$, with the lowest contour at the Galactic poles.

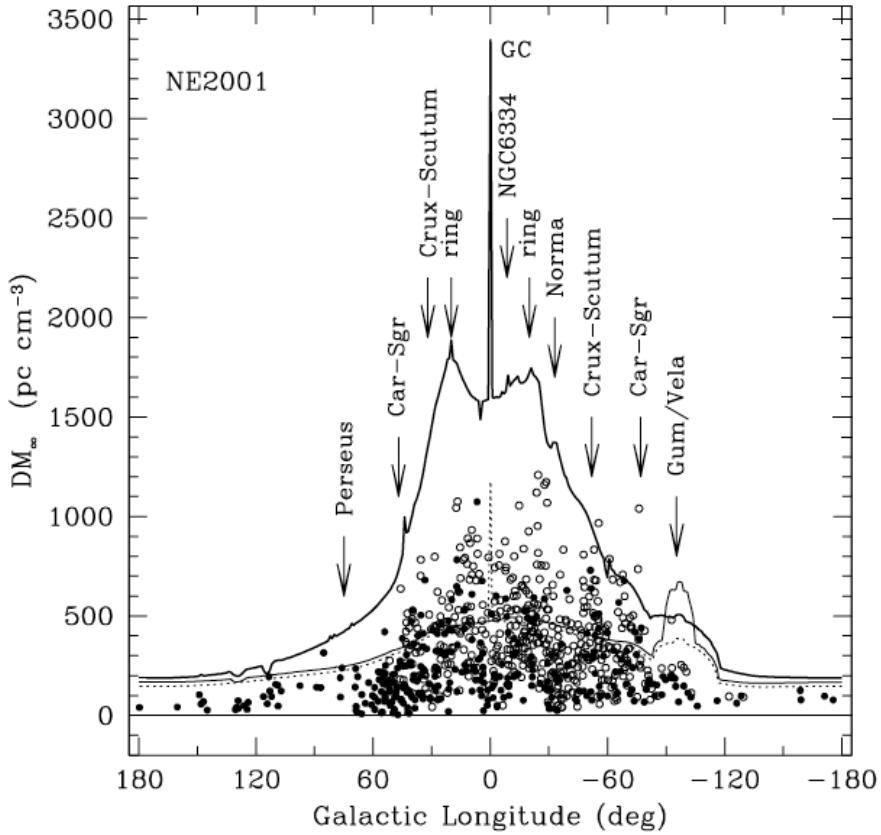

FIG. 11.— Plot of $DM_\infty(\ell, b)$, the maximum DM obtained by integrating the NE2001 model. Heavy solid line: $b = 0°$. Light solid line: $b = -5°$. Dotted line: $b = +5°$ (offset by -20 pc cm^{-3} in the vertical direction for clarity). Plotted points are pulsars with $|b| < 5°$. Filled circles: pulsars from the Princeton catalog. Open circles: pulsars from the public Parkes Multibeam catalog. Labelled features include tangents to the spiral arms and maxima associated with the ring component, the Gum Nebula and Vela supernova remnant, and the H II complex NGC 6334. The gaps near $\ell = +15°$ and $-20°$ and DM $\lesssim$ 200 pc cm^{-3} are real, appearing in both samples, and signify either the real absence of pulsars in the corresponding volume or the presence of large electron densities in these directions fairly close to the solar system. The absence of pulsars above $\sim$ 1200 pc cm^{-3} is due to selection against such objects by pulse broadening from dispersion smearing and scattering.

Cordes & Lazio 02

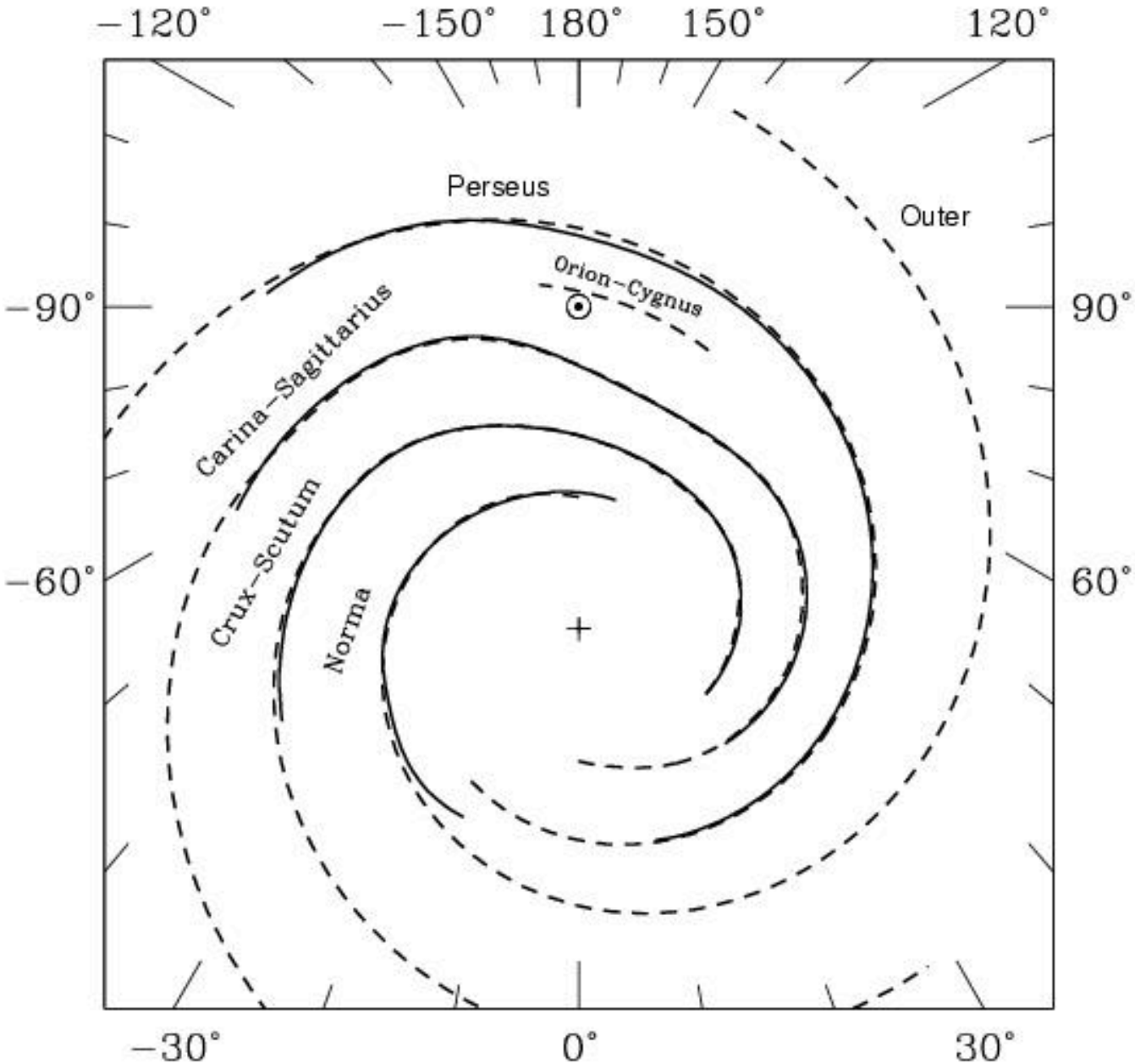
−120°
−150°
180°
150°
120°
Perseus
Outer
Orion−Cygnus
−90°
90°
Carina−Sagittarius
Crux−Scutum
−60°
60°
Norma
−30°
0°
30°

Table 1
Data Summary

	Number of Measurements					
Work	D[a]	DM	τ_d	$\Delta\nu_{\rm d}$	$\theta_{d,\rm Gal}$	$\theta_{d,\rm xgal}$
TC93	74	553	120	74	38	42
This paper	112	1143	159	110	118	94

[a]The number of distances is the number of distinct lines of sight. A globular cluster with multiple pulsars is counted as only one line of sight.

$P\dot{P}$ Diagram

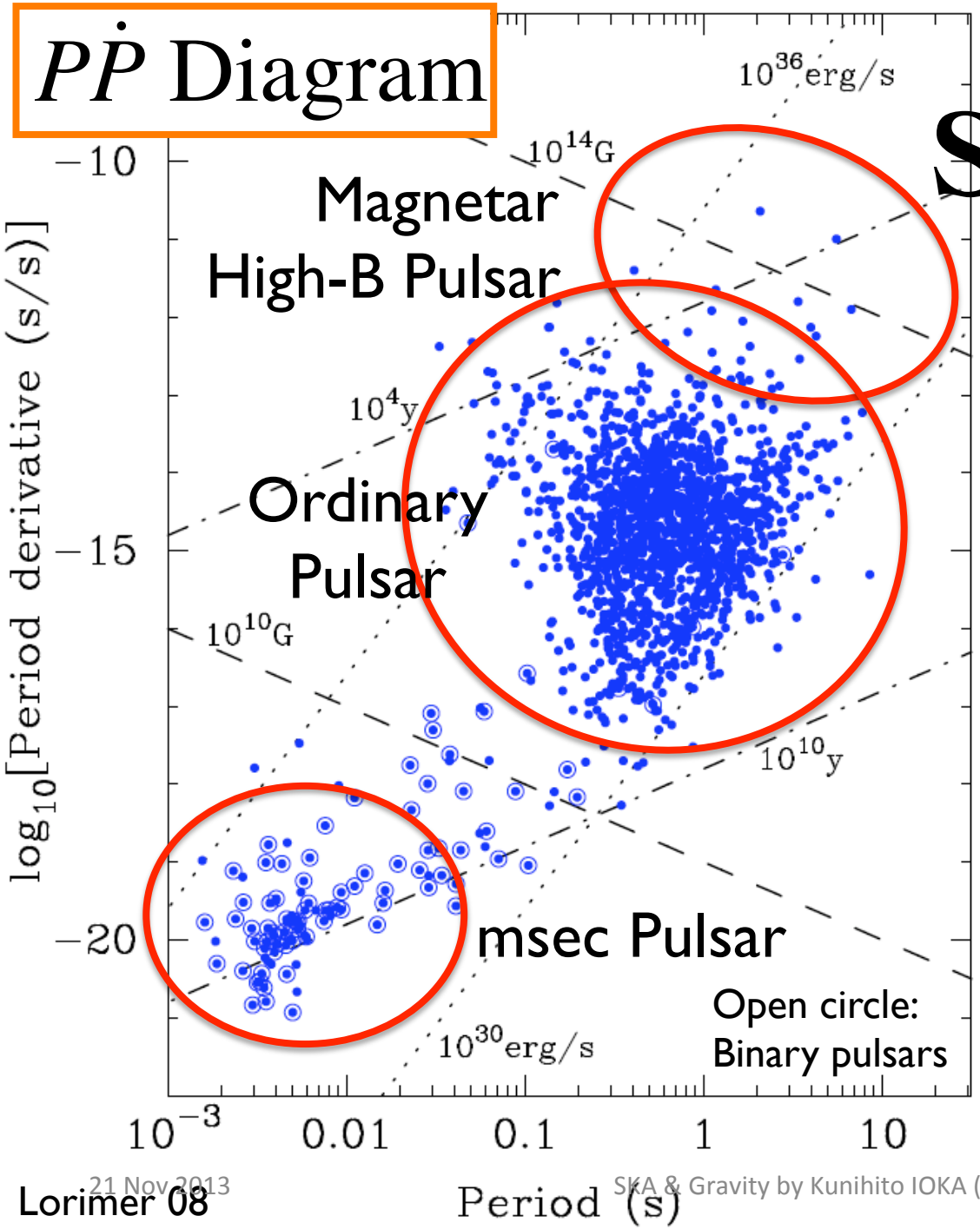

Lorimer 08

Spin-Down

$$|\mathbf{m}| \approx \frac{B_p R^3}{2}$$ Mag. Dipole

Mag. Dipole Formula

$$\dot{E} = -\frac{2}{3c^3}|\ddot{\mathbf{m}}|^2$$

$$\approx -\frac{B_p^2 R^6 \Omega^4 \sin^2\alpha}{6c^3}$$

$$\dot{E} = I\Omega\dot{\Omega},\ \Omega = \frac{2\pi}{P}$$

$$B_p = \sqrt{\frac{3c^3 I}{2\pi^2 R^6 \sin^2\alpha} P\dot{P}}$$

$\Rightarrow$ **$B \sim 10^{12}$G**

SKA1 PSR Survey Requirements

SKA Design Reference Mission: SKA Phase 1

Table 5-1. Pulsar Survey Scientific Requirements

Parameter	Value	
Pulsar luminosity	0.1 mJy kpc^2 at 1400 MHz within 10 kpc	>99.9% PSR
Pulsar period	0.5 ms–10 s	Currently 1.4ms-10s
Dispersion measure	At least 1500 pc cm^{-3}	For Galactic center
Sky coverage	Entire sky visible from its latitude on Earth, above notional elevation limit of 10 deg (TBC)	For MSP
Pulsar orbits	Orbital periods at least as short as 30 minutes	MSP in binary

Table 5-2 Pulsar Survey Technical Requirements

Parameter	Requirement	Comment
A_{eff}/T_{sys}	500 m^2 K^{-1}	Pulsar luminosity, period, DM
Frequency range	0.3–3 GHz	Pulsar spectra, period, DM
Frequency resolution	< 10 kHz	DM
Temporal resolution	50 μs	Pulsar duty cycle, period, DM
Array filling factor	"high"	Pulsar luminosity, processing; see text
Array data product	voltage time series over entire FoV	Processing, pulsar period, DM

Pulse width ~1ms×10%

SKA1 PSR Timing Requirement

SKA Design Reference Mission: SKA Phase 1

Table 6-1. Pulsar Timing Scientific Requirements

Parameter	Value
Pulsar luminosity	0.1 mJy kpc^2 at 1400 MHz within 10 kpc
Sky coverage	$> 2\pi$ sr
Gravitational wave strain	10^{-16}
Time resolution capability	100 ns

Table 6-2. Pulsar Timing Technical Requirements

Parameter	Requirement	Comment
A_{eff}/T_{sys}	$> 1000\ m^2\ K^{-1}$	Pulsar luminosity
Array data product	multiple independent voltage time series, notionally at least 20 such data streams	Processing
Frequency range	0.8–3 GHz	Pulsar spectra, timing precision
Frequency agility	switch between observing frequencies within 10 minutes or less	Timing precision
Polarization purity	40 dB	Timing precision, coupled to Array Data Product requirement; see text
Timing stability	connect pulse time of arrivals over at least 10 yr	Longer programs lead to ever higher precision tests; see text

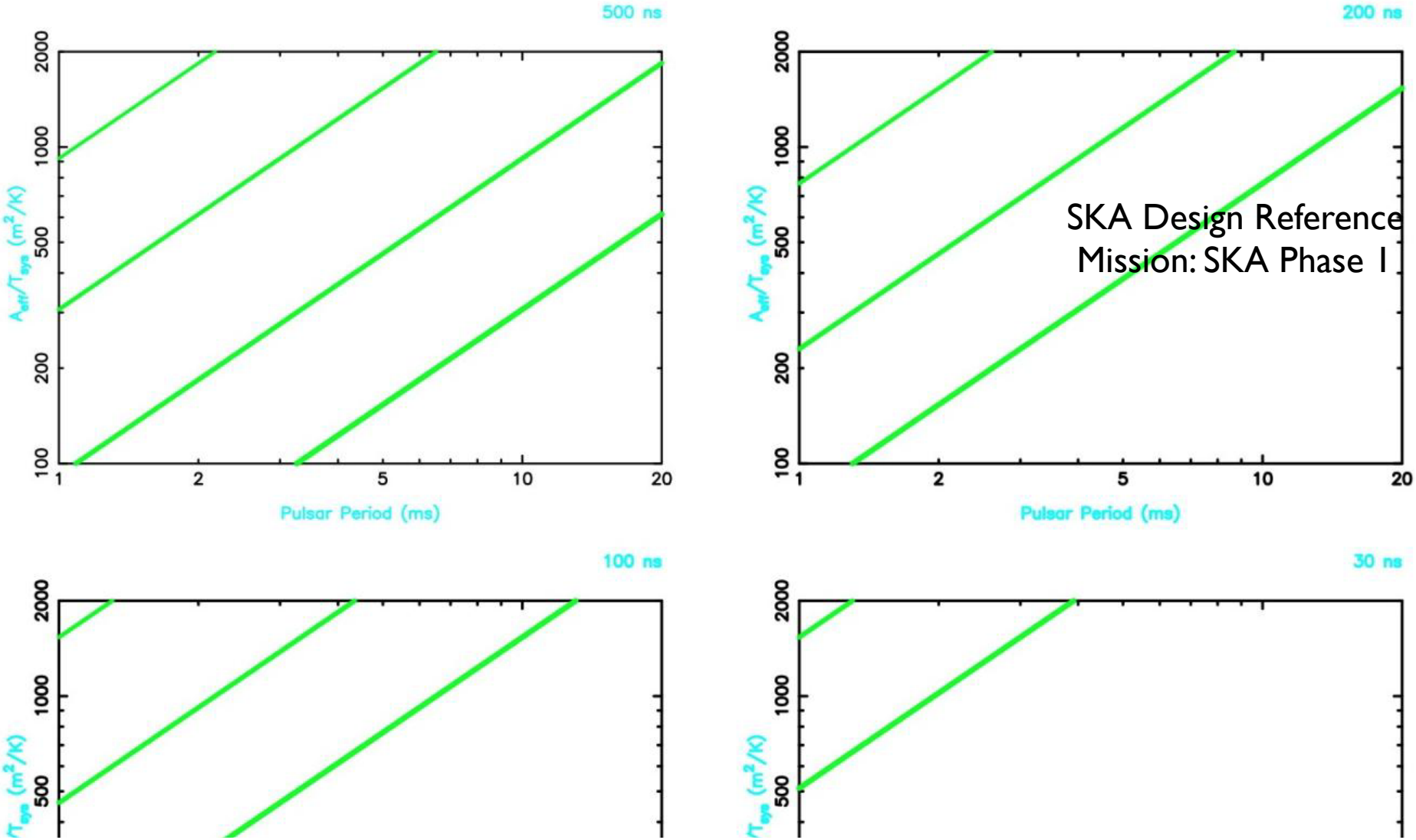

Figure 6-1. Each panel shows the sensitivity required, as a function of pulsar period, to obtain the required rms TOA level (500, 200, 100, and 30 ns). The curves are for flux densities of 30, 10, 3, and 1 mJy (in thickness, from stronger to weaker, or lower right to upper left). The curves also assume that the pulsar duty cycle is 10%, the time to acquire a pulse profile is 1 hr, and the bandwidth is 500 MHz for an observation frequency of 1400 MHz. These curves show the contribution from "white noise" or uncorrelated uncertainties; "red noise" contributions, e.g., from pulsar timing noise will lead to larger rms TOA levels.

SKA VLBI Requirement

Table 7.1. Scientific Requirements

Parameter	Value
Positional Accuracy	20 mas at low signal-to-noise ratio (5) 1 mas at high signal-to-noise-ratio (100)
Sky coverage	> 2π sr

Table 7.2. Pulsar Astrometry Technical Requirements

Parameter	Requirement	Comment
Observing Frequency	1 – 3 GHz	High signal-to-noise ratio, resolution, ionosphere calibration
Maximum baseline	200 km	positional accuracy
Instantaneous Accessible Solid Angle	> 0.25 deg^2	In-beam calibrators
Pulsar gating	Enable correlator to only record when pulsar is "on"	Improve signal-to-noise ratio of the pulsar

$2M_\odot$中性子星

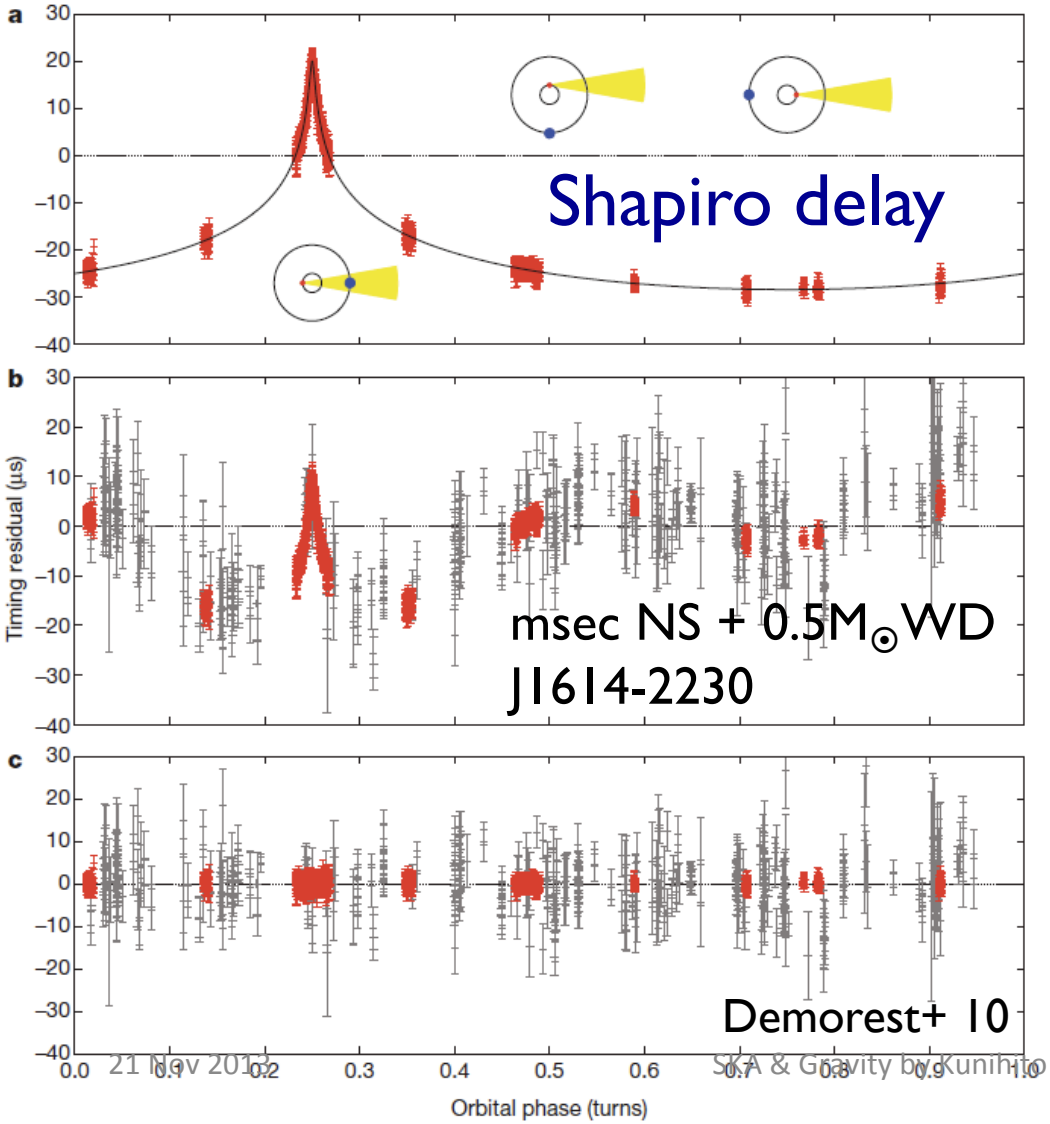

- ~(1.97±0.04)$M_\odot$
- 硬い状態方程式
- 中性子星がブラックホールに崩壊しにくい
- 連星中性子星合体
  ⇒ 超巨大中性子星
  ⇒ Short GRB
  の可能性を高める

See also Antoniadis+ 13

Maximum Mass

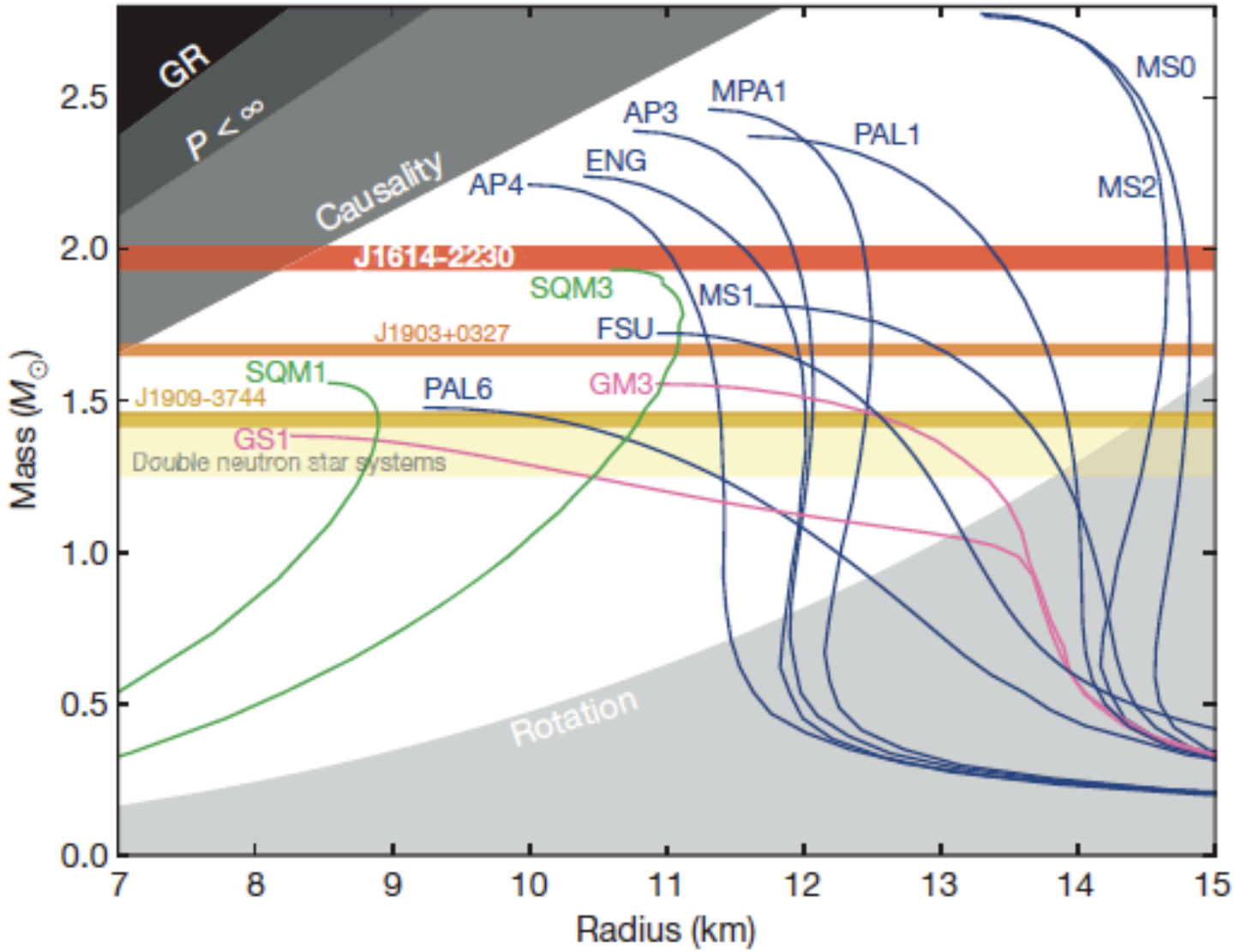

2M⊙

モデルを棄却

- ハイペロン
- 3体力
- ベクトル力

Demorest+ 10

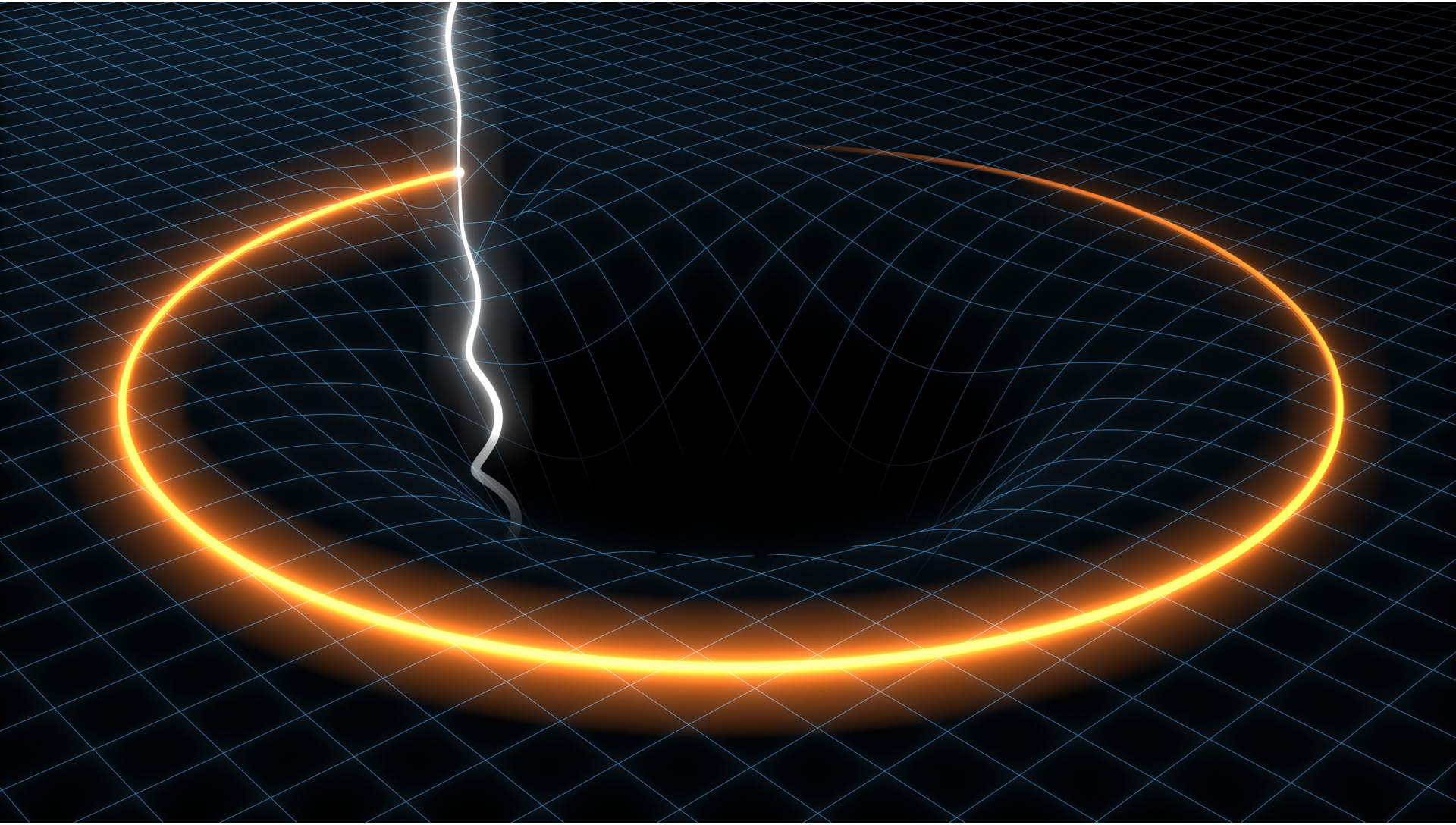

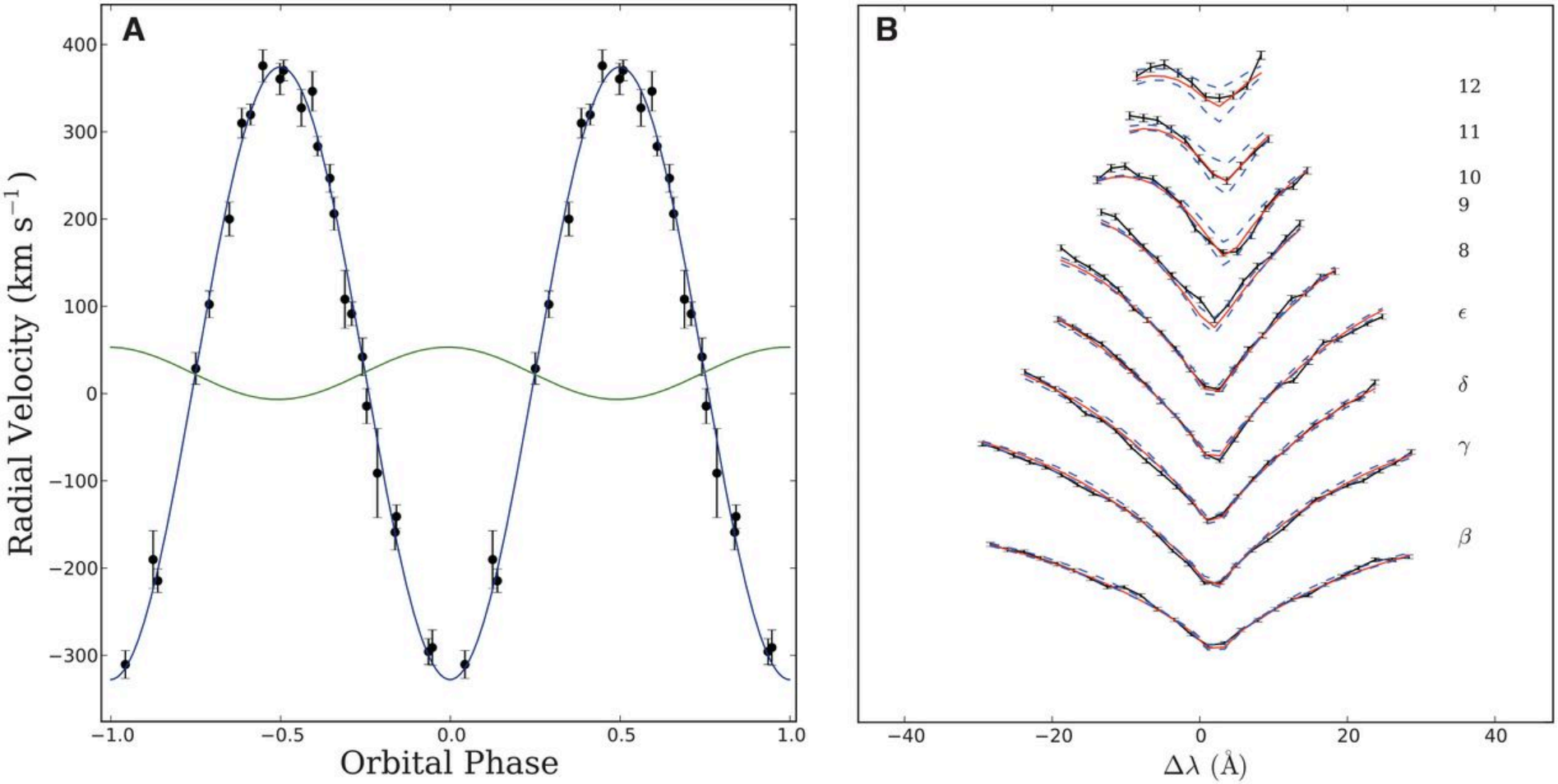
A
Radial Velocity (km s^{-1})
Orbital Phase
B
12
11
10
9
8
ϵ
δ
γ
β
Δλ (Å)

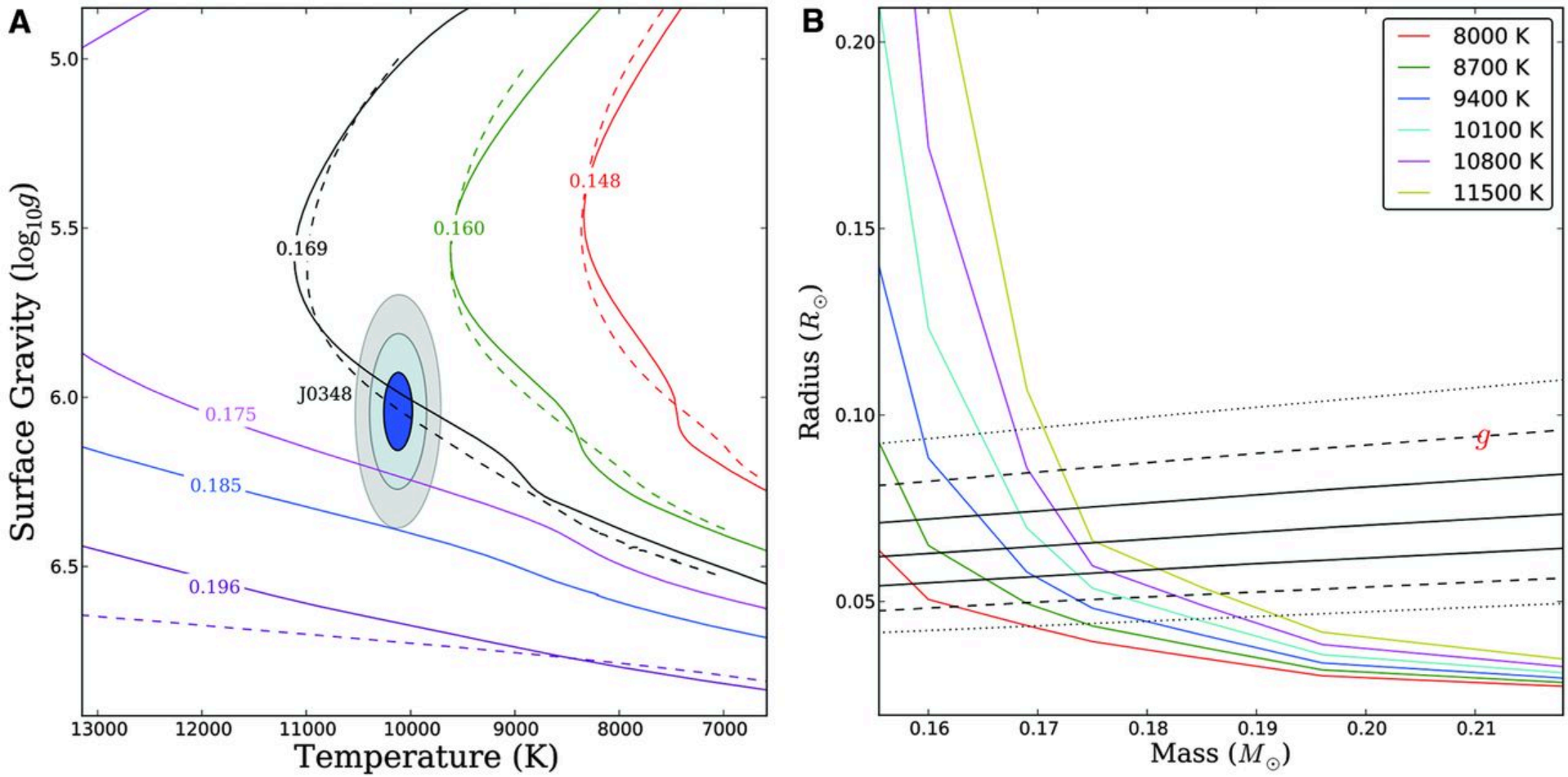
A
Surface Gravity ($\log_{10} g$)
Temperature (K)
0.169
0.160
0.148
J0348
0.175
0.185
0.196
B
Radius ($R_\odot$)
Mass ($M_\odot$)
8000 K
8700 K
9400 K
10100 K
10800 K
11500 K
g

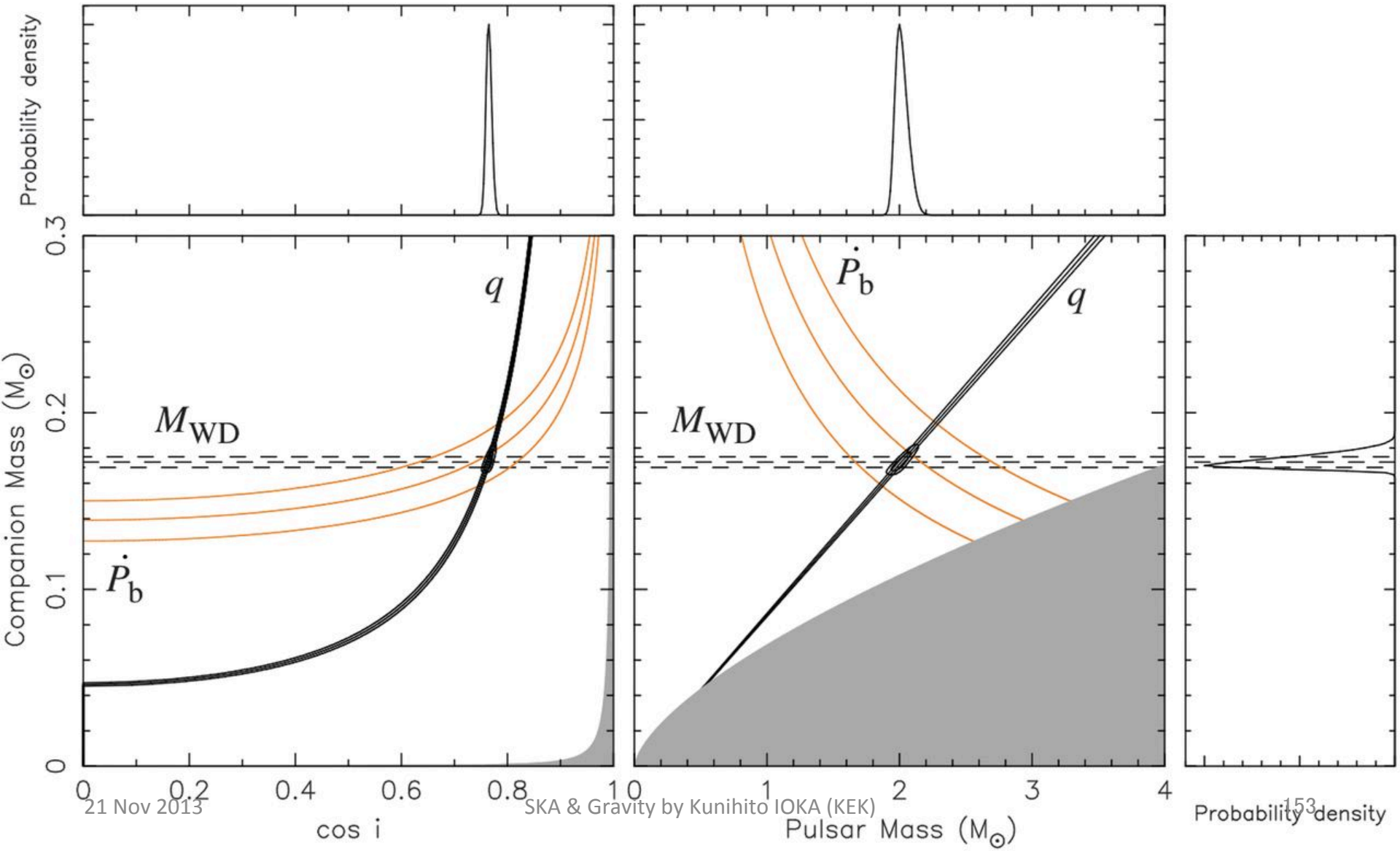
Probability density
Companion Mass ($M_\odot$)
0.3
0.2
0.1
0
q
M_{WD}
$\dot{P}_b$
0
0.2
0.4
0.6
0.8
1
cos i
$\dot{P}_b$
q
M_{WD}
0
1
2
3
4
Pulsar Mass ($M_\odot$)
Probability density

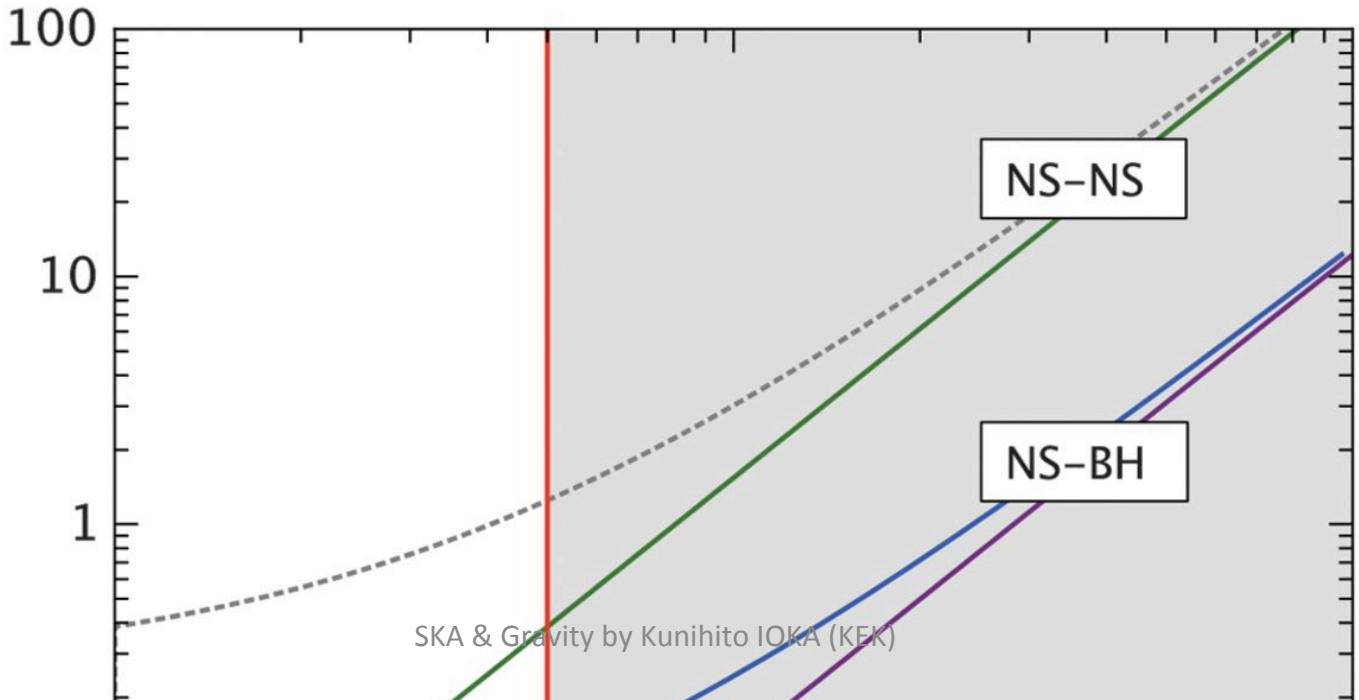
100
10
1
NS–NS
NS–BH

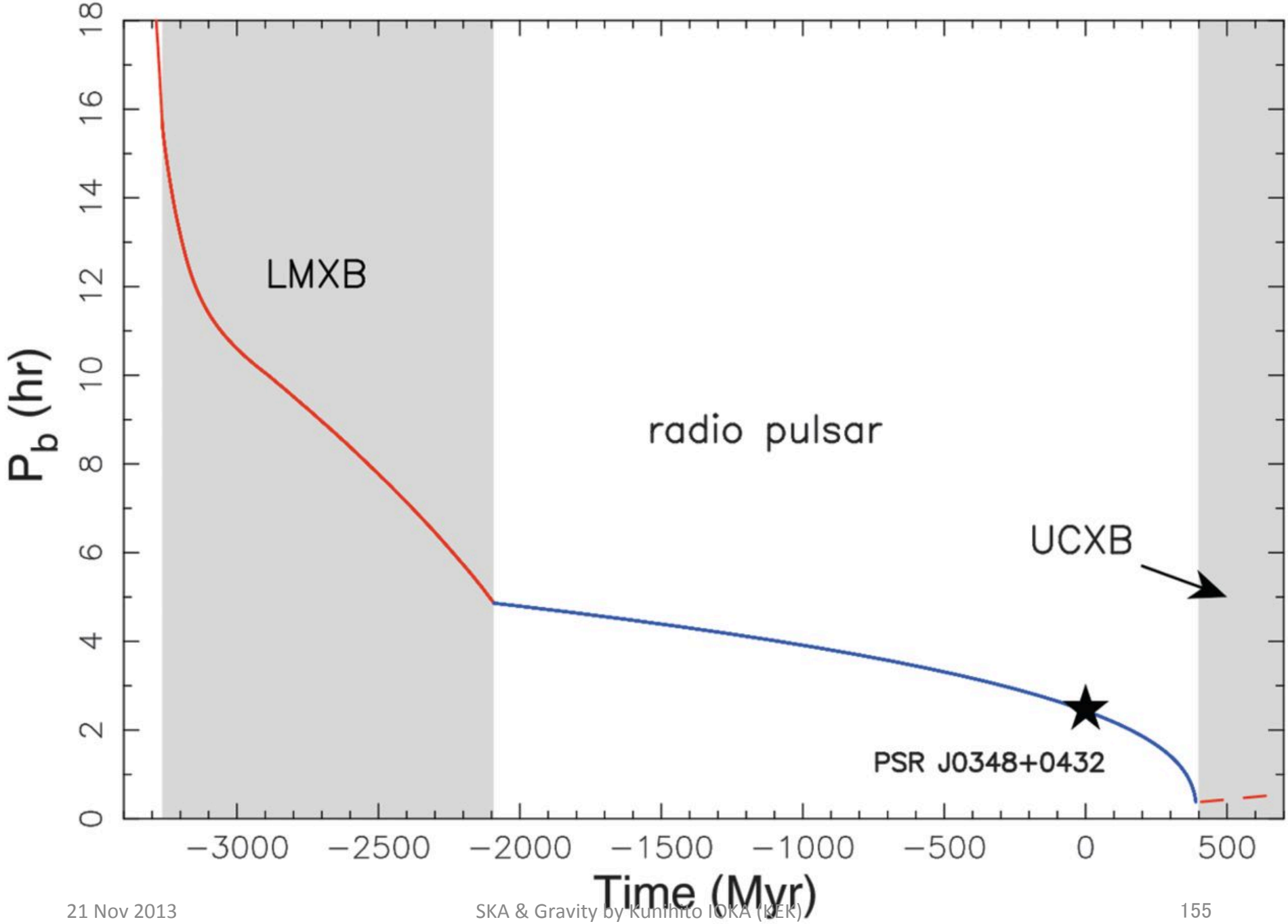
LMXB
radio pulsar
UCXB
PSR J0348+0432
P_b (hr)
Time (Myr)
0
2
4
6
8
10
12
14
16
18
−3000
−2500
−2000
−1500
−1000
−500
0
500

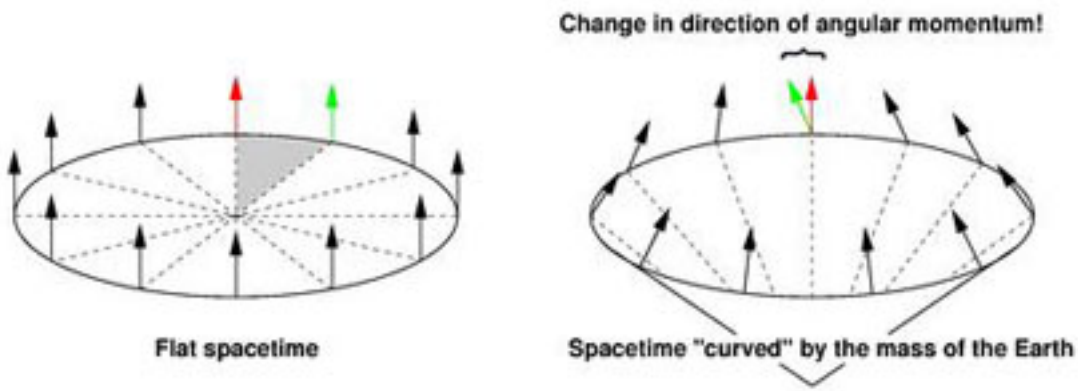
Change in direction of angular momentum!
Flat spacetime
Spacetime "curved" by the mass of the Earth